Understanding molecular mechanisms of striated muscle laminopathies using cellular and zebrafish models

Hannah Almira Nicolas

Thesis submitted to the University of Ottawa
in partial fulfillment of the requirements for the
Doctor of Philosophy in Biology

Department of Biology
Faculty of Science
University of Ottawa

Abstract

The Lamin A/C (*LMNA*) gene codes for the A-type lamins which are nuclear intermediate filaments that provide structural support to the nucleus and help regulate various nuclear processes such as gene expression. Mutations in *LMNA* cause a group of diseases collectively known as laminopathies. Laminopathies present with a diverse set of phenotypes with 79% of the cases affecting cardiac and/or skeletal muscles (striated muscle laminopathies). Striated muscle laminopathies tend to be severe and have poor patient prognosis.

The lamin A/C binding partner - Protein Kinase C alpha (PKC α), is a serine/threonine kinase that phosphorylates many proteins including other lamin A/C partners, and proteins associated with striated muscle laminopathies. Chapter 2 of this thesis determined PKC α involvement in striated muscle laminopathies by examining PKC α subcellular localization, lamin A/C interaction, and activation in various cellular models expressing WT or mutant lamin A/C. The results showed that in most of the mutations that we studied, cells expressing mutant lamin A/C presented with an abnormal increase in nuclear PKC α localization compared to WT. Patient and mice model myoblasts and/or fibroblasts also presented with altered PKC α-lamin A/C interaction and reduced PKC α activation compared to control. In parallel, activation of ERK 1/2, a downstream PKC α target associated with striated muscle laminopathies, was also decreased in patient myoblasts and mice model myoblasts. Altogether, these results suggested PKC α involvement in striated muscle laminopathies.

Chapter 3 of this thesis describes the creation of zebrafish with permanent *lmna* disruption, and characterization of the *lmna* mutants' phenotype. We induced a five base pair deletion in exon 2 of *lmna* that is predicted to result in a potential non-functional truncated protein of 180 amino acids lacking the PKC α binding site. Cardiac structure and function analyses of the *lmna* mutants

showed mild and transient cardiac defects during the first week of development. In addition, the *lmna* mutants displayed skeletal muscle structure fibre defects that likely contributed to their swim impairment. Expression of *jun* and *nfkb2* was decreased while activated Erk 1/2 was increased in mutants. Jun, NF-KB and Erk 1/2 are biomarkers for striated muscle laminopathies. Furthermore, activation of Pkc α, an upstream Erk 1/2 regulator, was increased in the *lmna* mutants compared to WT. Overall, the zebrafish *lmna* mutants presented a model of muscular laminopathies. These zebrafish *lmna* mutants can be used to test for drug efficacy or identify novel therapeutic targets to treat muscular laminopathies.

Résumé

Le gène Lamine A/C (*LMNA*) code pour les lamines de type A qui sont des filaments intermédiaires nucléaires qui fournissent un support structurel au noyau et aident à réguler divers processus nucléairs tels que l'expression des gènes. Les mutations de *LMNA* provoquent un ensemble de maladies connues sous le nom de laminopathies. Les laminopathies présentent un ensemble diversifié de phénotypes avec 79% des cas affectant les muscles cardiaques et/ou squelettiques (laminopathies musculaires striées). Les laminopathies musculaires striées ont tendance à être sévères et à conduire à de mauvais pronostic.

Le partenaire de liaison de la lamine A/C - la Protéine Kinase C alpha (PKC α), est une sérine/thréonine kinase qui phosphoryle de nombreuses protéines, y compris d'autres partenaires de la lamine A/C, et des protéines associées aux laminopathies musculaires striées. Le chapitre 2 de cette thèse visait à déterminer l'implication de PKC α dans les laminopathies musculaires striées en examinant la localisation subcellulaire de PKC α, son interaction avec la lamine A/C et son activation dans divers modèles cellulaires exprimant la lamine A/C de type sauvage (WT) ou différentes formes mutantes. Les résultats ont montré que pour la plupart des mutations que nous avons étudiées, les cellules exprimant la lamine A/C mutante présentaient une augmentation anormale de la localisation nucléaire de PKC α par rapport au WT. En revanche, les cellules exprimant une lamine A/C tronquée dépourvue du site de liaison à PKC α présentaient une localisation de PKC α qui était principalement cytoplasmique comme dans les cellules WT. Les myoblastes et/ou les fibroblastes de patients et de modèles souris présentaient également une interaction altérée entre la lamine A/C et PKC α, ainsi qu'une réduction de l'activation de PKC α par rapport au contrôle. Parallèlement, l'activation d'ERK 1/2, une cible de PKC α associée à des

laminopathies musculaires striées, est également diminuée dans les myoblastes de patients et de modèles murins. Dans l'ensemble, ces résultats suggèrent une implication de la PKC α dans les laminopathies musculaires striées.

Le chapitre 3 de cette thèse concerne la création de poisson zèbre avec une perturbation permanente du gène *lmna* et la caractérisation du phénotype des mutants de *lmna*. Nous avons induit une délétion de cinq paires de bases dans l'exon 2 de *lmna* qui devrait entraîner la synthèse d'une protéine tronquée non fonctionnelle de 180 acides aminés dépourvue du site de liaison de PKC α. Les analyses de la structure et de la fonction cardiaque des mutants de *lmna* ont montré des anomalies cardiaques légères et transitoires au cours de la première semaine de développement. De plus, les analyses de la structure et de la fonction des muscles squelettiques des mutants de *lmna* ont montré des défauts des fibres musculaires qui probablement contribuent à l'altération de la nage des mutants. L'expression de l'ARNm de *jun* et *nfkb2* est diminuée alors que celle d'Erk 1/2 activé est augmentée chez les mutants homozygotes *lmna*. Jun, NF-KB et Erk 1/2 sont des marqueurs des laminopathies musculaires striées. De plus, l'activation de Pkc α, un régulateur en amont d'Erk 1/2, est augmentée chez les mutants *lmna* par rapport à WT. Dans l'ensemble, les mutants *lmna* du poisson zèbre représentent un modèle de laminopathies musculaires. Ces mutants *lmna* du poisson zèbre peuvent être utilisés pour tester l'efficacité de médicaments ou identifier de nouvelles cibles thérapeutiques pour traiter les laminopathies musculaires.

Acknowledgements

Thank you to my supervisors - Dr. Frédérique Tesson and Dr. Marie-Andrée Akimenko for all the time, effort, and energy that they invested in me and my project. This has been an incredible learning experience.

Thank you to our collaborators - Dr. Gisèle Bonne and her team particularly Dr. Anne Bertrand Legout at the Myology Institute in Paris, France for sharing their samples and for welcoming me in their lab during my research stay. Thank you as well to Mr. Arturo Segura of the University of Ottawa Centre for Research Opportunities for helping fund my research visit in Paris.

Thank you to my previous and current thesis advisory committee members – Dr. Ilona Skerjanc, Dr. Mona Nemer, Dr. Marc Ekker and Dr. Laura Trinkle-Mulcahy for their hand at shaping and refining this project. Special thanks to Dr. Trinkle-Mulcahy for all her help particularly with the analyses of my cellular work results. Thank you as well to Dr. Gilles Lamothe for his guidance on the statistical analyses of the results.

Thank you to Mr. Vishal Saxena and the rest of the ACVS team (particularly Ms. Christine Archer) for all their immense work in maintaining the zebrafish facility. Thank you as well to Mr. Jacky Liang and Mr. Andrew Ochalski for their help and advice on sample imaging.

Thank you to the previous and current members of the Tesson, Akimenko, Ekker, Matar and Menzies labs especially - Pierrette Bolongo, Jing Zhang, Stephen Kutcher, Qing Ming Qu, Hailey Quigley, Joshua Ivare, Khang Hua, Robert Lalonde, Danick Goulet, Meaghan de Jesus, Marissa Northorp, Shea Keil, Reeham Kadhom, Mustafa Hamid and Bidemi Keshinro for their help with performing and/or trouble-shooting my experiments. Importantly, thank you for the friendship. I could not have gone through graduate school with a better group.

Thank you to one of my best friends who I met in grad school - Abishankari Rajkumar. Her kind, patient and empathetic nature has been a source of comfort and encouragement to me all these years. I am immensely grateful to have her as my friend.

Thank you to my friends outside the lab particularly – Himali Leung, Tasha Wagner, Cynthia Stang, Abhi Bhandari, Aatika Ahmed, Eva Watson and Deborah Michel for being an incredible source of support and encouragement.

Thank you to my family especially my maternal grandparents who were the main players during the early and formative years of my education.

Thank you to my parents. This thesis is my ode to their hard work, sacrifices, patience, understanding, support, and love for me.

Lastly, thank you God. This project has gone through immense challenges and near disasters but has miraculously survived owing to what I would call divine intervention.

Table of Contents

Appendix

List of Figures, Tables and Videos

Chapter 1

Chapter 2

Main Figures and Tables

Supplementary Figures and Tables

Chapter 3

Main Figures and Tables

Appendix

Review 1

Review 2

List of Abbreviations

a.a: amino acid(s)

Ab: antibody

ACE: angiotensin II converting enzyme

Akt: Protein kinase B

AF: Atrial fibrillation

ANP: atrial natriuretic peptide

AP-1: Activating Protein I

AVC: atrioventricular canal

BAF: barrier-to-autointegration factor

BNP: brain natriuretic peptide

BSA: bovine serum albumin

C: carboxyl

C*AAX* : cysteine-aliphatic-aliphatic-any amino acid

CD: conduction defect

Cdk1: Cyclin-dependent kinase 1

cmlc-1: cardiac myosin light chain-1

CMT2B1: Charcot–Marie–Tooth disease type 2B1

CRISPR/Cas9: Clustered regularly interspaced short palindromic repeats/CRISPR-associated protein 9

Csrp3: Cysteine And Glycine Rich Protein 3

Cx 40/43: Connexin 40/43

DCM: Dilated cardiomyopathy

DMD: Duchenne muscular dystrophy

DNA: deoxyribonucleic acid

dpf: day(s) post fertilization

E3.5: embryonic day 3.5

ECL: essential light chain of myosin

EDMD: Emery-Dreifuss muscular dystrophy

ef1α: elongation factor 1

ERK 1/2: Extracellular signal-regulated kinases 1/2

FHL2: four-and-a half LIM protein-2

FLNc: protein filamin C

FPLD2: Familial partial lipodystrophy Dunnigan-type 2

HDAC2: histone deacetylase 2

Hf1b/Sp4: Transcription factor Sp4

HGPS: Hutchinson-Gilford progeria syndrome

HF: Heart failure

hpf: hour(s) post fertilization

IDC: Idiopathic dilated cardiomyopathy

IF: immunofluorescence

Ig: immunoglobulin

iPSCs: induced pluripotent stem cells

IPSC-CMs: induced pluripotent stem cells derived cardiomyocytes

JNK: c-Jun N-terminal kinases

Keap1: Kelch-like ECH-associated protein 1

KASH: Klarsicht/ANC-1/Syne Homology

L-CMD: *LMNA*-related congenital muscular dystrophy

lama2: laminin α2

LAP2: Lamina-associated polypeptide 2

LEM: Lap2-emerin-MAN1

LGMD1B: Limb-girdle muscular dystrophy

LMNB1: lamin B1

LMNB2: lamin B2

LMNA: lamin A/C

MAPK: Mitogen-activated protein kinase

MEFs: Mouse embryonic fibroblasts

MEK 1/2: Dual-specificity mitogen-activated protein kinase kinase 1/2

miRNA: micro-RNA

MO: Morpholino

mpf: months post fertilization

mTor: mechanistic target of rapamycin

Myh6: myosin heavy-chain alpha

Myh7: myosin heavy-chain beta

mRNA: messenger RNA

N: amino

NAT10: N-Acetyltransferase 10

NF-κB: nuclear factor kappa B

NF-κB2: nuclear factor kappa B subunit 2

nm: nanometers

NMR: nuclear magnetic resonance

NPCs: Nuclear pore complexes

Nppb: Natriuretic peptide B

Nrf2: Nuclear factor erythroid-2-related factor 2

Nup153/154: Nucleoporin 153/154

p62/SQSTM1: Sequestosome-1 (ubiquitin-binding protein p62)

PCNA: Proliferating cell nuclear antigen

PDB: protein data bank

PKC: Protein kinase C

PKC α: Protein Kinase C alpha

PRKCA: Protein kinase C alpha (gene)

PLA: proximity ligation assay

PP-I: protein phosphatase-I

PPAR-gamma: Peroxisome proliferator-activated receptors gamma

RFP: red fluorescent protein

rpl13a: alpha ribosomal protein l13a

SERCA-2: sarcoplasmic/endoplasmic reticulum Ca^{2+}-ATPase

Smad 2/3: Mothers against decapentaplegic homolog 2/3

SREBF-1: Sterol regulatory element binding transcription factor 1

SRF: Serum response factor

SUMO1/2: Small ubiquitin-related modifier 1/2

syne1: Spectrin repeat-containing nuclear envelope protein 1

TF: Transcription factor

TGF-β: Transforming growth factor beta

TPA: 12-O-Tetradecanoylphorbol-13-acetate

TTN: titin

ttna: titin A

ttnb: titin B

WB: western blot

WNT: Wingless/Integrated

ywhaz: tyrosine 3-monooxygenase/tryptophan 5-monooxygenase activation protein, zeta polypeptide

Notes on Nomenclature

1. Gene and protein nomenclature in various species

Human

Gene: *LMNA*
Protein: LMNA

Zebrafish

Gene: *lmna*
Protein: Lmna

Mouse

Gene: *Lmna*
Protein: LMNA

2. Amino acid abbreviation

Alanine (Ala, A)

Arginine (Arg, R)

Asparagine (Asn, N)

Aspartic acid (Asp, D)

Cysteine (Cys, C)

Glutamine (Gln, Q)

Glutamic acid (Glu, E)

Glycine (Gly, G)

Histidine (His, H)

Isoleucine (Ile, I)

Leucine (Leu, L)

Lysine (Lys, K)

Methionine (Met, M)

Phenylalanine (Phe, F)

Proline (Pro, P)

Serine (Ser, S)

Threonine (Thr, T)

Tryptophan (Trp, W)

Tyrosine (Tyr, Y)

Valine (Val, V)

termination codon (X)

3. Protein variant nomenclature

p. H222P: protein sequence change affecting amino acid 222 and replacing histidine (H) with proline (P)

p.Y481X: protein sequence change affecting amino acid 481 and replacing tyrosine (Y) with a premature stop codon (X).

p.K32del: protein sequence change resulting in the deletion of lysine (K) at position 32

Chapter 1

General Introduction

1.1 Notes on Chapter 1

Several parts of the general introduction directly refer to sections and/or tables of two previously published reviews of which I am either a co-author or the primary author. These reviews are attached in the appendix of this thesis for reference. Where required, permission to use has been requested and granted.

Review 1 (pages 200 - 232)

Tesson, F., Saj, M., Uvaize, M. M., Nicolas, H., Płoski, R., & Bilińska, Z. (2014). Lamin A/C mutations in dilated cardiomyopathy. *Cardiology Journal*, *21*(4), 331–342. https://doi.org/10.5603/CJ.a2014.0037

1.1 a Author Contributions:

F Tesson – contributed to the content of the manuscript

M Saj – contributed to the content of the manuscript

M Mohamed Uvaize – contributed to the content of the manuscript

H Nicolas – contributed to the content of the manuscript

R Płoski – edited the manuscript

Z Bilińska – contributed to the content of the manuscript

1.1.b Review 1 Abstract

Dilated cardiomyopathy (DCM) is one of the leading causes of heart failure and heart transplant. Mutations in 60 genes have been associated with DCM. Approximately 6% of all DCM cases are caused by mutations in the lamin A/C gene (*LMNA*). *LMNA* codes for type-V intermediate filaments that support the structure of the nuclear membrane and are involved in chromatin structure and gene expression. Most *LMNA* mutations result in striated muscle diseases while the rest affects the adipose tissue, peripheral nervous system, multiple tissues or lead to progeroid syndromes/overlapping syndromes. Patients with *LMNA* mutations exhibit a variety of cellular and physiological phenotypes. This paper explores the current phenotypes observed in *LMNA*-caused DCM, the results and implications of the cellular and animal models of DCM and the prevailing theories on the pathogenesis of laminopathies.

Review 2 (pages 233 – 282)

Nicolas, H. A., Akimenko, M.-A., & Tesson, F. (2019). Cellular and Animal Models of Striated Muscle Laminopathies. *Cells*, *8*(4). https://doi.org/10.3390/cells8040291

1.1.c Author Contributions:

HA Nicolas – drafted the manuscript

MA Akimenko – edited the manuscript

F Tesson – contributed to the content of the manuscript, and edited the manuscript

1.1.d Review 2 Abstract

The lamin A/C (*LMNA*) gene codes for nuclear intermediate filaments constitutive of the nuclear lamina. *LMNA* has 12 exons and alternative splicing of exon 10 results in two major isoforms—lamins A and C. Mutations found throughout the *LMNA* gene cause a group of diseases collectively known as laminopathies, of which the type, diversity, penetrance and severity of phenotypes can vary from one individual to the other, even between individuals carrying the same mutation. The majority of the laminopathies affect cardiac and/or skeletal muscles. The underlying molecular mechanisms contributing to such tissue-specific phenotypes caused by mutations in a ubiquitously expressed gene are not yet well elucidated. This review will explore the different phenotypes observed in established models of striated muscle laminopathies and their respective contributions to advancing our understanding of cardiac and skeletal muscle-related laminopathies. Potential future directions for developing effective treatments for patients with lamin A/C mutation-associated cardiac and/or skeletal muscle conditions will be discussed.

1.2 The Nuclear Lamina

The nuclear lamina is a mechanically responsive orthogonal network of proteins that underlie the inner nuclear membrane (Aebi et al., 1986). It is primarily composed of the nuclear intermediate filaments A and B-type lamins (Aebi et al., 1986; Gerace et al., 1978). Membrane associated proteins such as ones with the LEM domain also compose the nuclear lamina (Broers et al., 2006). The A-type lamins are coded by the lamin A/C gene (*LMNA*) while the B-type lamins - B1 and B2, are coded by the lamin B1 gene (*LMNB1*) and lamin B2 gene (*LMNB2*), respectively. At the end of mitosis, the B-type lamins are incorporated first into the nuclear lamina followed by lamin A and then lamin C after which the respective A and B-type lamins networks exist in a 1:1 ratio relative to each other (González-Cruz et al., 2018; Holt et al., 2003; McKeon et al., 1986; Moir et al., 2000; Raharjo et al., 2001; Vaughan et al., 2001). Though the nuclear lamins are predominantly found in the nuclear periphery and cover about half of the nuclear surface, they are also localized in the nucleoplasm (Goldman et al., 2002; Moir et al., 2000; Sylvius et al., 2008; Turgay et al., 2017). During *in vitro* assembly, lamins A and C form homodimers and even polymers depending on the concentration (Adam & Goldman, 2012; Aebi et al., 1986). Cryo-electron tomography shows that the lamin filaments are 3.5 nm thick in mammalian cells, and immunostainings of A and B-type lamins show distinct networks with regions of co-localization (Delbarre et al., 2006; Goldberg et al., 2008; Moir et al., 2000; Nmezi et al., 2019; Shimi et al., 2008, 2015; Turgay et al., 2017). Furthermore, high resolution imaging in mammalian cells shows that the lamin B1 meshwork is closer to the inner nuclear membrane while the A-type lamins face the nucleoplasm (Nmezi et al., 2019). A 15-20 nm gap separates the two networks (Nmezi et al., 2019). A-type lamin structures are also noted to be denser and contribute more to nuclear rigidity than the B-type lamin structures (Adam & Goldman, 2012; Goldberg et al., 2008; Nmezi et al.,

2019). Nevertheless, *LMNB1* knockdown in mammalian cells results in increased A-type lamin mobility and mesh size demonstrating that the rigid A-type meshwork is complemented and supported by the more flexible B-type meshwork (Shimi et al., 2008). In addition, loss of lamin B1 results in an increased number of nuclear blebs suggesting a role of lamin B1 in preventing the protrusion of the A-type lamins (Nmezi et al., 2019). The absence of either nuclear lamins or presence of mutations in *LMNA* also severely disrupts the shape and/or structural integrity of the nucleus (Lammerding et al., 2006; Muchir et al., 2003; Nicolas et al., 2019; Vergnes et al., 2004). Moreover, in contrast to lamin B1 deficient cells, cells lacking lamin A/C present with significantly impaired nuclear stiffness and deformability under strain suggesting that the A-type lamins are critical in maintaining the nuclear structure (Lammerding et al., 2006). An expanded overview of the role and importance of A-type lamins in supporting and maintaining the nuclear structure can be found in sections 2.1 and 2.3-2.4 of Cellular and Animal Models of Striated Muscle Laminopathies (pages 237-239, 240-244) (Nicolas et al., 2019).

1.3 Lamin A/C

1.3.a Gene and Protein Structure

Human *LMNA* encoding the A-type lamins encompasses 24kbp in chromosome 1q21.3 and has 11 introns and 12 translated exons (Figure 1.1) (Lin & Worman, 1993; Wydner et al., 1996). At its 5' promoter region, there are several GC-rich areas, a CCAAT box and a TATA box-like sequence – TATTA (Lin & Worman, 1993). A-type lamins are primarily expressed in differentiated cells but they have been detected at very low levels in mouse embryonic stem cells and in the inner cell mass of mouse blastocysts at E3.5 (Eckersley-Maslin et al., 2013; Lin & Worman, 1993; Röber et al., 1989; Stewart & Burke, 1987). Alternative splicing of *LMNA* mRNA results in the translation of four isoforms – A, C, AΔ10 and C2. Lamins A and C are the more

abundant isoforms. Prelamin A (immature lamin A) and lamin C are produced by alternative splicing in exon 10 (Lin & Worman, 1993). Lamins A and C mRNAs share exons 1 through 9 after which lamin A mRNA contains only the first 90 nucleotides of exon 10 followed by exons 11 and 12 (Machiels et al., 1996). In contrast, lamin C mRNA possesses the complete exon 10 but lacks exons 11 and 12 (Machiels et al., 1996). As such, the resulting lamin A and lamin C proteins are identical in the first 566 amino acids (a.a) after which prelamin A contains a unique 98 a.a sequence while lamin C has an extra six unique a.a in its carboxyl terminus (McKeon et al., 1986). To produce mature lamin A (646 a.a), immature lamin A undergoes post translational processing involving the farnesylation of its C*AAX* (cysteine-aliphatic-aliphatic-any amino acid) motif, removal of the *AAX* part of the motif, methylation of the farnesylated cysteine and cleavage of the last 15 a.a (including the farnesylated and methylated cysteine) in its carboxyl end (Agarwal et al., 2003). Lamins A and C generally have comparable spatial (cell/tissue), temporal and stoichiometric expression profiles (Lin & Worman, 1993). Another lamin A/C isoform - AΔ10, is produced by alternative splicing (Machiels et al., 1996). Lamin AΔ10 mRNA lacks 90 nucleotides in exon 10 resulting in the deletion of 30 amino acids in the protein (Machiels et al., 1996). Lamin AΔ10 is expressed in various cancer cell lines and cell types including leukocytes and colon cells (Machiels et al., 1996). It is unknown if this isoform is found in striated muscles. The fourth isoform - lamin C2, uses an alternative exon 1 and is identical to lamin C except that the N terminus of lamin C2 contains a shorter stretch of non-alpha helical amino acids instead of the full length head and alpha helical coil 1A domain (Furukawa et al., 1994). This isoform is specifically found in mammalian spermatocytes (Alsheimer & Benavente, 1996; Furukawa et al., 1994).

Structurally, the A-type lamins have three major domains – the amino (N) globular head, the carboxyl (C) globular tail, and the alpha helical rod domain located in between the N and C

termini (Figure 1.1). The central rod domain facilitates the interaction of two lamin polypeptides forming parallel coiled-coil homodimers while the amino and carboxyl ends are involved in the interaction of these homodimers to assemble anti-parallel protofilaments (Strelkov et al., 2004; Stuurman et al., 1998). The combination of three or four of these protofilaments forms an intermediate filament which polymerizes to make up the 10 nm meshwork of the nuclear lamina (Dittmer & Misteli, 2011; Heald & McKeon, 1990). While lamins A and C form their separate networks, regions of overlap occur where the two interact (Shimi et al., 2015). Figure 1.2 illustrates these structural orders from lamin A/C subunits to lamin A/C polymer networks.

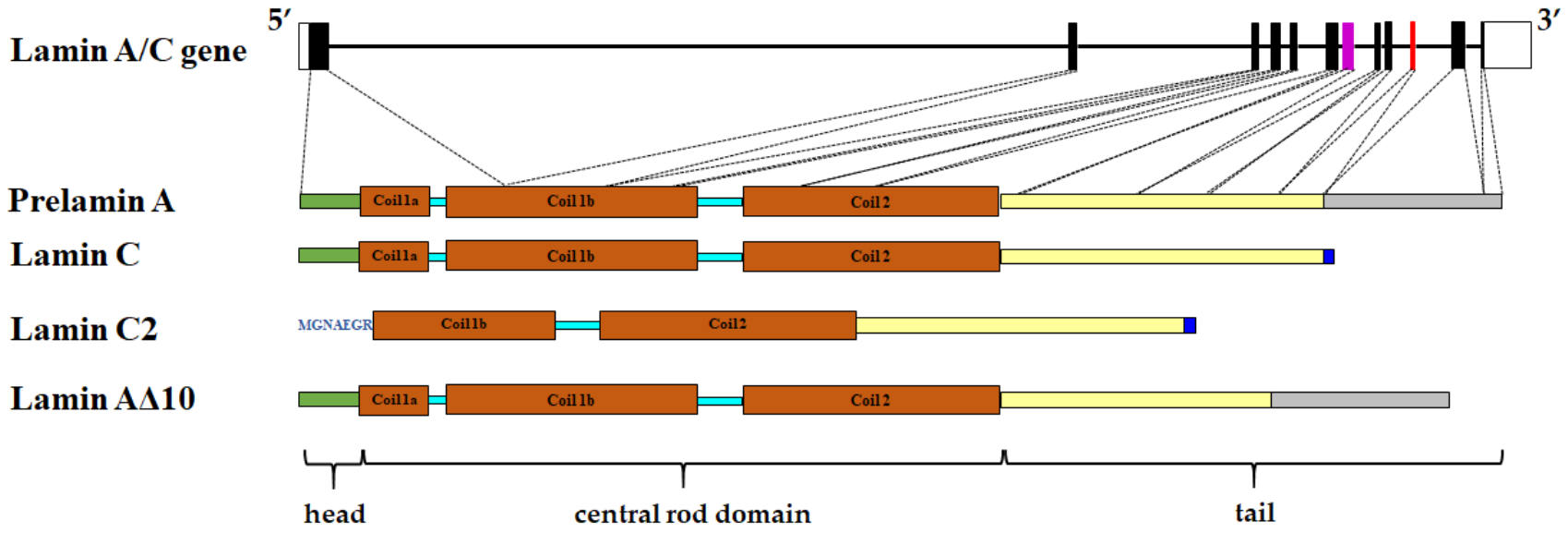

Figure 1.1: Schematic representation of the lamin A/C gene and the corresponding protein domains coded by each exon. Upper panel: The gene schematic illustrates the untranslated regions (white boxes), the introns (black solid lines), the exons (black, purple and red boxes), exon 7 where the nuclear localization signal is located (purple box), and exon 10 where the alternative splice site to produce lamins A and C is located (red box). Lower panel: The dash lines stemming from the exons indicate the corresponding coded protein domains in prelamin A, lamin C, and lamin AΔ10 except that lamin AΔ10 lacks exon 10. Lamin C2 uses an alternative exon 1 in intron 1 of lamin A/C. The amino head (green box), linkers 1 and 2 (cyan boxes), coils 1a, 1b and 2 (brown boxes) of the central rod domain, the carboxyl tail common to the A-type lamin isoforms (beige box), lamin A and AΔ10 specific C terminus (grey box), and lamin C and C2 specific C terminus (blue box) are shown. Lamin C2 specific amino acid sequence replacing the head and part of coil1b is also indicated.

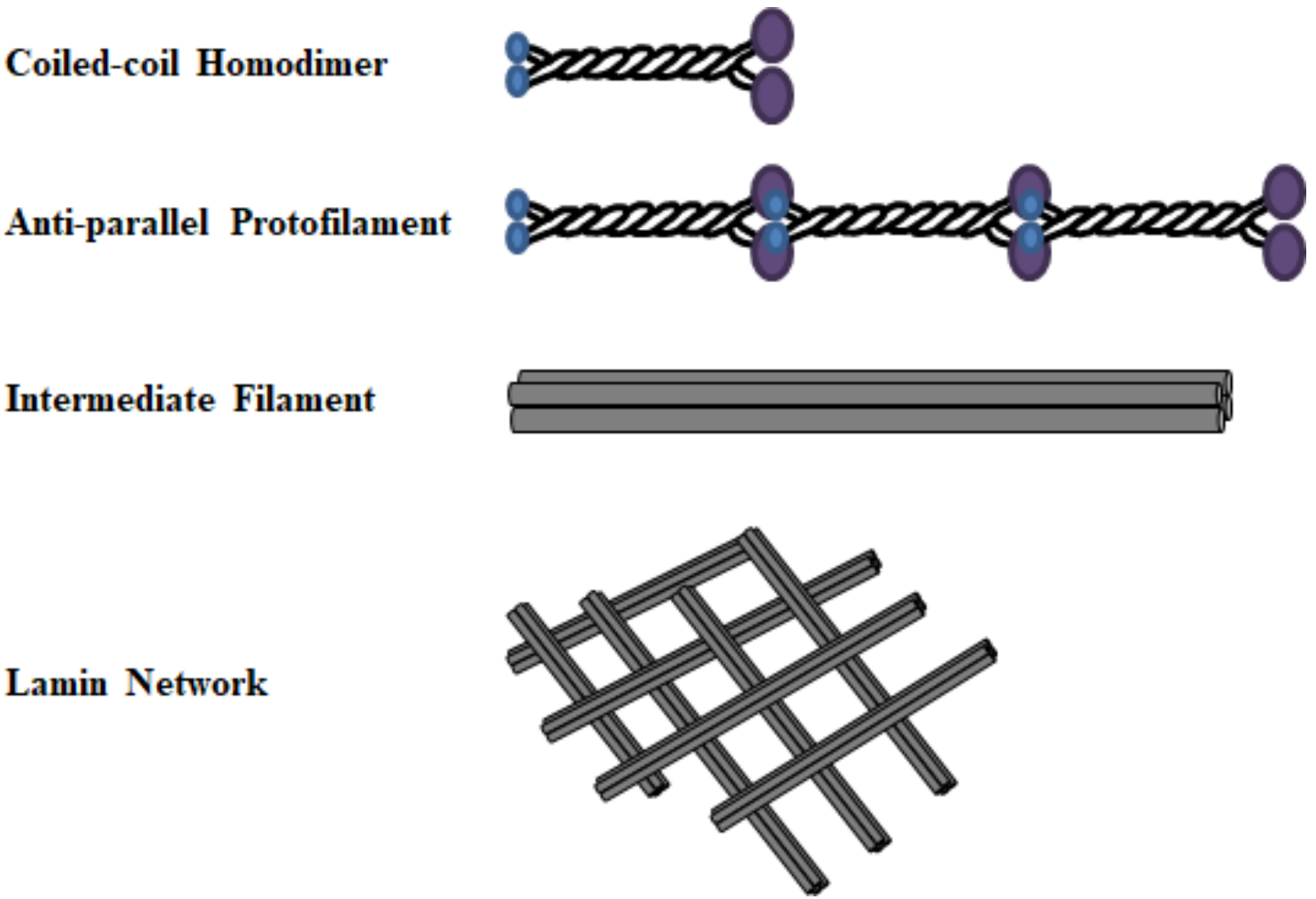

Figure 1.2: Schematic representations of the various structural orders of lamin A/C assembly to form the A-type lamins network in the nuclear lamina.

1.3.b Function and Regulation

In addition to nuclear structural support, the A-type lamins are also involved in connecting the nucleus to the rest of the cell. The SUN 1 and 2 proteins which span the inner nuclear membrane are binding partners of lamin A (Haque et al., 2006). In turn, SUN1/2 binds the transmembrane Klarsicht/ANC-1/Syne Homology (KASH) domains of Nesprins 1 and 2 which then interact with actin in the cytoskeleton (Haque et al., 2006). This chain of interactions physically connects the cytoskeleton and the nucleus via transmembrane proteins, and disruption of this link has been shown to contribute to laminopathies. For instance, patient myoblasts and neonatal rat ventricular myocytes (NRVMs) expressing striated muscle laminopathy mutations present with F actin disruption, and impaired focal adhesion and mechanosensing (Bertrand et al., 2014; Lanzicher et al., 2015; Laurini et al., 2018). Further discussion of the importance of A-type lamins in nuclear-cytoskeleton dynamics can be found in section 2.4 of Cellular and Animal Models of Striated Muscle Laminopathies (pages 241-244) (Nicolas et al., 2019).

Lamins A and C do not only affect the physical and mechanical attributes of the cell but also play a role in transducing cellular signals and regulating gene expression. Protein Kinase C alpha (PKC α) is a kinase binding partner of lamin A/C that is involved in multiple signaling pathways that transduce cellular stimulus into a cell response (Martelli et al., 2002; Nakashima, 2002). Further discussion about PKC α is found later in this chapter. Another protein involved in mediating cell response is the Activating Protein I (AP-1) transcription factor which functions in various cellular processes such as cell proliferation and apoptosis (Ivorra et al., 2006). One way to regulate AP-1 is by modifying the composition of its subunits (Ivorra et al., 2006). AP-1 composed of Fos and Jun preferably binds the 12-O-Tetradecanoylphorbol-13-acetate (TPA)-responsive element in the promoter of target genes (Ivorra et al., 2006). A study by Ivorra and colleagues

shows that the A-type lamins directly bind c-Fos via hydrophobic interaction and sequester it in the nuclear envelope (Ivorra et al., 2006). This prevents the formation of the Fos-Jun heterodimer resulting in the reduction of AP-1 transcription activity and an increase in cell cycle arrest (Ivorra et al., 2006). Similarly, the transcription factor MYC is sequestered by lamin A/C in the nuclear envelope thereby regulating its transcriptional activity (Myant et al., 2015). A-type lamins are also known to directly interact with chromosomes (Link et al., 2013). Lamin C2, which is found in spermatocytes, is discovered to be important in ensuring proper chromosomal positioning and synapsing during meiosis (Link et al., 2013). Male mice that lack this lamin isoform have profoundly defective meiosis which results in sterility (Link et al., 2013). Expression of a dominant negative truncated lamin A in either mammalian cells or frog interphase egg protein extracts is also detrimental, and results in the disruption of the nuclear lamina and formation of lamin nucleoplasmic aggregates (Spann et al., 1997). These nucleoplasmic aggregates trap the Replication factor C and PCNA required for elongation during DNA replication resulting in a significant decrease in DNA replication (Spann et al., 1997). Altogether, these results demonstrate how the A-type lamins affect cell response by regulating DNA replication and gene expression.

Aside from DNA transcription and replication regulation, the A-type lamins are involved in chromatin dynamics as well. Lamin A/C participates in chromatin regulation by anchoring chromatin in the nuclear lamina and by regulating histone modifiers (Mattioli et al., 2018; Mattout et al., 2007; Solovei et al., 2013; Taniura et al., 1995). Chromatin in the nuclear periphery is generally considered inactive while chromatin found in the nucleoplasm is active (Dietzel et al., 2004; Finlan et al., 2008; Meister et al., 2010). Consistent with this concept, deletion of lamin-1 (the functional equivalent of the nuclear lamins) in worms carrying fluorescently-tagged plasmids incorporated in the genome in tandem arrays shows relocalization of plasmid arrays to the nuclear

interior resulting in increased fluorescent marker expression signifying plasmid activation (Mattout et al., 2011). Previous work on mammals has also shown that lack of the A-type lamins and the lamin B receptor results in inversion of the chromatin architecture (i.e. heterochromatin shifts away from the nuclear periphery and towards the nuclear centre), and ectopic expression of lamin A in rods of mice retinas impedes chromatin inversion (Mattar et al., 2018; Solovei et al., 2013). Loss of the lamin A/C-mediated chromatin tether is also found to result in downregulation of muscle-related genes in myoblasts suggesting the importance of lamin A/C chromatin regulation in muscle differentiation (Solovei et al., 2013). However, in addition to chromatin tethering, the A-type lamins also regulate chromatin by interacting with histone modifiers such as the histone deacetylase 2 (HDAC2) (Mattioli et al., 2018). Histone deacetylases remove acetyl groups from histones allowing histones to wrap DNA more tightly promoting transcription repression. Mattioli et al discovered that lamin A/C interacts with HDAC2 at the promoter region of the *CDKN1A* gene where HDAC2 promotes deacetylation (Mattioli et al., 2018). The *CDKN1A* gene codes for the cyclin-dependent kinases 1 and 2 inhibitor - p21, which promotes cell cycle arrest. In skin fibroblasts of patients with premature aging laminopathy, HDAC2 and progerin (a truncated lamin A variant in premature aging laminopathy) interaction is reduced resulting in a decrease in HDAC2 activation, and an increase in p21 expression (Mattioli et al., 2018). Additionally, progerin is found to have impaired activation of HDAC2 resulting in increased acetylation of HDAC2 heterochromatin targets, and poorer response to and recovery from oxidative stress in progeric cells compared to control (Mattioli et al., 2018). Together, these results implicate lamin A/C dysregulation of HDAC2 in the impaired cell response and development of cellular senescence in progeroid cells.

Accordingly, due to the involvement of lamin A/C in diverse cellular processes, its regulation is evidently critical to avoid potentially adverse consequences. Micro-RNAs (miRNAs), sumoylation and phosphorylation are some of the known means to regulate lamin A/C (Boudreau et al., 2012; Jung et al., 2012; Kochin et al., 2014; Machowska et al., 2015; Zhang & Sarge, 2008). Micro-RNAs are short RNA sequences that regulate gene expression by promoting de-adenylation which hastens mRNA degradation, by blocking mRNA translation of the target gene and/or by cleaving the target gene's mRNA (Bartel, 2009; Fabian et al., 2010). In both mice and zebrafish brains, lamin C is noted to be much more highly expressed than lamin A (Jung et al., 2012; Koshimizu et al., 2011). The miRNA miR-9 is found to downregulate lamin A level, and mutation of its target site in prelamin A results in an increase in prelamin A amount (Jung et al., 2012). Sumoylation on the other hand is a post translational modification that adds small ubiquitin-like modifier (SUMO) to the lysine residues of target proteins (Yang et al., 2017). This process has many roles including regulation of protein subcellular localization and protein-protein interactions (Yang et al., 2017). Mammalian cells express SUMO 1, SUMO 2, SUMO 3, and 4 with SUMO 2 and 3 sharing 97% sequence identity, and SUMO 1 sharing about 50% sequence identity with SUMO 2/3 (Boudreau et al., 2012; Yang et al., 2017; Zhang & Sarge, 2008). SUMO 4 is not as well characterized as SUMO 1-3 (Yang et al., 2017). Previous work has shown that lamin A preferably binds SUMO 2 over SUMO 1 (Zhang & Sarge, 2008). Dilated cardiomyopathy (DCM) lamin A/C mutations that affect an amino acid position in the lamin A/C sumoylation consensus sequence present with decreased lamin A sumoylation (Zhang & Sarge, 2008). Furthermore, cells expressing the DCM lamin A/C variants have increased cell death compared to WT, and show abnormal lamin A/C aggregation in the nucleoplasm suggesting a role for lamin A/C sumoylation in cell viability and lamin A/C localization in the nuclear rim (Zhang & Sarge, 2008). In another

study, SUMO 1 is shown to be trapped in the DCM p.D192G lamin A/C variant aggregates (Sylvius et al., 2005). Expression of other DCM and muscular laminopathy-causing mutations in C2C12 and COS7 cells also result in SUMO 1 mislocalization and sequestration in the lamin A/C aggregates resulting in disturbance of cellular sumoylation level in mutant cells (Boudreau et al., 2012). Likewise, myoblasts and skeletal muscle tissue from the muscular laminopathy H222P mice model show similar results confirming cellular sumoylation defects in variant lamin A/C (Boudreau et al., 2012). Phosphorylation is another means to regulate lamin A/C at the protein level. The A-type lamins are phosphorylated primarily in three regions – the amino head, the proximal region of the carboxyl terminus, and the terminal region of the carboxyl tail specific to lamin A (Kochin et al., 2014). Ser22 and Ser392 in the N and C termini, respectively, are known as Cdk1 phosphorylation sites critical for lamin disassembly during cell division (Heald & McKeon, 1990; Kochin et al., 2014). Oocytes from older female mice have been shown to enter meiosis prematurely by having an increase in lamin A/C phosphorylation, and are observed to have accelerated lamin A/C structure disassembly in the region where the new spindle fibre is to be formed (Koncicka et al., 2018). Such quick progression through the cell cycle is thought to potentially contribute to the increase in chromosomal segregation errors found in oocytes of older females; thus illustrating the importance of lamin A/C phosphorylation status in maintaining cell cycle progression (Koncicka et al., 2018). In addition, loss of either or both Ser22 and Ser392 disturbs lamin A mobility and nucleoplasm distribution suggesting the importance of phosphorylation in lamin A dynamics (Kochin et al., 2014). Previous studies also found that phosphorylation of Ser403 and Ser404 located in the proximal region of the C terminus near the nuclear localization signal are important in lamin A nuclear import (Haas & Jost, 1993; Leukel & Jost, 1995). Similarly, amino acid substitution affecting Ser628 (lamin A specific) along with

substitutions affecting Ser22 and Ser392 result in considerable lamin A leakage in the cytoplasm (Kochin et al., 2014). Others also note hyper-phosphorylation of Ser458 or hypo-phosphorylation of Ser390 in the presence of pathogenic *LMNA* mutations further demonstrating the importance of lamin A/C phosphorylation in maintaining its normal functions (Mitsuhashi et al., 2010; Swift et al., 2013). Section 2.5 (pages 244-245) of Cellular and Animal Models of Striated Muscle Laminopathies gives a more detailed overview of the alteration in lamin A/C phosphorylation in cells and/or tissues of patients with myopathy caused by *LMNA* mutations (Nicolas et al., 2019). Overall, these studies highlight the importance of proper lamin A/C regulation and provide examples of the consequences if the cell fails to do so.

However, despite the multiple ways to regulate A-type lamins, lamin A/C dysfunction and/or dysregulation does occur and is unsurprisingly detrimental. Classical laminopathies are a group of diseases affecting various tissue types that are caused by mutations in *LMNA*. The succeeding section discusses laminopathies that affect the cardiac and skeletal muscles (striated muscle laminopathies).

1.4 Lamin A/C Mutations and Striated Muscle Laminopathies

Striated muscle laminopathies are presented by about 79% of individuals with pathogenic lamin A/C mutations (Tesson et al., 2014). Dilated cardiomyopathy is a cardiac disease that can be caused by *LMNA* mutations (Bonne & Quijano-Roy, 2013; Nicolas et al., 2019; Taylor et al., 2003; Tesson et al., 2014). About 6-8% of idiopathic DCM is caused by lamin A/C mutations and is predominantly transmitted in an autosomal dominant manner (Hasselberg et al., 2018; Hershberger & Morales, 1993; Taylor et al., 2003). DCM is characterized by dilation of the left ventricle or both ventricles and ventricular dysfunction (Pinto et al., 2016). Between 30% - 50% of *LMNA* mutation-caused DCM also present with conduction defects (CD) (Colombo et al.,

2008). Conduction defects are defined by the impairment of the electrical propagation in the heart which can result in various rhythm disturbances that can be fatal. In addition, DCM itself is a primary cause for heart transplant due to heart failure, and lamin A/C-associated DCM is more severe and results in poorer patient outcome compared to DCM caused by other genes (Hasselberg et al., 2018; Pasotti et al., 2008; Taylor et al., 2003; van Berlo et al., 2005). Thus, *LMNA* mutations causing DCM have been expressed (or generated) in various cell lines and animal models to elucidate the underlying mechanism for this phenotype. Sections 2.1, 2.3-2.6, 3.1-3.3, 3.4.3 (first paragraph), and 3.4.4 (pages 237-239, 240-247, 247-252, 255-256 and 257-263) of the Cellular and Animal Models of Striated Muscle Laminopathies report results from cellular and animal studies involving DCM mutations (Nicolas et al., 2019). Table 1 (pages 203-211) of the review titled Lamin A/C mutations in dilated cardiomyopathy also lists mutations in *LMNA* that cause DCM and the varied phenotypes that can co-present with it (Tesson et al., 2014). In addition to being severe, DCM caused by lamin A/C mutations is also worse and has an earlier onset in males than in females (Arimura et al., 2013; Ollila et al., 2017; van Rijsingen et al., 2013). This is mirrored in mice models of striated muscle laminopathies as discussed in sections 3.4.3-3.4.4 (pages 255-263) of the Cellular and Animal Models of Striated Muscle Laminopathies (Nicolas et al., 2019). The disparity in the severity and onset of DCM between sexes can be attributed to difference in sex hormones linked to a notable increase in the nuclear localization of androgen receptor and its co-factors in male mutant *LMNA* carriers than in females (Arimura et al., 2013). Castration or androgen receptor antagonist treatment of the male H222P muscular dystrophy mice model improves their symptoms while administration of testosterone in the H222P female mice aggravates their phenotype; thus implicating sex hormones in mediating the severity of the cardiac

laminopathy phenotype (Arimura et al., 2013). However, lamin A/C mutations do not only result in cardiac conditions, but they can also cause skeletal muscle diseases.

Emery-Dreifuss muscular dystrophy (EDMD) caused by *LMNA* mutations is predominantly an autosomal dominant muscular disorder that manifests in childhood (Bonne et al., 1999). An autosomal recessive form of EDMD is rare but is known to exist (Di Barletta et al., 2000). EDMD is hallmarked by joint contractures in the elbows and Achilles tendon, wasting of the muscles particularly of the forearm and lower front leg, and eventual development of cardiomyopathy with conduction defects (Bonne et al., 1999, 2000; Di Barletta et al., 2000). Muscle biopsies from individuals with muscular weakness exhibit classic muscle pathology which includes variation in fibre size, a notable increase in internal nuclei (nuclei are normally located in the periphery of muscle fibres), and in a few cases, a mild increase in necrotic fibres and endomysial connective tissue (Bonne et al., 2000). Slow-twitch muscle fibres (type I) are also predominant and are relatively atrophic (Bonne et al., 2000). However, creatinine kinase level, a marker of tissue damage, is variable in patients (Bonne et al., 2000). Several models of EDMD including the extensively studied H222P mice are discussed throughout the Cellular and Animal Models of Striated Muscle Laminopathies review (pages 233-282) (Nicolas et al., 2019). Of the pathways found to be associated with striated muscle laminopathies, the extracellular signal-regulated kinases 1 and 2 (ERK 1/2) has been comprehensively studied (Nicolas et al., 2019). ERKs 1 and 2 are members of the classical MAPK signaling cascade involved in a plethora of cellular activities from cell cycle progression, cell metabolism to cell migration (Jr, 2012). ERKs 1 and 2 are functionally very similar and are found in all tissue types including skeletal and cardiac tissues (Cargnello & Roux, 2011; Gonzalez et al., 1992; Uhlén et al., 2015). Upon activation, ERK 1/2 translocate from the cytoplasm to various cellular locations including the nucleus where they

activate targets such as the transcription factors c-Jun and Elk1 (Muchir et al., 2007; Wortzel & Seger, 2011). Both c-Jun and Elk1 are upregulated in the skeletal and/or cardiac tissues of the H222P mice (Muchir et al., 2007). Inhibition of ERK 1/2 and other MAPK members (p38, JNK) improves the cardiac and/or skeletal muscle phenotype of the H222P mice (Muchir, Shan, et al., 2009; Muchir, Reilly, et al., 2012; Muchir, Wu, et al., 2012; Muchir et al., 2013; Wu et al., 2010). Section 3.4.4 paragraph 4 (pages 260-261) and Table 2 (under Animal Models) (pages 270-271) of Cellular and Animal Models of Striated Muscle Laminopathies summarize the signaling pathways implicated in cardiac and skeletal laminopathies in the H222P EDMD mice model (Nicolas et al., 2019). The results from the work on the H222P mice has so far yielded a clinical trial (Clinical Trials ID: NCT03439514) testing the efficacy of p38 inhibitor treatment of patients with lamin A/C-associated DCM (MacRae, 2016). Phase 2 of the clinical trial has so far yielded promising results such as improved patient quality of life and physical activity capacity (MacRae, 2016).

Another laminopathy affecting the skeletal muscles is *LMNA*-related congenital muscular dystrophy (L-CMD). Similar to EDMD, L-CMD is an autosomal dominant disorder, and is the most severe form of striated muscle laminopathy (Quijano-Roy et al., 2008). Patients with L-CMD present with some clinical features that overlap with EDMD; however, L-CMD has an earlier onset (before the age of two), is progressive, and is very severe with some patients lacking muscular head control ("Dropped head syndrome") or trunk control (Bonne & Quijano-Roy, 2013; D'Amico et al., 2005; Quijano-Roy et al., 2008). Moreover, the cardiac phenotype (e.g. impairment of cardiac function, rhythm disturbance) of L-CMD patients has an earlier onset and is more progressive than in EDMD patients (Bonne & Quijano-Roy, 2013; Heller et al., 2017). A mouse model expressing p.K32del lamin A/C which causes L-CMD in humans was created to understand

the molecular mechanisms underlying this phenotype (Bertrand et al., 2012; Cattin et al., 2013; D'Amico et al., 2005). Briefly, the homozygous p.K32del mice died three weeks after birth and suffered severe metabolic deficiencies due to the depression of the sterol regulatory element binding transcription factor 1 (SREBF-1) important for adipogenesis and expression of various metabolism-related genes (Bertrand et al., 2012). On the other hand, the heterozygous mice eventually developed DCM because of the defective ubiquitin-proteasome system which failed to degrade the toxic p.K32del lamin A/C variant (Cattin et al., 2013). The fifth paragraph of section 3.4.4 of Cellular and Animal Models of Striated Muscle Laminopathies (pages 261-262) further describes these p.K32del mice (Nicolas et al., 2019).

Because of the severity of cardiac and skeletal muscle conditions caused by lamin A/C mutations, understanding the underlying mechanisms involved in the disease development and progression is important. Furthermore, identification of proteins involved in these pathogenic mechanisms is critical to develop effective therapeutic treatments. The kinase lamin A/C binding partner - PKC α, is potentially an interesting candidate for such purpose (Martelli et al., 2002).

1.5 Protein Kinase C alpha (PKC α)

PKC α is a serine/threonine kinase coded by the *PRKCA* gene. It is a ubiquitously expressed classical member of the PKC family that is involved in a plethora of cellular pathways (Igumenova, 2015; Nishizuka, 1988; Wetsel et al., 1992). PKC α is activated by calcium and lipids such as diacylglycerol and phosphatidylserine (Igumenova, 2015). Phorbol esters which mimic diacylglycerol can also bind PKC α (Goodnight et al., 1995). PKC α activation involves phosphorylation of three sites – Thr497, Thr638, and Ser657 (Bornancin & Parker, 1997; Cazaubon et al., 1994; Parekh et al., 2000). Phosphorylation of Ser657 is the benchmark for PKC α activation (Bornancin & Parker, 1997; Cazaubon et al., 1994; Parekh et al., 2000). PKC α

primarily resides in the cytoplasm but can move to various cellular locations including the cell periphery, mitochondria, and nucleus (Disatnik et al., 1994; Neri et al., 1998; Ruvolo et al., 1998; Schmalz et al., 1996; Singh et al., 2017; Wetsel et al., 1992). Mobile PKC α is thought to be in its active form as it is in these other subcellular localizations where PKC α phosphorylates its targets (Disatnik et al., 1994; Goodnight et al., 1995; Igumenova, 2015; Singh et al., 2017).

1.6 PKC alpha and Cardiac Diseases

As discussed in the preceding sections, cardiac laminopathies pose a serious risk because they tend to be severe and result in adverse outcomes. Up to 64% of patients with DCM caused by *LMNA* mutations develop heart failure (HF) with age-related penetrance (Charron et al., 2012; Taylor et al., 2003). Heart failure is defined by structural and functional cardiac defects resulting in impaired ventricle blood filling or ejection, and has various aetiologies (Inamdar & Inamdar, 2016). It is a major cause of mortality in both the developed and developing nations (Singh et al., 2017). PKC α is a critical regulator of cardiac function, and is the predominant classical PKC isoform in the rabbit and adult human hearts, and in mouse cardiac and skeletal muscles (Hambleton et al., 2006; Jensen et al., 2009; Pass et al., 2001; Ping et al., 1997). Changes in PKC α protein level and activity have been observed in hearts of patients with HF, and in various HF animal models (Bowling et al., 1999; Braz et al., 2004; Jalili et al., 1999; Rouet-Benzineb et al., 1996). For example, decrease in PKC α protein level is observed in a rabbit model of HF caused by double hemodynamic overload (Rouet-Benzineb et al., 1996). Reduction of left ventricular PKC α expression has also been associated with adverse cardiac remodelling (higher mass and enlarged diastolic dimension) and DCM risk in humans (Hu et al., 2018). However, in a zebrafish animal model, transient *prkca* knockdown did not result in any discernible cardiac phenotype at 3 days post fertilization (dpf) (Hu et al., 2018). Furthermore, in other studies, an increase instead of

a decrease in PKC α expression and/or activity is observed in cardiac disease. Upregulated PKC α level and/or activity is noted in failing human and rat hearts, and in the heart and skeletal muscles of hamsters with HF (Bowling et al., 1999; Braz et al., 2004; Wang et al., 1999; Wang et al., 2003). Moreover, over-expression of PKC α in rat cardiac myocytes results in hypocontractility while reduction of PKC α results in hypercontractility (Braz et al., 2004). Similarly, inhibition of PKC α in WT mice leads to increased contraction and restores cardiac function in rat and mice models of HF (Hambleton et al., 2006). Abolition of PKC α expression also rescues the DCM phenotype in the DCM *Csrp3* null mice model, and in the DCM mice model over-expressing protein phosphatase-I (PP-I) (Braz et al., 2004). Likewise, *Prkca* deletion (*Prkca* $^{-/-}$) protected the *Prkca* $^{-/-}$ mice from developing pressure overload-induced HF compared to WT mice (Braz et al., 2004). Altogether, these studies associate altered PKC α expression to cardiac disease, and PKC α's importance in cardiac function regulation.

1.7 Protein Kinase C alpha and Laminopathies

PKC α is a lamin A/C binding kinase involved in a variety of signaling pathways such as the MAPK cascade (Braz et al., 2002; Kim et al., 2014; Leitges et al., 2002; Martelli et al., 2002; Mauro et al., 2002; Nakashima, 2002; Naskar et al., 2014; Schönwasser et al., 1998). For instance, the MAPKs ERK 1/2 have been shown to be downstream targets of PKC α (Leitges et al., 2002; Naskar et al., 2014; Schönwasser et al., 1998). Previous work shows enhanced insulin-induced ERK activation in skeletal muscles of *Prkca* null mice (Leitges et al., 2002). In contrast, another study shows inhibition of TPA-induced ERK activation upon dominant negative PKC α expression, and decreased ERK 1/2 activation upon *Prkca* knockdown in mice (Naskar et al., 2014; Schönwasser et al., 1998). PKC α has also been shown to mediate cardiomyocyte hypertrophic growth by activating ERK 1/2, and dominant negative PKC α expression blocks PMA-induced

ERK 1/2 activation in neonatal rat cardiomyocyte (Braz et al., 2002). Collectively, these results illustrate the upstream role of PKC α in affecting ERK 1/2 activation in various cellular contexts and responses. Similarly, other members of the MAPK pathway – JNK and p38, are regulated by PKC α (Mauro et al., 2002). Protein Kinase B (also known as Akt), another protein associated with muscular laminopathies, is activated by PKC α as well (Li et al., 1999; Mitsuhashi et al., 2010). C-Fos, a lamin A/C binding partner that dimerizes with the MAPK downstream target c-Jun, is also regulated by PKC α (Ivorra et al., 2006; Soh et al., 1999; Soh & Weinstein, 2003). Overall, these studies demonstrate the involvement of PKC α in regulating many of the proteins that are already implicated in striated muscle laminopathies. A fact that then makes PKC α an interesting candidate for investigation of its potential involvement in cardiac and muscular laminopathies.

To facilitate the understanding of underlying mechanisms in striated muscle laminopathies, and to determine PKC α involvement in its pathogenesis, cellular and animal models were used in this thesis. Specifically, the tropical fish – zebrafish, served as the animal model to study cardiac and skeletal myopathies caused by lamin A/C mutations.

1.8 Zebrafish as a model of cardiac and skeletal muscle diseases

Zebrafish belongs to the Cyprinidae family. It is an established model organism for a wide variety of studies ranging from basic science to medical research. With its high fecundity, external fertilization, and optical transparency during the early stages of development, zebrafish can facilitate real-time phenotypic observation. Many of the available tools and techniques such as the CRISPR/Cas9 genome-editing technology can be used on zebrafish as well, making zebrafish accessible for various types of experiments, studies and manipulations. Importantly, the zebrafish orthologues of numerous human genes have been identified enabling translatable modelling of different human diseases such as cardiac and skeletal muscle conditions in zebrafish (Barbazuk et

al., 2000; Koshimizu et al., 2011; Mione & Trede, 2010; Poon & Brand, 2013; Shih et al., 2015; Steffen et al., 2007; Woods et al., 2000).

1.8.a Zebrafish as a cardiac disease model

Various cardiac diseases have been modelled in zebrafish (Bakkers, 2011; Poon & Brand, 2013; Shi et al., 2018; Verkerk & Remme, 2012). Though human and zebrafish hearts are anatomically different, many of the mechanisms underlying cardiac development and function in humans are conserved in zebrafish (Sarmah & Marrs, 2016). Similar to mammals but occurring at a different timescale, zebrafish cardiac development includes cardiac progenitor formation, differentiation, and migration to the embryonic midline, heart tube formation, cardiac looping (right-ward bending of the heart tube), and valve formation (Sarmah & Marrs, 2016). In zebrafish, cardiac progenitors can be identified at the blastula stage (2.25 – 5.25 hours post fertilization (hpf)) (Kimmel et al., 1995; Staudt & Stainier, 2012). By 16 and 17.5 hpf, these cardiac precursors begin to differentiate and migrate towards the embryonic midline (Glickman & Yelon, 2002). At 19.5 hpf, the cardiac cells merge into a cone, and by 24 hpf, the cone has stretched to form the zebrafish heart tube which contracts peristaltically (Bakkers, 2011; Glickman & Yelon, 2002). By 48 hpf, cardiac looping has occurred with the ventricle positioned to the right of the atrium, and the S-shaped heart is observed (Glickman & Yelon, 2002). By this point, sequential contraction of the atrium and ventricle has also replaced the initial peristaltic contraction of the heart (Glickman & Yelon, 2002; Shi et al., 2018). At 72 hpf, the ventricle and atrium have become distinct cardiac chambers separated by the atrioventricular canal (AVC) which has narrowed to efficiently prevent blood from regurgitating back into the atrium from the ventricle (Staudt & Stainier, 2012). By 96 hpf, the two valve leaflets of the atrioventricular valve have formed in the AVC completing the separation of the atrium and ventricle (Staudt & Stainier, 2012). Additionally, like in humans,

cardiac conduction in the zebrafish heart also propagates from the apex (bottom of the heart) to the base (top), and the generation and duration of cardiac action potential in the two species are comparable (Milan et al., 2006; Nemtsas et al., 2010; Sedmera et al., 2003). Nevertheless, despite these similarities between human and zebrafish heart development and physiology, differences do exist. For example, the basic zebrafish and human cardiac anatomies are different. While zebrafish have a two-chambered heart, humans have a four-chambered heart. Functionally, zebrafish also have a much lower E/A ratio (a measure of ventricle function relating to ventricular filling in between contractions), and blood pressure compared to humans (Genge et al., 2016; Ho et al., 2002; Hu et al., 2001). However, in spite of such discrepancies in cardiac structure and physiology between the two species, many groups have successfully modeled human cardiac diseases in zebrafish. These studies were primarily conducted on embryos and larvae though adult work also exist (Brown et al., 2016). The transparency of zebrafish during the early stages of development facilitates cardiac observation. In addition, since zebrafish is not reliant on the heart for oxygen delivery for up to 5 dpf, cardiac diseases that are embryonically lethal in mammals can be studied in this organism (Pelster & Burggren, 1996). This capacity is conducive for studying heart failure of which DCM is a primary cause. About 96% of human DCM-causing genes have an orthologue in zebrafish, and one of these genes is the titin gene (Shih et al., 2015). *TTN* codes for the titin protein, an essential part of the sarcomere. Mutations in *TTN* cause a group of sarcomeric diseases termed titinopathies which include both cardiomyopathy and skeletal muscle conditions (Gerull et al., 2002; Seeley et al., 2007). In zebrafish, the *TTN* gene has two orthologues – *ttna* and *ttnb* (Seeley et al., 2007). However, it is *ttna* that is expressed early on (at five somite stage) and at higher levels in the embryo heart compared to *ttnb* (Seeley et al., 2007). Morpholino knockdown or mutation of the N2A or N2B zebrafish cardiac titin isoforms encoded by *ttna* results in

pericardial edema, poor cardiac function, and disruption of the Z and A discs of the sarcomere (Seeley et al., 2007; Xu et al., 2002). The *ttna* morphants and mutants' phenotype of poorly contracting and dilated heart resemble DCM in humans therefore showing that these zebrafish *ttna* cardiomyopathy models can mimic the human disease presentation. Another zebrafish cardiac disease model is lazy susan (*laz*). This mutant possesses a nonsense mutation in the zebrafish cardiac myosin light chain-1 gene (*cmlc-1*) (Meder et al., 2009). *Cmlc-1* is the zebrafish orthologue of the essential light chain of myosin gene *(ECL)*. Mutations in *ECL* are known to cause cardiomyopathies in humans (Chen et al., 2008; Hernandez et al., 2007). Both *cmlc-1* morphants and mutant embryos/larvae (i.e. *laz* embryos/larvae) present with impaired or non-contractile myocytes (Chen et al., 2008; Meder et al., 2009). Furthermore, *cmlc-1* morphants are found to have larger ventricles and cardiomyocytes (Chen et al., 2008). Thus, like the *ttna* morphants and mutants, the *cmlc-1* morphants and *laz* zebrafish can phenocopy DCM in humans providing further evidence for relevant zebrafish cardiac disease modelling at the embryo/larval stages.

Aside from cardiac disease modelling at the embryo and larval stages, zebrafish adults have also been used to study cardiac conditions. This is the case for the *pitx2c* zebrafish knock-outs (Collins et al., 2018). PITX2C is the major cardiac isoform of the PITX2 transcription factor involved in cardiac morphogenesis and atrial fibrillation (AF), a cardiac rhythm disturbance condition (Collins et al., 2019). Abolition of *pitx2c* expression in zebrafish results in cardiac myocyte defects, cardiac dysfunction, atrial fibrosis and AF at the embryo, larval and adult stages with the adult mutants showing a more pronounced and penetrant phenotype than the mutant embryos and larvae (Collins et al., 2019). Evaluation of cardiac metabolism which is frequently impaired in AF also shows disturbance in expression of metabolic and oxidative stress genes in the homozygous *pitx2c* mutant embryos and adults (Collins et al., 2019). N-acetyl cysteine (a

reactive oxygen species scavenger) treatment of the *pitx2c* embryos/larvae lowered the number of *pitx2c* nulls with arrythmia further implicating metabolic dysfunction in this zebrafish AF model, and demonstrating how zebrafish can be used for drug testing as well (Collins et al., 2019).

1.8.b Zebrafish as a skeletal muscle disease model

Aside from modeling human cardiac diseases, zebrafish is also an established model of various skeletal muscle conditions as many of the genes and molecular mechanisms underlying mammalian skeletal muscle development and function are conserved in zebrafish (Bassett & Currie, 2003; Li et al., 2017; Steffen et al., 2007). The skeletal muscle makes up about 80% of a fish' body mass (Jackson & Ingham, 2013). In zebrafish, somite formation commences at 10 hpf, and by 17 hpf, muscle contraction begins (Jackson & Ingham, 2013; Kimmel et al., 1995). By 24 hpf, somitogenesis is completed, and is followed by the onset of swimming at 26 hpf (Jackson & Ingham, 2013; Kimmel et al., 1995). The slow and fast twitch muscle fibres are the two major types of skeletal muscle fibres. Similar to mammals, the slow-twitch muscle fibres have slower contraction and do not fatigue as quickly as the fast-twitch fibres which are for short bursts of activity (Guyon et al., 2007; Jackson & Ingham, 2013). Though the fast-twitch fibres make up most of the somites, the slow-twitch fibres enveloping the fast-twitch fibres are the first to develop, and are responsible for the first movements of zebrafish embryos at 24 hpf (Jackson & Ingham, 2013). Upon hatching at 3 dpf, zebrafish embryos primarily exhibit cyclic swim behaviour (i.e. consistent average swim speed between tail beats) (Müller et al., 2008; Müller & van Leeuwen, 2004). By 5 dpf, zebrafish larvae transition into intermittent swimming dominated by burst and coast swimming (Müller et al., 2009; Müller & van Leeuwen, 2004).

Duchenne Muscular Dystrophy (DMD) is an X-linked, rare and fatal muscular condition caused by mutations in the dystrophin gene (Aartsma-Rus et al., 2006; O'Brien & Kunkel, 2001).

Dystrophin is a cytoskeletal protein that is a component of the complex linking the cell membrane, cytoskeleton, and extracellular matrix (Li et al., 2014). The knockout DMD model *sapje* (*sap*) zebrafish carries a nonsense mutation in the dystrophin gene that results in a premature stop (Bassett et al., 2003). The *sap* mutation is recessive and lethal (Bassett et al., 2003). The embryonic and larval/juvenile (7-28 dpf) *sap* mutants resemble the patient DMD phenotype which includes progressive muscle degeneration, detachment of the embryonic muscle from the vertical myosepta, and muscular lesions (Bassett et al., 2003; Berger et al., 2010). Morpholino knockdown of dystrophin also mirrors these results (Bassett et al., 2003). In addition, consistent with results from previous studies, treatment of 3-5 dpf homozygous *sap* mutants with Ataluren, a drug that promotes read through a premature stop codon, increases dystrophin expression and improves the mutants' mechanical response to force and tension (Li et al., 2014). These results show that while the *sap* mutants are non-mammalian and nonX-linked DMD models, these zebrafish dystrophin null mutants recapitulate the disease presentation and provide results that are comparable to other mammalian models.

Another zebrafish muscular dystrophy model is the zebrafish *candyfloss* (*caf*) mutants (Hall et al., 2007). These are null mutants for the zebrafish laminin α2 (*lama2*) gene (Hall et al., 2007). Laminins are major structural components of the basal laminae (Hall et al., 2007). Homozygous null mutations in laminin α2 are known to cause congenital muscular dystrophy hallmarked by contractures, prominent loss of muscle tone, and muscle weakness (Helbling-Leclerc et al., 1995). The homozygous *caf* embryos exhibit dystrophic and detached muscles, and are incapable of hatching by themselves (Hall et al., 2007). Likewise, *caf* morphants present with muscular phenotype comparable to *caf* mutants (Hall et al., 2007). Consistent with *LAMA2* null patients, the homozygous *caf* mutants can also survive to adulthood despite the initially severe

phenotype allowing for phenotype characterization of this model at a later time point (Hall et al., 2007).

Altogether, the *sap* and *caf* zebrafish mutants present examples of successful and relevant human muscular dystrophy modeling in zebrafish. Furthermore, the *sap* mutants show how zebrafish models can facilitate high throughput drug tests and produce results that are comparable to the results from other mammalian models of the disease.

As such, with the demonstrated capacity of zebrafish to model human cardiac and skeletal muscle conditions, it is therefore a reasonable plausibility that zebrafish can adequately model striated muscle laminopathies.

1.9 Zebrafish and striated muscle laminopathies

Human lamin A/C has one orthologue in zebrafish. Both human and zebrafish lamin A/C have 12 exons. Zebrafish lamins A and C transcripts share *lmna* exons 1- 8 (Koshimizu et al., 2011). Lamin C retains the first six nucleotides of intron 9 which translates to two lamin C-specific a.a before the stop codon (Koshimizu et al., 2011). Lamin A does not retain any introns. In terms of the protein, zebrafish prelamin A shares 67% amino acid identity with human prelamin A. Zebrafish lamin A has 659 a.a while zebrafish lamin C has 554 a.a. (Koshimizu et al., 2011). Moreover, like the mammalian lamin A/C protein, zebrafish lamin A/C consist of an amino head, a rod domain, and a carboxyl globular tail (Koshimizu et al., 2011). Zebrafish *lmna* is expressed early on in development with lamin A being detected by 0.75 hpf and lamin C being detected starting at 9 hpf (Koshimizu et al., 2011). Lamin A is found to be consistently more highly expressed than lamin C throughout the early stages of embryo development, and during the first week of life (Koshimizu et al., 2011). It is unknown if the same trend persists in adulthood. Like mammalian lamin A/C, zebrafish lamin A/C is also localized in the nucleus and is expressed in

various tissue types including the heart and skeletal muscles (Koshimizu et al., 2011; Vogel et al., 2009).

Transient knockdown of *lmna* using morpholinos or transgenic expression of mutant *lmna* result in conditions mirroring the phenotypes of patients and other animal models of striated muscle laminopathies (Koshimizu et al., 2011; Vogel et al., 2009). Zebrafish *lmna* morphants present with disrupted nuclear membrane, and cardiac and skeletal muscle phenotypes such as cardiac edema, cardiac dysfunction, bradycardia, and damage to slow skeletal muscle fibres (Koshimizu et al., 2011; Vogel et al., 2009). Cardiac rhythm disturbances such as AF are occasionally noted in the *lmna* morphants as well (Vogel et al., 2009). Similarly, *lmna* transgenics with cardiac-specific expression of EDMD lamin A/C variants exhibit increased heart rate, lamin A aggregates, and misshapen nucleus (Verma & Parnaik, 2017).

Altogether, the data shows high conservation of lamin A/C structure and function between humans and zebrafish as evidenced by the phenotype observed in the *lmna* morphants and transgenics which recapitulates what has been observed in patients and other animal models of striated muscle laminopathies. Such genetic, functional, and phenotypic lamin A/C conservation between humans and zebrafish therefore provide support for zebrafish's capacity to model cardiac and skeletal muscle laminopathies.

1.10 Research Objectives

Due to PKC α's direct interaction with the A-type lamins, its regulation of other A-type lamin binding partners including the ones implicated in striated muscle laminopathies, and its importance in cardiac function, we hypothesize that PKC α is involved in the pathogenesis of striated muscle laminopathies. To provide evidence that will implicate PKC α in cardiac and muscular laminopathies, chapter 2 examined PKC α cellular localization, activation, and

interaction with the A-type lamins using various cellular models expressing different striated muscle laminopathy mutations. Furthermore, we also evaluated the activation level of one of PKC α's downstream targets, ERK 1/2, which have been previously implicated in striated muscle laminopathies.

In addition to the cellular models, we also created and evaluated a potential zebrafish model of muscular laminopathies described in chapter 3 of this thesis. We used the CRISPR/Cas9 technology to induce a mutation in *lmna* and disrupt *lmna* expression. Then, to determine if the zebrafish *lmna* mutants can mimic the phenotype of patients and other animal models of striated muscle laminopathies, we evaluated the cardiac and skeletal muscle structure and function of the *lmna* mutants. Moreover, we assessed the expression level of genes and activation level of proteins known to be involved in striated muscle laminopathies. PKC α expression and activation level were also examined to determine if PKC α is affected in the zebrafish *lmna* mutants.

Chapter 2

Protein Kinase C alpha cellular distribution, activity, and proximity with lamin A/C in striated muscle laminopathies

2.1 Notes on Chapter 2

2.1.a Study Introduction and Objectives

Dysregulated signaling pathways and compromised nuclear structure are attributed as major underlying mechanisms for the pathogenesis of striated muscle laminopathies. The kinase lamin A/C-binding partner PKC α is upstream of many signaling cascades including the ones implicated in striated muscle laminopathies. Furthermore, PKC α is important in cardiac function, which is frequently impaired and poses considerable mortality risk in patients with striated muscle laminopathies. Thus, to determine PKC α involvement in striated muscle laminopathies, we assessed PKC α subcellular localization, lamin A/C proximity, and activation in various cellular models expressing mutant lamin A/C. Furthermore, we evaluated the activation level of ERK 1/2, downstream PKC α targets to determine its activation status in relation to PKC α activation. The results from this study constitute a manuscript in preparation for submission to Cells.

2.1.b Author Contributions:

H.A. Nicolas – conceptualized and performed most of the experiments and data analyses, drafted the manuscript

A. Bertrand – collected and maintained patient and mouse cells, fixed patient and mouse cells for immunostaining and PLA experiments, edited the manuscript

S. Labib – performed initial experiments for the study and edited the manuscript

M Mohammed-Uvaize – performed initial experiments for the study and edited the manuscript

P. Bolongo – performed/assisted with plasmid cloning and C2C12/H9C2 transfection and immunostaining, edited the manuscript

W. Wu – performed some sets of the H9C2 transfection and immunostaining experiments, edited the manuscript

G. Bonne – funded experiments, edited the manuscript

MA. Akimenko – conceptualized and funded experiments, edited the manuscript

F. Tesson – conceptualized and funded experiments, edited the manuscript

2.2 Abstract

Striated muscle laminopathies are cardiac and skeletal muscle conditions caused by mutations in the lamin A/C gene (*LMNA*). *LMNA* codes for the A-type lamins, which are nuclear intermediate filaments that maintain the nuclear structure and nuclear processes such as gene expression. Protein Kinase C alpha (PKC α) interacts with lamin A/C as well as with several lamin A/C partners involved in striated muscle laminopathies. To determine PKC α involvement in muscular laminopathies, PKC α localization, activation, and interaction with the A-type lamins were examined in various cell types expressing pathogenic lamin A/C mutations. The results showed aberrant nuclear PKC α cellular distribution in mutant cells compared to WT. PKC α activation (phos-PKC α) was decreased or unchanged in the studied cells expressing *LMNA* mutations, and the activation of its downstream targets, ERK 1/2, paralleled PKC α activation alteration. Furthermore, the phos-PKC α - lamin A/C

proximity was altered. Overall, the data showed that PKC α localization, activation, and proximity with lamin A/C were affected by certain pathogenic *LMNA* mutations thus suggesting PKC α involvement in striated muscle laminopathies.

2.3 Introduction

Lamins A and C are A-type lamins coded by the lamin A/C (*LMNA*) gene. They are nuclear intermediate filaments important for structural support and maintenance of various nuclear processes such as gene expression (Broers et al., 2006). Mutations in *LMNA* cause a group of diseases called laminopathies with 79% affecting the heart and/or skeletal muscles (Tesson et al., 2014). One of the cardiac diseases that can be caused by lamin A/C mutations is dilated cardiomyopathy (DCM) with or without conduction defects (CD). DCM is defined by the enlargement of left or both ventricles and systolic dysfunction not caused by coronary artery disease or abnormal loading conditions (Pinto et al., 2016). Patients with DCM caused by lamin A/C mutations are afflicted with more severe phenotype and have poorer prognosis compared to patients with DCM caused by mutations in other genes (Hasselberg et al., 2018; Pasotti et al., 2008; Taylor et al., 2003; van Berlo et al., 2005). Moreover, individuals with DCM caused by *LMNA* mutations frequently present conduction defects, and/or develop heart failure requiring heart transplant (Colombo et al., 2008; Hasselberg et al., 2018; Pasotti et al., 2008; Taylor et al., 2003; van Berlo et al., 2005). Emery-Dreifuss muscular dystrophy (EDMD) and *LMNA*-related congenital muscular dystrophy (L-CMD) are skeletal muscle conditions also caused by lamin A/C mutations (Bonne et al., 1999, 2000; Quijano-Roy et al., 2008). Both dystrophies are childhood onset and have overlapping clinical presentations (Bonne & Quijano-Roy, 2013). However, L-CMD is more severe than EDMD (Bonne &

Quijano-Roy, 2013). The cardiac phenotype (arrhythmia, cardiac dysfunction) of the L-CMD patients are also more progressive and manifests at a younger age compared to EDMD (Bonne & Quijano-Roy, 2013; Heller et al., 2017).

Previous work suggests that disruption of lamin A/C interaction with its binding partners contributes to the pathophysiology of laminopathies (Bank et al., 2011; Lloyd et al., 2002; Mattioli et al., 2018; Samson et al., 2018; Simon et al., 2010; Vadrot et al., 2015). The lamin A/C binding partner, Protein Kinase C alpha (PKC α), is a classical member of the PKC family of serine/threonine kinases encoded by the *PRKCA* gene (Martelli et al., 2002; Nakashima, 2002). PKC α is mostly localized in the cytoplasm but it can translocate to various subcellular locations including the nucleus (Disatnik et al., 1994; Nakashima, 2002; Schmalz et al., 1996). It is presumed that PKC α found in other subcellular locations aside from the cytoplasm is active because it is in these locations where PKC α acts on its targets (Disatnik et al., 1994; Goodnight et al., 1995; Nakashima, 2002). PKC α is phosphorylated at Thr497, Thr638 and Ser657 for activation with phosphorylation of Ser657 important for full phosphorylation, activity and accumulation of mature PKC α (Bornancin & Parker, 1997; Cazaubon et al., 1994; Gysin & Imber, 1996; Keranen et al., 1995; Parekh et al., 2000). PKC α is the major classical PKC isoform in the mouse, rabbit and adult human heart, and is a fundamental regulator of cardiac contraction via intracellular calcium regulation (Braz et al., 2004; Hambleton et al., 2006; Pass et al., 2001; Ping et al., 1997). Change in PKC α expression is associated with DCM or heart failure in various patient and animal model studies (Bowling et al., 1999; Hu et al., 2018; Rouet-Benzineb et al., 1996; Song et al., 2015;

Wang et al., 2003). Genetic abolition of *Prkca* or pharmacological inhibition of PKC α/β results in either improved cardiac function or cardio-protection from heart failure in mice, rat and pig heart failure models therefore implicating PKC α in cardiac function and heart failure development and progression (Braz et al., 2004; Hambleton et al., 2006; Ladage et al., 2011; Liu et al., 2009). PKC α is also the major classical PKC isoform in adult mouse skeletal muscles (Jensen et al., 2009). *In vitro* work demonstrates its influence on myocyte structure and dynamics by regulating protein filamin C (FLNc) (Reimann et al., 2017). FLNc binds actin and is important in Z-discs assembly (Reimann et al., 2017). Phosphorylation of FLNc by PKC α inhibits FLNc cleavage and affects FLNc dynamics and mobility, thus regulating FLNc function (Reimann et al., 2017). Altogether, these data suggest PKC α involvement in myocyte structure and contraction.

Aside from the A-type lamins, PKC α also interacts with/regulates other lamin A/C partners including certain MAP kinases (Ivorra et al., 2006; Mauro et al., 2002; Naskar et al., 2014; Schönwasser et al., 1998; Soh et al., 1999; Soh & Weinstein, 2003). Cardiac and/or skeletal muscle tissue samples from the EDMD *Lmna* H222P mice model and in patients with DCM caused by lamin A/C mutations, show that members of the MAP kinase (MAPK) signaling pathway, particularly ERK 1/2 and several of its downstream targets, are highly expressed/active (Muchir et al., 2007; Muchir, Wu, et al., 2012; Muchir et al., 2013). ERK 1/2 inhibitor treatment of symptomatic EDMD H222P mice rescues cardiac and skeletal muscle function, improves the cardiac and skeletal muscle histology, and normalizes the abnormal gene expression profile while inhibitor treatment of asymptomatic H222P mice

delays disease onset and lessens the severity of the disease (Muchir et al., 2009, 2013; Muchir, Reilly, et al., 2012; Wu et al., 2011). Furthermore, *Erk 1* knockout alleviates the cardiac symptoms and improves survival of the H222P mice (Wu et al., 2014). However, this improvement in cardiac function is abolished by 20 weeks of age as ERK 2 activation gets elevated (Wu et al., 2014). Treatment of the *Erk 1* null H222P mice with a MEK inhibitor which prevents ERK activation restored the benefits of *Erk 1* knockout further confirming the role of ERK in the development of striated muscle laminopathies (Wu et al., 2014).

Previous studies suggest PKC α regulation of ERK 1/2 activation (Julian C. Braz et al., 2002; Leitges et al., 2002; Naskar et al., 2014; Schönwasser et al., 1998). Similarly, other members of the MAPK pathway – JNK and p38, which are also implicated in striated muscle laminopathies, are regulated by PKC α (Mauro et al., 2002; Soh et al., 1999; Soh & Weinstein, 2003). Thus, with the central role of PKC α in cardiac function, its interaction with A-type lamins and its regulation of several proteins associated with striated muscle laminopathies, we sought to determine the involvement of PKC α in cardiac and muscular laminopathies. In this study, we examined PKC α cellular distribution, activation and lamin A/C proximity in the presence of pathogenic lamin A/C mutations using cardiac and skeletal myoblast cell lines, striated muscle laminopathy mice model myoblasts, and fibroblasts and myoblasts from two L-CMD patients carrying distinct mutations. We show that in transfected cells expressing a DCM-causing *LMNA* mutation and in skeletal myoblasts from two individuals harbouring different L-CMD mutations, PKC α is found to have increased nuclear localization compared to cells expressing WT *LMNA*. On the other hand, transfected cells

expressing a truncated lamin A/C variant that lacks the PKC α binding domain present with PKC α that is mostly cytoplasmic. These data show that PKC α cellular localization is disturbed in the presence of *LMNA* mutations. Furthermore, PKC α and ERK 1/2 activations are decreased or unchanged in patient cells and in skeletal myoblasts from two different mice models of striated muscle laminopathies. In addition, PKC α-lamin A/C proximity is also altered in the patient cells and mice model myoblasts. Altogether, the results demonstrate for the first time the involvement of PKC α in cardiac and muscular laminopathies.

2.4 Materials and Methods

Approved Research Protocols for human cells and mice model cells

Collection and handling of human cells were performed in accordance with the French legislation on ethical rules. Primary mouse myoblasts were obtained following protocols conformed to French laws and were approved by the French Ministry of Higher Education and Research (approval n°00972.03).

Cell Culture and Maintenance

The H9C2 rat cardiac myoblasts (ATCC® CRL-1446™), the C2C12 mouse myoblasts (ATCC® CRL-1772™), and the human skin fibroblasts were cultured in complete medium made up of Dulbecco's Modified Eagle Medium (DMEM) supplemented with 10% Fetal Bovine Serum (FBS), 1% L-glutamine and 1% Pen/Strep at 37°C in 5% CO_2. The p.delK32 fibroblasts were collected as described in (Muchir et al., 2004) while the p.R249W fibroblasts were collected from the patient described in (Bertrand et al., 2014) during surgical intervention to reduce the patient's contractures.

Myoblasts from the H222P (Arimura et al., 2005) and ΔK32 (Bertrand et al., 2012) mice models were taken from the hind limb and cultured on 10% Matrigel coated plates in DMEM supplemented with 20% FBS, 10% Horse serum, 0.5% Chicken embryo extract and 1% Penicillin/Streptomycin at 37°C in 5% CO_2.

Human myoblasts from paraspinal (control), gluteus (p.delK32 patient) and deltoid (p.R249W patient) muscles (Bertrand et al., 2014) were cultured in DMEM supplemented with 16% medium 199, 20% FBS, 0.05% insulin (10 mg/mL stock), 0.025% fetuin (25 µg/mL stock), 0.005% hEGF (5 ng/mL stock), 0.005% bFGF (0.5 ng/mL stock), 0.2% dexamethasone (0.1 mg/mL stock) and 0.1% gentamycin at 37°C in 5% CO_2.

Cloning

To generate the plasmids for transfection, full length human lamins A and C cDNAs were cloned in-frame into eCFP-C1 and eYFP-C1 vectors (Clonetech Laboratories) respectively as described in (Boudreau et al., 2012; Sylvius et al., 2005). Full length human lamin A cDNA was also inserted into the eYFP-C1 vector between the BamHI and XbaI restriction sites. Electro-competent *E.coli* was transformed and grown on kanamycin plates to isolate bacterial colonies expressing the recombinant plasmid. Isolated bacterial clones were further grown in LB medium with kanamycin to propagate the recombinant plasmid. Recombinant plasmid extraction was performed using the Qiagen Plasmid Maxi Kit following the manufacturer's protocol. The fidelity of the inserts was confirmed by sequencing.

Cell Transfection

Cells were double transfected with WT or mutant human lamins A and C using Metafectene® Pro (Biontex) following the manufacturer's guideline. Transfection of both human lamins A and C was performed to maintain the stoichiometric amounts of A-type lamins normally found in cells. Briefly, fresh complete medium was added to cells prior to transfection. Two tubes containing DMEM were prepared per sample. DNA was added in one of the two tubes and Metafectene® Pro was added in the other tube. The DNA solution was then carefully added to the metafectene solution. The DNA/metafectene mix was left to incubate without disturbance at room temperature (RT) for at least 20 minutes prior to addition to the cells. Cells were incubated in the transfection solution for 21 hours.

Immunofluorescence

H9C2 and C2C12 cells were grown on coverslips and double transfected with WT or mutant human lamins A fused to eCFP and C fused to eYFP. At 21 hours post transfection, cells were fixed with 4% paraformaldehyde (PFA) for 20 minutes at RT and washed in PBS three times (5 min/wash). Following fixation, cells were blocked and permeabilized with 0.1% TritonX100 in 5% FBS for 20 minutes at RT. Cells were then incubated with the primary antibody for 1.5 hours at 37°C then washed in PBS three times (5 min/wash). Fluorescently-labeled secondary antibody incubation was performed for 1 hr at 37°C in the dark. The cells were then washed in PBS three times (5 min/wash). Coverslips were mounted on slides using ProLong™ Gold Antifade Mountant (Life Technologies P36930). Double immunostaining was performed in the same manner with the samples being incubated with

two primary antibodies first followed by incubation with two secondary antibodies. Supplementary Table 2.1 lists the antibodies that were used.

Human and mice model cells were fixed in 4% PFA for 10 minutes and washed in 1X PBS. Samples were then blocked and permeabilized with 5% BSA-PBST for 30 min at RT. Primary antibody incubation was for 1.5 hours at RT and secondary antibody incubation was for 1 hour at RT in the dark. All washes were done three times (5 min/wash) in PBST except the one after fixing which was done in PBS. Coverslips were mounted on slides using ProLong™ Gold Antifade Mountant (Life Technologies P36930). Supplementary Table 2.1 lists the antibodies that were used.

Confocal Microscopy

Z-stack images of transfected H9C2 and C2C12 cells were taken using the Zeiss LSM510 AxioImager M1 confocal microscope using the Plan Apochromat 63x (1.40 NA) oil immersion objective. The following lasers were used: 458 nm (emission filter 510-565 nm), 514 nm (emission filter 520 -555 nm) and 633 nm (emission filter 650LP).

Z-stack images of the human and mice model cells were taken using the Nikon A1RsiMP Confocal Workstation using the Plan Apochromat 60x (1.40 NA) oil immersion objective. The following lasers were used: 405 nm, 488 nm, 561 nm and 640 nm. When applicable, channel series was activated to prevent spectral bleed through between the channels.

ImageJ 1.47v 2.0.0-rc-43/1.52n (for Windows 64-bit) was used to analyze the raw fluorescent cell images. PKC α fluorescence intensity was measured in two regions in the

cytoplasm and one region in the nucleus. Background signal was measured from three different non-cellular regions on the image. The area of the selected region was kept constant throughout the measurements and between groups. PKC α fluorescence intensity measurements were performed on one of the middle z-stacks to ensure that the selected nuclear region is solely nuclear. Adjusted PKC α fluorescence intensity was determined by taking the integrated density of the selected region – (area of the selected region x mean fluorescence of background readings) (Gavet & Pines, 2010). The adjusted PKC α fluorescence intensities were then used to calculate the net PKC α fluorescence intensity which is the difference between the adjusted nuclear and cytoplasmic PKC α fluorescence intensities (i.e. net nuclear PKC α fluorescence intensity = adjusted nuclear PKC α fluorescence intensity – mean of the adjusted cytoplasmic PKC α fluorescence intensities). A positive value signifies an increase in nuclear PKC α localization and a negative value signifies that PKC α is mainly cytoplasmic. Adobe Photoshop CC 2019 was used to convert single channel images to black and white, increase image brightness for ease of visualization, annotate the images and prepare the figures.

Cell Sorting

Transfected cells expressing both human eCFP-lamin A and eYFP-lamin C were washed in PBS prior to addition of trypsin to detach the cells from the plate. Cells were then suspended in DMEM only and filtered through a 40 μm mesh (to minimize cell clumps). Transfected cells were then sorted and isolated using a Beckman Coulter MoFlo XDP

(Ottawa Hospital Research Institute Flow Cytometry and Cell Sorting Facility, Ottawa, ON, Canada).

Protein extraction and Western Blot

Nuclear protein extraction of double transfected and sorted C2C12 cells was performed using the Active Motif nuclear extraction kit (Active Motif 40010) following the manufacturer's protocol.

Whole-cell protein extraction was done using RIPA buffer (ThermoFisher Scientific 89901). The manufacturer's protocol was followed with some modification. Briefly, cells were washed with PBS prior to addition of trypsin to detach the cells. Cells were resuspended in complete medium and centrifuged. The cell pellet was rinsed with PBS and was resuspended in RIPA buffer with protease and phosphatase inhibitors. The sample was incubated on ice for 15 minutes, and centrifuged at 14,000g for 15 minutes. The supernatant was transferred into a pre-chilled micro-centrifuge tube for downstream application(s) or storage at -80°C.

Protein extracts were run on Bolt™ 4-12% Bis-Tris Plus gels at 180V for 50 minutes at RT. Transfer onto nitrocellulose membrane was performed for 1 hr at 250 mAmp on ice. Membranes were blocked in 5% BSA-PBST for 30 minutes at RT prior to incubation with the primary antibody at 4°C overnight on a shaking platform. Following primary antibody incubation, membranes were washed three times with PBST (5 min/wash) and incubated with the HRP-conjugated secondary antibody for 1 hr at RT on a shaking platform. Antibodies used are listed in supplementary Table 2.1. To remove previous antibody probing(s),

membranes were stripped using 1X stripping buffer (Millipore 2504). The ECL detection reagent kit (Amersham) was used to visualize the bands via the Bio-Rad VersaDoc Imaging System or the Bio-Rad ChemiDoc™ Touch. Raw membrane images were analyzed using Bio-Rad Image Lab 6.0.1 (software v 2.0.0.25).

Proximity Ligation Assay (PLA)

PLA experiments (Sigma-Aldrich DUO92101) were performed according to the manufacturer`s guideline when using one`s own blocking reagent (5% BSA-PBST) and antibody diluent (1% BSA-PBST). Hydrophobic pen was used to mark the area surrounding the coverslips for the PLA experiments. Briefly, PFA-fixed cells were incubated in 5% BSA-PBST for 30 min at RT for blocking and permeabilization. Samples were then incubated with the primary antibodies - 1:100 mouse anti lamin A/C (sc376248) and 1:100 rabbit anti phos-PKC α (sc12356-R) at RT for 1.5 hours. The negative control was incubated in phos-PKC α antibody only. After washing in PBST three times (5 min/wash), the manufacturer's protocol was followed from here onwards beginning with the incubation of the samples with the PLA probes. Z-stack images of samples were taken at 60x (1.40 NA oil objective) using the Nikon A1RsiMP Confocal Workstation (NIS-Elements AR 4.3 software). Channel series was activated to prevent spectral bleed through between the channels. The 405 nm and 561 nm lasers were used. Quantitative analysis of PLA results was manually performed using ImageJ 1.47v 2.0.0-rc-43/1.52n (for Windows 64-bit) according to (Borroni et al., 2018) except that a z-projection of the z-stacks for each nucleus were analyzed instead of a single stack per nucleus.

Data Analysis

GraphPad Prism 8.3.0 was used to perform statistical analyses. One-way ANOVA with Dunnett's correction for multiple tests or two-tailed t-test (with or without Welch's correction) was performed for analyses. Significance was accepted at $p < 0.05$.

2.5 Results

PKC α localization is disturbed in cells expressing various striated muscle laminopathy mutations

The locations of the pathogenic amino acid substitutions or deletions investigated in this study are shown in Figure 2.1. The amino acid changes span the entire protein, including locations in the head, central rod domain, and tail. The phenotype(s) associated with each variant is shown in Table 2.1, including DCM, DCM-CD, EDMD, and L-CMD.

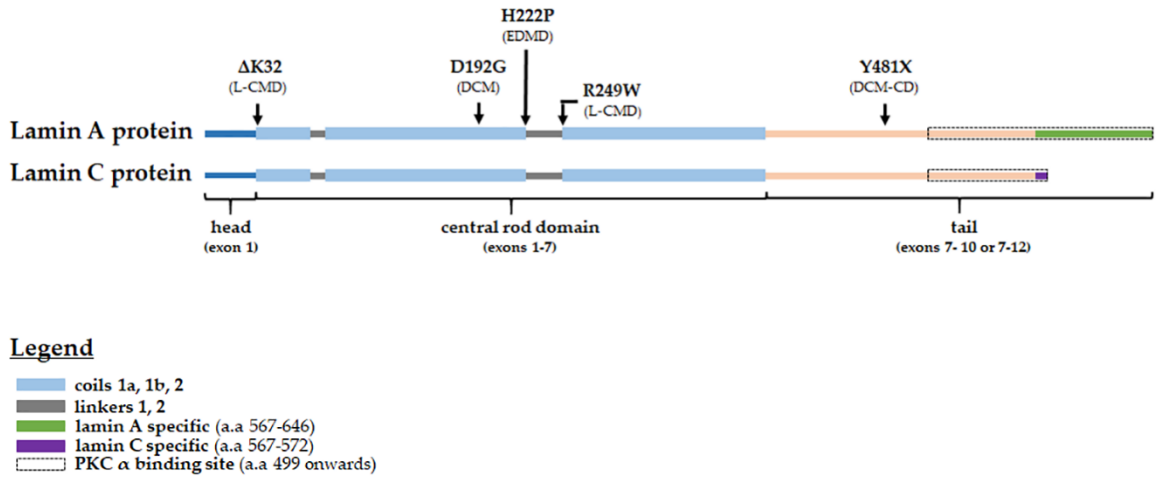

Figure 2.1: Lamin A/C protein schematic showing the location of the pathogenic amino acid changes studied, their corresponding phenotypes, and the PKC α binding site (indicated by black box). DCM – dilated cardiomyopathy, EDMD – Emery Dreifuss muscular dystrophy, L-CMD – *LMNA* related congenital muscular dystrophy, and DCM-CD – dilated cardiomyopathy with conduction defects.

Table 2.1: Phenotypes associated with the studied *LMNA* variants. DCM – dilated cardiomyopathy, DCM-CD – dilated cardiomyopathy with conduction defects, EDMD –

Emery Dreifuss muscular dystrophy, and L-CMD – *LMNA* related congenital muscular dystrophy.

Variant	Phenotype(s)	Reference(s)
p.delK32	L-CMD*, severe EDMD	(D'Amico et al., 2005; Vytopil et al., 2002)
p.D192G	severe DCM	(Fidzianska et al., 2008; Sylvius et al., 2005)
p.H222P	EDMD with arrhythmia	(G. Bonne et al., 2000)
p.R249W	L-CMD	(Quijano-Roy et al., 2008)
p.Y481X	DCM-CD	(Bilinska et al., 2006; Sylvius et al., 2005)

* Patient in this study was diagnosed with L-CMD.

To determine the effect of striated muscle laminopathy mutations on PKC α cellular distribution, H9C2 rat cardiac myoblasts and C2C12 mouse skeletal myoblasts were transfected with fluorescently conjugated wild type or mutant human lamins A and C. The fluorescent marker allowed for identification of cells expressing human lamins A and C. Transfected H9C2 (Figure 2.2A) and C2C12 (supplementary Figure 2.1A) cells were immunostained for endogenous total PKC α (both unphosphorylated and phosphorylated), and nuclear and cytoplasmic endogenous PKC α fluorescence intensities were measured. From the nuclear PKC α fluorescence intensity measurement, adjusted and net nuclear PKC α fluorescence intensities were then calculated, and the net nuclear PKC α fluorescence intensity was compared between the groups (Figure 2.2B, supplementary Figure 2.1B). PKC α was primarily found in the cytoplasm (Figure 2.2 and supplementary Figure 2.1) of H9C2 and C2C12 untransfected cells and transfected cells expressing wild type (WT) lamins. In contrast, transfected cells expressing the p.D192G lamin A/C variant displayed a significant increase in nuclear PKC α compared to WT (Figure 2.2 and supplementary Figure 2.1). On

the other hand, transfected cells expressing the p.H222P lamin A/C variant showed PKC α cellular localization that was comparable to WT (Figure 2.2). Likewise, the truncated p.Y481X lamin A/C that cannot bind PKC α had PKC α mostly in the cytoplasm (Figure 2.2) (Martelli et al., 2002).

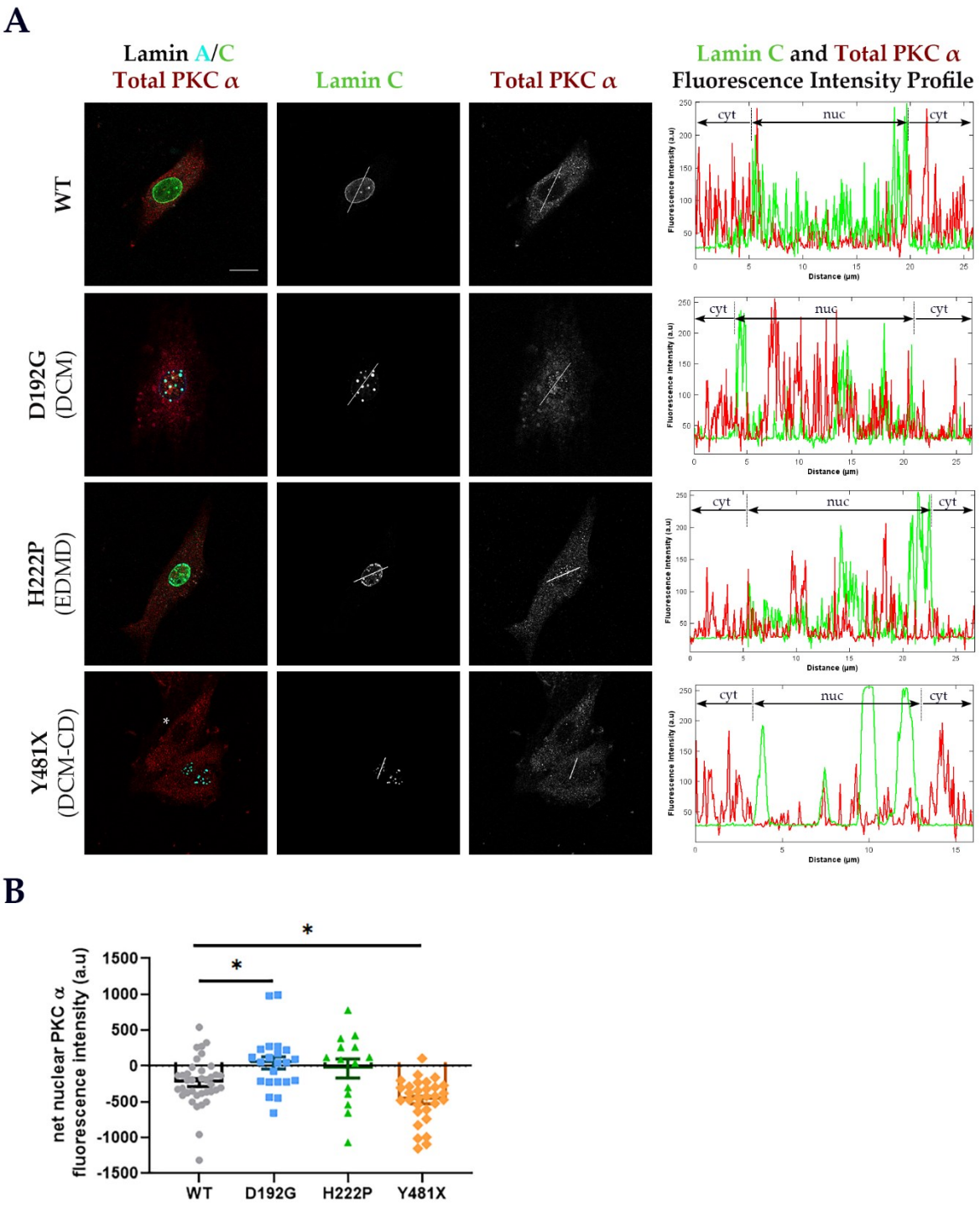

Figure 2.2: Cellular localization of total PKC α in transfected H9C2 cells expressing either WT or mutant human lamins A and C. **(A)** Exogenous eCFP-human lamin A and eYFP-human lamin C are shown with the immunostaining for endogenous PKC α (red) in WT and mutant *LMNA* expressing H9C2 cells. The composite image for each group is shown in the leftmost panel. A representative untransfected cell (indicated by a white asterisk) showing cytoplasmic PKC α localization comparable to PKC α localization in WT *LMNA* transfected cells. The white line across a cell in the second and third panels indicates the measurement path used to generate the fluorescence intensity profiles for lamin C and PKC α in the right most panel. The plot profile for lamin C is included to show nuclear demarcation of

fluorescence signal. Scale bar: 15 μm for all immunofluorescence images. **(B)** Mean (± SEM) net nuclear PKC α fluorescence intensity of each group: WT (grey circles), D192G (blue diamonds), H222P (green triangle) and Y481X (orange diamonds)**.** The net nuclear PKC α fluorescence intensity of each cell = adjusted nuclear PKC α fluorescence intensity – mean of the adjusted cytoplasmic PKC α fluorescence intensities. n ≥ 3 independent sets are analyzed (≥14 cells/group are analyzed). Significance (*) is set at $p < 0.05$.

To confirm the results from the transfected cell lines, cellular distribution of PKC α phosphorylated at Ser657 (phos-PKC α) was examined in human and mice myoblasts carrying lamin A/C mutations. Phosphorylated PKC α was further studied as this is the active form of the protein. Control and L-CMD patient myoblasts (one patient/variant) and myoblasts from WT mice, the EDMD H222P mice model and the L-CMD p.K32del (ΔK32) mice model were immunostained for endogenous phos-PKC α. Phos-PKC α was predominantly cytoplasmic in the control myoblasts (Figure 2.3 and supplementary Figure 2.2). Similarly, phos-PKC α cellular distribution in the H222P mice myoblasts remained mostly cytoplasmic (supplementary Figure 2.2). In contrast, both patient myoblasts and ΔK32 mice myoblasts displayed an increase in nuclear phos-PKC α localization compared to control (Figure 2.3 and supplementary Figure 2.2).

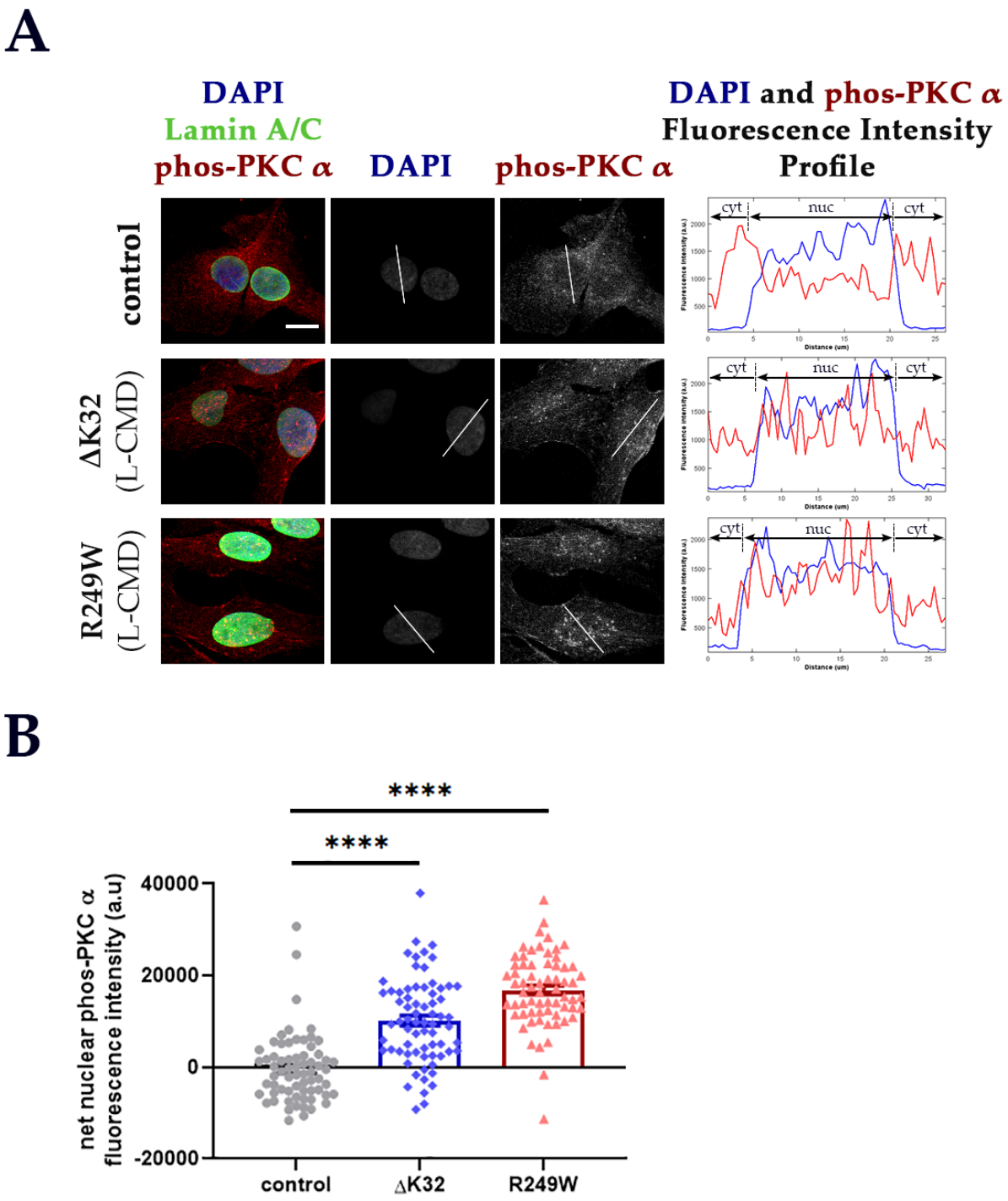

Figure 2.3: Cellular localization of phosphorylated PKC α (phos-PKC α) in control and patient myoblasts. **(A)** Immunostaining for DAPI, lamin A/C and phos-PKC α in control and patient myoblasts. The composite image for each group is shown in the leftmost panel. The white line across a cell in the second and third panels indicates the measurement path used to generate the fluorescence intensity profiles for DAPI and phos-PKC α in the right most panel. The plot profile for DAPI is included to show nuclear demarcation of fluorescence signal. Scale bar: 15 µm for all immunofluorescence images. **(B)** Mean (± SEM) net nuclear phos-PKC α fluorescence intensity of each group: control (grey circles), ΔK32 (blue diamonds), and R249W (pink triangles)**.** The net nuclear phos-PKC α fluorescence intensity

of each cell = adjusted nuclear phos-PKC α fluorescence intensity – mean of the adjusted cytoplasmic phos-PKC α fluorescence intensities. n = 2 technical replicates (one patient/group; ≥ 66 cells/group are analyzed). Significance (*) is set at $p < 0.05$; **** means $p < 0.0001$.

To eliminate a possible factor that could have influenced PKC α localization, *LMNA* over-expression was examined. Western blot analyses of nuclear extracts from sorted C2C12 cells expressing WT or mutant *LMNA* showed comparable levels of lamin A/C over-expression (supplementary Figure 2.3) suggesting that lamin A/C over-expression unlikely caused the aberrant PKC α localization.

To verify that the observed increase in PKC α nuclear localization was not caused by a compromised nuclear membrane where proteins can passively move into the nucleus, immunostaining for another protein - HSP60, was performed on human myoblasts (supplementary Figure 2.4). HSP60 is a chaperone protein found in various subcellular localizations such as the cytoplasm, mitochondria, and nucleus (Deniset et al., 2018; Itoh et al., 1995; Itoh et al., 2002; Meng et al., 2018). It has a molecular weight of 60 kDa which is smaller than the 80 kDa PKC α; thus making it easier and more likely for HSP60 to get into the nucleus than PKC α if the observed PKC α mislocalization was due to compromised nuclear permeability. Qualitative analyses of patient myoblasts HSP60 immunostaining images showed that similar to what was observed in the control myoblasts, HSP60 remained primarily outside of the nucleus in cells expressing mutant *LMNA* (supplementary Figure 2. 4). This suggested that the increased nuclear localization of phos-PKC α in the patient myoblasts was unlikely caused by a compromised nuclear membrane where proteins can

easily get into the nucleus. Overall, the results revealed PKC α mislocalization in the presence of pathogenic *LMNA* mutations.

PKC α activation is disturbed by lamin A/C mutations

To determine if the activation level of PKC α was changed in the presence of pathogenic lamin A/C mutations, western blot analyses of whole-cell protein extracts from human myoblasts and fibroblasts, and mice model myoblasts were performed. PKC α activation was significantly lower in the R249W patient myoblasts and fibroblasts compared to control (Figures 2.4A, B and supplementary Figure 2.5). In ΔK32 patient myoblasts, a trend of reduced phos-PKC α was observed (Figures 2.4A, B and supplementary Figure 2.5). On the other hand, PKC α activation level was comparable to WT in the H222P mice myoblasts (Figures 2.4C, D).

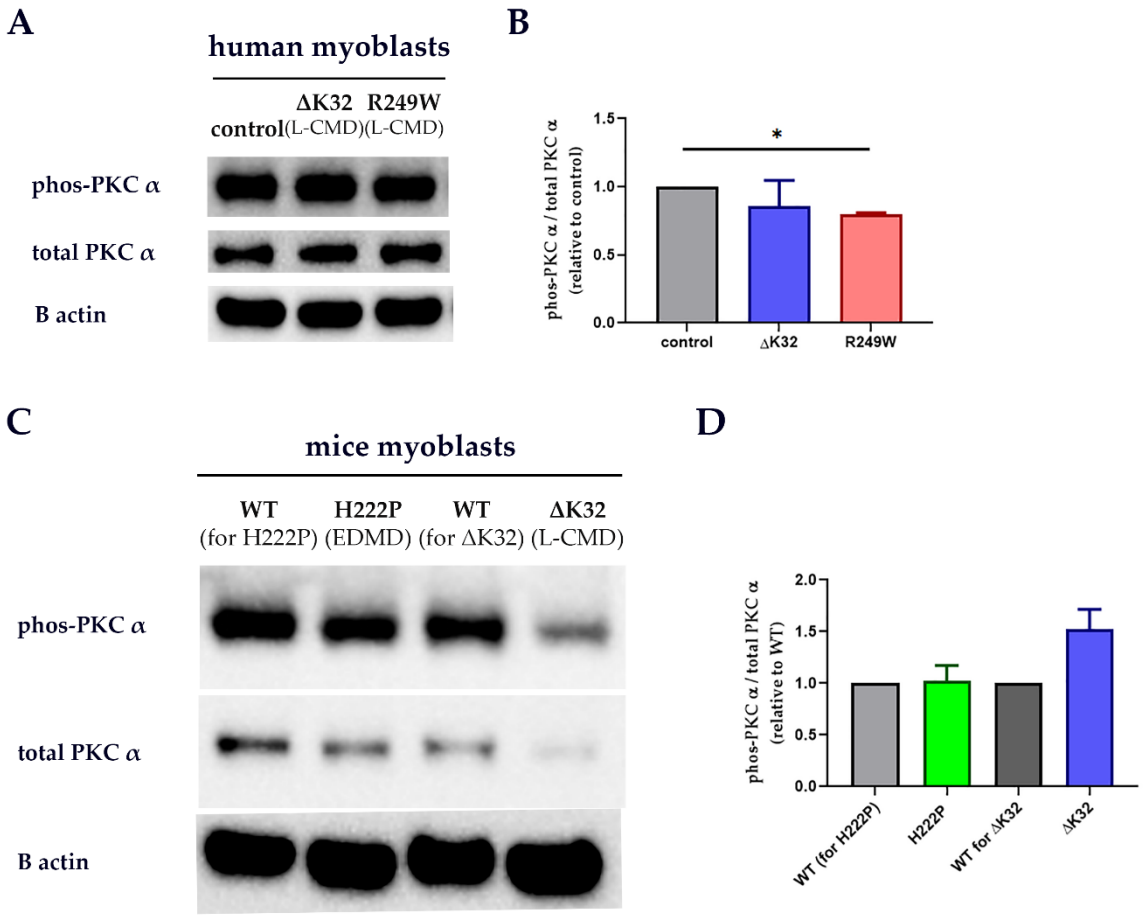

Figure 2.4: Western blot analyses for PKC α in whole cell protein extracts from patient and mice model myoblasts. Representative blots for human myoblasts **(A)** and mice model myoblasts **(C)**. Mean (± SEM) protein level relative to control (or WT) is shown for human myoblasts **(B)** and mice model myoblasts **(D)**. $n \geq 3$ technical replicates (one patient or mice model/group). Significance (*) is set at $p < 0.05$.

PKC α and lamin A/C proximity is disrupted by lamin A/C mutations

To determine if *LMNA* mutations affected the proximity of PKC α and lamin A/C to each other, proximity ligation assay (PLA) was performed on human myoblasts and fibroblasts, and mice model myoblasts. A PLA signal is obtained if the target proteins are within 40 nm of each other (Alam, 2018). Both ΔK32 and R249W human myoblasts and fibroblasts showed a significant increase in the number of PLA signals/nucleus compared to control (Figures 2.5A, B and supplementary Figure 2.6). Similarly, an increase in PLA signal was noted in the ΔK32 mice myoblasts suggesting increased occurrence of lamin A/C and

phos-PKC α proximity in these cells. (Figures 2.5C, D). On the other hand, the H222P mice model myoblasts had fewer PLA signals than WT myoblasts (Figures 2.5C, D).

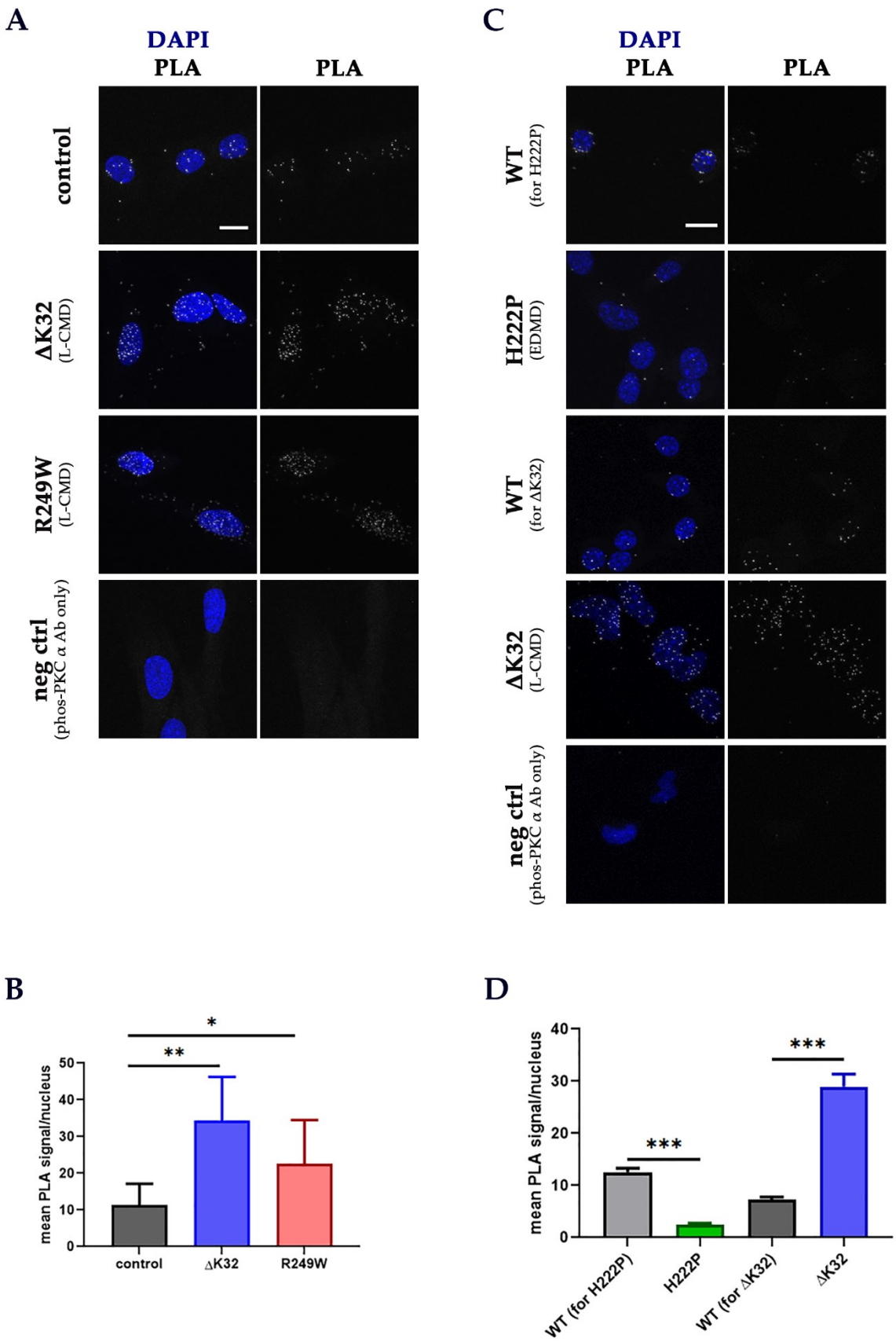

Figure 2.5: Proximity ligation assay (PLA) between lamin A/C and phos-PKC α in human **(A)** and mice models **(C)** myoblasts. Mean (± SEM) PLA signal/nucleus in human **(B)** and mice models **(D)** myoblasts. The nucleus is stained with DAPI (blue) and the PLA signal

representing the proximity of lamin A/C and phos-PKC α is in white. n = 2 technical replicates (one patient/group; ≥ 92 nuclei/group are analyzed) for human myoblasts and n = 1 experimental set (≥ 46 nuclei/group are analyzed) for mice models myoblasts. Scale bar: 15 μm for all PLA images. Significance (*) is set at $p < 0.05$; ** means $p < 0.01$ and *** means $p < 0.001$.

ERK 1/2 activation is downregulated in patient and mice model myoblasts

ERK 1/2 is known to be regulated by PKC α and is implicated in the development and progression of striated muscle laminopathies (Leitges et al., 2002; Mauro et al., 2002; Muchir et al., 2007, 2009, 2013; Muchir, Reilly, et al., 2012; Naskar et al., 2014; Schönwasser et al., 1998). Western blots were performed to estimate phos-ERK 1/2 level in whole-cell protein extracts from human myoblasts and fibroblasts, and mice model myoblasts. Phos-ERK 1/2 was significantly downregulated in both the ΔK32 and R249W patient myoblasts compared to control (Figures 2.6A, B). Likewise, ERK 1/2 activation was dampened in both the H222P and ΔK32 mice myoblasts (Figures 2.6C, D). However, no significance was obtained in the human fibroblasts (Supplementary Figure 2.5).

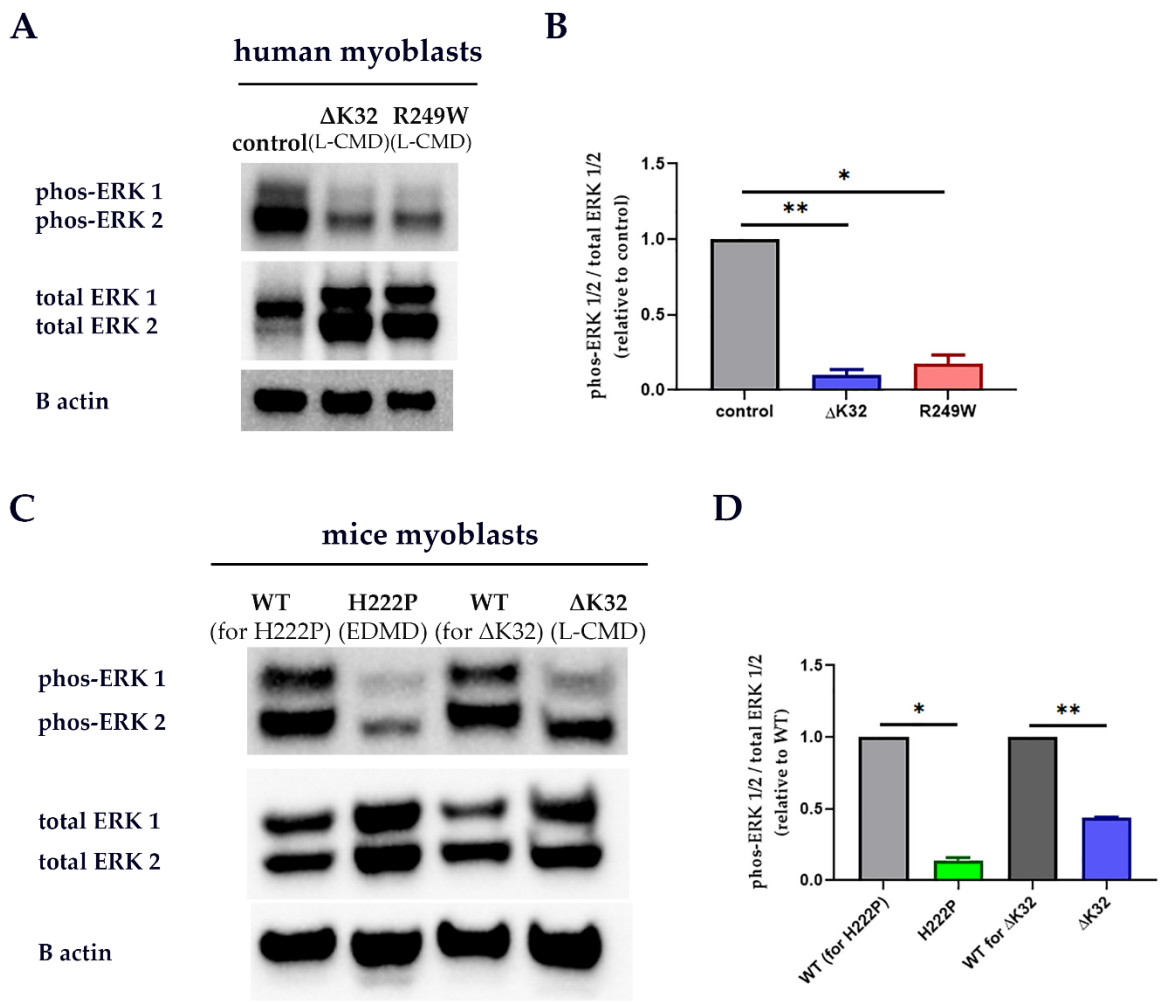

Figure 2.6: Western blot analyses for ERK 1/2 in whole cell protein extracts from patient and mice model myoblasts. Representative blots for human myoblasts **(A)** and mice model myoblasts **(C)**. Mean (± SEM) protein level relative to control (or WT) is shown for human myoblasts **(B)** and mice model myoblasts **(D)**. $n \geq 2$ technical replicates (one patient or mice model/group). Significance (*) is set at $p < 0.05$; ** means $p < 0.01$ and *** means $p < 0.001$.

2.6 Discussion

Striated muscle laminopathies affect the majority of individuals carrying pathogenic lamin A/C mutations (Tesson et al., 2014). Unfortunately, there is currently no available cure or effective treatment for these patients. To further understand the molecular mechanisms contributing to the development and progression of striated muscle laminopathies, we studied PKC α, one of lamin A/C's kinase binding partners. Due to the central role of PKC α in cardiac function, its interaction with the A-type lamins and its regulation of other lamin A/C partners including ones implicated in striated muscle laminopathies, we sought to determine

if PKC α was involved in cardiac and muscular diseases caused by lamin A/C mutations. Our study provides evidence linking PKC α to striated muscle laminopathies by assessing PKC α cellular localization, activation, and proximity with the A-type lamins. We show that PKC α nuclear distribution is increased in most of the lamin A/C mutations that we studied. PKC α is highly localized in the nucleus of cardiac and skeletal myoblast cell lines expressing a DCM-causing lamin A/C mutation. This increase in nuclear PKC α localization is unlikely caused by lamin A/C over-expression or compromised nuclear permeability. Additionally, it is unlikely caused by the fluorescent tag as the L-CMD patient and ΔK32 mice model myoblasts present with comparable results to the cell lines. The increase in nuclear PKC α is paralleled by an increase in lamin A/C- phos-PKC α PLA signal suggesting more frequent proximity conducive for interaction of lamin A/C and phos-PKC α in patient fibroblasts and myoblasts, and in ΔK32 mice model myoblasts. We also show that in L-CMD patients' myoblasts and fibroblasts, whole-cell PKC α phosphorylation status is reduced, suggesting decreased PKC α. Activation of ERK 1/2, a downstream PKC α target previously associated with striated muscle laminopathies, is decreased in L-CMD patient myoblasts as well as in H222P and ΔK32 mice myoblasts. On the other hand, cells expressing the DCM-CD p.Y481X truncated lamin A/C lacking the PKC α binding region in the C-terminus show more cytoplasmic (i.e. less nuclear) PKC α subcellular localization than WT. Previous work determined that lamin A binds PKC α downstream of amino acid 499 (Martelli et al., 2002). Thus, our data provide evidence to warrant further study of PKC α in the context of pathogenic *LMNA* mutations.

Various patient and heart failure animal model studies found contradicting results regarding PKC α expression. In cardiac tissues from various heart failure animal models and patients with heart failure due to dilated cardiomyopathy (DCM) or ischemic cardiomyopathy, PKC α expression is upregulated (Bowling et al., 1999; Braz et al., 2004;

Song et al., 2015; Wang et al., 1999; Wang et al., 2003). In contrast, a rabbit heart failure model has reduced PKC α expression in failing ventricles (Rouet-Benzineb et al., 1996). Decreased *PRKCA* expression in the left ventricle has also been associated with adverse cardiac remodeling and increased DCM risk in patients (Hu et al., 2018). In our study, PKC α activation is downregulated in L-CMD patient myoblasts and fibroblasts. ERK 1/2 activation is reduced as well. PKC α activation has been shown to be upstream of the ERK 1/2 cascade mediating cardiac myocyte hypertrophy (Braz et al., 2002; Naskar et al., 2014). Adverse cardiac remodeling is a hallmark of DCM with cardiolaminopathy patients having improper cardiac remodeling and many presenting mildly DCM (systolic dysfunction without severe left ventricle enlargement) (Gigli et al., 2017; Taylor et al., 2003). In our study, the p.D192G and p.Y481X lamin A/C patients had DCM with the p.D192G patient presenting a milder left ventricle dilatation compared to the p.Y481X patient (Bilinska et al., 2006; Sylvius et al., 2005). Interestingly, p.D192G cells have increased nuclear PKC α while p.Y481X cells have mostly cytoplasmic PKC α. Considering PKC α involvement in transducing cellular signals, aberrant PKC α activation and localization might contribute to the abnormal cellular response to physical stimuli in cells expressing mutant lamin A/C resulting in the development of phenotype in mechanically-stressed tissues such as the heart. The impaired ability of PKC α to localize in the nucleus in p.Y481X cells potentially exacerbate the mechano-transduction defect in these cells as PKC α is less able to reach its nuclear targets resulting in more pronounced cardiac remodeling (i.e. more significant left ventricle dilation) in the p.Y481X patient compared to the p.D192G patient (Bilinska et al., 2006; Sylvius et al., 2005). On the other hand, in myoblasts from one-month old H222P mice, PKC α activation and cellular localization is comparable to WT. The H222P mice do not present any notable phenotype at 4 weeks old (Arimura et al., 2005; Muchir et al., 2007).

Regarding lamin A/C interaction with a binding partner, one of the ways by which lamin A/C regulates proteins is by sequestering the target protein and/or its regulator or substrate (González et al., 2008; Ivorra et al., 2006; Myant et al., 2015; Rodríguez et al., 2010). Protein interaction mediated by the A-type lamins have been documented such as in the lamin A/C – c-Fos – ERK 1/2 complex (González et al., 2008). In this example, lamin A/C anchors both ERK 1/2 and c-Fos enabling ERK 1/2 to phosphorylate c-Fos and free it from lamin A/C. Upon release from the nuclear lamina, c-Fos is then able to dimerize with c-Jun and assemble the AP-1 transcription factor (González et al., 2008). In the present study, the formation of the lamin A/C – ERK 1/2 - PKC α complex is plausible as lamin A/C is able to bind both ERK 1/2 and PKC α (González et al., 2008; Martelli et al., 2002). In cells expressing p.D192G, p.K32del or p.R249W lamin A/C, an increase in nuclear PKC α is observed. Concomitant with this increase in nuclear PKC α is an increase in lamin A/C- PKC α proximity. This enhanced proximity between lamin A/C and PKC α likely keeps PKC α in the nucleus by tethering PKC α to the A-type lamins. However, structural changes incurred due to the lamin A/C mutations could have disrupted lamin A/C – ERK 1/2 interaction thus impeding ERK 1/2 – PKC α interaction and resulting in decreased ERK 1/2 activation. Recent work on CRISPR knock-in mutant C2C12 myoblasts expressing p.R249W also show a lack of ERK 1/2 activation in western blot analyses compared to control (Gómez-Domínguez et al., 2020). Disruption of lamin A/C - ERK 1/2 association is plausible especially in the p.R249W variant as amino acid 249 is located in the region that binds ERK 1/2 (González et al., 2008). However, even if the affected amino acid is not located in the PKC α or ERK 1/2 binding sites, such as in the p.K32del variant, previous work has noted disruption of lamin A/C – partner interaction (Lloyd et al., 2002). Studies have also shown misassembly of p.K32del filaments potentially disturbing lamin A/C partner binding and/or interactions mediated by lamin A/C (Bank et al., 2011; Zwerger et al., 2013). Alternatively, lamin A/C –

ERK 1/2 interaction might not have been affected but the overall conformational change in the lamin A/C variants might have disrupted the ERK 1/2 - PKC α interaction resulting in reduced ERK activation. Similarly, downregulation of ERK 1/2 activation is noted in the H222P mice myoblasts. However, in these myoblasts, a decrease in PKC α – lamin A/C proximity is observed. The reduction in lamin A/C - PKC α proximity possibly impeded the lamin A/C-mediated ERK 1/2 - PKC α interaction resulting in downregulation of ERK 1/2 activation. Previous work by another group on H222P myoblasts also does not note ERK 1/2 activation at baseline (Muchir et al., 2007). In addition, C2C12 cells stably expressing p.H222P lamin A show elevated ERK 1/2 activation only after AICAR treatment, glucose starvation or osmotic shock (Choi et al., 2012; Muchir et al., 2013). ERK 1/2 hyperactivation is also noted in C2C12 and Cos7 cells transiently transfected with p.H222P lamin A and in striated muscle tissues from symptomatic H222P mice suggesting involvement of physiological stress in upregulating ERK 1/2 phosphorylation in the context of the p.H222P lamin A/C variant (Choi et al., 2012; Muchir et al., 2007, 2013). Since the myoblasts we studied were collected from one-month old H222P mice which were still asymptomatic, physiological stress might not have been significant enough to result in notable ERK 1/2 activation (Arimura et al., 2005; Muchir et al., 2007). Dysregulation of a lamin A/C partner's function as a consequence of disrupted lamin A/C binding has been demonstrated with other lamin A/C mutations. For instance, several lamin A/C variants with amino acid substitutions affecting the region that binds the transcription factor SREBF-1 (important for adipogenesis and metabolism) show impaired SREBF-1 binding (Lloyd et al., 2002). This reduced binding resulted in SREBF-1 dysregulation, and abnormal expression of downstream SREBF-1 target genes contributing to lipodystrophy in patients (Vadrot et al., 2015). Likewise, the lamin A/C variants p.R527P and p.L530P which have amino acid substitutions affecting the region that binds actin present with a notable decrease in actin binding (Simon et al., 2010). Individuals

expressing either of these lamin A/C variants have EDMD (Bonne et al., 1999). Actin is involved in the transduction of mechanical signal in the cell and is part of the network that connects the cytoskeleton to the nucleus. Therefore, disruption of its association with the A-type lamins unsurprisingly results in a phenotype involving muscles which are tissues under constant mechanical and physical stress.

In conclusion, our results show that PKC α cellular localization, activation, and proximity with the A-type lamins are affected by striated muscle laminopathy mutations. Furthermore, the data hint at a potential correlation between the severity of the patient phenotype and abnormal PKC α cellular localization, activation and proximity with lamin A/C. Results from cells expressing p.H222P (EDMD) or p.Y481X (DCM-CD) lamin A/C suggest that a predominantly cytoplasmic PKC α localization in combination with decreased PKC α - lamin A/C proximity, and decreased PKC α and ERK 1/2 phosphorylation result in less severe muscular and/or cardiac phenotype. On the other hand, cells expressing variant lamin A/C (e.g. p.D192G, p.K32del, p.R249W) with increased nuclear PKC α localization, increased PKC α - lamin A/C association and decreased PKC α and ERK 1/2 activation result in more severe cardiac and/or skeletal laminopathy. Future studies evaluating ERK 1/2 – lamin A/C interaction in cells expressing mutant lamin A/C are needed to determine the effects of the mutations on lamin A/C – ERK 1/2 binding. In addition, future work to determine ERK 1/2 – lamin A/C - PKC α assembly, and to characterize the interplay between these proteins can also be performed. Other downstream PKC α targets can be examined as well to further understand the role of PKC α in striated muscle laminopathies, and to identify other proteins that could potentially be therapeutic targets to treat striated muscle laminopathies.

2.7 Supplementary Information

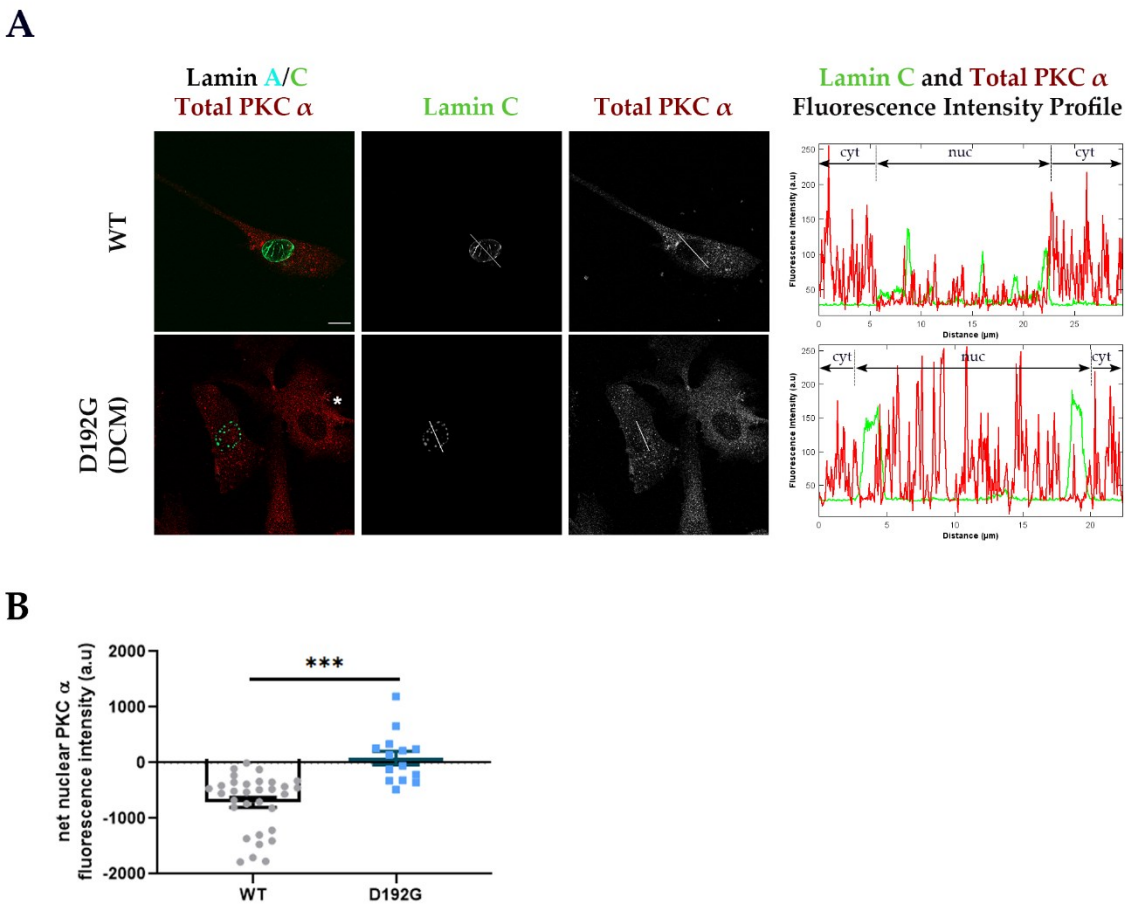

Supplementary Figure 2.1: Cellular localization of PKC α in transfected C2C12 cells expressing either WT or mutant human lamins A and C. **(A)** Exogenous eCFP-human lamin A and eYFP-human lamin C are shown with the immunostaining for endogenous PKC α (in red) in WT and mutant *LMNA* expressing C2C12 cells. The composite image for each group is shown in the leftmost panel. A representative untransfected cell (indicated by a white asterisk) showing cytoplasmic PKC α localization comparable to PKC α localization in WT *LMNA* transfected cells. The white line across a cell in the second and third panels indicates the measurement path used to generate the fluorescence intensity profiles for lamin C and PKC α in the right most panel. The plot profile for lamin C is included to show nuclear demarcation of fluorescence signal. Scale bar: 15 μm for all immunofluorescence images. **(B)** Mean (± SEM) net nuclear PKC α fluorescence intensity of each group: WT (grey circles) and D192G (blue squares). The net nuclear PKC α fluorescence intensity of each cell = adjusted nuclear PKC α fluorescence intensity – mean of the adjusted cytoplasmic PKC α fluorescence intensities. n ≥ 3 independent sets (≥14 cells/group are analyzed). Significance (*) is set at $p < 0.05$ and *** means $p < 0.001$.

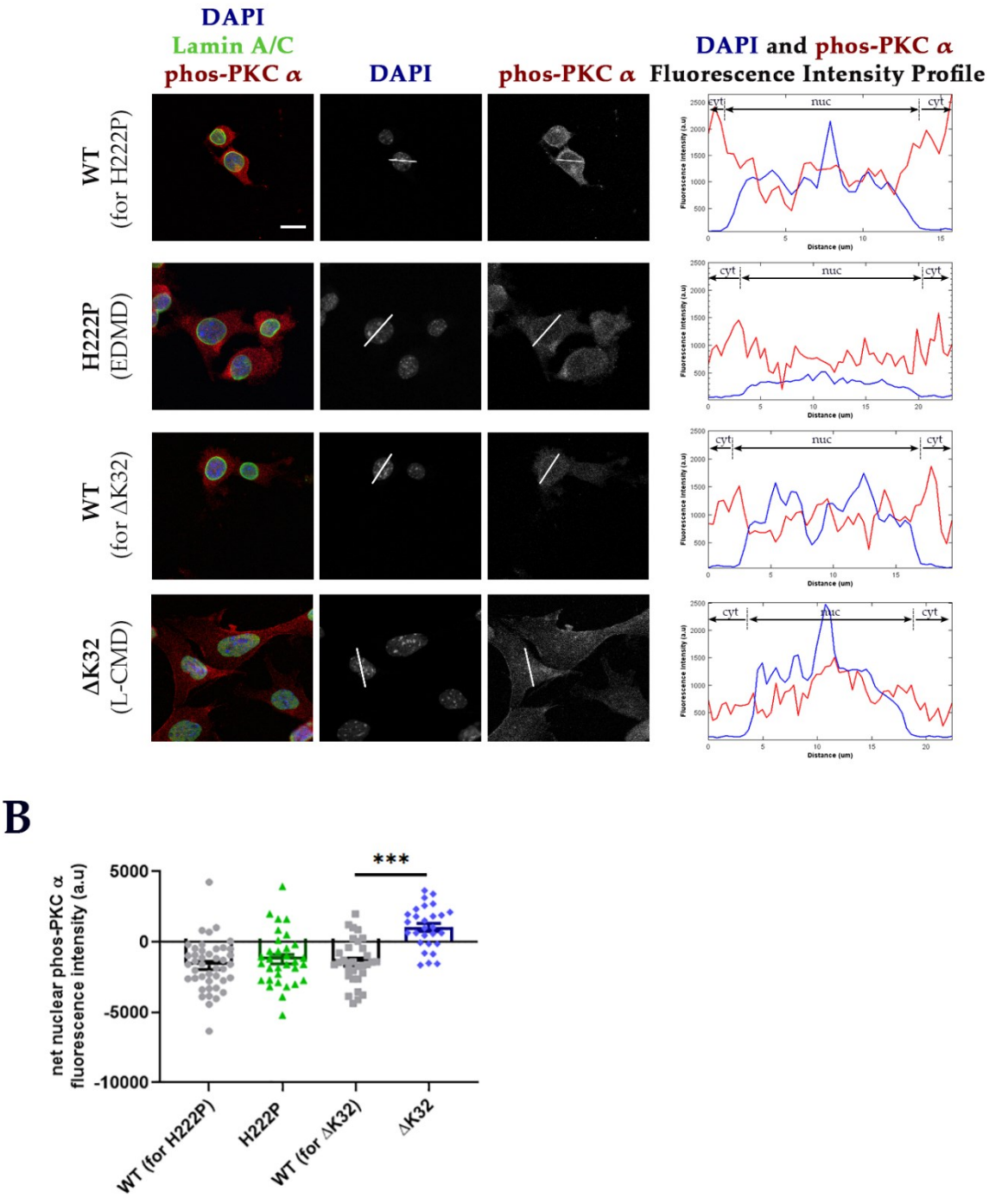

Supplementary Figure 2.2: Cellular localization of phosphorylated PKC α (phos-PKC α) in WT and mice model myoblasts. **(A)** Immunostaining for DAPI, lamin A/C and phos-PKC α in WT and mice model myoblasts. The composite image for each group is shown in the leftmost panel. The white line across a cell in the middle panels indicates the measurement path used to generate the fluorescence intensity profiles (right most panel) for DAPI and phos-PKC α. The plot profile for DAPI is included to show nuclear demarcation of fluorescence signal. Scale bar: 15 μm for all immunofluorescence images. **(B)** Mean (± SEM) net nuclear phos-PKC α fluorescence intensity of each group: WT for H222P (grey circles),

H222P (green triangles), WT for ΔK32 (grey square) and ΔK32 (blue diamonds)**.** The net nuclear phos-PKC α fluorescence intensity of each cell = adjusted nuclear phos-PKC α fluorescence intensity – mean of the adjusted cytoplasmic phos-PKC α fluorescence intensities. n = 1 experimental set (≥ 30 nuclei/group are analyzed). Significance (*) is set at $p < 0.05$; *** means $p < 0.001$.

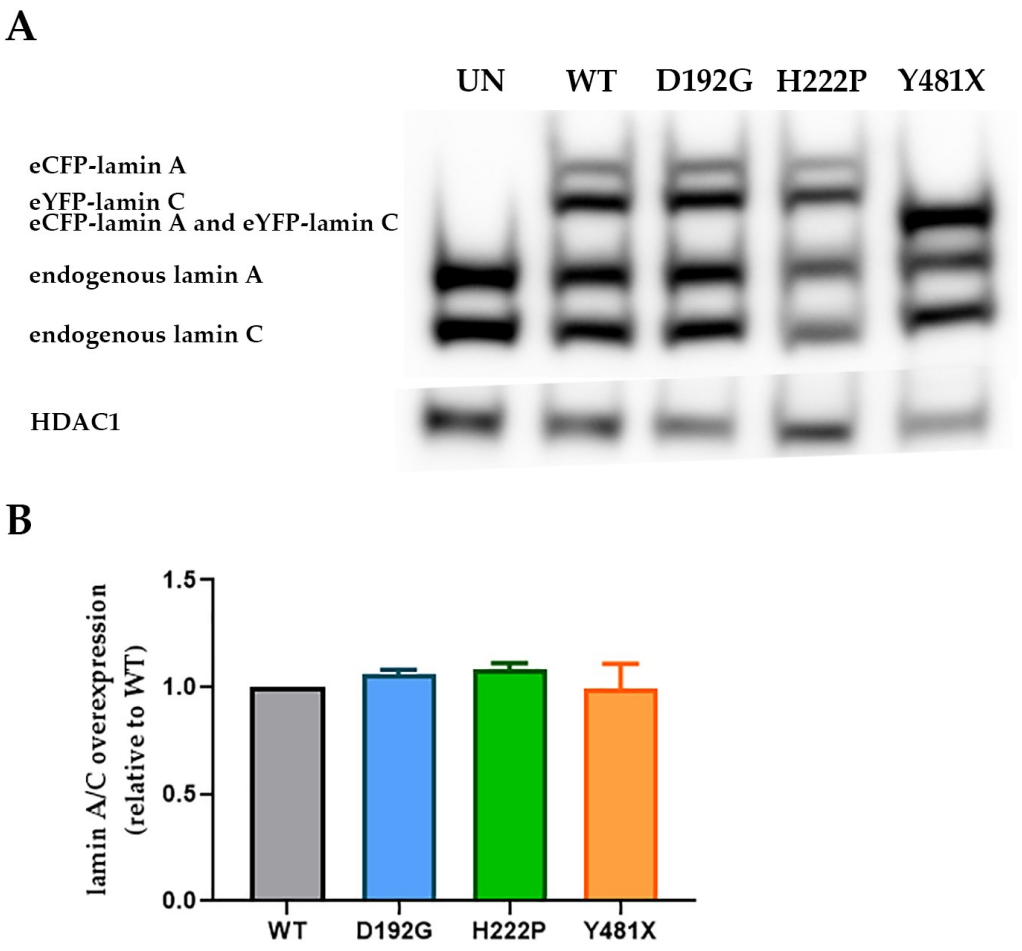

Supplementary Figure 2.3: Exogenous (transfected) and endogenous lamin A/C protein levels analyses of nuclear extracts from transfected and sorted C2C12 cells expressing WT or mutant human eCFP-lamin A and eYFP-lamin C. **(A)** Representative western blot for lamin A/C in untransfected (UN) cells, WT and mutant *LMNA* expressing cells. **(B)** Comparison of lamin A/C overexpression between the WT and mutants. Mean ± SEM. n ≥ 2 independent sets. Significance (*) is set at $p < 0.05$.

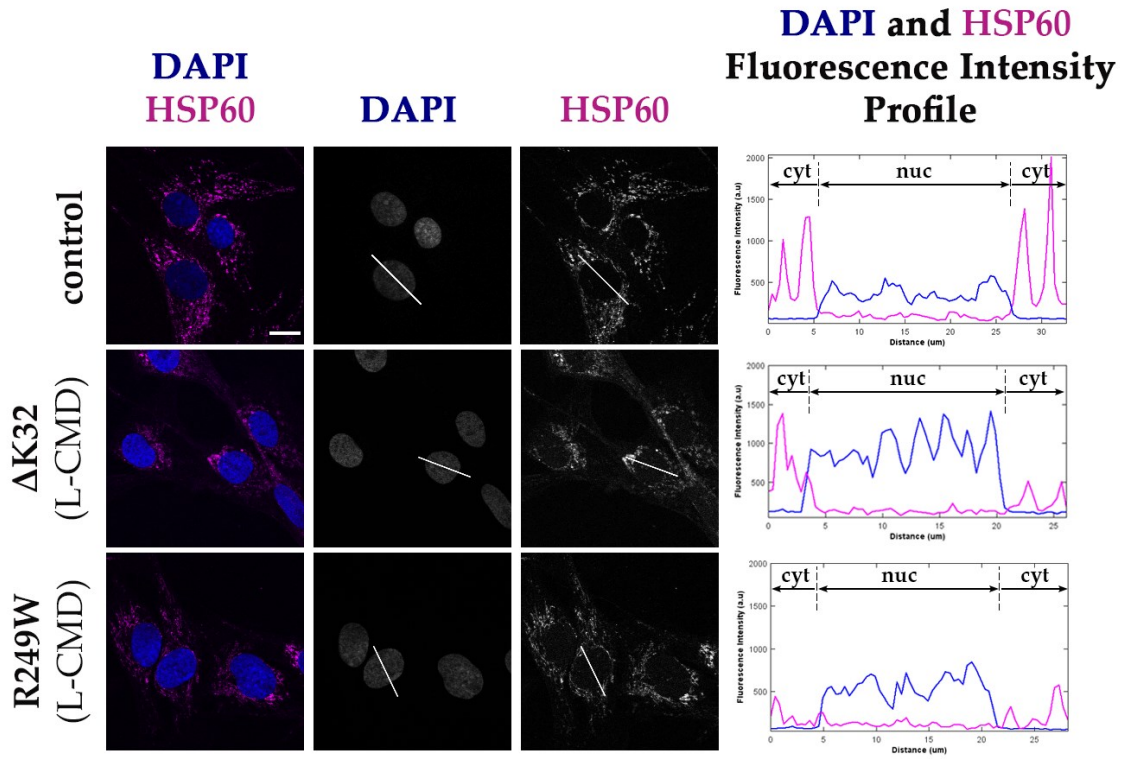

Supplementary Figure 2.4: Immunostaining for HSP60 (in magenta) and DAPI (in blue) in control and patient myoblasts. The composite image for each group is shown in the leftmost panel. The white line across a cell in the second and third panels indicates the measurement path used to generate the fluorescence intensity profiles for DAPI and HSP60 in the right most panel. The plot profile for DAPI is included to show nuclear demarcation of fluorescence signal. n = 1 experimental set (one patient/group; ≥ 50 cells/group are analyzed). Scale bar: 15 μm for all immunofluorescence images.

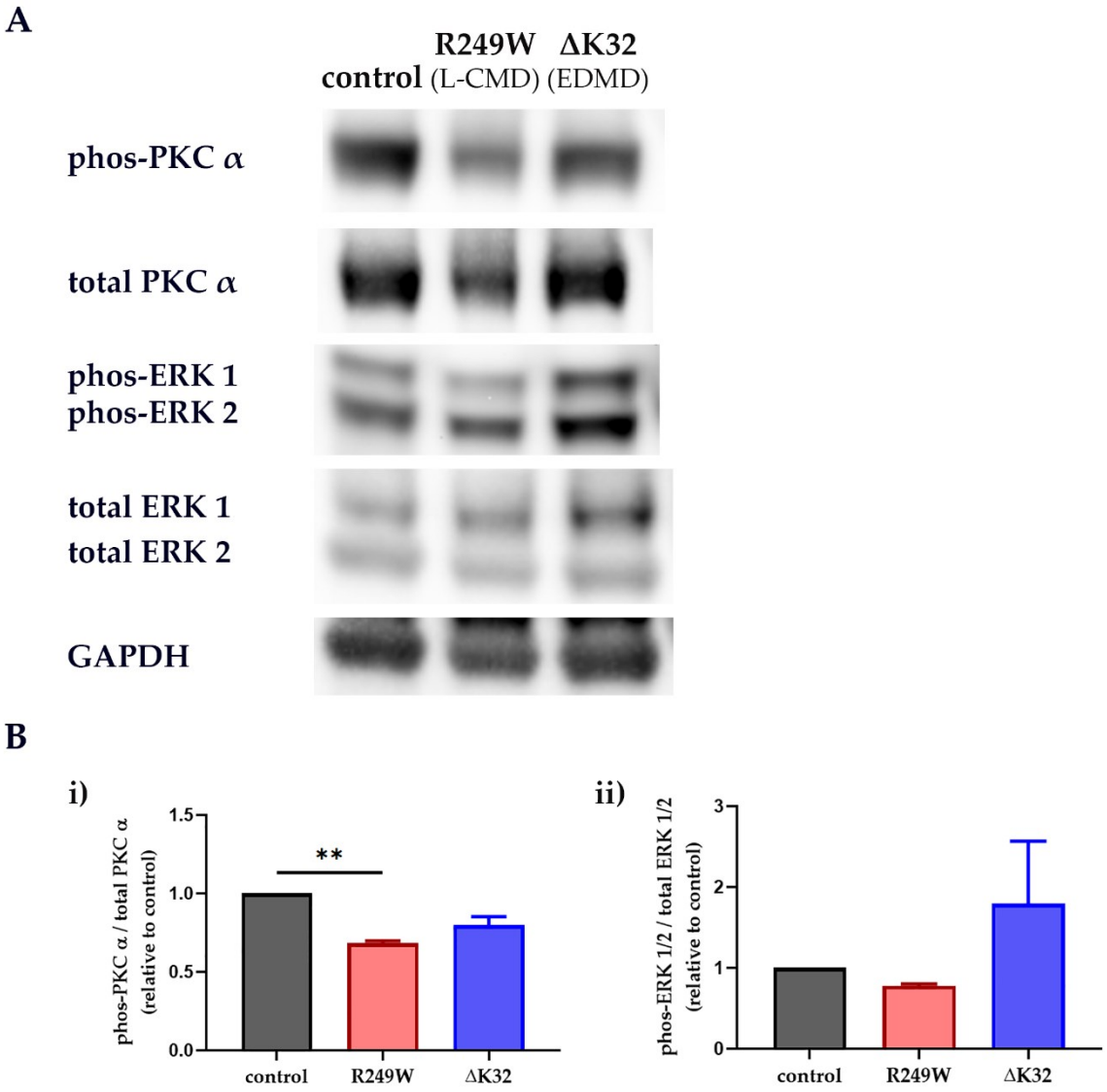

Supplementary Figure 2.5: Western blot analyses for PKC α and ERK 1/2 levels in whole cell protein extracts from human fibroblasts. **(A)** Representative blots for PKC α and ERK 1/2 probings. **(B)** Levels of activated PKC α **(i)** and activated ERK 1/2 **(ii)** are graphed. Mean (± SEM) is shown. n ≥ 2 technical replicates (one patient/group). Significance (*) is set at $p < 0.05$; ** means $p < 0.01$.

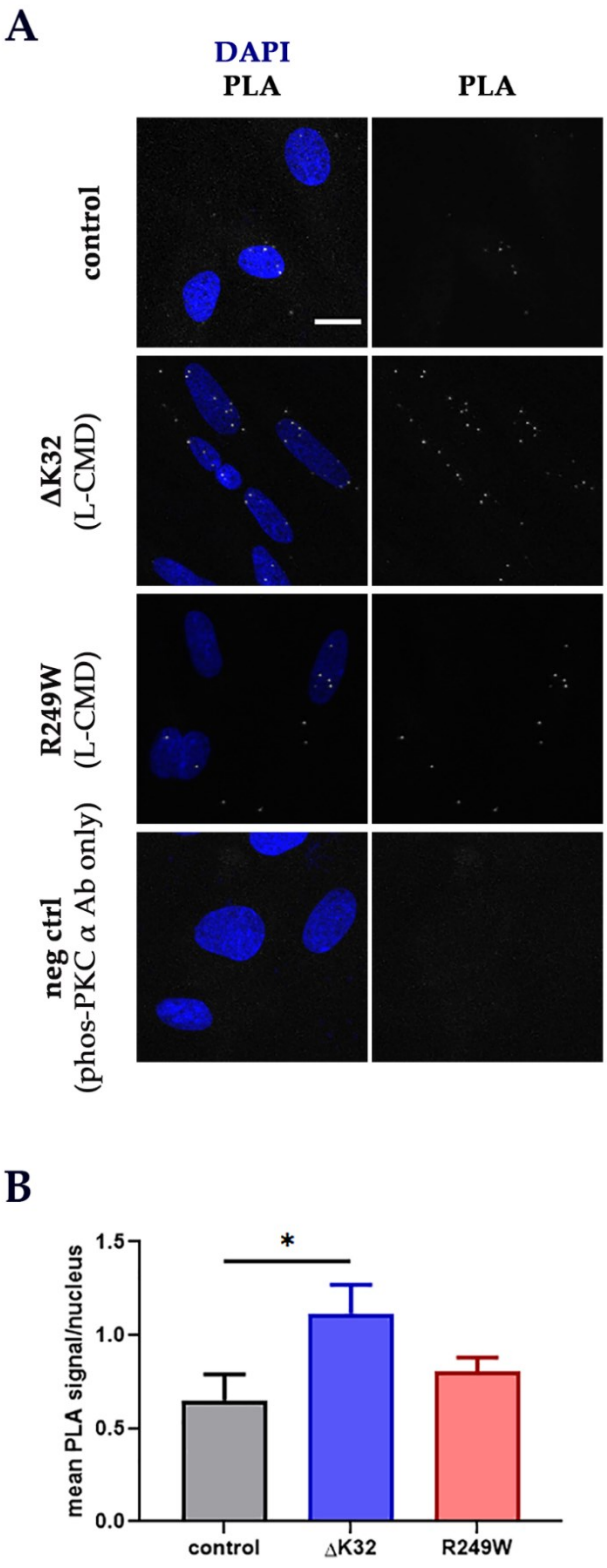

Supplementary Figure 2.6: Proximity ligation assay (PLA) between lamin A/C and phos-PKC α in human fibroblasts **(A)**. The nucleus is stained with DAPI (blue) and the PLA signal representing the proximity of lamin A/C and phos-PKC α is in white. Scale bar: 15 µm for all PLA images. **(B)** Mean (± SEM) PLA signal/nuclei in human fibroblasts**.** n = 2 technical replicates (one patient/group ≥ 115 cells/group are analyzed). Significance (*) is set at $p < 0.0$

Supplementary Table 2.1: List of antibodies and DNA stain used in the study. The respective dilutions for the application(s) are also indicated. IF means immunofluorescence, WB means western blot and PLA means proximity ligation assay.

Antibody/Stain	Application(s)
mouse anti-total PKC α (sc-8393)	IF (1:100), WB (1:500)
mouse anti-B actin (sc-47778)	WB (1:2000)
mouse anti-HSP60 (sc-13115)	IF (1:250)
mouse anti-lamin A/C (sc-376248)	IF/PLA (1:100)
rabbit anti-total PKC α (sc-208)	IF (1:250), WB (1:2000)
rabbit anti-phos PKC α (sc-12356-R)	IF/PLA (1:100), WB (1:2000)
rabbit anti-phos ERK 1/2 (Cell Signaling Technology 9101)	WB (1:2000)
rabbit anti-total ERK 1/2 (Cell Signaling Technology 9102)	WB (1:2000)
rabbit anti-HDAC1 (Ab33278)	WB (1:2000)
rabbit anti-GAPDH (Ab22555)	WB (1:15000)
goat anti-lamin A/C (sc-6215)	WB (1:2000)
anti-mouse Alexa Fluor 488 or 594 or 647	IF (1:500)
anti-rabbit Alexa Fluor 488 or 594	IF (1:500)
anti-rabbit or anti-mouse or anti-goat HRP-conjugated secondary	WB (1:5000)
DAPI	IF (1:5000)

2.8 Acknowledgements

Experiments in this study were funded by the Heart and Stroke Foundation Grant NA 6628 (F.T.), CIHR grant DEV312217 (M-A.A.) and INSERM, the Association Institut de Myologie (AIM) and Sorbonne Université-Médecine (G.B.). Funding for the research stay of H.A.N. at the Myology Institute in Paris was provided by the University of Ottawa's Faculty of Science graduate office, and the University of Ottawa Centre for Research Opportunities office. We would also like to thank Dr. Gilles Lamothe (Department of Mathematics, University of Ottawa) for his guidance in the statistical analyses of the data, Dr. Laura Trinkle-Mulcahy (Department of Cellular and Molecular Medicine, University of Ottawa) for her critiques on the image analyses, Dr. Laurie Chan (Department of Biology, University of Ottawa) for the H9C2 cells, Dr. Jason Fernandez (formerly from OHRI) for sorting the cells even during after hours, weekends and holidays, Joshua Ivare for help with analyzing the human fibroblasts data, and previous undergraduate students in the Tesson lab for their help in maintaining the cells.

2.9 Conflict of Interest

The authors declare no conflict of interest.

2.10 References

Alam, M. S. (2018). Proximity Ligation Assay (PLA). *Current Protocols in Immunology*, *123*(1), e58. https://doi.org/10.1002/cpim.58

Arimura, T., Helbling-Leclerc, A., Massart, C., Varnous, S., Niel, F., Lacene, E., Fromes, Y., Toussaint, M., Mura, A. M., Keller, D. I., Amthor, H., Isnard, R., Malissen, M., Schwartz, K., & Bonne, G. (2005). Mouse model carrying H222P-Lmna mutation develops muscular dystrophy and dilated cardiomyopathy similar to human striated muscle laminopathies. *Human Molecular Genetics*, *14*(1), 155–169.

Bank, E. M., Ben-Harush, K., Wiesel-Motiuk, N., Barkan, R., Feinstein, N., Lotan, O., Medalia, O., & Gruenbaum, Y. (2011). A laminopathic mutation disrupting lamin filament assembly causes disease-like phenotypes in Caenorhabditis elegans. *Molecular Biology of the Cell*, *22*(15), 2716–2728. https://doi.org/10.1091/mbc.E11-01-0064

Bertrand, A. T., Renou, L., Papadopoulos, A., Beuvin, M., Lacène, E., Massart, C., Ottolenghi, C., Decostre, V., Maron, S., Schlossarek, S., Cattin, M.-E., Carrier, L., Malissen, M., Arimura, T., & Bonne, G. (2012). DelK32-lamin A/C has abnormal location and induces incomplete tissue maturation and severe metabolic defects leading to premature death. *Human Molecular Genetics*, *21*(5), 1037–1048. https://doi.org/10.1093/hmg/ddr534

Bertrand, A. T., Ziaei, S., Ehret, C., Duchemin, H., Mamchaoui, K., Bigot, A., Mayer, M., Quijano-Roy, S., Desguerre, I., Lainé, J., Ben Yaou, R., Bonne, G., & Coirault, C. (2014). Cellular microenvironments reveal defective mechanosensing responses and elevated YAP signaling in LMNA-mutated muscle precursors. *Journal of Cell Science*, *127*(Pt 13), 2873–2884. https://doi.org/10.1242/jcs.144907

Bilinska, Z. T., Sylvius, N., Grzybowski, J., Fidzianska, A., Michalak, E., Walczak, E., Walski, M., Bieganowska, K., Szymaniak, E., Kusmierczyk-Droszcz, B., Lubiszewska, B., Wagner, T., Tesson, F., & Ruzyllo, W. (2006). Dilated cardiomyopathy caused by LMNA mutations. Clinical and morphological studies. *Kardiologia Polska*, *64*(8), 812–819; discussion 820-1.

Bonne, G., Barletta, M. R. D., Varnous, S., Becane, H. M., Hammouda, E. H., Merlini, L., Muntoni, F., Greenberg, C. R., Gary, F., Urtizberea, J. A., Duboc, D., Fardeau, M., Toniolo, D., & Schwartz, K. (1999). Mutations in the gene encoding lamin A/C cause

autosomal dominant Emery-Dreifuss muscular dystrophy. *Nature Genetics*, *21*(3), 285–288.

Bonne, G., Mercuri, E., Muchir, A., Urtizberea, A., Becane, H. M., Recan, D., Merlini, L., Wehnert, M., Boor, R., Reuner, U., Vorgerd, M., Wicklein, E. M., Eymard, B., Duboc, D., Penisson-Besnier, I., Cuisset, J. M., Ferrer, X., Desguerre, I., Lacombe, D., … Muntoni, F. (2000). Clinical and molecular genetic spectrum of autosomal dominant Emery-Dreifuss muscular dystrophy due to mutations of the lamin A/C gene. *Annals of Neurology*, *48*(2), 170–180.

Bonne, Gisèle, & Quijano-Roy, S. (2013). Emery-Dreifuss muscular dystrophy, laminopathies, and other nuclear envelopathies. *Handbook of Clinical Neurology*, *113*, 1367–1376. https://doi.org/10.1016/B978-0-444-59565-2.00007-1

Bornancin, F., & Parker, P. J. (1997). Phosphorylation of protein kinase C-alpha on serine 657 controls the accumulation of active enzyme and contributes to its phosphatase-resistant state. *The Journal of Biological Chemistry*, *272*(6), 3544–3549. https://doi.org/10.1074/jbc.272.6.3544

Borroni, A. P., Emanuelli, A., Shah, P. A., Ilić, N., Apel-Sarid, L., Paolini, B., Manikoth Ayyathan, D., Koganti, P., Levy-Cohen, G., & Blank, M. (2018). Smurf2 regulates stability and the autophagic-lysosomal turnover of lamin A and its disease-associated form progerin. *Aging Cell*, *17*(2). https://doi.org/10.1111/acel.12732

Boudreau, E., Labib, S., Bertrand, A. T., Decostre, V., Bolongo, P. M., Sylvius, N., Bonne, G., & Tesson, F. (2012). Lamin A/C mutants disturb sumo1 localization and sumoylation in vitro and in vivo. *PloS One*, *7*(9), e45918.

Bowling, N., Walsh, R. A., Song, G., Estridge, T., Sandusky, G. E., Fouts, R. L., Mintze, K., Pickard, T., Roden, R., Bristow, M. R., Sabbah, H. N., Mizrahi, J. L., Gromo, G., King, G. L., & Vlahos, C. J. (1999). Increased protein kinase C activity and expression of Ca2+-sensitive isoforms in the failing human heart. *Circulation*, *99*(3), 384–391.

Braz, J. C., Gregory, K., Pathak, A., Zhao, W., Sahin, B., Klevitsky, R., Kimball, T. F., Lorenz, J. N., Nairn, A. C., Liggett, S. B., Bodi, I., Wang, S., Schwartz, A., Lakatta, E. G., DePaoli-Roach, A. A., Robbins, J., Hewett, T. E., Bibb, J. A., Westfall, M. V., … Molkentin, J. D. (2004). PKC-alpha regulates cardiac contractility and propensity toward heart failure. *Nature Medicine*, *10*(3), 248–254.

Braz, Julian C., Bueno, O. F., De Windt, L. J., & Molkentin, J. D. (2002). PKC alpha regulates the hypertrophic growth of cardiomyocytes through extracellular signal-regulated kinase1/2 (ERK1/2). *The Journal of Cell Biology*, *156*(5), 905–919. https://doi.org/10.1083/jcb.200108062

Broers, J. L., Ramaekers, F. C., Bonne, G., Yaou, R. B., & Hutchison, C. J. (2006). Nuclear lamins: Laminopathies and their role in premature ageing. *Physiological Reviews*, *86*(3), 967–1008.

Cazaubon, S., Bornancin, F., & Parker, P. J. (1994). Threonine-497 is a critical site for permissive activation of protein kinase C alpha. *The Biochemical Journal*, *301 (Pt 2)*, 443–448. https://doi.org/10.1042/bj3010443

Choi, J. C., Wu, W., Muchir, A., Iwata, S., Homma, S., & Worman, H. J. (2012). Dual specificity phosphatase 4 mediates cardiomyopathy caused by lamin A/C (LMNA) gene mutation. *The Journal of Biological Chemistry*, *287*(48), 40513–40524. https://doi.org/10.1074/jbc.M112.404541

Colombo, M. G., Botto, N., Vittorini, S., Paradossi, U., & Andreassi, M. G. (2008). Clinical utility of genetic tests for inherited hypertrophic and dilated cardiomyopathies. *Cardiovascular Ultrasound*, *6*, 62. https://doi.org/10.1186/1476-7120-6-62

D'Amico, A., Haliloglu, G., Richard, P., Talim, B., Maugenre, S., Ferreiro, A., Guicheney, P., Menditto, I., Benedetti, S., Bertini, E., Bonne, G., & Topaloglu, H. (2005). Two patients with "Dropped head syndrome" due to mutations in LMNA or SEPN1 genes. *Neuromuscular Disorders: NMD*, *15*(8), 521–524. https://doi.org/10.1016/j.nmd.2005.03.006

Deniset, J. F., Hedley, T. E., Hlaváčková, M., Chahine, M. N., Dibrov, E., O'Hara, K., Maddaford, G. G., Nelson, D., Maddaford, T. G., Fandrich, R., Kardami, E., & Pierce, G. N. (2018). Heat shock protein 60 involvement in vascular smooth muscle cell proliferation. *Cellular Signalling*, *47*, 44–51. https://doi.org/10.1016/j.cellsig.2018.03.011

Disatnik, M. H., Buraggi, G., & Mochly-Rosen, D. (1994). Localization of protein kinase C isozymes in cardiac myocytes. *Experimental Cell Research*, *210*(2), 287–297. https://doi.org/10.1006/excr.1994.1041

Fidzianska, A., Bilinska, Z. T., Tesson, F., Wagner, T., Walski, M., Grzybowski, J., Ruzyllo, W., & Hausmanowa-Petrusewicz, I. (2008). Obliteration of cardiomyocyte nuclear architecture in a patient with LMNA gene mutation. *Journal of the Neurological Sciences*, *271*(1–2), 91–96.

Gavet, O., & Pines, J. (2010). Progressive activation of CyclinB1-Cdk1 coordinates entry to mitosis. *Developmental Cell*, *18*(4), 533–543.

Gigli, M., Stolfo, D., Merlo, M., Barbati, G., Ramani, F., Brun, F., Pinamonti, B., & Sinagra, G. (2017). Insights into mildly dilated cardiomyopathy: Temporal evolution and long-term prognosis. *European Journal of Heart Failure*, *19*(4), 531–539. https://doi.org/10.1002/ejhf.608

Gómez-Domínguez, D., Epifano, C., Miguel, F. de, Castaño, A. G., Vilaplana-Martí, B., Martín, A., Amarilla-Quintana, S., Bertrand, A. T., Bonne, G., Ramón-Azcón, J., Rodríguez-Milla, M. A., & Pérez de Castro, I. (2020). Consequences of Lmna Exon 4 Mutations in Myoblast Function. *Cells*, *9*(5). https://doi.org/10.3390/cells9051286

González, J. M., Navarro-Puche, A., Casar, B., Crespo, P., & Andrés, V. (2008). Fast regulation of AP-1 activity through interaction of lamin A/C, ERK1/2, and c-Fos at the nuclear envelope. *The Journal of Cell Biology*, *183*(4), 653–666. https://doi.org/10.1083/jcb.200805049

Goodnight, J. A., Mischak, H., Kolch, W., & Mushinski, J. F. (1995). Immunocytochemical localization of eight protein kinase C isozymes overexpressed in NIH 3T3 fibroblasts. Isoform-specific association with microfilaments, Golgi, endoplasmic reticulum, and nuclear and cell membranes. *The Journal of Biological Chemistry*, *270*(17), 9991–10001. https://doi.org/10.1074/jbc.270.17.9991

Gysin, S., & Imber, R. (1996). Replacement of Ser657 of protein kinase C-alpha by alanine leads to premature down regulation after phorbol-ester-induced translocation to the membrane. *European Journal of Biochemistry*, *240*(3), 747–750. https://doi.org/10.1111/j.1432-1033.1996.0747h.x

Hambleton, M., Hahn, H., Pleger, S. T., Kuhn, M. C., Klevitsky, R., Carr, A. N., Kimball, T. F., Hewett, T. E., 2nd, G. W. D., Koch, W. J., & Molkentin, J. D. (2006). Pharmacological-

and gene therapy-based inhibition of protein kinase Calpha/beta enhances cardiac contractility and attenuates heart failure. *Circulation*, *114*(6), 574–582.

Hasselberg, N. E., Haland, T. F., Saberniak, J., Brekke, P. H., Berge, K. E., Leren, T. P., Edvardsen, T., & Haugaa, K. H. (2018). Lamin A/C cardiomyopathy: Young onset, high penetrance, and frequent need for heart transplantation. *European Heart Journal*, *39*(10), 853–860. https://doi.org/10.1093/eurheartj/ehx596

Heller, F., Dabaj, I., Mah, J. K., Bergounioux, J., Essid, A., Bönnemann, C. G., Rutkowski, A., Bonne, G., Quijano-Roy, S., & Wahbi, K. (2017). Cardiac manifestations of congenital LMNA-related muscular dystrophy in children: Three case reports and recommendations for care. *Cardiology in the Young*, *27*(6), 1076–1082. https://doi.org/10.1017/S1047951116002079

Hu, R., Morley, M. P., Brandimarto, J., Tucker, N. R., Parsons, V. A., Zhao, S. D., Meder, B., Katus, H. A., Rühle, F., Stoll, M., Villard, E., Cambien, F., Lin, H., Smith, N. L., Felix, J. F., Vasan, R. S., van der Harst, P., Newton-Cheh, C., Li, J., … Cappola, T. P. (2018). Genetic Reduction in Left Ventricular Protein Kinase C-α and Adverse Ventricular Remodeling in Human Subjects. *Circulation. Genomic and Precision Medicine*, *11*(3), e001901. https://doi.org/10.1161/CIRCGEN.117.001901

Itoh, H., Kobayashi, R., Wakui, H., Komatsuda, A., Ohtani, H., Miura, A. B., Otaka, M., Masamune, O., Andoh, H., & Koyama, K. (1995). Mammalian 60-kDa stress protein (chaperonin homolog). Identification, biochemical properties, and localization. *The Journal of Biological Chemistry*, *270*(22), 13429–13435. https://doi.org/10.1074/jbc.270.22.13429

Itoh, Hideaki, Komatsuda, A., Ohtani, H., Wakui, H., Imai, H., Sawada, K.-I., Otaka, M., Ogura, M., Suzuki, A., & Hamada, F. (2002). Mammalian HSP60 is quickly sorted into the mitochondria under conditions of dehydration. *European Journal of Biochemistry*, *269*(23), 5931–5938. https://doi.org/10.1046/j.1432-1033.2002.03317.x

Ivorra, C., Kubicek, M., González, J. M., Sanz-González, S. M., Alvarez-Barrientos, A., O'Connor, J.-E., Burke, B., & Andrés, V. (2006). A mechanism of AP-1 suppression through interaction of c-Fos with lamin A/C. *Genes & Development*, *20*(3), 307–320. https://doi.org/10.1101/gad.349506

Jensen, T. E., Maarbjerg, S. J., Rose, A. J., Leitges, M., & Richter, E. A. (2009). Knockout of the predominant conventional PKC isoform, PKCalpha, in mouse skeletal muscle does not affect contraction-stimulated glucose uptake. *American Journal of Physiology.Endocrinology and Metabolism*, *297*(2), E340-8.

Keranen, L. M., Dutil, E. M., & Newton, A. C. (1995). Protein kinase C is regulated in vivo by three functionally distinct phosphorylations. *Current Biology : CB*, *5*(12), 1394–1403. https://doi.org/10.1016/s0960-9822(95)00277-6

Ladage, D., Tilemann, L., Ishikawa, K., Correll, R. N., Kawase, Y., Houser, S. R., Molkentin, J. D., & Hajjar, R. J. (2011). Inhibition of PKCα/β with ruboxistaurin antagonizes heart failure in pigs after myocardial infarction injury. *Circulation Research*, *109*(12), 1396–1400. https://doi.org/10.1161/CIRCRESAHA.111.255687

Leitges, M., Plomann, M., Standaert, M. L., Bandyopadhyay, G., Sajan, M. P., Kanoh, Y., Farese, R. V., & Letiges, M. (2002). Knockout of PKC alpha enhances insulin signaling through PI3K. *Molecular Endocrinology (Baltimore, Md.)*, *16*(4), 847–858. https://doi.org/10.1210/mend.16.4.0809

Liu, Q., Chen, X., Macdonnell, S. M., Kranias, E. G., Lorenz, J. N., Leitges, M., Houser, S. R., & Molkentin, J. D. (2009). Protein kinase Calpha, but not PKCbeta or PKCgamma, regulates contractility and heart failure susceptibility: Implications for ruboxistaurin as a novel therapeutic approach. *Circulation Research*, *105*(2), 194–200.

Lloyd, D. J., Trembath, R. C., & Shackleton, S. (2002). A novel interaction between lamin A and SREBP1: Implications for partial lipodystrophy and other laminopathies. *Human Molecular Genetics*, *11*(7), 769–777.

Martelli, A. M., Bortul, R., Tabellini, G., Faenza, I., Cappellini, A., Bareggi, R., Manzoli, L., & Cocco, L. (2002). Molecular characterization of protein kinase C-alpha binding to lamin A. *Journal of Cellular Biochemistry*, *86*(2), 320–330.

Mattioli, E., Andrenacci, D., Garofalo, C., Prencipe, S., Scotlandi, K., Remondini, D., Gentilini, D., Di Blasio, A. M., Valente, S., Scarano, E., Cicchilitti, L., Piaggio, G., Mai, A., & Lattanzi, G. (2018). Altered modulation of lamin A/C-HDAC2 interaction and p21 expression during oxidative stress response in HGPS. *Aging Cell*, *17*(5), e12824. https://doi.org/10.1111/acel.12824

Mauro, A., Ciccarelli, C., Cesaris, P. D., Scoglio, A., Bouche, M., Molinaro, M., Aquino, A., & Zani, B. M. (2002). PKCalpha-mediated ERK, JNK and p38 activation regulates the myogenic program in human rhabdomyosarcoma cells. *Journal of Cell Science*, *115*(Pt 18), 3587–3599.

Meng, Q., Li, B. X., & Xiao, X. (2018). Toward Developing Chemical Modulators of Hsp60 as Potential Therapeutics. *Frontiers in Molecular Biosciences*, *5*, 35. https://doi.org/10.3389/fmolb.2018.00035

Muchir, A., Kim, Y. J., Reilly, S. A., Wu, W., Choi, J. C., & Worman, H. J. (2013). Inhibition of extracellular signal-regulated kinase 1/2 signaling has beneficial effects on skeletal muscle in a mouse model of Emery-Dreifuss muscular dystrophy caused by lamin A/C gene mutation. *Skeletal Muscle*, *3*(1), 17-5040-3–17.

Muchir, A., Medioni, J., Laluc, M., Massart, C., Arimura, T., van der Kooi, A. J., Desguerre, I., Mayer, M., Ferrer, X., Briault, S., Hirano, M., Worman, H. J., Mallet, A., Wehnert, M., Schwartz, K., & Bonne, G. (2004). Nuclear envelope alterations in fibroblasts from patients with muscular dystrophy, cardiomyopathy, and partial lipodystrophy carrying lamin A/C gene mutations. *Muscle & Nerve*, *30*(4), 444–450. https://doi.org/10.1002/mus.20122

Muchir, A., Pavlidis, P., Decostre, V., Herron, A. J., Arimura, T., Bonne, G., & Worman, H. J. (2007). Activation of MAPK pathways links LMNA mutations to cardiomyopathy in Emery-Dreifuss muscular dystrophy. *The Journal of Clinical Investigation*, *117*(5), 1282–1293.

Muchir, A., Reilly, S. A., Wu, W., Iwata, S., Homma, S., Bonne, G., & Worman, H. J. (2012). Treatment with selumetinib preserves cardiac function and improves survival in cardiomyopathy caused by mutation in the lamin A/C gene. *Cardiovascular Research*, *93*(2), 311–319.

Muchir, A., Shan, J., Bonne, G., Lehnart, S. E., & Worman, H. J. (2009). Inhibition of extracellular signal-regulated kinase signaling to prevent cardiomyopathy caused by mutation in the gene encoding A-type lamins. *Human Molecular Genetics*, *18*(2), 241–247.

Muchir, A., Wu, W., Choi, J. C., Iwata, S., Morrow, J., Homma, S., & Worman, H. J. (2012). Abnormal p38alpha mitogen-activated protein kinase signaling in dilated cardiomyopathy caused by lamin A/C gene mutation. *Human Molecular Genetics*, *21*(19), 4325–4333.

Myant, K., Qiao, X., Halonen, T., Come, C., Laine, A., Janghorban, M., Partanen, J. I., Cassidy, J., Ogg, E.-L., Cammareri, P., Laiterä, T., Okkeri, J., Klefström, J., Sears, R. C., Sansom, O. J., & Westermarck, J. (2015). Serine 62-Phosphorylated MYC Associates with Nuclear Lamins and Its Regulation by CIP2A Is Essential for Regenerative Proliferation. *Cell Reports*, *12*(6), 1019–1031. https://doi.org/10.1016/j.celrep.2015.07.003

Nakashima, S. (2002). Protein kinase C alpha (PKC alpha): Regulation and biological function. *Journal of Biochemistry*, *132*(5), 669–675.

Naskar, S., Datta, K., Mitra, A., Pathak, K., Datta, R., Bansal, T., & Sarkar, S. (2014). Differential and conditional activation of PKC-isoforms dictates cardiac adaptation during physiological to pathological hypertrophy. *PloS One*, *9*(8), e104711.

Parekh, D. B., Ziegler, W., & Parker, P. J. (2000). Multiple pathways control protein kinase C phosphorylation. *The EMBO Journal*, *19*(4), 496–503. https://doi.org/10.1093/emboj/19.4.496

Pasotti, M., Klersy, C., Pilotto, A., Marziliano, N., Rapezzi, C., Serio, A., Mannarino, S., Gambarin, F., Favalli, V., Grasso, M., Agozzino, M., Campana, C., Gavazzi, A., Febo, O., Marini, M., Landolina, M., Mortara, A., Piccolo, G., Viganò, M., … Arbustini, E. (2008). Long-term outcome and risk stratification in dilated cardiolaminopathies. *Journal of the American College of Cardiology*, *52*(15), 1250–1260. https://doi.org/10.1016/j.jacc.2008.06.044

Pass, J. M., Gao, J., Jones, W. K., Wead, W. B., Wu, X., Zhang, J., Baines, C. P., Bolli, R., Zheng, Y. T., Joshua, I. G., & Ping, P. (2001). Enhanced PKC beta II translocation and PKC beta II-RACK1 interactions in PKC epsilon-induced heart failure: A role for RACK1. *American Journal of Physiology. Heart and Circulatory Physiology*, *281*(6), H2500-2510. https://doi.org/10.1152/ajpheart.2001.281.6.H2500

Ping, P., Zhang, J., Qiu, Y., Tang, X. L., Manchikalapudi, S., Cao, X., & Bolli, R. (1997). Ischemic preconditioning induces selective translocation of protein kinase C isoforms epsilon and eta in the heart of conscious rabbits without subcellular redistribution of total protein kinase C activity. *Circulation Research*, *81*(3), 404–414. https://doi.org/10.1161/01.res.81.3.404

Pinto, Y. M., Elliott, P. M., Arbustini, E., Adler, Y., Anastasakis, A., Böhm, M., Duboc, D., Gimeno, J., de Groote, P., Imazio, M., Heymans, S., Klingel, K., Komajda, M., Limongelli, G., Linhart, A., Mogensen, J., Moon, J., Pieper, P. G., Seferovic, P. M., … Charron, P. (2016). Proposal for a revised definition of dilated cardiomyopathy, hypokinetic non-dilated cardiomyopathy, and its implications for clinical practice: A position statement of the ESC working group on myocardial and pericardial diseases. *European Heart Journal*, *37*(23), 1850–1858. https://doi.org/10.1093/eurheartj/ehv727

Quijano-Roy, S., Mbieleu, B., Bönnemann, C. G., Jeannet, P.-Y., Colomer, J., Clarke, N. F., Cuisset, J.-M., Roper, H., De Meirleir, L., D'Amico, A., Ben Yaou, R., Nascimento, A., Barois, A., Demay, L., Bertini, E., Ferreiro, A., Sewry, C. A., Romero, N. B., Ryan, M., … Estournet, B. (2008). De novo LMNA mutations cause a new form of congenital muscular dystrophy. *Annals of Neurology*, *64*(2), 177–186. https://doi.org/10.1002/ana.21417

Reimann, L., Wiese, H., Leber, Y., Schwäble, A. N., Fricke, A. L., Rohland, A., Knapp, B., Peikert, C. D., Drepper, F., van der Ven, P. F. M., Radziwill, G., Fürst, D. O., & Warscheid, B. (2017). Myofibrillar Z-discs Are a Protein Phosphorylation Hot Spot with Protein Kinase C (PKCα) Modulating Protein Dynamics. *Molecular & Cellular Proteomics: MCP*, *16*(3), 346–367. https://doi.org/10.1074/mcp.M116.065425

Rodríguez, J., Calvo, F., González, J. M., Casar, B., Andrés, V., & Crespo, P. (2010). ERK1/2 MAP kinases promote cell cycle entry by rapid, kinase-independent disruption of retinoblastoma-lamin A complexes. *The Journal of Cell Biology*, *191*(5), 967–979. https://doi.org/10.1083/jcb.201004067

Rouet-Benzineb, P., Mohammadi, K., Pérennec, J., Poyard, M., Bouanani Nel-H, null, & Crozatier, B. (1996). Protein kinase C isoform expression in normal and failing rabbit hearts. *Circulation Research*, *79*(2), 153–161. https://doi.org/10.1161/01.res.79.2.153

Samson, C., Petitalot, A., Celli, F., Herrada, I., Ropars, V., Le Du, M.-H., Nhiri, N., Jacquet, E., Arteni, A.-A., Buendia, B., & Zinn-Justin, S. (2018). Structural analysis of the ternary complex between lamin A/C, BAF and emerin identifies an interface disrupted in autosomal recessive progeroid diseases. *Nucleic Acids Research*, *46*(19), 10460–10473. https://doi.org/10.1093/nar/gky736

Schmalz, D., Kalkbrenner, F., Hucho, F., & Buchner, K. (1996). Transport of protein kinase C alpha into the nucleus requires intact cytoskeleton while the transport of a protein containing a canonical nuclear localization signal does not. *Journal of Cell Science*, *109 (Pt 9)*(Pt 9), 2401–2406.

Schönwasser, D. C., Marais, R. M., Marshall, C. J., & Parker, P. J. (1998). Activation of the mitogen-activated protein kinase/extracellular signal-regulated kinase pathway by

conventional, novel, and atypical protein kinase C isotypes. *Molecular and Cellular Biology*, *18*(2), 790–798. https://doi.org/10.1128/mcb.18.2.790

Simon, D. N., Zastrow, M. S., & Wilson, K. L. (2010). Direct actin binding to A- and B-type lamin tails and actin filament bundling by the lamin A tail. *Nucleus (Austin, Tex.)*, *1*(3), 264–272. https://doi.org/10.4161/nucl.1.3.11799

Soh, J. W., Lee, E. H., Prywes, R., & Weinstein, I. B. (1999). Novel roles of specific isoforms of protein kinase C in activation of the c-fos serum response element. *Molecular and Cellular Biology*, *19*(2), 1313–1324.

Soh, J.-W., & Weinstein, I. B. (2003). Roles of specific isoforms of protein kinase C in the transcriptional control of cyclin D1 and related genes. *The Journal of Biological Chemistry*, *278*(36), 34709–34716. https://doi.org/10.1074/jbc.M302016200

Song, X., Qian, X., Shen, M., Jiang, R., Wagner, M. B., Ding, G., Chen, G., & Shen, B. (2015). Protein kinase C promotes cardiac fibrosis and heart failure by modulating galectin-3 expression. *Biochimica Et Biophysica Acta*, *1853*(2), 513–521. https://doi.org/10.1016/j.bbamcr.2014.12.001

Sylvius, N., Bilinska, Z. T., Veinot, J. P., Fidzianska, A., Bolongo, P. M., Poon, S., McKeown, P., Davies, R. A., Chan, K. L., Tang, A. S., Dyack, S., Grzybowski, J., Ruzyllo, W., McBride, H., & Tesson, F. (2005). In vivo and in vitro examination of the functional significances of novel lamin gene mutations in heart failure patients. *Journal of Medical Genetics*, *42*(8), 639–647.

Taylor, M. R., Fain, P. R., Sinagra, G., Robinson, M. L., Robertson, A. D., Carniel, E., Lenarda, A. D., Bohlmeyer, T. J., Ferguson, D. A., Brodsky, G. L., Boucek, M. M., Lascor, J., Moss, A. C., Li, W. L., Stetler, G. L., Muntoni, F., Bristow, M. R., Mestroni, L., &

Group, F. D. C. R. R. (2003). Natural history of dilated cardiomyopathy due to lamin A/C gene mutations. *Journal of the American College of Cardiology*, *41*(5), 771–780.

Tesson, F., Saj, M., Uvaize, M. M., Nicolas, H., Płoski, R., & Bilińska, Z. (2014). Lamin A/C mutations in dilated cardiomyopathy. *Cardiology Journal*, *21*(4), 331–342. https://doi.org/10.5603/CJ.a2014.0037

Vadrot, N., Duband-Goulet, I., Cabet, E., Attanda, W., Barateau, A., Vicart, P., Gerbal, F., Briand, N., Vigouroux, C., Oldenburg, A. R., Lund, E. G., Collas, P., & Buendia, B. (2015). The p.R482W substitution in A-type lamins deregulates SREBP1 activity in Dunnigan-type familial partial lipodystrophy. *Human Molecular Genetics*, *24*(7), 2096–2109. https://doi.org/10.1093/hmg/ddu728

van Berlo, J. H., de Voogt, W. G., van der Kooi, A. J., van Tintelen, J. P., Bonne, G., Yaou, R. B., Duboc, D., Rossenbacker, T., Heidbüchel, H., de Visser, M., Crijns, H. J. G. M., & Pinto, Y. M. (2005). Meta-analysis of clinical characteristics of 299 carriers of LMNA gene mutations: Do lamin A/C mutations portend a high risk of sudden death? *Journal of Molecular Medicine (Berlin, Germany)*, *83*(1), 79–83. https://doi.org/10.1007/s00109-004-0589-1

Vytopil, M., Ricci, E., Dello Russo, A., Hanisch, F., Neudecker, S., Zierz, S., Ricotti, R., Demay, L., Richard, P., Wehnert, M., Bonne, G., Merlini, L., & Toniolo, D. (2002). Frequent low penetrance mutations in the Lamin A/C gene, causing Emery Dreifuss muscular dystrophy. *Neuromuscular Disorders: NMD*, *12*(10), 958–963.

Wang, J., Liu, X., Arneja, A. S., & Dhalla, N. S. (1999). Alterations in protein kinase A and protein kinase C levels in heart failure due to genetic cardiomyopathy. *The Canadian Journal of Cardiology*, *15*(6), 683–690.

Wang, Jingwei, Liu, X., Sentex, E., Takeda, N., & Dhalla, N. S. (2003). Increased expression of protein kinase C isoforms in heart failure due to myocardial infarction. *American Journal of Physiology. Heart and Circulatory Physiology*, *284*(6), H2277-2287. https://doi.org/10.1152/ajpheart.00142.2002

Wu, W., Iwata, S., Homma, S., Worman, H. J., & Muchir, A. (2014). Depletion of extracellular signal-regulated kinase 1 in mice with cardiomyopathy caused by lamin A/C gene mutation partially prevents pathology before isoenzyme activation. *Human Molecular Genetics*, *23*(1), 1–11.

Wu, W., Muchir, A., Shan, J., Bonne, G., & Worman, H. J. (2011). Mitogen-activated protein kinase inhibitors improve heart function and prevent fibrosis in cardiomyopathy caused by mutation in lamin A/C gene. *Circulation*, *123*(1), 53–61.

Zwerger, M., Jaalouk, D. E., Lombardi, M. L., Isermann, P., Mauermann, M., Dialynas, G., Herrmann, H., Wallrath, L. L., & Lammerding, J. (2013). Myopathic lamin mutations impair nuclear stability in cells and tissue and disrupt nucleo-cytoskeletal coupling. *Human Molecular Genetics*, *22*(12), 2335–2349. https://doi.org/10.1093/hmg/ddt079

Chapter 3

A CRISPR/Cas9 zebrafish lamin A/C mutant model of muscular laminopathy

3.1 Notes on Chapter 3

3.1.a Study Introduction and Objectives

While cellular models provide phenotype characterization at a cellular and molecular level, animal models allow for further study of how such underlying molecular mechanisms manifest in an organism. Previous work on morpholino *lmna* knockdown and transgenic expression of EDMD lamin A/C variants in zebrafish demonstrated zebrafish's capacity to mimic the phenotype of patients and other animal models of striated muscle laminopathies. As such, we created zebrafish with stable *lmna* interruption, and assessed the cardiac and skeletal muscle structure and function of the *lmna* mutants. Expression and activation levels of genes and proteins previously associated with striated muscle laminopathies were assessed as well to determine if the *lmna* mutants share the same molecular disturbances observed in patients and other models of striated muscle laminopathies. Lastly, PKC α expression and activation were also examined to determine if these are affected in the *lmna* mutants. The results from this study constitute a manuscript in preparation for PLoS ONE.

3.1.b Author Contributions:

HA. Nicolas – conceptualized and performed most of the experiments and data analyses, drafted the manuscript

K. Hua – performed RNA extraction, qRT experiments and analyses, scored cardiac function, edited the manuscript

F. Tesson – conceptualized and funded experiments, edited the manuscript

MA. Akimenko – conceptualized and funded experiments, edited the manuscript

3.2 Abstract

Pathogenic mutations in the lamin A/C gene (*LMNA*) frequently result in cardiac and/or skeletal muscle diseases referred to as striated muscle laminopathies. We created a zebrafish muscular laminopathy model using CRISPR/Cas9 technology to target the zebrafish *lmna* gene. Both heterozygous and homozygous *lmna* mutants present skeletal muscle damage at 1 day post fertilization (dpf), and mobility impairment at 4-7 dpf. Cardiac structure and function analyses during the first week of development show mild and transient defects in the *lmna* mutants compared to wild type fish. Quantitative PCR analysis of genes implicated in striated muscle laminopathies show a decrease in *jun* and *nfκb2* expression in 7 dpf homozygous *lmna* mutants compared to wild type larvae. In addition, homozygous *lmna* mutants have a 1.38 fold increase in activated (phosphorylated) ERK 1/2, which are kinases associated with striated muscle laminopathies, compared to wild type larvae at 7 dpf. Activated (phosphorylated) Protein Kinase C alpha (Pkc α), a kinase that binds lamin A/C and many lamin A/C-binding partners including Erk 1/2, is also upregulated in the 7 dpf homozygous *lmna* mutants compared to wild type larvae. Overall, this study presents an animal model of skeletal muscle laminopathy where both heterozygous and homozygous *lmna* mutants exhibit prominent skeletal muscle abnormalities during the first week of development. Furthermore, this is the first animal model that potentially implicates Pkc α in muscular laminopathies.

3.3 Introduction

The lamin A/C gene (*LMNA)* encodes the type V intermediate filaments A-type lamins, which are found in the nucleus and are major components of the nuclear lamina. Lamin A/C supports the nuclear membrane and participates in various nuclear functions such as regulation of gene expression (Broers et al., 2006; Ivorra et al., 2006). Pathogenic *LMNA* mutations cause a

group of diseases that affect different tissue types with about 79% of these mutations resulting in cardiac and/or skeletal muscles conditions that are collectively termed striated muscle laminopathies (Tesson et al., 2014).

The skeletal muscle diseases Emery-Dreifuss muscular dystrophy (EDMD), *LMNA*-related congenital muscular dystrophy (L-CMD) and Limb-girdle muscular dystrophy (LGMD1B) are myopathies that are primarily caused by autosomal dominant *LMNA* mutations (Bonne & Quijano-Roy, 2013). EDMD is an early onset disease defined by joint contractures and wasting of the muscles in the humeroperoneal region (Bonne et al., 2000). In addition, EDMD patients frequently develop cardiac conditions such as dilated cardiomyopathy (DCM) and/or conduction defects (Bonne & Quijano-Roy, 2013). DCM is characterized by dilation of the left or both ventricles and systolic dysfunction not resulting from abnormal cardiac loading or coronary artery disease (Pinto et al., 2016). L-CMD shares some clinical features with EDMD but has an earlier disease onset and more severe muscular degeneration with some patients lacking neck muscle control (dropped head syndrome) (Bonne & Quijano-Roy, 2013). LGMD1B has a slower progression and predominantly affects different muscle groups than EDMD; however, LGMD1B patients also present cardiac conduction defects with age related penetrance (Muchir et al., 2000; Vytopil et al., 2002). DCM is the most common type of cardiomyopathy (Wexler et al., 2009). Patients with DCM caused by lamin A/C mutations frequently present with conduction defects (Colombo et al., 2008). As such, *LMNA*-caused DCM results in poorer patient outcomes compared to other familial DCM (Hasselberg et al., 2018; Pasotti et al., 2008; Taylor et al., 2003; van Berlo et al., 2005).

Various cellular and animal models of striated muscle laminopathies have been created and used to study signaling pathways associated with cardiac and muscular laminopathies. These models were recently reviewed in (Nicolas et al., 2019). The serine/threonine kinases ERKs 1 and

2 of the MAP kinase signaling pathway are upregulated and activated in heart tissues of some patients with *LMNA*-associated cardiomyopathy, as well as in cardiac and skeletal muscle samples from the H222P lamin A/C EDMD mice model (Muchir et al., 2007, 2012, 2013). Treatment of the H222P mice with an ERK 1/2 inhibitor improves the cardiac and skeletal function and tissue histology of the H222P mice, and normalizes the H222P mice's abnormal gene expression profile (Muchir, Shan, et al., 2009; Muchir et al., 2012, 2013; Wu et al., 2011). In addition, JUN, a downstream target of the JNK branch of the MAP kinase signaling pathway, is upregulated in heart tissues from the H222P mice compared to wild type (WT) (Muchir et al., 2007). JNK inhibition is shown to either delay the onset of cardiac dilation or improve cardiac function in symptomatic H222P mice and lower the transcript levels of cardiac disease markers (Wu et al., 2010, 2011). Gene transcription regulated by the NF-κB signaling pathway is also decreased in mechanically or cytokine-stimulated mouse embryo fibroblasts of a mice model that produces a truncated lamin A (Jahn et al., 2012; Lammerding et al., 2004; Sullivan et al., 1999).

Protein Kinase C α (PKC α) is a serine/threonine lamin A/C-binding kinase encoded by the *PRKCA* gene (Martelli et al., 2002; Nakashima, 2002). It regulates the activation of members of various signaling pathways such as ERK 1/2 of the MAP kinase cascade (Braz et al., 2002; Kim et al., 2014; Leitges et al., 2002; Mauro et al., 2002; Nakashima, 2002; Naskar et al., 2014; Schönwasser et al., 1998). PKC α is the predominant conventional PKC isoform in rabbit and adult human hearts, and in mouse hearts and skeletal muscles (Hambleton et al., 2006; Jensen et al., 2009; Pass et al., 2001; Ping et al., 1997). Furthermore, PKC α is important in cardiac contraction as it regulates intracellular calcium levels (Braz et al., 2004). Abnormal PKC α activation and expression is associated with heart failure and DCM in humans, and the inhibition or genetic abrogation of PKC α in heart failure (HF) animal models results in improvement of cardiac

function (Bowling et al., 1999; Braz et al., 2004; Hu et al., 2018; Ladage et al., 2011; Wang et al., 2003). In addition, PKC α is involved in skeletal muscle structure and function by regulating protein filamin C (FLNc) which is critical for anchoring actin and establishing the Z-discs structure (Leber et al., 2016; Reimann et al., 2017). Phosphorylation of FLNc by PKC α prevents FLNc cleavage; thus affecting FLNc kinetics and mobility (Reimann et al., 2017). Altogether, these data implicate PKC α in cardiac and skeletal muscle structure and function.

Zebrafish are an established model of multiple cardiac and skeletal muscle diseases (Bassett & Currie, 2003; Li et al., 2017; Seeley et al., 2007; Steffen et al., 2007; Verma & Parnaik, 2017; Vogel et al., 2009; Xu et al., 2002). Many of the zebrafish genes and molecular mechanisms underlying skeletal muscle development and function have a mammalian counterpart (Bassett & Currie, 2003; Li et al., 2017; Steffen et al., 2007). Various muscular dystrophies are modelled in zebrafish including the *dmd* zebrafish morphants and mutants mimicking Duchenne muscular dystrophy (Bassett et al., 2003; Berger et al., 2010). Similarly, zebrafish models of different cardiac diseases such as DCM (e.g. titin morphants and mutants, lamin A/C morphants and transgenics) are created (Seeley et al., 2007; Verma & Parnaik, 2017; Vogel et al., 2009; Xu et al., 2002). Despite the genome duplication event that occurred in the teleost lineage, there is only one lamin A/C gene (*lmna*) in the zebrafish genome. Both the human and zebrafish lamin A/C genes have 12 exons encoding for the lamin A and C proteins. Zebrafish lamins A and C transcripts are similar up until exon 8 after which lamin C retains the first six nucleotides of intron 9. (Koshimizu et al., 2011). These six nucleotides are then translated to two lamin C-specific amino acids (a.a) that precede the stop codon (Koshimizu et al., 2011). All introns are spliced out to generate the lamin A transcript. Human lamins A and C share the first 566 a.a after which mature lamin A has an additional 80 unique a.a and lamin C possesses six unique a.a. In zebrafish, lamin A has 659

a.a while lamin C has 554 a.a (Koshimizu et al., 2011). Lamins are highly conserved and zebrafish prelamin A shares 67% amino acid identity with human prelamin A. Lamins A and C form distinct but interacting networks in the nuclear lamina, and both networks provide structural and mechanical support for the nucleus (Lammerding et al., 2006; Shimi et al., 2015). Nevertheless, while many of the properties and functions of lamins A and C overlap, some differences exist such as the differential effect of some lamin A/C mutations on the respective capacities of lamins A and C to bind a partner (Motsch et al., 2005; Sylvius et al., 2008). Like mammalian lamin A/C, zebrafish *lmna* is expressed ubiquitously with the lamin A/C proteins localized underneath the nuclear membrane (Koshimizu et al., 2011; Vogel et al., 2009). Mammalian lamins A and C are expressed at comparable levels in the heart and skeletal muscles but zebrafish lamin A is shown to be more abundant than zebrafish lamin C in adult zebrafish hearts (Al-Saaidi & Bross, 2015; Koshimizu et al., 2011). However, in the brain, lamin C is more highly expressed in both mammals and zebrafish (Jung et al., 2012; Koshimizu et al., 2011).

Functional analysis in zebrafish using morpholino-mediated gene knockdown of *lmna* results in bradycardia, progressive decrease in fractional shortening from 2 – 4 dpf as well as slow muscle fibre damage at 1 dpf and disrupted nuclear membrane (Koshimizu et al., 2011; Vogel et al., 2009). Zebrafish transgenics with cardiac-specific expression of EDMD lamin A/C variants also present increased heart rates at 3.5 and 5.5 dpf compared to WT, and disrupted nuclear membrane (Verma & Parnaik, 2017). Altogether, these results demonstrate the ability to simulate striated muscle laminopathies in zebrafish. However, since morpholino-mediated gene knockdown is transient, we created zebrafish *lmna* mutants with five base pair deletion (5bp Δ) in exon 2 of *lmna* using the CRISPR/Cas9 technology to allow for long term analysis of *lmna* mutants. Both heterozygous and homozygous *lmna* mutants present with skeletal muscle structure defects and

impaired swimming. On the other hand, the cardiac structure and function impairment in the *lmna* mutants is mild and transient. Expression of *jun* and *nfkb2* is decreased while activated (phosphorylated) Pkc α and Erk 1/2 are increased in the *lmna* mutants suggesting that similar molecular pathways to the ones implicated in patients and other models of striated muscle laminopathies are also affected in the zebrafish *lmna* mutants. Furthermore, our results suggest that Pkc α is potentially involved in muscular laminopathies.

3.4 Materials Methods

Zebrafish Husbandry and Maintenance

Zebrafish were housed in a controlled environment room (28.5°C room and water temperature; 14 h light/10 h dark cycle). Animal handling and experimentation followed the guidelines set by the Canadian Council on Animal Care (under the Ontario Animals for Research Act). The approved institute ethics protocol ID is BL 2399-R3 A1.

Cas9 mRNA and Guide RNA synthesis

The process of creating a CRISPR zebrafish mutant was based on (Hwang et al., 2013; Hwang et al., 2013). The ZiFit program for CRISPR/Cas9 Nucleases was used to identify potential guide RNA (gRNA) sequences in zebrafish lamin A/C (sequence ID: NM_152971) (Sander et al., 2007, 2010). The selected gRNA sequence in the second translated exon of the zebrafish lamin A/C gene was: 5'GGGGGAGAAGAGAACACTGG'3. The exon 2 gRNA oligonucleotide was inserted between the BsaI and DraI restriction sites of the pDR274 plasmid and transcribed using the mMessage mMachine® T7 kit (Ambion) following the manufacturer's protocol. The Cas9 mRNA was prepared according to (Hwang et al., 2013). Briefly, the Cas9 mRNA was transcribed from the MLM3613 (Addgene 42251) plasmid which was linearized at the Not1 site. Cas9 mRNA transcription was then performed using the mMessage mMachine® T7 kit (Ambion) following the

manufacturer's protocol. The Cas9/gRNA micro-injection solution was prepared based on (Hwang et al., 2013; Hwang et al., 2013). About 1-2 nL of the micro-injection solution (1 µL of Cas9 mRNA [720 ng/µL stock] + 1µL of exon 2 gRNA [30 ng/µL stock] + 0.4 µL of 0.5% phenol red) was micro-injected into one-cell stage WT zebrafish embryos. Micro-injected zebrafish were raised to adulthood and screened for germline transmission of *lmna* mutation through natural breeding.

DNA extraction and genotyping

DNA extraction of WT and mutant *lmna* zebrafish was performed based on (Meeker et al., 2007). PCR was run using these primers - *lmna* Fwd primer 1: 5' GAACGGTAAGAAAGAAGCAG 3' and *lmna* Rev primer 1: 5' AATTATCCAGCCTTCAGGAG 3'. This primer pair produces a 184 bp amplicon in WT samples. To confirm the genotype, a separate set of PCR was ran using a second set of primers - *lmna* Fwd primer 2: 5' CCATGCTACTTGGCAAATGTTA 3' and *lmna* Rev primer 2: 5' CACTTTATTTGTGTCCCCAGTAGAA 3'. This primer pair produces an 834 bp amplicon in WT samples. Heteroduplex mobility assays were performed based on (Zhu et al., 2014) to identify *lmna* mutants. To differentiate between WT and homozygous fish, two PCR reactions were prepared for each sample. One reaction contained only the DNA sample to be genotyped while the second reaction contained the DNA sample to be genotyped and a known WT DNA. The PCR program was as follows: 95°C for 4 min followed by 35 cycles of 95°C for 1 min, 56°C for 1 min and 72°C for 1 min (for the first primer pair) or 30 s (for the second primer pair). Last extension was at 72°C for 8 min. Amplicons were run on 12% polyacrylamide gels for 40 min at 180 V (PCR using the first primer pair) or 50 min at 180 V (PCR using the second primer pair). Mutant

genotypes were verified and identified by sending representative samples for sequencing at the Ottawa Hospital Research Institute (OHRI) sequencing facility.

Immunostaining

Whole-mount immunostaining –

WT and *lmna* mutant 1 dpf embryos were anesthetized using tricaine (MS-222) and then fixed in 4% PFA overnight at 4°C or for 2 hours at room temperature (RT). Permeabilization was done by incubating the samples in 2% PBST for 30 minutes at 37° C. The embryos were blocked in 5% BSA-PBST for 2 hours at 37° C. Primary antibody incubation was done overnight at 37° C. Secondary antibody and rhodamine phalloidin incubation was done for 3 hours at 37° C. Supplementary Table 3.1 lists the antibodies and stains used. The embryos were mounted on slides using glycerol. At least 7 embryos/genotype were imaged using a confocal microscope and analyzed using ImageJ.

Immunostaining on sections –

WT and *lmna* mutant 7 dpf larvae were anesthetized using tricaine (MS-222) and then fixed in 4% PFA overnight at 4°C and washed twice in PBS (5 min/wash). After which the larvae were incubated in 30% sucrose at 4°C overnight for cryoprotection, and then embedded the next day in 2/3 OCT and 1/3 30% sucrose solution for sectioning. Embedded larvae were flash frozen using isopentane and were either sectioned or stored in -80°C for later use. The pericardial sac region was sectioned longitudinally at 12 μm. Sample slides were blocked with 5% BSA-PBST for 2 hours at RT and incubated with the primary antibody overnight at 37° C. Secondary antibody incubation was performed for 3 hours at 37° C. Supplementary Table 3.1 lists the antibodies used. Slides were mounted using Aqua Polymount. At least 3 larvae/genotype (≥3 sections per sample)

were imaged using a confocal microscope and analyzed using ImageJ 2.0.0-rc-43/1.52n (for Windows 64-bit).

Cardiac Function Analyses

Heart Rate (HR) Analyses -

The heart rate of progenies of WT crosses and of heterozygous crosses were manually and independently counted by four different individuals (genotype blind) based on 10 second heart videos of zebrafish embryos/larvae (3 – 7dpf) that were taken using the Lumenera Infinity 3-1UC camera mounted on a Leica MZ FLIII microscope, and recorded using the Infinity Capture (v 6.4.0) program. The videos were taken at 6.5x magnification at a resolution of 1024 pixels x 768 pixels. Zebrafish embryos/larvae were positioned laterally in the troughs of a micro-injection plate (an agarose plate moulded with narrow troughs). The embryos/larvae were left to acclimatize for one minute on the wet micro-injection plate before the videos were taken. Zebrafish were not sedated prior to video taking to avoid the depressive effect of tricaine (MS-222) on heart rate (Collymore et al., 2014). A frame rate of ≥ 19 frames/s was used to capture the videos. The heart rate per minute was estimated by multiplying the number of counted heart beats by six. There were ≥ 9 fish/genotype/time point.

Ventricular dimension measurement and Fractional Shortening analyses –

Using the same videos used for heart rate analyses, ventricular dimensions and fractional shortening were measured in 3 – 4 dpf zebrafish larvae according to (Hoage et al., 2012). The pixel lengths were converted to mm using this scale: 621.312 pixels/mm. Cardiac videos were opened in ImageJ 2.0.0-rc-43/1.52n (for Windows 64-bit), and the end diastolic and systolic ventricular diameters were measured at the beginning, middle and end of each video. Two or three individuals, who were genotype blind, independently performed the measurements at each time point and the

mean of the pooled data for each time point was used for analyses. There were ≥ 8 fish/genotype/time point.

Confocal Microscopy

Z-stack confocal images of whole-mount or sections samples were taken using either the Plan Fluor 20x (0.75 NA) water/glycerol immersion objective or the Plan Apochromat 60x (1.40 NA) oil immersion objective of the Nikon A1RsiMP Confocal Workstation**.** The following lasers were used – 405 nm, 488 nm and 561 nm. Channel series was activated to prevent spectral bleed through between the channels. Image analyses of raw files were performed using ImageJ 2.0.0-rc-43/1.52n (for Windows 64-bit). Adobe Photoshop CC 2019 was used to annotate the images and create the figures.

Swim Ability and Movement Analyses

Swim and movement analyses of 4 – 7 dpf WT and *lmna* mutant larvae were performed using ZebraBox (ViewPoint Behaviour Technology). One larva was placed per well of a 24-well plate. One mL of embryo medium (3mL 0.01% methylene blue + 16mL 60X E3 embryo medium [17.2g NaCl + 0.76g KCl + 4.9g $MgSO_4 \cdot 7H_2O$ + 2.9g $CaCl_2 \cdot 2H_2O$ + 1L H_2O] + 981mL H_2O) was added in each well. The larvae were left to acclimatize for a few minutes before recording. Swim activity was captured per minute for five minutes for each larva using the ZebraLab software and the ZebraBox tracking system. The ZebraBox tracking system is composed of a mounted camera, infrared illumination and LED lights. Arbitrary speed thresholds were set: 2 mm/s for inactive/small movements and 10.0 mm/s for small/large movements. Speed, distance, and number of movement readouts for each larva were verified by watching the swim videos and checking the swim map that tracked the movement of each larva. Average swim speed and mean total distance swam were calculated for each larva per time point. Mean total number of movements (combined

slow and fast) were calculated for each larva for the entire period of observation. Genotyping was performed after data collection. There were ≥ 7 larvae/group/time point.

RNA extraction and quantitative RT-PCR

RNA was extracted from pools of 5 whole zebrafish larvae at 7 dpf using a pestle for homogenization in TRIzol reagent (Invitrogen) following manufacturer protocol. Integrity of the RNA was checked by gel electrophoresis, and purity of the RNA was determined using the NanoDrop 1000 Spectrophotometer (ThermoFisher). Only samples with clear 28S and 18S rRNA bands at an approximate intensity ratio of 2:1 and an A260/280 absorbance ratio of 1.8-2.1 were used for cDNA synthesis using the iScript™ Reverse Transcription Supermix for RT-qPCR kit (Bio-Rad) according to the manufacturer protocol. For all genes, standard 10 µL qRT-PCR reactions were assembled as follows: 5 µl of SsoFast™ EvaGreen® Supermix (Bio-Rad), 0.4 µl of forward primer (10 µM), 0.4 µl of reverse primer (10µM), 4 µl of template cDNA and 0.2 µl of nuclease-free water. For no template negative controls, template cDNA was replaced by nuclease-free water. All reactions were carried out in triplicate using the Bio-Rad CFX96 system. The PCR conditions were 95 ºC for 30 s, followed by 40 cycles of 95 ºC for 5 s and 59 ºC for 5 s. Normalized gene expression values were determined using the comparative Cq method and each gene was normalized against three reference genes, elongation factor 1 alpha (*ef1α*), ribosomal protein l13a (*rpl13a*), and tyrosine 3-monooxygenase/tryptophan 5-monooxygenase activation protein, zeta polypeptide (*ywhaz*). Supplementary Table 3.2 lists the primers used.

Protein extraction and Western Blot Analyses

Whole larval lysates from ≥ 3 pooled 7 dpf larvae/genotype/set were extracted using RIPA lysis and extraction buffer (ThermoFisher Scientific 89901). Halt™ Protease and Phosphatase Inhibitor Cocktail (ThermoFisher Scientific 78440) was added to the extraction buffer to

prevent protein degradation. The accompanying manufacturer's protocol was followed for protein extraction. Protein extracts were loaded on to Bolt™ 4-12% Bis-Tris Plus gels and ran at 180V for 50 minutes at RT. After which the transfer onto nitrocellulose membrane was ran for 1 hr at 250 mAmp on ice. Membranes were blocked in 5% BSA-PBST for 30 minutes at RT prior to incubation with the primary antibody at 4°C overnight on a shaker. Following primary antibody incubation, membranes were washed three times with PBST (5 min/wash) and incubated with the HRP-conjugated secondary antibody for 1 hr at RT on a shaker. Supplementary Table 3.1 lists the antibodies used. The ECL detection reagent kit (Amersham) was used to visualize the bands using the Bio-Rad ChemiDoc™ Touch imager. Bio-Rad ImageLab 6.0.1 (software v 2.0.0.25) was used to analyze the raw membrane images.

Statistical Analyses

GraphPad Prism 8.1.1 was used to conduct statistical tests and to generate graphs. Chi-square test was performed to confirm adherence to Mendelian ratio. Unpaired two-tailed t-test (with or without Welch's correction) was performed to compare two groups. One-way ANOVA with correction for multiple tests (Dunnett's or Tukey's correction) was used to compare the means of more than two groups. Mean ± SEM was presented. Adjusted p-values after multiple tests correction were reported and significance was set at $p < 0.05$.

3.5 Results

Creation of zebrafish *lmna* mutants

In this study, the CRISPR/Cas9 genome editing technology was used to create a five base pair deletion (5bp Δ) in the second coding exon of the zebrafish *lmna* gene (Figure 3.1A and B). *In silico* analysis of the 5bp Δ is predicted to create a premature stop codon in exon 3 resulting in

a truncated protein of 180 a.a. lacking many of the functional and binding domains including the Pkc α binding site located in the C-terminus (Figure 3.1C).

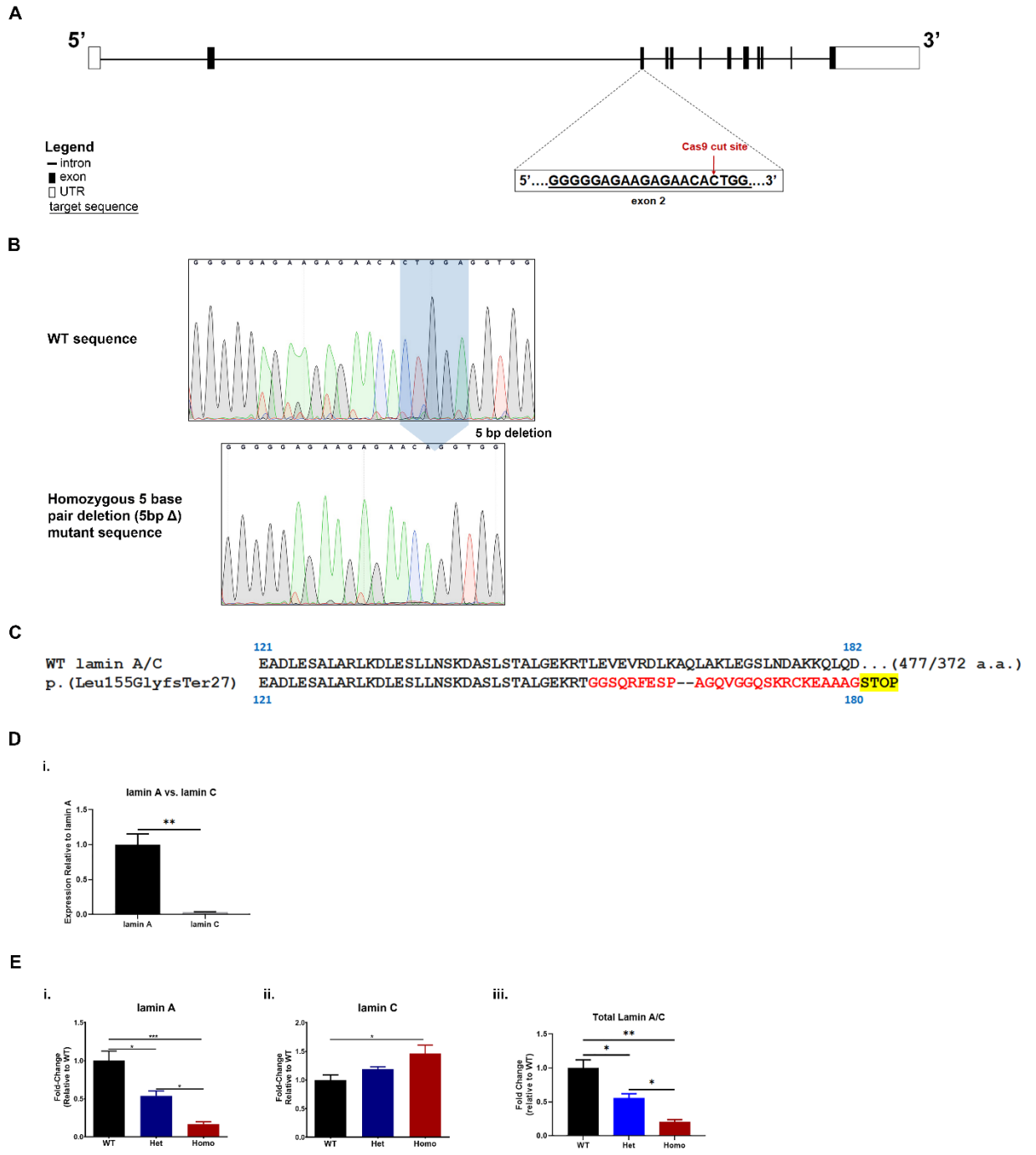

Figure 3.1: Creation and identification of zebrafish lamin A/C (*lmna*) mutants. (A) Schematic representation of the zebrafish *lmna* gene illustrating its untranslated regions (UTRs), introns, exons, the CRISPR-Cas9 target sequence, and the Cas9 cut site in exon 2. **(B)** WT sequence and homozygous *lmna* mutant sequence with five base pair deletion (5bp Δ) in exon 2. **(C)** Amino acid sequence alignment between the WT sequence and the putative sequence of the variant produced

by the 5 bp Δ. **(D) (i)** Whole-larval quantitative PCR analyses of lamins A and C transcripts (mean ± SEM) in 7 dpf WT larvae. **(E)** Whole-larval quantitative PCR analyses of lamins A and C transcripts (mean ± SEM) in 7 dpf WT and *lmna* mutant larvae. n = 3 independent sets (5 larvae/genotype/set). Significance (*) is set at $p < 0.05$; ** means $p < 0.01$ and *** means $p < 0.001$.

Heteroduplex mobility assays were used to genotype 52 randomly chosen embryos obtained from a cross of heterozygous parents. The genotype of the embryos from the resulting three different profiles were verified by sequencing analysis: 11 are WT (21%), 31 are heterozygous (59.6%) and 10 are homozygous (19.25%). A chi-square test showed that these values did not significantly differ from the expected Mendelian genotype ratio of 1:2:1 in a cross between heterozygous parents. Random genotyping of 41 adult zebrafish obtained from a cross between heterozygous parents at 5 months post fertilization (mpf) also approximated the expected Mendelian ratio and gave a distribution of 8 WT (19.5%)/ 25 Het (61%)/ 8 Homo (19.5%) suggesting that there is no notable difference in the survival of WT and *lmna* mutants at 5 mpf.

In the absence of a lamin A/C antibody that cross-reacts with the zebrafish protein, quantitative PCR was performed to measure zebrafish lamins A and C transcript levels in WT and *lmna* mutants. Consistent with previous results from another study, lamin A is more highly expressed than lamin C during the first week of development (Koshimizu et al., 2011). Lamin C mRNA expression is 28 folds less than lamin A in WT larvae at 7 dpf (Figure 3.1Di). A profound decrease in lamin A transcript level is observed in the RNA extracts of 7 dpf heterozygous and homozygous *lmna* mutant larvae compared to WT (Figure 3.1Ei). In contrast, an increase in lamin C mRNA is observed in homozygous *lmna* mutants compared to WT (Figure 3.1Eii). Nevertheless, total lamins A and C transcript level is significantly reduced in both heterozygous and homozygous *lmna* mutants compared to WT (Figure 3.1Eiii).

Heterozygous and homozygous *lmna* mutants display mild and transient cardiac structure and/or function defects.

Zebrafish *lmna* morphants exhibit cardiac structure and function abnormalities (Vogel et al., 2009). To determine if the zebrafish *lmna* mutants also present similar defects, embryos from heterozygous crosses were monitored during the first week of development. In addition, embryos from crosses of the WT siblings of the heterozygous parents were also assessed. Non-specific pericardial edema was observed at 3 dpf but by 7 dpf, the pericardial edema has subsided. No notable abnormal cardiac shape and positioning were noted in the *lmna* mutants. Ventricular diameter at the end of systole and diastole was also measured as illustrated in supplementary Figure 3.1. At 3 dpf, homozygous *lmna* mutants have significantly narrower ventricular diameters at the end of systole and diastole compared to WT (Figure 3.2A). However, by 4 dpf, this difference in ventricular diameter is no longer significant.

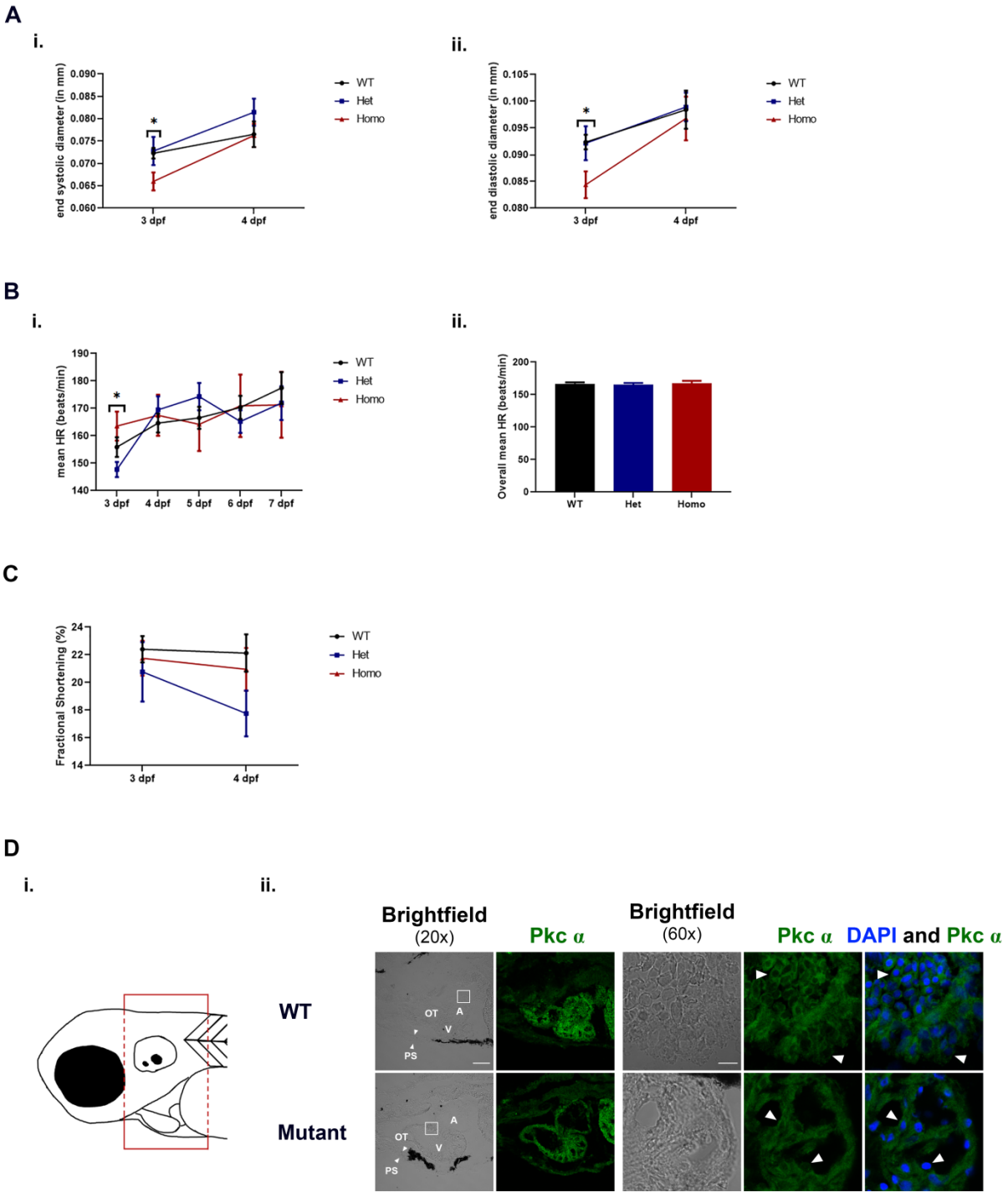

Figure 3.2: Cardiac structure and function evaluation and Pkc α immunostaining in WT and mutant *lmna* zebrafish. (A) (i) end systolic and **(ii)** end diastolic diameters of WT and *lmna* mutants at 3 and 4 dpf displaying statistical significance at 3dpf between WT and homozygous mutant fish. **(B) (i)** Average heart rate per time point of WT and mutant *lmna* zebrafish from 3 – 7 dpf displaying statistical significance at 3dpf between WT and heterozygous mutant fish. **(ii)** Overall mean heart rate of WT and mutant *lmna* during the period of observation. **(C)** WT and mutant *lmna* larvae fractional shortening at 3 and 4 dpf. n ≥ 8 fish/genotype/time point. Mean ±

SEM is presented. Significance (*) is set at $p < 0.05$. **(D) (i)** Schematic showing the region and section orientation (red box) of the images shown in (ii). **(ii)** Pkc α immunostaining of 7 dpf WT and mutant *lmna* larvae longitudinal cardiac sections. The maximum projection of the confocal z-stack images taken are shown at 20x and 60x magnification. The region enclosed in a white box in the 20x brightfield image is taken at 60x magnification. DAPI marks the nucleus. White arrowheads point to cells. PS, pericardial sac, OT, outflow tract, V, ventricle and A, atrium. Scale bars: 50 μm (20x) and 10 μm (60x). $n \geq 3$ larvae/genotype.

To assess the cardiac function of WT and *lmna* mutants, heart rate (HR; beats/min) was scored from 3 – 7 dpf. Previous work shows bradycardia in *lmna* morphants at 1 - 3 dpf (Vogel et al., 2009). Similarly, the heterozygous *lmna* mutants in this study have a lower HR compared to WT at 3 dpf (Figure 3.2Bi and supplementary videos 3.1 and 3.2.) A trend towards bradycardia is also noted in the homozygous *lmna* mutants at 5 and 7 dpf (Figure 3.2Bi). However, the overall mean HR during the period of observation is comparable between WT and *lmna* mutants (Figure 3.2Bii). In addition, fractional shortening (FS) was calculated from the end systolic and diastolic ventricular diameters of WT and *lmna* mutants at 3 and 4 dpf to estimate ventricular function. A previous study on zebrafish lamin A/C morphants noted decreased FS at 2 - 4 dpf compared to controls (Vogel et al., 2009). In this study, the *lmna* mutants present a trend towards decreased FS compared to control at 3 and 4 dpf (Figure 3.2C).

As a regulator of cardiac structure and function, expression of Pkc α in cardiac tissues was determined by immunostaining cardiac sections of 7 dpf WT and *lmna* mutant larvae. Genome duplication in zebrafish resulted in two *PRKCA* zebrafish paralogues – *prkcaa* and *prkcab*. The Pkc α-a and Pkc α-b proteins share 85% a.a. identity with each other. Furthermore, zebrafish Pkc α-a and Pkc α-b share 84% and 82% a.a. identity respectively with human PKC α. The available Pkc α antibody that works on zebrafish samples does not discriminate between the two zebrafish Pkc α proteins. The immunostaining results show similar Pkc α expression in cardiac tissues of 7 dpf WT and mutant *lmna* larvae (Figure 3.2D).

Heterozygous and homozygous *lmna* mutants display abnormal skeletal muscle structure and function

Patients and animal models of striated muscle laminopathies frequently present with skeletal muscle structure defects and/or dysfunction (Nicolas et al., 2019). The *lmna* morphants also show slow muscle fibre defects at 1 dpf (Koshimizu et al., 2011). Thus, to determine if skeletal muscle damage is also present in the *lmna* mutants, slow muscle fibres of progenies from WT crosses and heterozygous crosses were immunostained for myosin heavy chain using the F59 antibody at 1 dpf. Consistent with results from the *lmna* morphants, all 9 of the homozygous and 9/11 of the heterozygous *lmna* mutants present with slow muscle fibre damage (fibre waviness, tears and irregular spacing) compared to 3/9 of WT embryos (Figure 3.3A). A sample was considered abnormal if ≥ 3 of its somites present any of the aforementioned defects. F-actin organization was also examined using rhodamine phalloidin staining of 1 dpf WT and *lmna* mutants. We observe F-actin structural defects in the muscle of the *lmna* mutants mirroring that of the myosin heavy chain (Figure 3Aii).

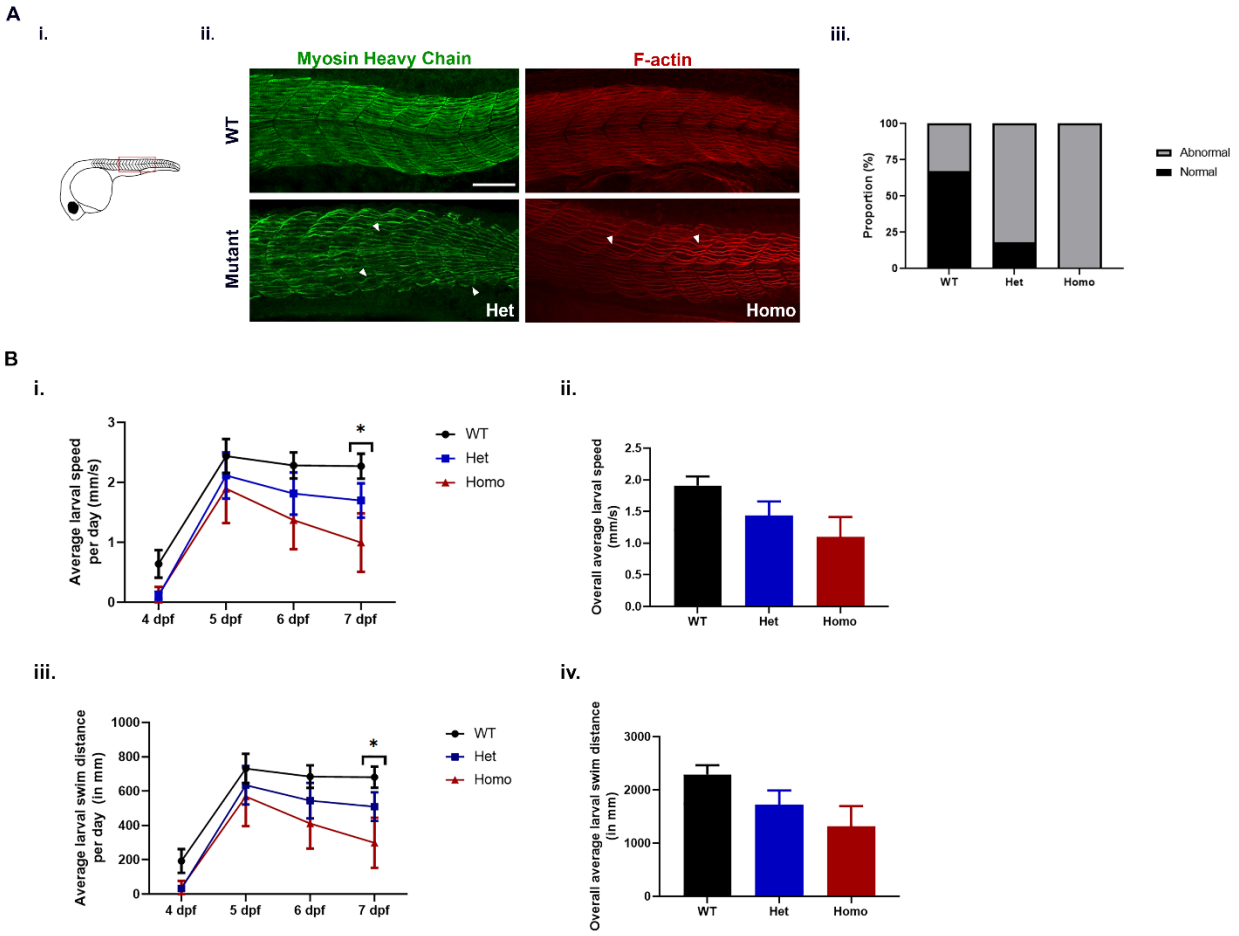

Figure 3.3: Skeletal muscle structure and swim capacity analyses of WT and mutant *lmna* zebrafish. (A) (i) Schematic representation of 1 dpf zebrafish embryo illustrating the region (in red box) presented in (ii). **(ii)** Maximum projection of confocal z-stack images showing normal and abnormal myosin heavy chain and F-actin staining in whole-mount 1 dpf WT and *lmna* mutant zebrafish embryos. White arrowheads point to fibre defects. Myosin heavy chain and F-actin staining show the same fibre defects. Heterozygous and homozygous mutants show comparable phenotypes. **(iii)** Frequency of WT and *lmna* mutant embryos presenting with slow muscle fibre defects in the trunk. n ≥ 9 embryos/genotype. **(B)** Swim analyses of WT and *lmna* mutant zebrafish from 4 dpf – 7 dpf. **(i)** The average larval speed (mm/s) at each time point per genotype displaying statistical significance at 7 dpf between WT and homozygous mutant fish. **(ii)** The overall average larval speed (mm/s) during the entire period of observation for each genotype. **(iii)** The average larval distance (in mm) swam per day per genotype displaying statistical significance at 7 dpf between WT and homozygous mutant fish. **(iv)** The overall average larval distance swam during the entire period of observation. n ≥ 7 larvae/genotype. Mean ± SEM is shown. Significance (*) is set at $p < 0.05$. Scale bar: 75 µm.

Skeletal muscle function was assessed by examining the number of movement and swim capacity of WT and mutant *lmna* larvae at 4 – 7dpf to determine if there is mobility impairment in the *lmna* mutants as a potential result of skeletal muscle defects. Swim activity was recorded for

each fish for five minutes/time point and analyzed in WT and *lmna* mutants from 4 – 7 dpf. Heterozygous and homozygous *lmna* mutant larvae are slower on average, swim a shorter total distance and move less compared to WT (Figure 3.3B and supplementary Figure 3.2).

Expression of genes and activation of proteins associated with striated muscle laminopathies are perturbed in the homozygous *lmna* mutants.

To determine if levels of striated muscle laminopathy biomarkers are also affected in the *lmna* mutants, the expression level of *nfκb2* and *jun*, and phosphorylation of Erk 1/2 were assessed. *Nfκb2* is a downstream target of NF-κB and *jun* codes for c-Jun, a target of the JNK branch of the MAP kinase signaling pathway. Quantitative PCR performed on RNA extracts of 7 dpf larvae show a notable attenuation of *nfκb2* and *jun* mRNA levels in the homozygous *lmna* mutants compared to WT (Figure 3.4A). Western blot analysis of activated (phosphorylated) Erk 1/2 (phos-Erk 1/2) in protein extracts of 7 dpf larvae show a 1.38 fold increase in phos-Erk 1/2 level in the homozygous *lmna* mutants compared to WT (Figure 3.4B). The residues involved in human ERK 1/2 activation (Thr202/Tyr204 for ERK 1 and Thr185/Tyr187 for ERK 2) are conserved in zebrafish (Jr, 2012). Similarly, the residues (Thr497, Thr638 and Ser657) involved in human PKC α activation are conserved in zebrafish except that Ser657 is substituted with a threonine in zebrafish (Bornancin & Parker, 1997; Cazaubon et al., 1994; Gysin & Imber, 1996; Keranen et al., 1995; Parekh et al., 2000). Phosphorylated Pkc α (phos- Pkc α) is also upregulated in protein extracts from 7 dpf *lmna* mutant larvae (Figure 3.4B). Phos- Pkc α in 7 dpf WT larvae protein extracts is not detectable.

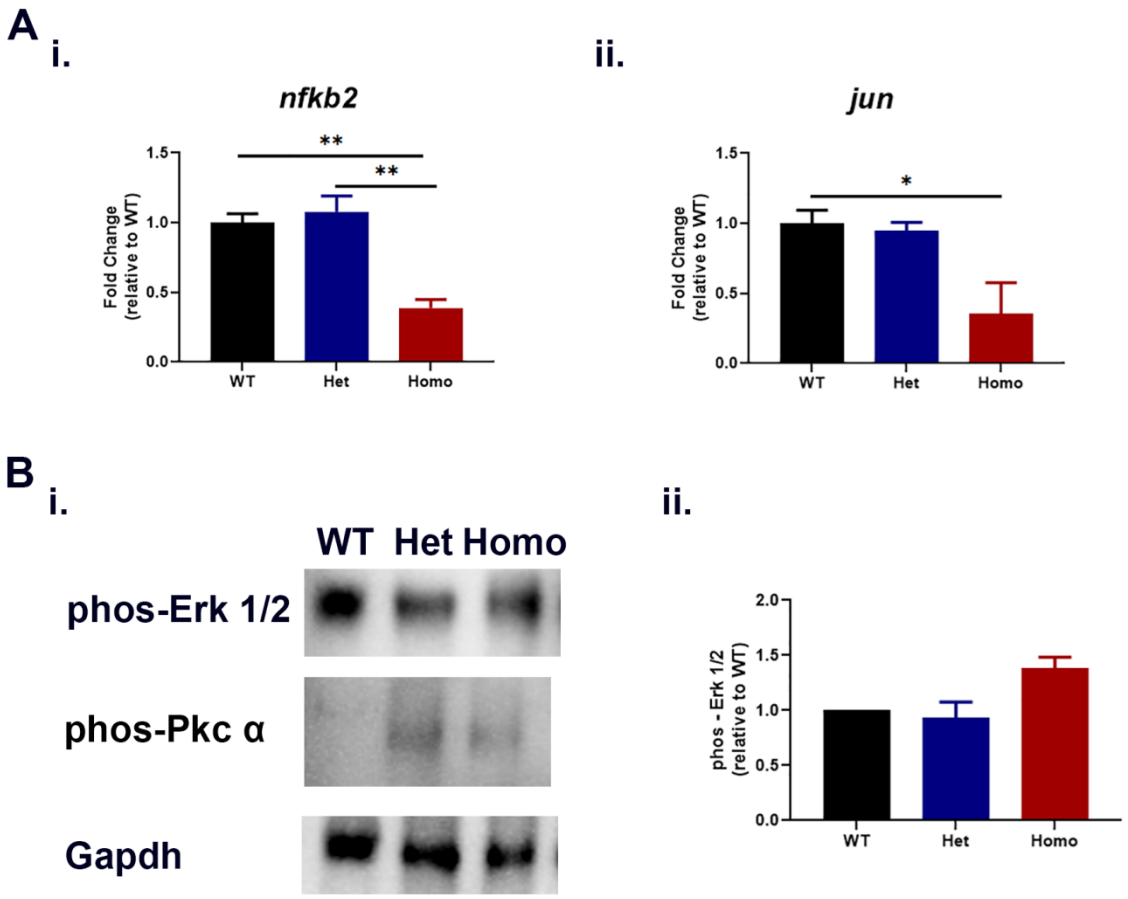

Figure 3.4: Quantitative PCR and western blot analyses of striated muscle laminopathy biomarkers in 7 dpf WT and mutant *lmna* zebrafish larvae. (A) Quantitative PCR of *nfκb2* and *jun* transcript levels. n = 3 independent sets (5 pooled larvae/genotype/set). **(B) (i)** Representative western blot for activated Erk 1/2 (phos-Erk 1/2) and activated Pkc α (phos- Pkc α) in WT and mutant *lmna* zebrafish larvae **(ii)** Western blot analyses of phos-Erk 1/2 in WT and mutant *lmna* zebrafish larvae. n = 2 independent sets (≥ 3 pooled larvae/genotype/set). Mean ± SEM is presented. Significance (*) is set at $p < 0.05$; ** means $p < 0.01$.

3.6 Discussion

Mutations in the lamin A/C gene primarily result in cardiac and/or skeletal muscle conditions in patients (Tesson et al., 2014). Multiple animal models including zebrafish have been created to study striated muscle laminopathies (Nicolas et al., 2019). However, there is currently limited or no information on the cardiac and skeletal muscle phenotypes of zebrafish with permanent *lmna* interruption. In this study, we created zebrafish with permanent *lmna* disruption

by inducing a five base pair deletion in the second exon of zebrafish lamin A/C using the CRISPR/Cas9 technology. Heterozygous and homozygous *lmna* mutants both have reduced lamin A, and combined lamins A and C transcript levels. Zebrafish *lmna* mutants do not suffer premature death and have comparable survival to their WT siblings at 5 mpf. The *lmna* mutants exhibit mild and transient cardiac defects. At 1 dpf, the *lmna* mutants present skeletal structure abnormalities. In addition, the *lmna* mutants on average move less, swim slower and cover a smaller mean total distance at 4 – 7 dpf than WT larvae. Furthermore, expression of genes and proteins implicated in striated muscle laminopathies is disturbed. In particular, *jun* and *nfκb2* transcript levels are reduced and phos-Erk 1/2 is increased in the homozygous *lmna* mutants. Activated Pkc α, an upstream regulator of Erk 1/2 and Jun, is increased in the *lmna* mutants as well. Altogether, the *lmna* mutants show marked skeletal muscle phenotype, and aberrant expression of genes and proteins previously linked to striated muscle laminopathies in patients and other animal models.

The *Lmna* null mice models ($Lmna^{GT\,-/-}$ and $Lmna^{\Delta/\Delta}$) have hypotrophic cardiac and skeletal muscles but neither exhibit abnormal cardiac structure (e.g. fibrosis or cardiac chamber enlargement) nor dystrophic skeletal muscles (Kim & Zheng, 2013; Kubben et al., 2011). In contrast, zebrafish with transient *lmna* knockdown present with cardiac structural and functional defects and skeletal muscle damage (Koshimizu et al., 2011; Vogel et al., 2009). In this study, the 5bp Δ in *lmna* shifts the reading frame creating a premature stop that may result in a truncated lamin A/C of 180 amino acids lacking many of its functional and binding domains including the regions that interact with Erk 1/2 and Pkc α (González et al., 2008; Martelli et al., 2002). The presence or absence of the truncated lamin A/C variant cannot be confirmed due to lack of lamin A/C antibody that can detect zebrafish lamin A/C. However, quantitative PCR analyses show reduction in lamin A transcript level in the homozygous *lmna* mutants. In contrast, lamin C

transcript level is found to be 1.46 fold higher in the homozygous mutants compared to WT. Previous work from Koshimizu et al provide evidence for the presence of zebrafish lamin C at the mRNA and protein levels (Koshimizu et al., 2011). However, *in silico* work by Peter and Stick suggest that lamin C is present in mammals only (Peter & Stick, 2012). Using the forward primer located in *lmna* exon 8 and reverse primer in *lmna* intron 9 published by Koshimizu et al, we found that these primers that were also used in this study cover a region common to the putative zebrafish lamin C and another untranslated *lmna* transcript that retains an intron (Ensembl *lmna* ID: ENSDARG00000013415; transcript ID: lmna-201). Thus, the observed increase in lamin C mRNA in the homozygous mutants might have included the lmna-201 transcript. Nevertheless, since lamin C is significantly less abundant than lamin A, total lamins A and C expression in the mutants is significantly decreased compared to WT making the heterozygous mutants lamin A/C haploinsufficient and the homozygous mutants lamin A/C deficient. The remaining lamin A/C transcripts in the mutants may result from alternative means of mutant mRNA processing such as exon skipping and activation of cryptic splice sites that could bypass nonsense-mediated mRNA decay (Anderson et al., 2017).

Previous studies show lamin A/C deficiency or haploinsufficiency resulting in death or striated muscle laminopathy in patients respectively (Al-Saaidi et al., 2013; Gupta et al., 2010; Siu et al., 2012; van Engelen et al., 2005). Likewise, transient knockdown of *lmna* in zebrafish results in cardiac and skeletal muscle abnormalities (Koshimizu et al., 2011; Vogel et al., 2009). Consistent with these observations, the zebrafish homozygous *lmna* mutants display slow muscle fibre damage at 1 dpf. Interestingly, unlike most animal models of striated muscle laminopathies, the zebrafish heterozygous *lmna* mutants also present an abnormal muscular phenotype (Nicolas et al., 2019). Myosin heavy chain and F-actin staining of muscle fibres show wavy fibres, irregular

spacing between the muscle fibres, and muscle fibre tears in the *lmna* mutants compared to WT at 1 dpf. F-actin defects have been noted in patient myoblasts, neonatal rat ventricular myocytes (NRVMs) and fruit flies expressing striated muscle laminopathy mutations (Bertrand et al., 2014; Dialynas et al., 2015; Laurini et al., 2018). Actin is part of the network that physically links the nucleus to the cytoskeleton (Haque et al., 2006). It is also known to directly interact with the C terminus of lamin A/C making F-actin intimately involved in the transduction of force in the nucleus and the rest of the cell (Simon et al., 2010). In this study, the truncation of lamin A/C removes the F-actin binding sites potentially disrupting the proper handling of mechanical stimulus which is critical in cells under constant physical stress such as myocytes. Patient myoblasts and mutant NRVMs with disrupted F-actin present with compromised mechanosensitivity, nuclear stability and cell adhesion owing to the disruption of the nucleo-cytoskeletal structure (Bertrand et al., 2014; Laurini et al., 2018). Consistent with the mobility issues observed in various animal models expressing various striated muscle laminopathy variants, our zebrafish *lmna* mutants have impaired swim capacity compared to WT (Arimura et al., 2005; Bank et al., 2011; Dialynas et al., 2015).

In some patients with striated muscle laminopathy and in the H222P EDMD mice, elevated expression and activity of several members of the MAP kinase signaling pathway are observed (Muchir et al., 2007, 2012, 2013). This aberrant gene expression profile is thought to contribute to the development of muscular dystrophy and cardiomyopathy (Muchir et al., 2007, 2013). Likewise, the homozygous *lmna* zebrafish mutants present with abnormal activation or expression of MAP kinase members. The homozygous *lmna* mutants have an upregulation of phosphorylated Erk 1/2 compared to WT. An increase in phos-ERK 1/2 has been previously noted in HeLa (human epithelial cell line) and C2C12 (mouse myoblast cell line) cells upon lamin A/C knockdown

(Muchir, Wu, et al., 2009). Thus, like the H222P mice, abnormal expression and activation of ERK 1/2 in the homozygous *lmna* mutants likely contributed to the development of their muscular dystrophy phenotype. Additionally, consistent with results from mouse embryo fibroblasts of a *Lmna* mice model that produces a truncated lamin A, NF-κB-regulated gene transcription is decreased as evidenced by the reduction in *nfκb2* expression level in the homozygous *lmna* mutants compared to WT further implicating the NF-κB pathway in muscular laminopathies (Jahn et al., 2012; Lammerding et al., 2004; Sullivan et al., 1999).

Regarding cardiac structure, the *lmna* morphants present with pericardial edema and cardiac chamber dilation (Vogel et al., 2009). In this study, the homozygous *lmna* mutants have a narrower ventricle at 3 dpf compared to WT. No other significant and specific cardiac structural defect is observed in the *lmna* mutants at the embryo and early larval stages. Cardiac function assessment was performed beginning at 3 dpf when the zebrafish ventricle and atrium are distinct chambers contracting sequentially and are separated by the developing valve leaflets in the atrioventricular canal (Staudt & Stainier, 2012). Previous work notes bradycardia in the $Lmna^{GT\text{-}/\text{-}}$ mice, and lower HR at 1-3 dpf and decreased fractional shortening at 2-4 dpf in the *lmna* morphants compared to control (Kubben et al., 2011; Vogel et al., 2009). Similarly, the heterozygous *lmna* mutants present with significantly decreased HR at 3 dpf compared to WT. Furthermore, the homozygous *lmna* mutants have a narrower ventricle compared to WT suggesting that their ventricle does not relax as much as WT during diastole at 3 dpf. Consequently, a trend towards poorer fractional shortening is observed in the *lmna* mutants compared to WT at 3 dpf which persists at 4 dpf. These results are supported by recent work from Hayashi and colleagues showing bradycardia at 2 dpf and impaired cardiac conduction at 3 dpf in homozygous CRISPR mutants with 4bp Δ in *lmna* exon 1 (Hayashi et al., 2020). Zebrafish *lmna* exon 6 crispants (i.e.

CRISPR/*lmna* guide RNA micro-injected embryos with mosaic *lmna* interruption) also present similar results confirming cardiac dysfunction in *lmna* mutants during the embryonic stage (Hayashi et al., 2020). However, by 7 dpf, the cardiac function defects noted in our *lmna* mutants are no longer observable suggesting transient and mild cardiac dysfunction in these mutants. In individuals with muscular laminopathies, the skeletal muscle phenotype precedes the presentation of cardiac abnormalities although some patients might not develop a cardiac phenotype (Gisèle Bonne & Quijano-Roy, 2013; Vytopil et al., 2002). Therefore, the lack of significant cardiac structure and function abnormalities in the *lmna* mutants during the first week of development mimics observations in EDMD and L-CMD patients. Alternatively, the significant drop in *c-jun* expression in the homozygous mutants might also contribute to the lack of prominent cardiac phenotype in these mutant larvae. In the H222P mice, *c-Jun* transcript level is upregulated prior to detection of notable abnormal cardiac structure and function suggesting that elevated *c-Jun* expression contributes to cardiac disease in the H222P mice (Muchir et al., 2007). Furthermore, genetic compensation might also account for the transient and weak cardiac abnormalities in the *lmna* mutants and the phenotypic difference between zebrafish mutants and morphants (Kok et al., 2015; Rossi et al., 2015). To check for genetic compensation, *lmnb1* transcript level was assessed in WT and *lmna* mutant larvae. *Lmnb1* codes for another nuclear lamina protein, lamin B1, which forms its own network in the nuclear lamina and supports the A-type lamins (Shimi et al., 2008, 2015). However, instead of an upregulation, *lmnb1* expression is significantly reduced in the homozygous *lmna* mutants (supplementary Figure 3.3) suggesting that another gene with a comparable function to the A-type lamins could be compensating.

Expression and activation of the A-type lamin binding partner - Pkc α, a kinase central to cardiac function and an upstream regulator of several members of the MAP kinase signaling

pathway, were also assessed in WT and *lmna* mutants. Pkc α is found to be expressed in the heart of both WT and *lmna* mutant fish. Furthermore, phosphorylated Pkc α level is increased in 7 dpf whole mutant larvae protein extract compared to WT. It should be noted that *prkca* morphants do not manifest any notable cardiac phenotype at 3 dpf while *Prkca* null mice present with hypercontractile hearts and *Prkca* over-expression results in hypocontractile hearts (Braz et al., 2004; Hu et al., 2018). Therefore, the increase in activated Pkc α in the zebrafish *lmna* mutants might contribute to the trend towards decreasing cardiac contractility observed in the *lmna* mutants compared to WT.

Altogether, the data shows evident skeletal muscle phenotype in the zebrafish *lmna* mutants with mild and transient cardiac abnormalities. This phenotype could serve as a model for skeletal myopathies such as EDMD which usually present with marked muscle damage in childhood and late onset or no cardiac conditions (Bonne & Quijano-Roy, 2013; Vytopil et al., 2002). Future studies on older *lmna* mutants should be performed to determine if the mutants develop a more prominent cardiac phenotype. Furthermore, these *lmna* mutants could be used to test the efficiency of muscular laminopathy drugs or to identify other potential therapeutic targets. Lastly, future work could include additional Pkc α characterization in zebrafish carrying other pathogenic *lmna* mutations to confirm Pkc α involvement in muscular laminopathies.

3.7 Supplementary Information

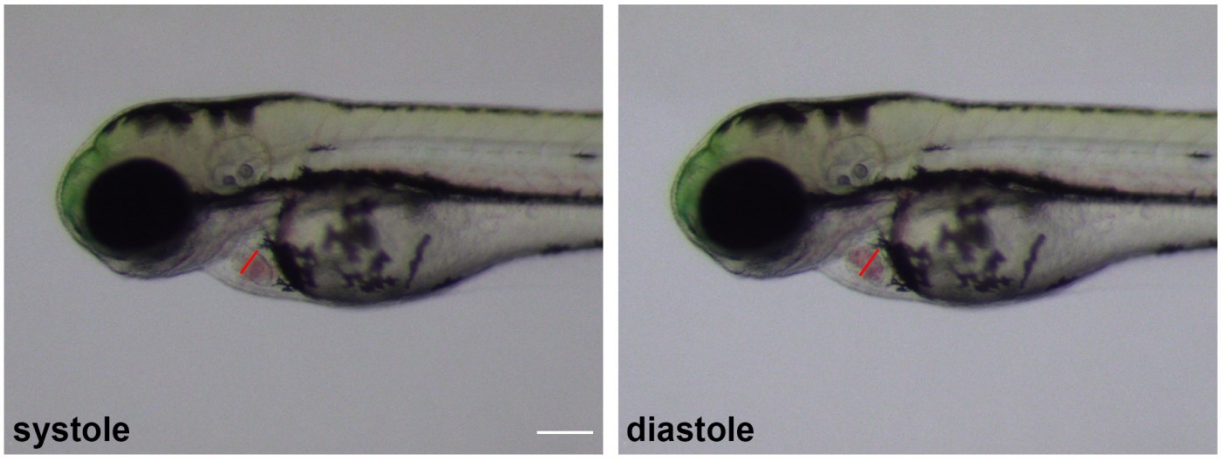

Supplementary Figure 3.1: Image of a 3 dpf zebrafish showing how the end systolic and end diastolic ventricular diameters are measured. The length of the red line represents the ventricular diameter. Scale bar: 1 mm.

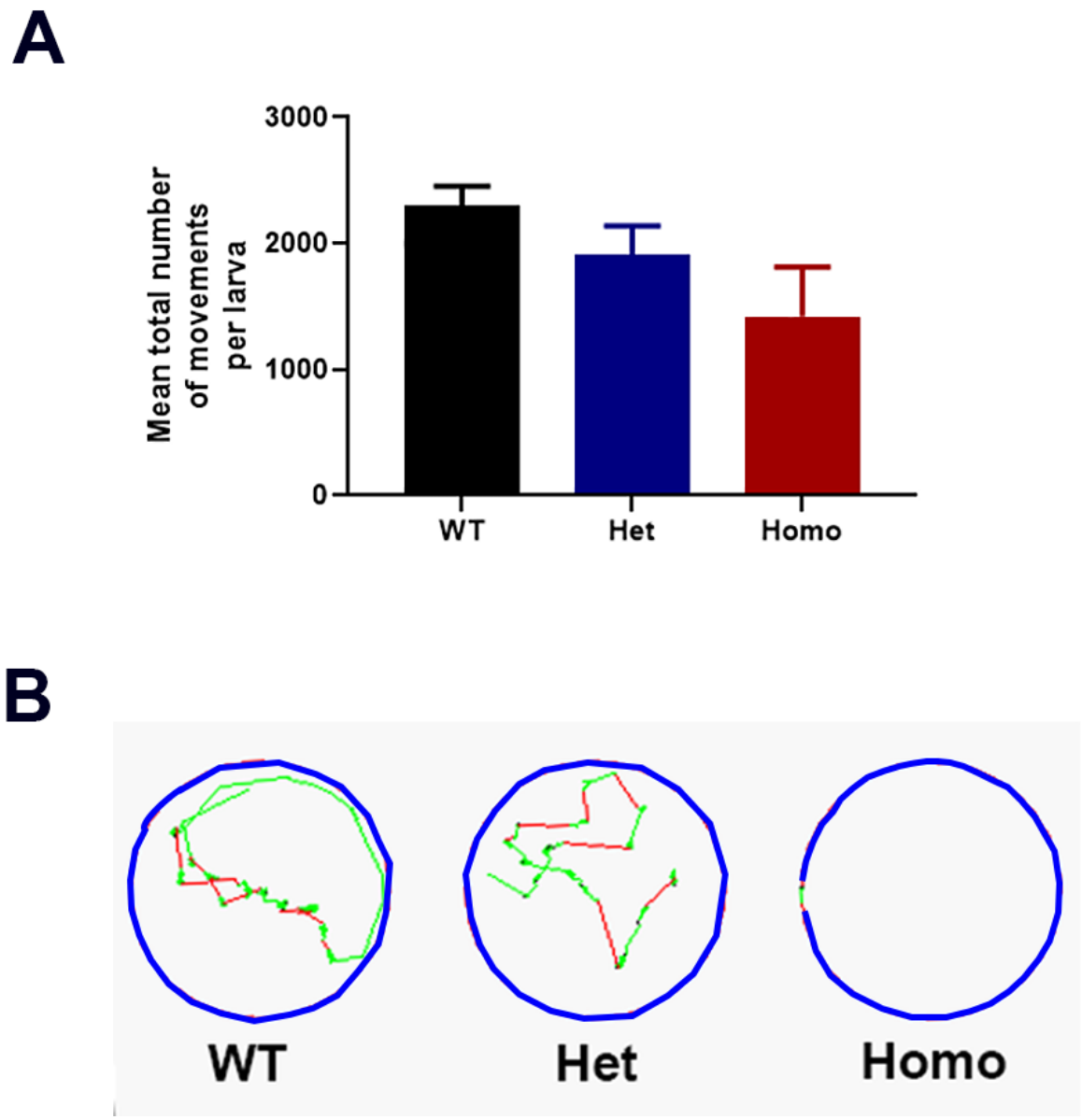

Supplementary Figure 3.2: Movement analysis of WT and *lmna* mutant larvae. **(A)** Average number of movements per larva from 4 – 7 dpf. **(B)** An example of a swim map tracking the swim path of 7 dpf WT and *lmna* mutant larvae for one minute. The red tracks indicate fast movement and the green tracks indicate slow movement. The blue circle signifies the well. n ≥ 7 larvae/genotype. Mean ± SEM is shown. Significance (*) is set at $p < 0.05$.

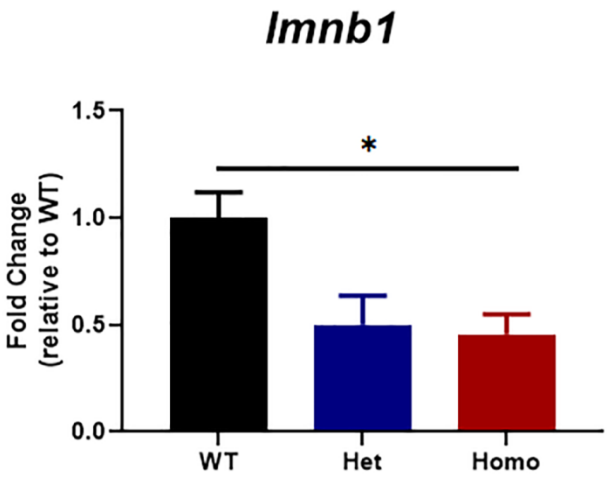

Supplementary Figure 3.3: Quantitative PCR analysis of lamin b1 (*lmnb1*) transcript level in whole larval RNA extracts of 7 dpf WT and *lmna* mutant zebrafish. n = 3 sets (5 larvae/genotype/set). Mean ± SEM was presented. Significance (*) is set at $p < 0.05$.

Supplementary Video 3.1: Cardiac video of a WT zebrafish at 3 dpf.

Supplementary Video 3.2: Cardiac video of a heterozygous zebrafish at 3 dpf.

Supplementary Table 3.1: List of antibodies and stains used and their respective application(s) and dilution(s).

Antibody/Stain	Application(s)
rabbit polyclonal anti-total PKCα (sc-208)	IF (1:250)
mouse monoclonal anti-total PKCα (sc-8393)	IF (1:100)
mouse monoclonal anti-myosin heavy chain (DSHB F59)	IF (1:10)
Alexa Fluor™ 594 phalloidin (ThermoFisher Scientific A12381)	IF (1:250)
goat anti-mouse IgG Alexa Fluor™ 488 (ThermoFisher Scientific A-11001)	IF (1:500)
goat anti-mouse IgG1 Alexa Fluor™ 488 (ThermoFisher Scientific A-21121)	IF (1:500)
goat anti-rabbit IgG Alexa Fluor™ 488 (ThermoFisher Scientific A32731)	IF (1:500)
DAPI (Roche 10236276001)	IF (1:5000)
rabbit polyclonal anti-phos PKC α (sc-12356-R)	WB (1:2000)
rabbit polyclonal anti-phos ERK 1/2 (Cell Signalling Tech 9101)	WB (1:2000)
rabbit polyclonal anti-GAPDH (Ab22555)	WB (1:10000)
goat anti-rabbit IgG-HRP (sc-2004)	WB (1:5000)

Supplementary Table 3.2: List of primers used in the quantitative PCR experiments.

Gene (sequence ID)	**Fwd primer** (5' --> 3')	**Rev primer** (5' --> 3')	**Reference**
lmna (NM_152971.1)			(Koshimizu et al., 2011)
lamin A	TTTGTTCCAGACCACCCTCATC	AAGCACAGATGGTCAGGGTTTG	
lamin C	TGGCAGGTGAAGAGGCAGATTG	GACCCGCAACATAAAGGCTA	
lmnb1 (NM_152972.2)	ACCCGCGGCAAGAGAAAGCG	TCCTGCCATCGGCTGGTCCT	(Ye et al., 2015)
jun (NM_199987.1)	CGCTTTCTCTCAGCATGACAGT	GATTGAGCGTCATGTTGTGTTTC	(Bugel et al., 2016)
nfkb2 (NM_001001840.3)	AGTATCCAGTCCATCTCGCTGT	GCTTCTTCTCGCTCTCTTCATC	(Bugel et al., 2016)
ef1α (ENSDART00000023156)	CTGGAGGCCAGCTCAAACAT	ATCAAGAAGAGTAGTACCGCTAGCATTAC	(Tang et al., 2007)
rpl13a (NM_212784)	TCTGGAGGACTGTAAGAGGTATGC	AGACGCACAATCTTGAGAGCAG	(Tang et al., 2007)
ywhaz (BC044412)	TCTGCAATGATGTGTTGGAGC	TCAATGGTTGCTTTCTTGTCGTC	(Tang et al., 2007)

3.8 Acknowledgements

We would like to thank the University of Ottawa Animal Care and Veterinary Services for their help in maintaining and managing the fish. We would also like to thank Akimenko lab members Hailey Quigley and Joshua Ivare for their assistance with genotyping the fish and cardiac function analyses. Thank you as well to Célia Boumghar (University of Ottawa) for her help in heart rate analyses, to other University of Ottawa undergraduate students who helped with optimizing experiments (Meaghan de Jesus and Danick Goulet) or identifying *lmna* mutants (Katyanna Ménard, Nirali Shukla, Laurianne Perron and Caroline Awada) and to Raoul Salmon (Université de Lorraine) for also identifying *lmna* mutants. This study was supported by the following grants: CIHR grant DEV312217 to M-A.A and Heart and Stroke Foundation Grant NA 6628 to F.T.

3.9 Conflict of Interest

The authors declare no conflict of interest.

3.10 References

Al-Saaidi, R., & Bross, P. (2015). Do lamin A and lamin C have unique roles? *Chromosoma*, *124*(1), 1–12. https://doi.org/10.1007/s00412-014-0484-7

Al-Saaidi, R., Rasmussen, T. B., Palmfeldt, J., Nissen, P. H., Beqqali, A., Hansen, J., Pinto, Y. M., Boesen, T., Mogensen, J., & Bross, P. (2013). The LMNA mutation p.Arg321Ter associated with dilated cardiomyopathy leads to reduced expression and a skewed ratio of lamin A and lamin C proteins. *Experimental Cell Research*, *319*(19), 3010–3019. https://doi.org/10.1016/j.yexcr.2013.08.024

Anderson, J. L., Mulligan, T. S., Shen, M.-C., Wang, H., Scahill, C. M., Tan, F. J., Du, S. J., Busch-Nentwich, E. M., & Farber, S. A. (2017). MRNA processing in mutant zebrafish

lines generated by chemical and CRISPR-mediated mutagenesis produces unexpected transcripts that escape nonsense-mediated decay. *PLoS Genetics*, *13*(11), e1007105. https://doi.org/10.1371/journal.pgen.1007105

Arimura, T., Helbling-Leclerc, A., Massart, C., Varnous, S., Niel, F., Lacene, E., Fromes, Y., Toussaint, M., Mura, A. M., Keller, D. I., Amthor, H., Isnard, R., Malissen, M., Schwartz, K., & Bonne, G. (2005). Mouse model carrying H222P-Lmna mutation develops muscular dystrophy and dilated cardiomyopathy similar to human striated muscle laminopathies. *Human Molecular Genetics*, *14*(1), 155–169.

Bank, E. M., Ben-Harush, K., Wiesel-Motiuk, N., Barkan, R., Feinstein, N., Lotan, O., Medalia, O., & Gruenbaum, Y. (2011). A laminopathic mutation disrupting lamin filament assembly causes disease-like phenotypes in Caenorhabditis elegans. *Molecular Biology of the Cell*, *22*(15), 2716–2728. https://doi.org/10.1091/mbc.E11-01-0064

Bassett, D. I., Bryson-Richardson, R. J., Daggett, D. F., Gautier, P., Keenan, D. G., & Currie, P. D. (2003). Dystrophin is required for the formation of stable muscle attachments in the zebrafish embryo. *Development (Cambridge, England)*, *130*(23), 5851–5860. https://doi.org/10.1242/dev.00799

Bassett, D. I., & Currie, P. D. (2003). The zebrafish as a model for muscular dystrophy and congenital myopathy. *Human Molecular Genetics*, *12 Spec No 2*, R265-270. https://doi.org/10.1093/hmg/ddg279

Berger, J., Berger, S., Hall, T. E., Lieschke, G. J., & Currie, P. D. (2010). Dystrophin-deficient zebrafish feature aspects of the Duchenne muscular dystrophy pathology. *Neuromuscular Disorders: NMD*, *20*(12), 826–832. https://doi.org/10.1016/j.nmd.2010.08.004

Bertrand, A. T., Ziaei, S., Ehret, C., Duchemin, H., Mamchaoui, K., Bigot, A., Mayer, M., Quijano-Roy, S., Desguerre, I., Lainé, J., Ben Yaou, R., Bonne, G., & Coirault, C. (2014). Cellular microenvironments reveal defective mechanosensing responses and elevated YAP signaling in LMNA-mutated muscle precursors. *Journal of Cell Science*, *127*(Pt 13), 2873–2884. https://doi.org/10.1242/jcs.144907

Bonne, G., Mercuri, E., Muchir, A., Urtizberea, A., Becane, H. M., Recan, D., Merlini, L., Wehnert, M., Boor, R., Reuner, U., Vorgerd, M., Wicklein, E. M., Eymard, B., Duboc, D., Penisson-Besnier, I., Cuisset, J. M., Ferrer, X., Desguerre, I., Lacombe, D., … Muntoni, F. (2000). Clinical and molecular genetic spectrum of autosomal dominant Emery-Dreifuss muscular dystrophy due to mutations of the lamin A/C gene. *Annals of Neurology*, *48*(2), 170–180.

Bonne, Gisèle, & Quijano-Roy, S. (2013). Emery-Dreifuss muscular dystrophy, laminopathies, and other nuclear envelopathies. *Handbook of Clinical Neurology*, *113*, 1367–1376. https://doi.org/10.1016/B978-0-444-59565-2.00007-1

Bornancin, F., & Parker, P. J. (1997). Phosphorylation of protein kinase C-alpha on serine 657 controls the accumulation of active enzyme and contributes to its phosphatase-resistant state. *The Journal of Biological Chemistry*, *272*(6), 3544–3549. https://doi.org/10.1074/jbc.272.6.3544

Bowling, N., Walsh, R. A., Song, G., Estridge, T., Sandusky, G. E., Fouts, R. L., Mintze, K., Pickard, T., Roden, R., Bristow, M. R., Sabbah, H. N., Mizrahi, J. L., Gromo, G., King, G. L., & Vlahos, C. J. (1999). Increased protein kinase C activity and expression of Ca2+-sensitive isoforms in the failing human heart. *Circulation*, *99*(3), 384–391.

Braz, J. C., Gregory, K., Pathak, A., Zhao, W., Sahin, B., Klevitsky, R., Kimball, T. F., Lorenz, J. N., Nairn, A. C., Liggett, S. B., Bodi, I., Wang, S., Schwartz, A., Lakatta, E. G., DePaoli-Roach, A. A., Robbins, J., Hewett, T. E., Bibb, J. A., Westfall, M. V., … Molkentin, J. D. (2004). PKC-alpha regulates cardiac contractility and propensity toward heart failure. *Nature Medicine*, *10*(3), 248–254.

Braz, Julian C., Bueno, O. F., De Windt, L. J., & Molkentin, J. D. (2002). PKC alpha regulates the hypertrophic growth of cardiomyocytes through extracellular signal-regulated kinase1/2 (ERK1/2). *The Journal of Cell Biology*, *156*(5), 905–919. https://doi.org/10.1083/jcb.200108062

Broers, J. L., Ramaekers, F. C., Bonne, G., Yaou, R. B., & Hutchison, C. J. (2006). Nuclear lamins: Laminopathies and their role in premature ageing. *Physiological Reviews*, *86*(3), 967–1008.

Bugel, S. M., Wehmas, L. C., La Du, J. K., & Tanguay, R. L. (2016). Phenotype anchoring in zebrafish reveals a potential role for matrix metalloproteinases (MMPs) in tamoxifen's effects on skin epithelium. *Toxicology and Applied Pharmacology*, *296*, 31–41. https://doi.org/10.1016/j.taap.2016.02.013

Cazaubon, S., Bornancin, F., & Parker, P. J. (1994). Threonine-497 is a critical site for permissive activation of protein kinase C alpha. *The Biochemical Journal*, *301 (Pt 2)*, 443–448. https://doi.org/10.1042/bj3010443

Collymore, C., Tolwani, A., Lieggi, C., & Rasmussen, S. (2014). Efficacy and safety of 5 anesthetics in adult zebrafish (Danio rerio). *Journal of the American Association for Laboratory Animal Science : JAALAS*, *53*(2), 198–203.

Colombo, M. G., Botto, N., Vittorini, S., Paradossi, U., & Andreassi, M. G. (2008). Clinical utility of genetic tests for inherited hypertrophic and dilated cardiomyopathies. *Cardiovascular Ultrasound*, *6*, 62. https://doi.org/10.1186/1476-7120-6-62

Dialynas, G., Shrestha, O. K., Ponce, J. M., Zwerger, M., Thiemann, D. A., Young, G. H., Moore, S. A., Yu, L., Lammerding, J., & Wallrath, L. L. (2015). Myopathic lamin mutations cause reductive stress and activate the nrf2/keap-1 pathway. *PLoS Genetics*, *11*(5), e1005231. https://doi.org/10.1371/journal.pgen.1005231

González, J. M., Navarro-Puche, A., Casar, B., Crespo, P., & Andrés, V. (2008). Fast regulation of AP-1 activity through interaction of lamin A/C, ERK1/2, and c-Fos at the nuclear envelope. *The Journal of Cell Biology*, *183*(4), 653–666. https://doi.org/10.1083/jcb.200805049

Gupta, P., Bilinska, Z. T., Sylvius, N., Boudreau, E., Veinot, J. P., Labib, S., Bolongo, P. M., Hamza, A., Jackson, T., Ploski, R., Walski, M., Grzybowski, J., Walczak, E., Religa, G., Fidzianska, A., & Tesson, F. (2010). Genetic and ultrastructural studies in dilated cardiomyopathy patients: A large deletion in the lamin A/C gene is associated with cardiomyocyte nuclear envelope disruption. *Basic Research in Cardiology*, *105*(3), 365–377.

Gysin, S., & Imber, R. (1996). Replacement of Ser657 of protein kinase C-alpha by alanine leads to premature down regulation after phorbol-ester-induced translocation to the membrane. *European Journal of Biochemistry*, *240*(3), 747–750. https://doi.org/10.1111/j.1432-1033.1996.0747h.x

Hambleton, M., Hahn, H., Pleger, S. T., Kuhn, M. C., Klevitsky, R., Carr, A. N., Kimball, T. F., Hewett, T. E., 2nd, G. W. D., Koch, W. J., & Molkentin, J. D. (2006). Pharmacological-

and gene therapy-based inhibition of protein kinase Calpha/beta enhances cardiac contractility and attenuates heart failure. *Circulation*, *114*(6), 574–582.

Haque, F., Lloyd, D. J., Smallwood, D. T., Dent, C. L., Shanahan, C. M., Fry, A. M., Trembath, R. C., & Shackleton, S. (2006). SUN1 interacts with nuclear lamin A and cytoplasmic nesprins to provide a physical connection between the nuclear lamina and the cytoskeleton. *Molecular and Cellular Biology*, *26*(10), 3738–3751. https://doi.org/10.1128/MCB.26.10.3738-3751.2006

Hasselberg, N. E., Haland, T. F., Saberniak, J., Brekke, P. H., Berge, K. E., Leren, T. P., Edvardsen, T., & Haugaa, K. H. (2018). Lamin A/C cardiomyopathy: Young onset, high penetrance, and frequent need for heart transplantation. *European Heart Journal*, *39*(10), 853–860. https://doi.org/10.1093/eurheartj/ehx596

Hayashi, K., Teramoto, R., Nomura, A., Asano, Y., Beerens, M., Kurata, Y., Kobayashi, I., Fujino, N., Furusho, H., Sakata, K., Onoue, K., Chiang, D. Y., Kiviniemi, T. O., Buys, E., Sips, P., Burch, M. L., Zhao, Y., Kelly, A. E., Namura, M., … Takamura, M. (2020). Impact of functional studies on exome sequence variant interpretation in early-onset cardiac conduction system diseases. *Cardiovascular Research*. https://doi.org/10.1093/cvr/cvaa010

Hoage, T., Ding, Y., & Xu, X. (2012). Quantifying cardiac functions in embryonic and adult zebrafish. *Methods in Molecular Biology (Clifton, N.J.)*, *843*, 11–20. https://doi.org/10.1007/978-1-61779-523-7_2

Hu, R., Morley, M. P., Brandimarto, J., Tucker, N. R., Parsons, V. A., Zhao, S. D., Meder, B., Katus, H. A., Rühle, F., Stoll, M., Villard, E., Cambien, F., Lin, H., Smith, N. L., Felix, J. F., Vasan, R. S., van der Harst, P., Newton-Cheh, C., Li, J., … Cappola, T. P. (2018).

Genetic Reduction in Left Ventricular Protein Kinase C-α and Adverse Ventricular Remodeling in Human Subjects. *Circulation. Genomic and Precision Medicine*, *11*(3), e001901. https://doi.org/10.1161/CIRCGEN.117.001901

Hwang, W. Y., Fu, Y., Reyon, D., Maeder, M. L., Tsai, S. Q., Sander, J. D., Peterson, R. T., Yeh, J. R., & Joung, J. K. (2013). Efficient genome editing in zebrafish using a CRISPR-Cas system. *Nature Biotechnology*, *31*(3), 227–229.

Hwang, Woong Y., Fu, Y., Reyon, D., Maeder, M. L., Kaini, P., Sander, J. D., Joung, J. K., Peterson, R. T., & Yeh, J.-R. J. (2013). Heritable and precise zebrafish genome editing using a CRISPR-Cas system. *PloS One*, *8*(7), e68708. https://doi.org/10.1371/journal.pone.0068708

Ivorra, C., Kubicek, M., González, J. M., Sanz-González, S. M., Alvarez-Barrientos, A., O'Connor, J.-E., Burke, B., & Andrés, V. (2006). A mechanism of AP-1 suppression through interaction of c-Fos with lamin A/C. *Genes & Development*, *20*(3), 307–320. https://doi.org/10.1101/gad.349506

Jahn, D., Schramm, S., Schnolzer, M., Heilmann, C. J., de Koster, C. G., Schutz, W., Benavente, R., & Alsheimer, M. (2012). A truncated lamin A in the Lmna -/- mouse line: Implications for the understanding of laminopathies. *Nucleus (Austin, Tex.)*, *3*(5), 463–474. https://doi.org/10.4161/nucl.21676

Jensen, T. E., Maarbjerg, S. J., Rose, A. J., Leitges, M., & Richter, E. A. (2009). Knockout of the predominant conventional PKC isoform, PKCalpha, in mouse skeletal muscle does not affect contraction-stimulated glucose uptake. *American Journal of Physiology.Endocrinology and Metabolism*, *297*(2), E340-8.

Jr, R. R. (2012). ERK1/2 MAP kinases: Structure, function, and regulation. *Pharmacological Research : The Official Journal of the Italian Pharmacological Society*, *66*(2), 105–143.

Jung, H.-J., Coffinier, C., Choe, Y., Beigneux, A. P., Davies, B. S. J., Yang, S. H., Barnes, R. H., Hong, J., Sun, T., Pleasure, S. J., Young, S. G., & Fong, L. G. (2012). Regulation of prelamin A but not lamin C by miR-9, a brain-specific microRNA. *Proceedings of the National Academy of Sciences of the United States of America*, *109*(7), E423-431. https://doi.org/10.1073/pnas.1111780109

Keranen, L. M., Dutil, E. M., & Newton, A. C. (1995). Protein kinase C is regulated in vivo by three functionally distinct phosphorylations. *Current Biology : CB*, *5*(12), 1394–1403. https://doi.org/10.1016/s0960-9822(95)00277-6

Kim, S., Lee, J., Lee, S. K., Bae, S. Y., Kim, J., Kim, M., Kil, W. H., Kim, S. W., Lee, J. E., & Nam, S. J. (2014). Protein kinase C-α downregulates estrogen receptor-α by suppressing c-Jun phosphorylation in estrogen receptor-positive breast cancer cells. *Oncology Reports*, *31*(3), 1423–1428. https://doi.org/10.3892/or.2013.2936

Kim, Y., & Zheng, Y. (2013). Generation and characterization of a conditional deletion allele for Lmna in mice. *Biochemical and Biophysical Research Communications*, *440*(1), 8–13. https://doi.org/10.1016/j.bbrc.2013.08.082

Kok, F. O., Shin, M., Ni, C.-W., Gupta, A., Grosse, A. S., van Impel, A., Kirchmaier, B. C., Peterson-Maduro, J., Kourkoulis, G., Male, I., DeSantis, D. F., Sheppard-Tindell, S., Ebarasi, L., Betsholtz, C., Schulte-Merker, S., Wolfe, S. A., & Lawson, N. D. (2015). Reverse genetic screening reveals poor correlation between morpholino-induced and mutant phenotypes in zebrafish. *Developmental Cell*, *32*(1), 97–108. https://doi.org/10.1016/j.devcel.2014.11.018

Koshimizu, E., Imamura, S., Qi, J., Toure, J., Jr, D. M. V., Carr, C. E., Hanai, J., & Kishi, S. (2011). Embryonic senescence and laminopathies in a progeroid zebrafish model. *PloS One*, *6*(3), e17688.

Kubben, N., Voncken, J. W., Konings, G., van Weeghel, M., van den Hoogenhof, M. M., Gijbels, M., van Erk, A., Schoonderwoerd, K., van den Bosch, B., Dahlmans, V., Calis, C., Houten, S. M., Misteli, T., & Pinto, Y. M. (2011). Post-natal myogenic and adipogenic developmental: Defects and metabolic impairment upon loss of A-type lamins. *Nucleus (Austin, Tex.)*, *2*(3), 195–207. https://doi.org/10.4161/nucl.2.3.15731

Ladage, D., Tilemann, L., Ishikawa, K., Correll, R. N., Kawase, Y., Houser, S. R., Molkentin, J. D., & Hajjar, R. J. (2011). Inhibition of PKCα/β with ruboxistaurin antagonizes heart failure in pigs after myocardial infarction injury. *Circulation Research*, *109*(12), 1396–1400. https://doi.org/10.1161/CIRCRESAHA.111.255687

Lammerding, J., Fong, L. G., Ji, J. Y., Reue, K., Stewart, C. L., Young, S. G., & Lee, R. T. (2006). Lamins A and C but not lamin B1 regulate nuclear mechanics. *The Journal of Biological Chemistry*, *281*(35), 25768–25780. https://doi.org/10.1074/jbc.M513511200

Lammerding, J., Schulze, P. C., Takahashi, T., Kozlov, S., Sullivan, T., Kamm, R. D., Stewart, C. L., & Lee, R. T. (2004). Lamin A/C deficiency causes defective nuclear mechanics and mechanotransduction. *The Journal of Clinical Investigation*, *113*(3), 370–378. https://doi.org/10.1172/JCI19670

Laurini, E., Martinelli, V., Lanzicher, T., Puzzi, L., Borin, D., Chen, S. N., Long, C. S., Lee, P., Mestroni, L., Taylor, M. R. G., Sbaizero, O., & Pricl, S. (2018). Biomechanical defects and rescue of cardiomyocytes expressing pathologic nuclear lamins. *Cardiovascular Research*, *114*(6), 846–857. https://doi.org/10.1093/cvr/cvy040

Leber, Y., Ruparelia, A. A., Kirfel, G., van der Ven, P. F. M., Hoffmann, B., Merkel, R., Bryson-Richardson, R. J., & Fürst, D. O. (2016). Filamin C is a highly dynamic protein associated with fast repair of myofibrillar microdamage. *Human Molecular Genetics*, *25*(13), 2776–2788. https://doi.org/10.1093/hmg/ddw135

Leitges, M., Plomann, M., Standaert, M. L., Bandyopadhyay, G., Sajan, M. P., Kanoh, Y., Farese, R. V., & Letiges, M. (2002). Knockout of PKC alpha enhances insulin signaling through PI3K. *Molecular Endocrinology (Baltimore, Md.)*, *16*(4), 847–858. https://doi.org/10.1210/mend.16.4.0809

Li, M., Hromowyk, K. J., Amacher, S. L., & Currie, P. D. (2017). Muscular dystrophy modeling in zebrafish. *Methods in Cell Biology*, *138*, 347–380. https://doi.org/10.1016/bs.mcb.2016.11.004

Martelli, A. M., Bortul, R., Tabellini, G., Faenza, I., Cappellini, A., Bareggi, R., Manzoli, L., & Cocco, L. (2002). Molecular characterization of protein kinase C-alpha binding to lamin A. *Journal of Cellular Biochemistry*, *86*(2), 320–330.

Mauro, A., Ciccarelli, C., Cesaris, P. D., Scoglio, A., Bouche, M., Molinaro, M., Aquino, A., & Zani, B. M. (2002). PKCalpha-mediated ERK, JNK and p38 activation regulates the myogenic program in human rhabdomyosarcoma cells. *Journal of Cell Science*, *115*(Pt 18), 3587–3599.

Meeker, N. D., Hutchinson, S. A., Ho, L., & Trede, N. S. (2007). Method for isolation of PCR-ready genomic DNA from zebrafish tissues. *BioTechniques*, *43*(5), 610, 612, 614.

Motsch, I., Kaluarachchi, M., Emerson, L. J., Brown, C. A., Brown, S. C., Dabauvalle, M.-C., & Ellis, J. A. (2005). Lamins A and C are differentially dysfunctional in autosomal

dominant Emery-Dreifuss muscular dystrophy. *European Journal of Cell Biology*, *84*(9), 765–781. https://doi.org/10.1016/j.ejcb.2005.04.004

Muchir, A., Bonne, G., van der Kooi, A. J., van Meegen, M., Baas, F., Bolhuis, P. A., de Visser, M., & Schwartz, K. (2000). Identification of mutations in the gene encoding lamins A/C in autosomal dominant limb girdle muscular dystrophy with atrioventricular conduction disturbances (LGMD1B). *Human Molecular Genetics*, *9*(9), 1453–1459.

Muchir, A., Kim, Y. J., Reilly, S. A., Wu, W., Choi, J. C., & Worman, H. J. (2013). Inhibition of extracellular signal-regulated kinase 1/2 signaling has beneficial effects on skeletal muscle in a mouse model of Emery-Dreifuss muscular dystrophy caused by lamin A/C gene mutation. *Skeletal Muscle*, *3*(1), 17-5040-3–17.

Muchir, A., Pavlidis, P., Decostre, V., Herron, A. J., Arimura, T., Bonne, G., & Worman, H. J. (2007). Activation of MAPK pathways links LMNA mutations to cardiomyopathy in Emery-Dreifuss muscular dystrophy. *The Journal of Clinical Investigation*, *117*(5), 1282–1293.

Muchir, A., Reilly, S. A., Wu, W., Iwata, S., Homma, S., Bonne, G., & Worman, H. J. (2012). Treatment with selumetinib preserves cardiac function and improves survival in cardiomyopathy caused by mutation in the lamin A/C gene. *Cardiovascular Research*, *93*(2), 311–319.

Muchir, A., Shan, J., Bonne, G., Lehnart, S. E., & Worman, H. J. (2009). Inhibition of extracellular signal-regulated kinase signaling to prevent cardiomyopathy caused by mutation in the gene encoding A-type lamins. *Human Molecular Genetics*, *18*(2), 241–247.

Muchir, A., Wu, W., & Worman, H. J. (2009). Reduced expression of A-type lamins and emerin activates extracellular signal-regulated kinase in cultured cells. *Biochimica et Biophysica Acta*, *1792*(1), 75–81.

Nakashima, S. (2002). Protein kinase C alpha (PKC alpha): Regulation and biological function. *Journal of Biochemistry*, *132*(5), 669–675.

Naskar, S., Datta, K., Mitra, A., Pathak, K., Datta, R., Bansal, T., & Sarkar, S. (2014). Differential and conditional activation of PKC-isoforms dictates cardiac adaptation during physiological to pathological hypertrophy. *PloS One*, *9*(8), e104711.

Nicolas, H. A., Akimenko, M.-A., & Tesson, F. (2019). Cellular and Animal Models of Striated Muscle Laminopathies. *Cells*, *8*(4). https://doi.org/10.3390/cells8040291

Parekh, D. B., Ziegler, W., & Parker, P. J. (2000). Multiple pathways control protein kinase C phosphorylation. *The EMBO Journal*, *19*(4), 496–503. https://doi.org/10.1093/emboj/19.4.496

Pasotti, M., Klersy, C., Pilotto, A., Marziliano, N., Rapezzi, C., Serio, A., Mannarino, S., Gambarin, F., Favalli, V., Grasso, M., Agozzino, M., Campana, C., Gavazzi, A., Febo, O., Marini, M., Landolina, M., Mortara, A., Piccolo, G., Viganò, M., … Arbustini, E. (2008). Long-term outcome and risk stratification in dilated cardiolaminopathies. *Journal of the American College of Cardiology*, *52*(15), 1250–1260. https://doi.org/10.1016/j.jacc.2008.06.044

Pass, J. M., Gao, J., Jones, W. K., Wead, W. B., Wu, X., Zhang, J., Baines, C. P., Bolli, R., Zheng, Y. T., Joshua, I. G., & Ping, P. (2001). Enhanced PKC beta II translocation and PKC beta II-RACK1 interactions in PKC epsilon-induced heart failure: A role for

RACK1. *American Journal of Physiology. Heart and Circulatory Physiology*, *281*(6), H2500-2510. https://doi.org/10.1152/ajpheart.2001.281.6.H2500

Peter, A., & Stick, R. (2012). Evolution of the lamin protein family: What introns can tell. *Nucleus (Austin, Tex.)*, *3*(1), 44–59. https://doi.org/10.4161/nucl.18927

Ping, P., Zhang, J., Qiu, Y., Tang, X. L., Manchikalapudi, S., Cao, X., & Bolli, R. (1997). Ischemic preconditioning induces selective translocation of protein kinase C isoforms epsilon and eta in the heart of conscious rabbits without subcellular redistribution of total protein kinase C activity. *Circulation Research*, *81*(3), 404–414. https://doi.org/10.1161/01.res.81.3.404

Pinto, Y. M., Elliott, P. M., Arbustini, E., Adler, Y., Anastasakis, A., Böhm, M., Duboc, D., Gimeno, J., de Groote, P., Imazio, M., Heymans, S., Klingel, K., Komajda, M., Limongelli, G., Linhart, A., Mogensen, J., Moon, J., Pieper, P. G., Seferovic, P. M., … Charron, P. (2016). Proposal for a revised definition of dilated cardiomyopathy, hypokinetic non-dilated cardiomyopathy, and its implications for clinical practice: A position statement of the ESC working group on myocardial and pericardial diseases. *European Heart Journal*, *37*(23), 1850–1858. https://doi.org/10.1093/eurheartj/ehv727

Reimann, L., Wiese, H., Leber, Y., Schwäble, A. N., Fricke, A. L., Rohland, A., Knapp, B., Peikert, C. D., Drepper, F., van der Ven, P. F. M., Radziwill, G., Fürst, D. O., & Warscheid, B. (2017). Myofibrillar Z-discs Are a Protein Phosphorylation Hot Spot with Protein Kinase C (PKCα) Modulating Protein Dynamics. *Molecular & Cellular Proteomics: MCP*, *16*(3), 346–367. https://doi.org/10.1074/mcp.M116.065425

Rossi, A., Kontarakis, Z., Gerri, C., Nolte, H., Hölper, S., Krüger, M., & Stainier, D. Y. R. (2015). Genetic compensation induced by deleterious mutations but not gene knockdowns. *Nature*, *524*(7564), 230–233. https://doi.org/10.1038/nature14580

Sander, J. D., Maeder, M. L., Reyon, D., Voytas, D. F., Joung, J. K., & Dobbs, D. (2010). ZiFiT (Zinc Finger Targeter): An updated zinc finger engineering tool. *Nucleic Acids Research*, *38*(Web Server issue), W462-468. https://doi.org/10.1093/nar/gkq319

Sander, J. D., Zaback, P., Joung, J. K., Voytas, D. F., & Dobbs, D. (2007). Zinc Finger Targeter (ZiFiT): An engineered zinc finger/target site design tool. *Nucleic Acids Research*, *35*(Web Server issue), W599-605. https://doi.org/10.1093/nar/gkm349

Schönwasser, D. C., Marais, R. M., Marshall, C. J., & Parker, P. J. (1998). Activation of the mitogen-activated protein kinase/extracellular signal-regulated kinase pathway by conventional, novel, and atypical protein kinase C isotypes. *Molecular and Cellular Biology*, *18*(2), 790–798. https://doi.org/10.1128/mcb.18.2.790

Seeley, M., Huang, W., Chen, Z., Wolff, W. O., Lin, X., & Xu, X. (2007). Depletion of zebrafish titin reduces cardiac contractility by disrupting the assembly of Z-discs and A-bands. *Circulation Research*, *100*(2), 238–245. https://doi.org/10.1161/01.RES.0000255758.69821.b5

Shimi, T., Kittisopikul, M., Tran, J., Goldman, A. E., Adam, S. A., Zheng, Y., Jaqaman, K., & Goldman, R. D. (2015). Structural organization of nuclear lamins A, C, B1, and B2 revealed by superresolution microscopy. *Molecular Biology of the Cell*, *26*(22), 4075–4086. https://doi.org/10.1091/mbc.E15-07-0461

Shimi, T., Pfleghaar, K., Kojima, S., Pack, C.-G., Solovei, I., Goldman, A. E., Adam, S. A., Shumaker, D. K., Kinjo, M., Cremer, T., & Goldman, R. D. (2008). The A- and B-type

nuclear lamin networks: Microdomains involved in chromatin organization and transcription. *Genes & Development*, *22*(24), 3409–3421. https://doi.org/10.1101/gad.1735208

Simon, D. N., Zastrow, M. S., & Wilson, K. L. (2010). Direct actin binding to A- and B-type lamin tails and actin filament bundling by the lamin A tail. *Nucleus (Austin, Tex.)*, *1*(3), 264–272. https://doi.org/10.4161/nucl.1.3.11799

Siu, C.-W., Lee, Y.-K., Ho, J. C.-Y., Lai, W.-H., Chan, Y.-C., Ng, K.-M., Wong, L.-Y., Au, K.-W., Lau, Y.-M., Zhang, J., Lay, K. W., Colman, A., & Tse, H.-F. (2012). Modeling of lamin A/C mutation premature cardiac aging using patient-specific induced pluripotent stem cells. *Aging*, *4*(11), 803–822. https://doi.org/10.18632/aging.100503

Staudt, D., & Stainier, D. (2012). Uncovering the molecular and cellular mechanisms of heart development using the zebrafish. *Annual Review of Genetics*, *46*, 397–418. https://doi.org/10.1146/annurev-genet-110711-155646

Steffen, L. S., Guyon, J. R., Vogel, E. D., Beltre, R., Pusack, T. J., Zhou, Y., Zon, L. I., & Kunkel, L. M. (2007). Zebrafish orthologs of human muscular dystrophy genes. *BMC Genomics*, *8*, 79.

Sullivan, T., Escalante-Alcalde, D., Bhatt, H., Anver, M., Bhat, N., Nagashima, K., Stewart, C. L., & Burke, B. (1999). Loss of A-type lamin expression compromises nuclear envelope integrity leading to muscular dystrophy. *The Journal of Cell Biology*, *147*(5), 913–920.

Sylvius, N., Hathaway, A., Boudreau, E., Gupta, P., Labib, S., Bolongo, P. M., Rippstein, P., McBride, H., Bilinska, Z. T., & Tesson, F. (2008). Specific contribution of lamin A and lamin C in the development of laminopathies. *Experimental Cell Research*, *314*(13), 2362–2375.

Tang, R., Dodd, A., Lai, D., McNabb, W. C., & Love, D. R. (2007). Validation of zebrafish (Danio rerio) reference genes for quantitative real-time RT-PCR normalization. *Acta Biochimica Et Biophysica Sinica*, *39*(5), 384–390. https://doi.org/10.1111/j.1745-7270.2007.00283.x

Taylor, M. R., Fain, P. R., Sinagra, G., Robinson, M. L., Robertson, A. D., Carniel, E., Lenarda, A. D., Bohlmeyer, T. J., Ferguson, D. A., Brodsky, G. L., Boucek, M. M., Lascor, J., Moss, A. C., Li, W. L., Stetler, G. L., Muntoni, F., Bristow, M. R., Mestroni, L., & Group, F. D. C. R. R. (2003). Natural history of dilated cardiomyopathy due to lamin A/C gene mutations. *Journal of the American College of Cardiology*, *41*(5), 771–780.

Tesson, F., Saj, M., Uvaize, M. M., Nicolas, H., Płoski, R., & Bilińska, Z. (2014). Lamin A/C mutations in dilated cardiomyopathy. *Cardiology Journal*, *21*(4), 331–342. https://doi.org/10.5603/CJ.a2014.0037

van Berlo, J. H., de Voogt, W. G., van der Kooi, A. J., van Tintelen, J. P., Bonne, G., Yaou, R. B., Duboc, D., Rossenbacker, T., Heidbüchel, H., de Visser, M., Crijns, H. J. G. M., & Pinto, Y. M. (2005). Meta-analysis of clinical characteristics of 299 carriers of LMNA gene mutations: Do lamin A/C mutations portend a high risk of sudden death? *Journal of Molecular Medicine (Berlin, Germany)*, *83*(1), 79–83. https://doi.org/10.1007/s00109-004-0589-1

van Engelen, B. G. M., Muchir, A., Hutchison, C. J., van der Kooi, A. J., Bonne, G., & Lammens, M. (2005). The lethal phenotype of a homozygous nonsense mutation in the lamin A/C gene. *Neurology*, *64*(2), 374–376. https://doi.org/10.1212/01.WNL.0000149763.15180.00

Verma, A. D., & Parnaik, V. K. (2017). Heart-specific expression of laminopathic mutations in transgenic zebrafish. *Cell Biology International*, *41*(7), 809–819. https://doi.org/10.1002/cbin.10784

Vogel, B., Meder, B., Just, S., Laufer, C., Berger, I., Weber, S., Katus, H. A., & Rottbauer, W. (2009). In-vivo characterization of human dilated cardiomyopathy genes in zebrafish. *Biochemical and Biophysical Research Communications*, *390*(3), 516–522.

Vytopil, M., Ricci, E., Dello Russo, A., Hanisch, F., Neudecker, S., Zierz, S., Ricotti, R., Demay, L., Richard, P., Wehnert, M., Bonne, G., Merlini, L., & Toniolo, D. (2002). Frequent low penetrance mutations in the Lamin A/C gene, causing Emery Dreifuss muscular dystrophy. *Neuromuscular Disorders: NMD*, *12*(10), 958–963.

Wang, J., Liu, X., Sentex, E., Takeda, N., & Dhalla, N. S. (2003). Increased expression of protein kinase C isoforms in heart failure due to myocardial infarction. *American Journal of Physiology. Heart and Circulatory Physiology*, *284*(6), H2277-2287. https://doi.org/10.1152/ajpheart.00142.2002

Wexler, R. K., Elton, T., Pleister, A., & Feldman, D. (2009). Cardiomyopathy: An overview. *American Family Physician*, *79*(9), 778–784.

Wu, W., Muchir, A., Shan, J., Bonne, G., & Worman, H. J. (2011). Mitogen-activated protein kinase inhibitors improve heart function and prevent fibrosis in cardiomyopathy caused by mutation in lamin A/C gene. *Circulation*, *123*(1), 53–61.

Wu, W., Shan, J., Bonne, G., Worman, H. J., & Muchir, A. (2010). Pharmacological inhibition of c-Jun N-terminal kinase signaling prevents cardiomyopathy caused by mutation in LMNA gene. *Biochimica et Biophysica Acta*, *1802*(7–8), 632–638.

Xu, X., Meiler, S. E., Zhong, T. P., Mohideen, M., Crossley, D. A., Burggren, W. W., & Fishman, M. C. (2002). Cardiomyopathy in zebrafish due to mutation in an alternatively spliced exon of titin. *Nature Genetics*, *30*(2), 205–209. https://doi.org/10.1038/ng816

Ye, L., Robertson, M. A., Hesselson, D., Stainier, D. Y. R., & Anderson, R. M. (2015). Glucagon is essential for alpha cell transdifferentiation and beta cell neogenesis. *Development (Cambridge, England)*, *142*(8), 1407–1417. https://doi.org/10.1242/dev.117911

Zhu, X., Xu, Y., Yu, S., Lu, L., Ding, M., Cheng, J., Song, G., Gao, X., Yao, L., Fan, D., Meng, S., Zhang, X., Hu, S., & Tian, Y. (2014). An efficient genotyping method for genome-modified animals and human cells generated with CRISPR/Cas9 system. *Scientific Reports*, *4*, 6420. https://doi.org/10.1038/srep06420

Chapter 4
General Discussion

4.1 The three hypotheses regarding laminopathies

Laminopathies are a group of diseases that affect various tissue types ranging from adipose tissues to myocytes. However, laminopathies can also manifest a multisystem phenotype such as in the premature aging condition - Hutchinson-Gilford progeria syndrome (HGPS). For a gene such as lamin A/C that is expressed in most cell types, the resulting diverse and tissue-specific phenotypes of patients with various lamin A/C mutations are intriguing. How can mutations in a widely expressed gene present with tissue-specific phenotypes? How can two individuals with the same *LMNA* mutation present with different conditions or one be asymptomatic while the other is gravely ill? Three overarching hypotheses seek to explain the underlying mechanisms for the development of laminopathy in patients and these hypotheses are not mutually exclusive. The first hypothesis proposes that toxic and misprocessed A-type lamins cause the phenotypes. The second hypothesis attributes the diseases to abnormal gene expression regulation by variant lamin A/C. Lastly, the third hypothesis proposes that the disruption of lamin A/C's role in nuclear and chromatin support and mechanical transduction causes the phenotypes.

The first hypothesis attributes the disease phenotype as primarily caused by the accumulation of toxic and misprocessed lamin A/C. The misprocessed lamin A/C is detrimental to the cell and eventually causes a disease. The classic case supporting this notion is with HGPS. Most HGPS patients possess a mutation in exon 11 of *LMNA* that affects amino acid 608 (Eriksson et al., 2003). The HGPS mutation results in the activation of a cryptic splice that produces a variant lacking 50 amino acids in the C terminus (Eriksson et al., 2003). Due to alternative splicing in exon 10, exons 11 and 12 are lamin A specific; thus, lamin C is unaffected. This truncated lamin A (also known as progerin) retains its C*AAX* motif and is not cleaved by ZMPSTE24 to generate mature lamin A (Eriksson et al., 2003). A farnesyl group is added to the cysteine of this *CAXX*

motif by farnesyl transferase, and this is the first of the post-translational modifications that prelamin A goes through to yield mature lamin A (Agarwal et al., 2003). Individuals with the progeric mutation affecting amino acid 608 express the misprocessed and truncated premature lamin A that remains farnesylated. Two mice models expressing either farnesylated progerin (*Lmna*^{HG}) or non-farnesylated progerin (*Lmna*^{nHG}) were created (Yang et al., 2005, 2008). Both *Lmna*^{HG} and *Lmna*^{nHG} mice presented with progeric syndrome (growth delay, osteoporosis, lipodystrophy, premature death) but the *Lmna*^{nHG} mice had a less severe phenotype (Yang et al., 2006, 2008). Inhibition of farnesyl transferase in the heterozygous *Lmna*^{HG} mice decreased the number of nuclei with blebs, improved weight gain, and reduced fat loss and bone fracture (Yang et al., 2005, 2006). Similarly, farnesyl transferase inhibition in the heterozygous *Lmna*^{nHG} mice reduced nuclear blebs (Yang et al., 2008). In cellular models, expression of progerin in control foreskin fibroblasts and in HeLa cells recapitulated the cellular phenotype (misshapen nuclei, mislocalization of some nuclear proteins, loss of heterochromatin) seen in HGPS patient fibroblasts (Goldman et al., 2004b). However, expression of WT lamin A in HGPS patient cells did not rescue the abnormal cellular phenotype suggesting that the truncated HGPS lamin A variant behaved in a dominant negative manner (Scaffidi & Misteli, 2005). Unsurprisingly, treatment of HGPS patient fibroblasts with morpholino that blocked the activated splice site in exon 11 preventing the production of the truncated lamin A, rescued the cellular abnormalities noted in the patient cells (Scaffidi & Misteli, 2005). The treatment also normalized the expression of several genes associated with HGPS (Scaffidi & Misteli, 2005). Altogether, these data show that progerin causes the HGPS phenotype.

However, persistence of immature lamin A/C does not always result in progeria. It can also lead to cardiomyopathy. Mice that express non-farnesylated prelamin A (nPLA) only or WT (i.e.

farnesylated) prelamin A (PLA) only were created (Davies et al., 2010). The non-farnesylated prelamin A was localized in both the nuclear rim and the nucleoplasm just like lamin A in WT mice, and WT prelamin A in the PLA mice (Davies et al., 2010). Nuclear stiffness did not differ between the mouse embryo fibroblasts (MEFs) of PLA and nPLA mice though nuclear deformations were noted in the cells of the nPLA mice (Davies et al., 2010). PLA and nPLA litter were also comparable up until 20 weeks old after which the nPLA mice developed DCM and cardiac dysfunction resulting in death of all male nPLA mice by 44 weeks and all nPLA female mice by 80 weeks (Davies et al., 2010). Crossing the PLA mice with the *Zmpste24* null mice (gene that encodes ZMPSTE24) also resulted in an increase in prelamin A production that led to worse outcome (lower body weight and poorer survival rate) in the PLA$^{-/-}$ or $^{+/-}$ *Zmpste24*$^{-/-}$ mice compared to controls; thus confirming that the unprocessed lamin A was toxic to the cells and caused the cardiac phenotype (Davies et al., 2010). .

Another mice model which was initially thought to be *Lmna* null (from here on will be referred to as *Lmna*$^{\Delta 8\text{-}11}$) actually expresses a truncated lamin A that lacks the C terminus of the protein (Jahn et al., 2012; Sullivan et al., 1999). Homozygous *Lmna*$^{\Delta 8\text{-}11}$ mice were initially indistinguishable from their heterozygous and WT siblings but by week 2 to 3, the homozygous mice had growth delay and displayed gait defects by week 3-4 post birth (Sullivan et al., 1999). Furthermore, by 8 weeks old, the homozygous *Lmna*$^{\Delta 8\text{-}11}$ mice were all dead (Sullivan et al., 1999). In contrast, the heterozygous *Lmna*$^{\Delta 8\text{-}11}$ mice presented with cardiac dysfunction at 10 weeks old and by 50 weeks old, the mice had cardiac chamber dilation and decreased fractional shortening (Wolf et al., 2008). While haploinsufficiency might contribute to DCM development in the heterozygous *Lmna*$^{\Delta 8\text{-}11}$ mice, it is also probable that the truncated lamin A that was expressed in these mutant mice acted in a dominant negative manner that was harmful to the mice.

Taken together, the presented studies on progerin, misprocessed and/or truncated lamin A give support to the detrimental effects of "toxic" lamin A/C and its contribution to the development of laminopathies.

The second hypothesis endeavoring to explain laminopathies ascribes the diversity of phenotypes as a consequence of the disturbance in gene expression regulation by lamin A/C. As discussed earlier in the introduction (section 1.3.b pages 12-17), the A-type lamins are known to bind proteins as a means to regulate their functions (Ivorra et al., 2006; Myant et al., 2015; Rodríguez et al., 2010). Such interaction can keep a transcription factor from reaching and acting on its target(s) and/or prevents it from interacting with its regulator(s). Alternatively, lamin A/C can also facilitate the transcription factor's interactions by binding both the transcription factor and its target or regulator. Nonetheless, the downstream effect would affect gene expression. The p.H222P variant is the best characterized striated muscle laminopathy variant (Nicolas et al., 2019). The MAPK signaling pathway was implicated in striated muscle laminopathies primarily from studies involving the H222P EDMD mice model. The A-type lamins are known to bind ERKs in the region spanning amino acids 247-355 (González et al., 2008). Though H222 is outside this region, the mutation affecting this position disturbed ERK 1/2 activity and cellular localization. An increase in nuclear ERK 1/2 was noted and its activation was pronounced in the H222P EDMD mutant mice (Muchir et al., 2007). The other MAPK members - JNK and p38, along with the MAPKs downstream targets such as ELK-1, a transcription factor, were similarly upregulated (Muchir et al., 2007). This abnormal increase in transcription factor expression and activation followed by the consequent changes in the expression profile of their respective target genes was thought to contribute to the disease development as the cells respond to stimuli and stress in the context of an abnormal gene expression profile.

In another example, *C. elegans* carrying fluorescently-tagged plasmids that are incorporated in the genome in tandem arrays were studied (Mattout et al., 2011). As mentioned in the introduction (section 1.3.b pages 13-14), lamin-1 depletion resulted in a shift of the plasmid arrays towards the nuclear interior, and expression of the green fluorescent marker suggesting plasmid de-repression, and lamin-1 function in plasmid arrays tethering and gene expression regulation (Mattout et al., 2011). To determine if lamin mutations affect the nuclear periphery sequestration and/or repositioning of heterochromatin in a tissue-specific manner, a plasmid array expressing red fluorescent protein (RFP) under *myo-3*, a muscle-specific promoter, was assessed in the muscle cells of WT worms and mutant worms expressing the EDMD p.Y59C lamin-1 variant (Mattout et al., 2011). In the muscle cells of WT worms, the array under the *myo-3* promoter had shifted from the nuclear rim to the nucleoplasm (Mattout et al., 2011). On the other hand, in the muscle cells of mutant worms, half of the muscle-specific arrays were retained in the nuclear periphery (Mattout et al., 2011). Consequently, the mutant worms also displayed defects in muscle integrity (e.g. F actin disorganization in the trunk), and impaired swim capacity (Mattout et al., 2011). To verify if the effect of p.Y59C lamin-1 is cell/tissue-specific, the expression of other arrays was examined. In the gut cells of both WT and mutant worms, plasmid arrays with intestine-specific promoters were unaffected and had shifted accordingly from the nuclear periphery to the nuclear centre thus confirming that the the EDMD lamin -1 variant effect on gene expression is cell/tissue-specific (Mattout et al., 2011).

Altogether, the MAPK studies on the H222P mice and the worm study illustrate how gene expression can be altered in the presence of pathogenic *LMNA* mutations. These studies also show how expression of lamin A/C variants can result in tissue-specific phenotypes. Moreover, the *C.*

elegans example segues into the third laminopathy hypothesis that examines how compromising the structural integrity of the A-type lamins can result in a disease phenotype.

The third laminopathy hypothesis attributes the tissue-specific phenotypes to the structural role of the A-type lamins in maintaining the nuclear and chromatin architecture and transducing mechanical signals. Because of the involvement of the A-type lamins in nuclear and cytoskeletal structure and dynamics, compromising lamin A/C will make cells and tissues vulnerable to physical stress. This function is particularly crucial for myocytes and muscular tissues which experience constant mechanical stimulus. For instance, a previous study observed nuclear envelope disturbances (e.g. nuclear blebbing, nucleoplasm extrusion into the cytoplasm) in cardiomyocytes of patients with lamin A/C-associated dilated cardiomyopathy (DCM) (Bilinska et al., 2006; Fidzianska et al., 2008; Gupta et al., 2010; Sylvius et al., 2005). Likewise, cells from the *Lmna*$^{\Delta 8\text{-}11}$ mice showed nuclear envelope disruption and impaired nuclear capacity to handle mechanical stress (Lammerding et al., 2004, 2006; Sullivan et al., 1999). Application of strain caused notable nuclear deformation in the mutant cells compared to WT suggesting the importance of A-type lamins in nuclear handling of physical stress (Lammerding et al., 2004). Additionally, low pressure micro-injection of fluorescently-labelled dextran into the nucleus resulted in dextran leaking into the cytoplasm of mutant cells but not in the WT cells thus providing further evidence for the importance of the A-type lamins in maintaining nuclear membrane integrity (Bilinska et al., 2006; Fidzianska et al., 2008; Gupta et al., 2010; Lammerding et al., 2004; Sylvius et al., 2005).

The nuclear membrane integrity is also important in facilitating the assembly of replication and transcription complexes as the nuclear lamins serve as docking sites for these factors (Misteli & Scaffidi, 2005). As mentioned in the introduction (section 1.3.b pages 13), DNA replication was disrupted in cells expressing a truncated lamin A as PCNA and the replication factor C were

trapped in the lamin aggregates (Spann et al., 1997). Similarly, MEFs from *Zmpste24* null mice expressing immature lamin A (i.e. prelamin A) only presented with DNA replication arrest, cellular senescence, increased micronuclei and chromosomal aggregation signaling genomic instability (Liu et al., 2005). Fibroblasts from *Zmpste24* null mice and from HGPS patients also showed increased DNA damage and defective DNA damage response in progeroid cells (Liu et al., 2005). Expression of variant prelamin A that cannot be cleaved by ZMPSTE24 in WT MEFs mirrored the phenotype of the *Zmpste24* null mice MEFs (Liu et al., 2005). Likewise, expression of WT ZMPSTE24 in *Zmpste24* null mice MEFs rescued the progeric cellular phenotype suggesting that the immature lamin A drove genomic instability and impaired DNA damage response in progeric cells (Liu et al., 2005). Loss of heterochromatin in the nuclear periphery correlating with the increase in progerin was also observed in fibroblasts of patients with HGPS, and in cardiomyocytes of patients with DCM caused by lamin A/C mutations (Goldman et al., 2004; Gupta et al., 2010; McCord et al., 2013). In addition, abnormal histone methylation and lamin A/C-DNA interactions were noted in the HGPS fibroblasts (McCord et al., 2013). Since the A-type lamins anchor chromatin in the nuclear lamina, the disruption of the lamin A/C network and accumulation of the misprocessed lamin A impaired heterochromatin tethering and disrupted the regulation of factors such as the histone modifiers involved in gene expression regulation (Mattout et al., 2007; Solovei et al., 2013; Taniura et al., 1995).

However, the A-type lamins do not only maintain the structure of the nucleus but also connect the nucleus to the rest of the cell. As such, others have examined the effect of lamin A/C mutations on F actin organization, cell adhesion and stress-strain response using neonatal rat ventricular cardiomyocytes (NRVMs) expressing either WT or mutant *LMNA*. Interestingly, one of the DCM with conduction defects (DCM-CD) lamin A/C variants expressed in the NRVMs was

p.D192G which was also studied in chapter 2 of this thesis. Laurini and colleagues observed that the NRVMs expressing mutant lamin A/C displayed nuclear deformations (e.g. blebs, nuclear elongation), F actin disorganization and weaker F actin staining signal compared to WT cells (Laurini et al., 2018). In addition, *in silico* simulation of stress-strain response of WT and variant lamin A dimers predicted that the DCM variants p.N195K and especially the p.D192G were more easily unfolded compared to WT dimers suggesting that the nuclear stiffness was compromised in the mutant NRVMs (Laurini et al., 2018). Cell adhesion and plasticity (capacity of the cytoskeleton to handle elastic energy) were compromised as well in the mutant NRVMs as they were more easily deformed due to the impaired mechanical stress transmission from the membrane to the nucleus caused by destabilized actin structure (Laurini et al., 2018). To further probe the effects of this mechano-transduction defect in the mutant NRVMs, gene expression was examined in WT and mutant cells particularly in the context of the p38 branch of the MAPK signaling pathway. P38 is thought to interact with actin, and p38 activation has been implicated in striated muscle laminopathies (Laurini et al., 2018; Muchir et al., 2007; Muchir, Wu, et al., 2012). Previous work had also shown therapeutic benefits of inhibiting p38 in the H222P EDMD mice model, and in phase 2 clinical trial of patients with DCM-caused by lamin A/C mutations (clinical trial ID: NCT02057341) (MacRae, 2016; Muchir et al., 2007; Muchir, Wu, et al., 2012). Therefore, mutant NRVMs were treated with a p38 inhibitor to see if inhibition of p38 will rescue the mutant cells' phenotype. Indeed, F actin organization was restored, and the plasticity, adhesion and stiffness of the mutant NRVMs were improved; thus demonstrating the interplay between gene expression (via the p38 MAPK), actin and mechanical transduction in laminopathies (Laurini et al., 2018).

4.2 The p.K32del lamin A/C variant phenotype: a case explained by the three laminopathy hypotheses

To demonstrate how the three hypotheses can converge to explain a laminopathy phenotype, the p.K32del variant that results in L-CMD or severe EDMD in patients will be discussed (D'Amico et al., 2005; Vytopil et al., 2002). Aside from HGPS cases, "toxic" lamin A/C was also found to be involved in the pathogenesis of striated muscle laminopathy in the p.K32del variant. The homozygous p.K32del mice model presented with severe growth retardation compounded by lethal metabolic defects while the heterozygous mutant mice eventually developed DCM (Bertrand et al., 2012; Cattin et al., 2013). DCM pathogenesis in the heterozygous mutant mice was marked by two stages. In young heterozygous mutant mice, there was haploinsufficiency as the amount of total lamin A/C in these mice was half of the WT amount (Cattin et al., 2013). This was due to the degradation of p.K32del lamin A/C. However, as the heterozygous mutant mice got older and became symptomatic, their total lamin A/C level normalized to WT suggesting that the degradation of p.K32del lamin A/C became impaired (Cattin et al., 2013). Upon examination, the group discovered that there was a cardiac-specific dysfunction of the ubiquitin proteasome system responsible for degrading p.K32del lamin A/C resulting in p.K32del accumulation (Cattin et al., 2013). This accumulation of p.K32del lamin A/C was detrimental to the mice and contributed to DCM development.

On the other hand, immunostaining for lamin A/C in the homozygous p.K32del mutant mice showed that the p.K32del lamin A/C did not localize in the nuclear rim and remained nucleoplasmic (Bertrand et al., 2012). The A-type lamins are known to bind and regulate transcription factors by keeping them in the nuclear lamina. The loss of this function might have contributed to the cardiac and skeletal muscle maturation defects observed in the homozygous mutant mice (Bertrand et al., 2012). Furthermore, the homozygous mutant mice also suffered severe metabolic problems (Bertrand et al., 2012). These metabolic deficits were associated with

the profound reduction in the expression of the sterol regulatory element binding transcription factor 1 (SREBF-1) and its downstream target genes (Bertrand et al., 2012). SREBF-1 is known to bind the A-type lamins and the data suggest that the p.K32del variant exert a dominant-negative effect on the activity of SREBF-1 in the homozygous mutant mice (Bertrand et al., 2012; Lloyd et al., 2002).

At the cellular level, experiments to assess mechanical handling and processing in cells expressing mutant *LMNA* were performed. Of the studied patients myoblasts, two of the samples were from unrelated individuals who carry the mutation producing p.K32del lamin A/C (Bertrand et al., 2014). The myoblasts were cultured in 3D or 2D (soft or hard) settings (Bertrand et al., 2014). Mutant myoblasts failed to orient properly in 3D culture (Bertrand et al., 2014). Actin stress fibres were also prominent compared to control myoblasts in both 3D and 2D (soft substrate) cultures (Bertrand et al., 2014). In addition, mutant cells spread over a larger area compared to controls, and substrate stiffness did not affect cell spreading in mutant cells (Bertrand et al., 2014). Vinculin and focal adhesion kinase, both of which are cell adhesion proteins, were disturbed in the mutant cells as well (Bertrand et al., 2014). Furthermore, cyclic stretching of mutant myoblasts damaged the actin cytoskeleton structure, reduced vinculin immunostaining fluorescence intensity and induced nuclear deformations; thus suggesting that the capacity of the mutant myoblasts to handle mechanical stress was impaired (Bertrand et al., 2014). Evaluation of the MKL1-SRF and YAP transcription factors involved in cytoskeletal component expression and regulation showed abnormal expression and/or localization in the patient myoblasts compared to controls suggesting that compromised nuclear structure can have a downstream effect on transcription activity (Bertrand et al., 2014).

Overall, the example of the p.K32del lamin A/C variant demonstrates how the accumulation of "toxic" lamin A/C, aberrant gene expression combined with the disrupted cellular and nuclear mechanical response can result in a tissue-specific phenotype.

4.3 The thesis results in the context of the three hypotheses

To frame the results of this thesis in the context of the three main hypotheses explaining laminopathies, the thesis data contributed primarily to support the second and third hypotheses. Another group's work on p.K32del lamin A/C showed that the accumulation of this variant in older heterozygous ΔK32 mice resulted in the development of DCM suggesting that this lamin A/C variant acted as a toxic molecule in the cell, and contributed to the development of the cardiac phenotype (Cattin et al., 2013). However, in this thesis, we did not perform studies to determine and evaluate if and how the other variants of chapter 2 (p.D192G, p.H222P, p.R249W and p.Y481X) potentially behave as a toxic molecule although our data may suggest such as the presence of these lamin A/C variants result in dysregulation of PKC α and ERK 1/2 signalling. As for the results from the zebrafish *lmna* mutants in chapter 3, the muscular dystrophy phenotype resulted from lamin A/C deficit in the homozygous *lmna* mutants and haploinsufficiency in the heterozygous *lmna* mutants instead of toxic lamin A/C.

Regarding the second hypothesis that proposes gene expression dysregulation resulting from disrupted lamin A/C function, the results from the cellular and zebrafish models showed abnormal expression profile of genes and proteins implicated in striated muscle laminopathies. The cellular studies expanded the list of known *LMNA* mutations that also lead to abnormal ERK 1/2 activation while the zebrafish *lmna* mutants showed aberrant ERK 1/2 activation in the context of reduced lamin A/C expression. Altogether, these results provide further evidence supporting the integral role of ERK 1/2 in the development and progression of striated muscle laminopathies.

However, the main contribution of the results from chapter 2 was implicating PKC α in cardiac and muscular laminopathies. The results demonstrated how PKC α, a regulator of many proteins including ERK 1/2, was perturbed in its cellular localization, activation, and proximity to lamin A/C in the presence of pathogenic *LMNA* mutations. Figure 4.1 presents models of WT and variant lamin A from chapter 2 revealing how the truncations and amino acid substitutions could potentially alter the secondary structure of the A-type lamins, and consequently affect the interaction between lamin A/C and PKC α. These models were created using I-TASSER which simulates protein structure based on iterations and analyses of published structures in the Protein Data Bank (PDB) (Roy et al., 2012; Yang & Zhang, 2015; Zhang, 2009). The models with the best scores were selected and presented. Currently, there are 14 published lamin A/C structures on PDB although none of them is the full-length protein. Regardless, these PDB structures have contributed to our understanding of how lamin A/C mutations can cause structural and/or assembly changes that can disturb lamin A/C function leading to disease development. Structure 6JLB for instance identified amino acids important for lamin A/C homodimer and protofilament assembly (Ahn et al., 2019). Such information provides insight on how a specific mutation can affect lamin A/C assembly, and thus have structural and/or functional consequences. Of the 14 available lamin A/C structures, three (PDB IDs: 1IFR, 1IVT and 3GEF) cover a part of the region that binds PKC α in the C-terminus (Dhe-Paganon et al., 2002; Krimm et al., 2002; Magracheva et al., 2009). All three structures showed an immunoglobulin (Ig) like conformation for this region of the C-terminus. Based on structure 1IFR for example, the lipodystrophy mutations are found to affect amino acids that are clustered in a small exposed region of the protein while the muscular laminopathy mutations affect amino acids both in the core of the Ig domain involved in structural support and on the surface potentially involved in interactions with lamin A/C partners (Dhe-Paganon et al.,

2002). Similar observations were made by Krimm et al with structure 1IVT (Krimm et al., 2002). In another study characterizing the interaction interface of the lamin A/C – emerin - barrier-to-autointegration factor (BAF) complex (structure 6GHD), the results showed how the progeroid variants and not the EDMD and lipodystrophy variants interrupted lamin A/C - BAF association; thus, implicating lamin A/C – BAF interaction in progeria and further demonstrating how certain amino acid changes affecting specific lamin A/C interaction(s) can lead to a particular phenotype (Samson et al., 2018). Therefore, based on the data and results from these structural studies, indeed, the lamin A/C variants that we studied affected the interaction between lamin A/C and PKC α. For instance, in chapter 2, p.K32del lamin A/C was observed to have increased interaction with PKC α (Figure 2.5 page 57). Despite the shift in position of the amino acids downstream of K32 upon its deletion (Figure 4.1A helical wheel), the predicted structure of p.K32del does not present significant conformational changes on the overall structure of the protein (Figure 4.1A). Alignment of the PKC α binding region of WT and p.K32del lamin A showed overlap but a gain of a short alpha helix is noted in the variant. Such gain could have potentially contributed to the increase in lamin A/C - PKC α binding. In contrast, p.H222P lamin A/C was shown to have decreased PKC α interaction (Figure 2.5 page 57) even though the p.H222P lamin A model does not show considerable structural changes in the protein. However, the predicted gain of alpha helices in the PKC α binding site (Figure 4.1C) of the variant seemed to be detrimental to lamin A/C - PKC α binding and PKC α was primarily found in the cytoplasm. Similarly, the truncation of p.Y481X leads to the loss of the rest of the C terminus downstream of position 481 (Figure 4.1E) impairing the ability of lamin A/C to bind PKC α resulting in lesser PKC α in the nucleus of cells expressing p.Y481X compared to WT (Figure 2.2 page 50). Future studies including co-immunoprecipitation experiments can be done to further confirm our protein interaction results. Moreover, X-ray

crystallography and nuclear magnetic resonance (NMR) spectroscopy can also be employed to determine the actual protein structure of the lamin A/C variants. X-ray crystallography is a method that allows for the determination of the 3D structure of a molecule from its crystal (Smyth & Martin, 2000). The protein crystals are bombarded by X-ray from which the diffraction patterns and spots are analyzed to produce the molecular structure of the protein (Smyth & Martin, 2000). On the other hand, NMR is a technique that takes advantage of the inherent magnetic properties (aka spin) of certain atomic nuclei (Berg et al., 2002). Since each magnetic nucleus has its unique chemical shifts, these shifts can then be used and analyzed to construct the 3D conformation of a molecule (Berg et al., 2002).

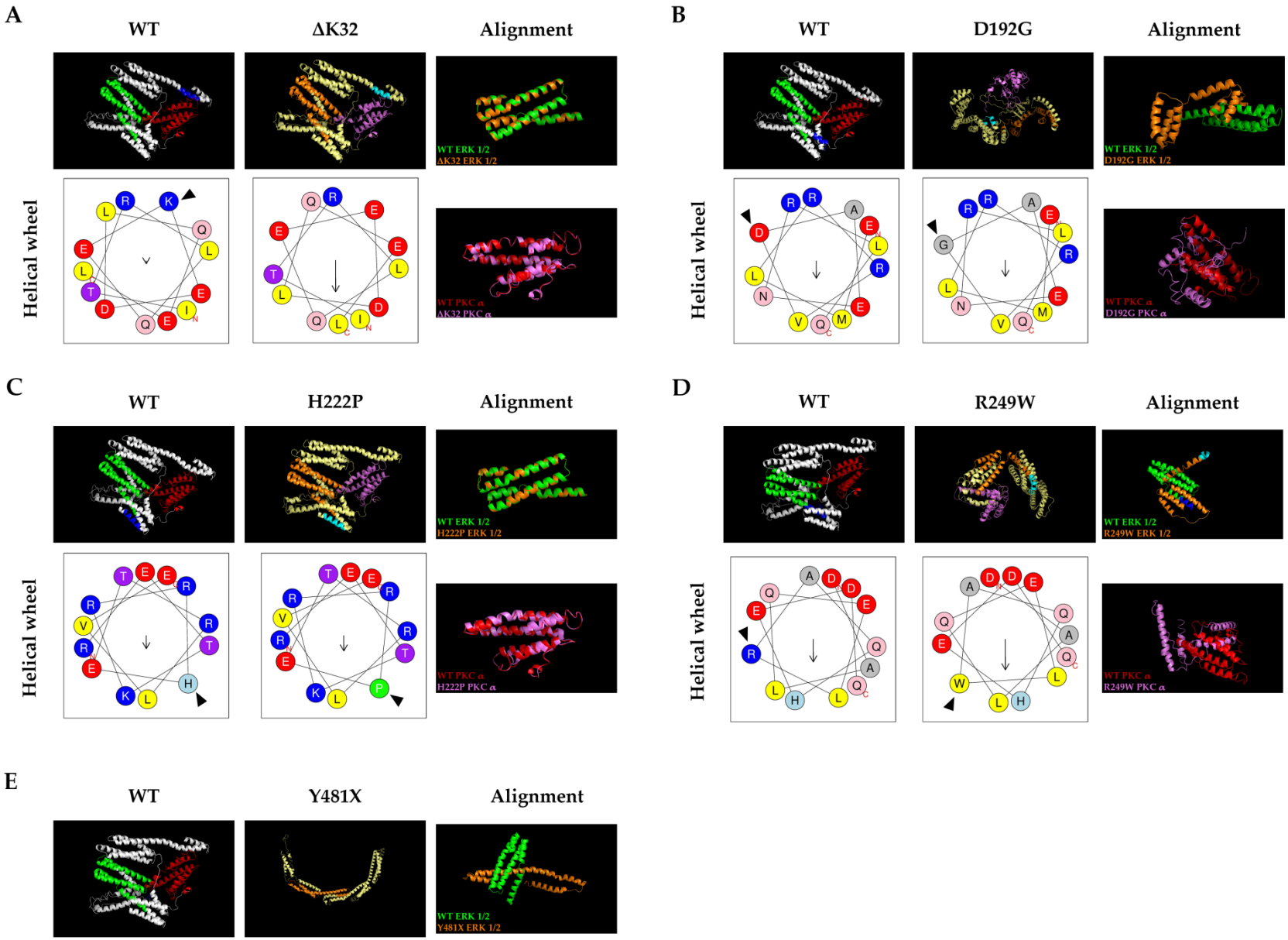
A
WT
ΔK32
Alignment
WT ERK 1/2
ΔK32 ERK 1/2
Helical wheel
WT PKC α
ΔK32 PKC α
B
WT
D192G
Alignment
WT ERK 1/2
D192G ERK 1/2
Helical wheel
WT PKC α
D192G PKC α
C
WT
H222P
Alignment
WT ERK 1/2
H222P ERK 1/2
Helical wheel
WT PKC α
H222P PKC α
D
WT
R249W
Alignment
WT ERK 1/2
R249W ERK 1/2
Helical wheel
WT PKC α
R249W PKC α
E
WT
Y481X
Alignment
WT ERK 1/2
Y481X ERK 1/2

Figure 4.1: Simulated protein models of mature WT lamin A and lamin A variants. Top panel: WT simulated model (left most panel), simulated variant model (middle panel) and alignment (right most panel) of the ERK 1/2 binding region in WT (in green) and variant (in orange) lamin A/C. Lower panel: helical wheel of the WT (left most panel), helical wheel of the variant (middle panel) and alignment (right most panel) of the PKC α binding region in WT (in green) and variant (in lavender) lamin A/C. The affected helix used to generate the helical wheel is shown in blue for WT and cyan in the variants. Where applicable, the affected amino acid is shown as a stick figure (blue in WT; cyan in variant). Note that a portion of the ERK 1/2 binding site is shown in blue or cyan in the WT and R249W models respectively since the affected position 249 is in the ERK 1/2 binding region. The amino and carboxyl ends are annotated by N and C respectively and the affected amino acid (a.a) is indicated by a black arrowhead in the helical wheel. The black arrow in the helical wheel indicates the direction of the hydrophobic moment. Polar, basic and positively charged a.a are in blue, polar, acidic and negatively charged a.a are in red, aliphatic or aromatic, nonpolar and neutral a.a. are in yellow, amide, polar and neutral a.a are in pink, small, aliphatic and non-polar a.a are in grey, proline (P) which is cyclic, nonpolar and neutral is in green, threonine (T) which is hydroxyl-containing, polar and neutral is in purple, and histidine (H) which is basic, aromatic, polar, and can either be positively charged or neutral is in light blue. Models are rendered using PyMol (The PyMOL Molecular Graphics System, Version 2.3.4 Schrödinger, LLC, n.d.).

In parallel to the changes in lamin A/C - PKC α interaction, the activation level of the PKC α target - ERK 1/2, was also disturbed. Since lamin A/C can bind ERK 1/2 and PKC α (Figure 4.2), lamin A/C might serve as the docking site for these two proteins and facilitate PKC α phosphorylation of ERK 1/2. However, in the presence of lamin A/C mutations, the resulting amino acid changes might cause conformational alterations in the protein that will affect its ability to bind its partners. In our study, the p.R249W and p.K32del variants presented with increased lamin A/C - PKC α interaction but decreased ERK 1/2 activation. Structural changes in the lamin A/C variants might have impeded lamin A/C – ERK 1/2 binding; thus, though lamin A/C - PKC α interaction was increased, a reduction in ERK 1/2 activation was noted. Future studies could evaluate the effect of various lamin A/C mutations on ERK 1/2 – lamin A/C interaction. Alternatively, lamin A/C – ERK 1/2 binding might not have been perturbed but the overall change in lamin A/C conformation might have impaired ERK 1/2 – PKC α interaction resulting in downregulation of ERK 1/2 activation. Likewise, ERK 1/2 activation was also reduced in the H222P mice myoblasts. However, in these cells, lamin A/C - PKC α association was decreased. Therefore, in the H222P mice myoblasts, the decrease in lamin A/C - PKC α interaction resulted in limited ERK 1/2 - PKC α interaction, and thus decreased ERK 1/2 activation. Figure 4.3 illustrates a potential mechanism for PKC α and ERK 1/2 interaction mediated by the A-type lamins in cells expressing WT lamin A/C (Figure 4.3A) and in cells expressing mutant lamin A/C that cause striated muscle laminopathies (Figure 4.3B).

Nevertheless, though previous work provided evidence for the plausibility of the lamin A/C – ERK 1/2 - PKC α assembly, it is necessary to confirm that the complex in Figure 4.3A exists. Localization and co-immunoprecipitation experiments will determine whether PKC α, lamin A/C and ERK 1/2 are found in the same subcellular location and if they form a complex. X-

ray crystallography can also potentially solve the structure or the interaction interface of this tri-protein assembly. A precedent has already been set by the PDB structure 6GHD which solved the interaction interface of the emerin – lamin A/C – BAF ternary complex (Samson et al., 2018). Future work involving protein interaction studies and kinase assay can also be performed to confirm direct PKC α phosphorylation of ERK 1/2 in the presence of lamin A/C mutations (Figure 4.3B). In addition, PKC α knockdown and PKC α over-expression experiments can be performed concomitant with the analysis of ERK 1/2 activation to confirm the correlation between ERK 1/2 activation and PKC α in the context of lamin A/C mutations. Other PKC α downstream targets could also be assessed to determine if their expression and/or activity levels are altered as well in the presence of *LMNA* mutations. Such targets can include c-Fos and the AP-1 transcription factor. C-Fos along with c-Jun are subunits of the AP-1 transcription factor (Ivorra et al., 2006). While c-Jun is known to be involved in striated muscle laminopathies, it is currently unknown whether c-Fos and the AP-1 transcription complex are also involved in cardiac and skeletal muscle laminopathies (Muchir et al., 2007). The A-type lamins are known binding partners of c-Fos and have been shown to sequester c-Fos in the nuclear lamina thus preventing it from dimerizing with c-Jun to assemble the AP-1 complex, and consequently affecting downstream gene expression (Ivorra et al., 2006). Moreover, c-Fos is a target of ERK 1/2, and phosphorylation of c-Fos by ERK 1/2 does not only activate c-Fos but also releases c-Fos from the nuclear lamina thereby allowing c-Fos to dimerize with c-Jun (González et al., 2008; Monje et al., 2003). Interestingly, lamin A/C facilitates this c-Fos – ERK 1/2 interaction by serving as a scaffold for ERK 1/2 to act on c-Fos (González et al., 2008). Incidentally, PKC α has been shown to regulate ERK 1/2 activity and c-Fos expression (Abate et al., 1991; Muramatsu et al., 1989; Soh et al., 1999). As such, it would be interesting to determine the involvement of c-Fos and the AP-1 transcription factor in striated

muscle laminopathies and to characterize the role of PKC α via these proteins in cardiac and skeletal muscle laminopathies.

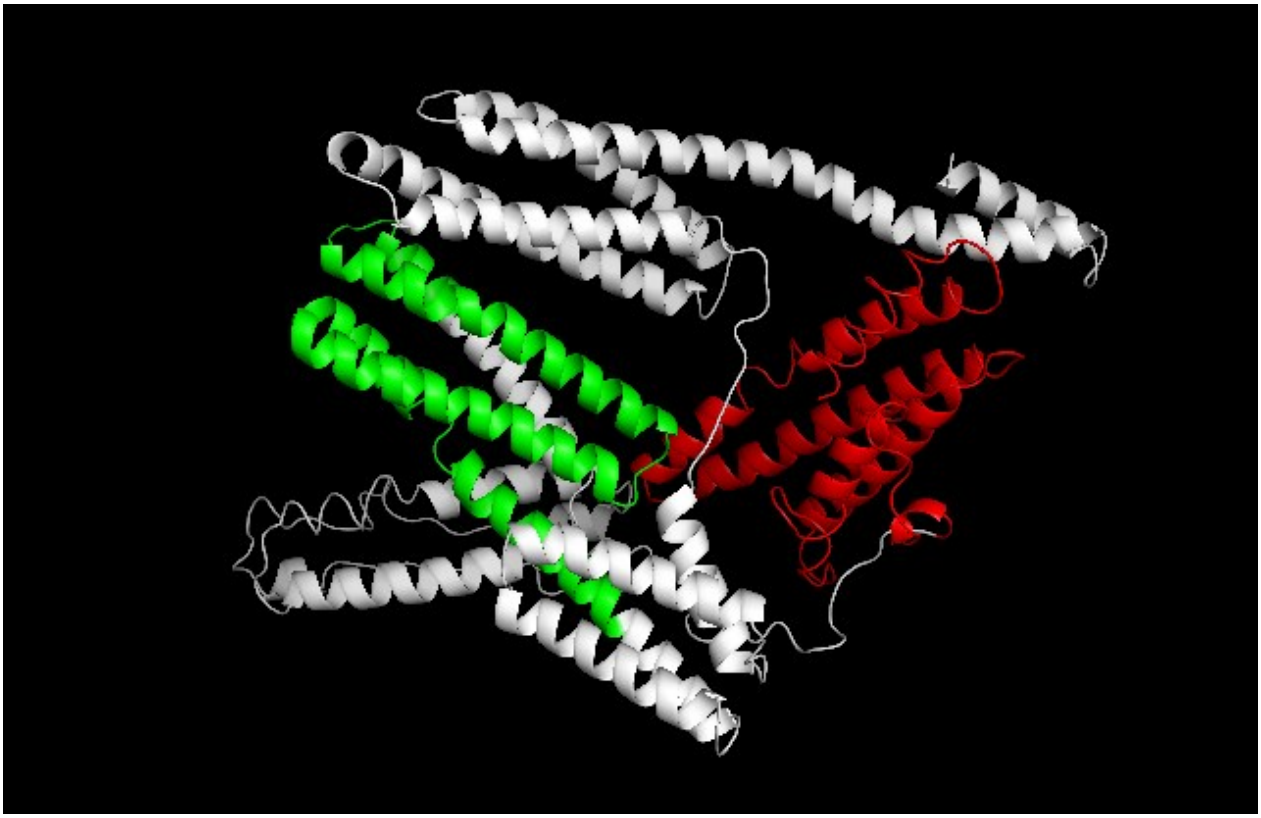

Figure 4.2: Simulated model of WT lamin A showing the regions on lamin A that bind ERK 1/2 (in green) and PKC α (in red). Models are rendered using PyMol (The PyMOL Molecular Graphics System, Version 2.3.4 Schrödinger, LLC, n.d.)

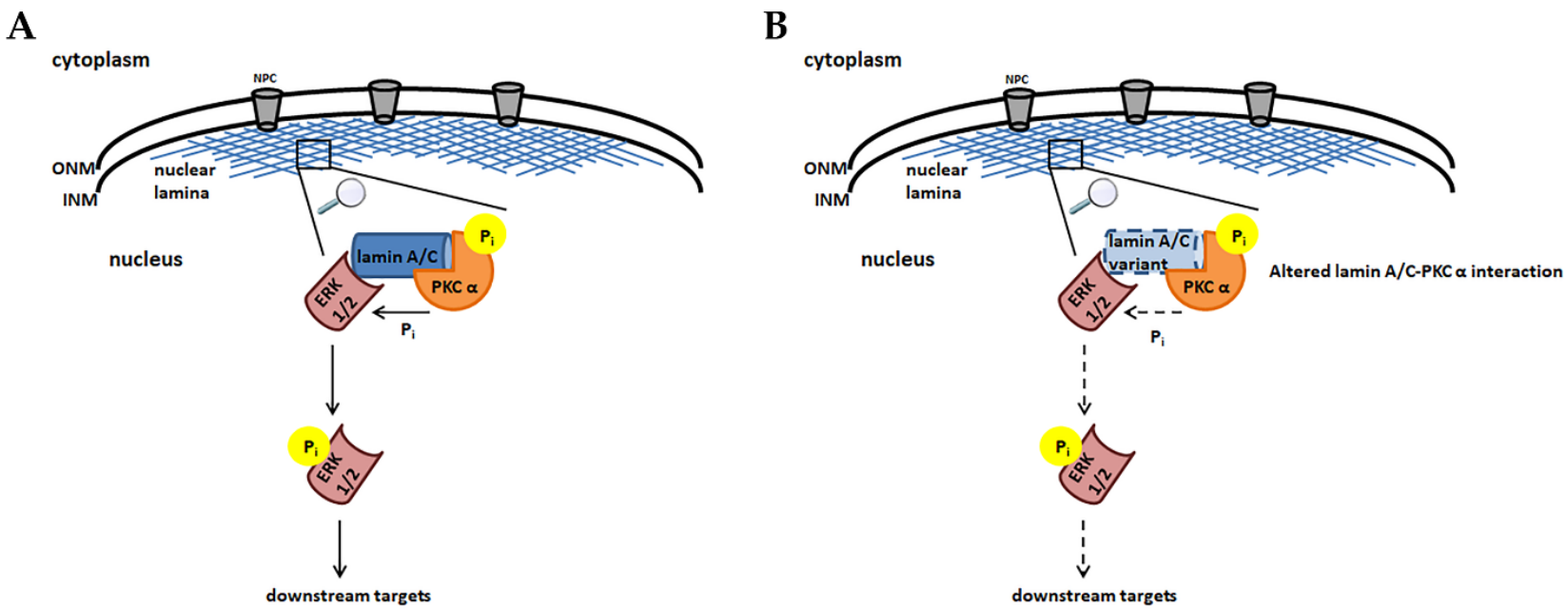

Figure 4.3: Schematic of proposed model for PKC α involvement in striated muscle laminopathies. **(A)** PKC α and ERK 1/2 interaction is mediated by lamin A/C. In normal circumstances, ERK 1/2 – lamin A/C - PKC α assemble, and ERK 1/2 gets activated by PKC α phosphorylation. Activated ERK 1/2 is now able to act on its downstream targets. **(B)** In cells expressing mutant lamin A/C, altered lamin A/C - PKC α interaction impairs lamin A/C – PKC α - ERK 1/2 interactions which result in reduced ERK 1/2 activation. ONM (outer nuclear membrane); INM (inner nuclear membrane); P_i (phosphate group); NPC (nuclear protein complex).

Like in the cellular models of chapter 2, activated ERK 1/2 and PKC α levels were also assessed in the zebrafish *lmna* mutants carrying a five base pair deletion in the second exon of *lmna* (chapter 3). Quantitative PCR showed that the *lmna* mutants presented with significant decrease in lamin A, and an overall reduction in total lamins A and C transcripts (Koshimizu et al., 2011). However, the presence or absence of the variant lamin A/C protein cannot be verified due to current lack of antibody that can detect zebrafish lamin A/C. Nonetheless, it is predicted that the five base pair deletion in *lmna* results in a premature stop that truncates the translated protein into a 180 amino acid polypeptide lacking many of its functional and binding sites including the ERK 1/2 and PKC α binding regions. Alternatively, if the mutant lamin A/C mRNA protein is not translated, the heterozygous *lmna* mutants will express only half the amount of lamin A/C compared to WT (i.e. lamin A/C haploinsufficiency) while the homozygous *lmna* mutants will be knock-outs. Either way, the *lmna* mutants have significantly reduced levels of lamin A/C compared to WT. Previous work on patient samples and on various cellular and animal models of striated muscle laminopathies showed disturbances in the expression and/or activation of genes and proteins such as the MAPK members and their downstream targets (Nicolas et al., 2019). Consistent with these data and the results from chapter 2, the *lmna* mutants also presented with aberrant expression or activation of two members of the MAPK signaling pathway: Jun and Erk 1/2. In the homozygous *lmna* mutants, an increase in activated Erk 1/2 was noted. Similarly, lamin A/C siRNA knockdown in C2C12 and HeLa cells resulted in upregulation of ERK 1/2 activation (Muchir, Wu, et al., 2009). The MAPK target *jun* was also reduced in the homozygous *lmna* mutants compared to WT. Likewise, abnormal *c-Jun* expression has been observed in the H222P mice model (Muchir et al., 2007). Expression of *nfκb2*, a downstream target of the Nfκb transcription factor, was also reduced in the homozygous *lmna* mutants. Previous work on cytokine

or mechanically-induced *Lmna*$^{\Delta 8\text{-}11}$ mouse embryo fibroblasts showed attenuation of Nfκb-regulated gene transcription (Lammerding et al., 2004). Altogether, in accordance with results from other studies, the homozygous *lmna* mutants presented with abnormal expression/activation of striated muscle laminopathies biomarkers but in the context of lamin A/C haploinsufficiency or protein deficit.

In terms of structural and functional consequences, the *lmna* mutant embryos and larvae exhibited skeletal muscle structure defects and swim impairment. Cardiac structure and function defects were mild and transient. Future work on the *lmna* mutants can include cardiac structure and function analyses on older *lmna* mutants to determine if they will develop significant cardiac dysfunction since DCM caused by lamin A/C mutations generally has an adult onset (Hasselberg et al., 2018; Taylor et al., 2003). Skeletal muscle structure analyses and swim tests can also be performed on older *lmna* mutants to examine the progression of their skeletal muscle phenotype. Nevertheless, the muscular phenotype of the *lmna* mutants suggests how lamin A/C deficit is detrimental particularly in tissues that are constantly under mechanical strain and stress.

Regarding PKC α, like in cells expressing the truncated p.Y481X lamin A/C lacking the PKC α binding site, the *lmna* mutants presented with a predominantly cytoplasmic Pkc α cellular distribution (Figure 3.2Dii page 105). Increased phos- Pkc α was also observed in whole-larval protein extracts of the *lmna* mutants compared to WT thus suggesting PKC α involvement in muscular laminopathies in the context of lamin A/C deficit. Nevertheless, further studies on Pkc α in zebrafish expressing other variant and non-truncated lamin A/C can be performed to confirm Pkc α involvement in cardiac and/or skeletal muscle laminopathies.

In whole, *LMNA* mutations cause a diverse set of phenotypes owing to the wide-ranging functions and associations of the A-type lamins. The mutations in *LMNA* which results in

truncations or substitutions can alter lamin A/C protein structure itself. Such change at the fundamental level affects the protein's ability to interact with its binding partners, and in turn will have downstream effects on gene expression which could be detrimental to the cells. This thesis provides evidence to implicate PKC α in cardiac and muscular laminopathies. Further study of PKC α in the context of lamin A/C mutations is warranted as PKC α might turn out to be key in determining and understanding laminopathies due to its known association not only with the A-type lamins themselves but also with many of the lamin A/C partners including the ones associated with striated muscle laminopathies. As for the zebrafish *lmna* mutants, this model is a convenient and accessible animal model that can be used to further study muscular laminopathies specifically in the context of lamin A/C deficit (as in the homozygous mutants). In addition, since the heterozygous *lmna* mutants also presented with a phenotype, they can also be used to further examine muscular laminopathy in the context of lamin A/C haploinsufficiency as previous work has associated lamin A/C haploinsufficiency in striated muscle laminopathies (Al-Saaidi et al., 2013; Cattin et al., 2013; Gupta et al., 2010; Wolf et al., 2008).

References

Aartsma-Rus, A., Van Deutekom, J. C. T., Fokkema, I. F., Van Ommen, G.-J. B., & Den Dunnen, J. T. (2006). Entries in the Leiden Duchenne muscular dystrophy mutation database: An overview of mutation types and paradoxical cases that confirm the reading-frame rule. *Muscle & Nerve*, *34*(2), 135–144. https://doi.org/10.1002/mus.20586

Abate, C., Marshak, D. R., & Curran, T. (1991). Fos is phosphorylated by p34cdc2, cAMP-dependent protein kinase and protein kinase C at multiple sites clustered within regulatory regions. *Oncogene*, *6*(12), 2179–2185.

Adam, S. A., & Goldman, R. D. (2012). Insights into the differences between the A- and B-type nuclear lamins. *Advances in Biological Regulation*, *52*(1), 108–113. https://doi.org/10.1016/j.advenzreg.2011.11.001

Aebi, U., Cohn, J., Buhle, L., & Gerace, L. (1986). The nuclear lamina is a meshwork of intermediate-type filaments. *Nature*, *323*(6088), 560–564. https://doi.org/10.1038/323560a0

Agarwal, A. K., Fryns, J.-P., Auchus, R. J., & Garg, A. (2003). Zinc metalloproteinase, ZMPSTE24, is mutated in mandibuloacral dysplasia. *Human Molecular Genetics*, *12*(16), 1995–2001.

Ahn, J., Jo, I., Kang, S.-M., Hong, S., Kim, S., Jeong, S., Kim, Y.-H., Park, B.-J., & Ha, N.-C. (2019). Structural basis for lamin assembly at the molecular level. *Nature Communications*, *10*(1), 3757. https://doi.org/10.1038/s41467-019-11684-x

Al-Saaidi, R., Rasmussen, T. B., Palmfeldt, J., Nissen, P. H., Beqqali, A., Hansen, J., Pinto, Y. M., Boesen, T., Mogensen, J., & Bross, P. (2013). The LMNA mutation p.Arg321Ter associated with dilated cardiomyopathy leads to reduced expression and a skewed ratio of lamin A and lamin C proteins. *Experimental Cell Research*, *319*(19), 3010–3019. https://doi.org/10.1016/j.yexcr.2013.08.024

Alsheimer, M., & Benavente, R. (1996). Change of karyoskeleton during mammalian spermatogenesis: Expression pattern of nuclear lamin C2 and its regulation. *Experimental Cell Research*, *228*(2), 181–188. https://doi.org/10.1006/excr.1996.0315

Arimura, T., Onoue, K., Takahashi-Tanaka, Y., Ishikawa, T., Kuwahara, M., Setou, M., Shigenobu, S., Yamaguchi, K., Bertrand, A. T., Machida, N., Takayama, K., Fukusato, M., Tanaka, R., Somekawa, S., Nakano, T., Yamane, Y., Kuba, K., Imai, Y., Saito, Y., …

Kimura, A. (2013). Nuclear accumulation of androgen receptor in gender difference of dilated cardiomyopathy due to lamin A/C mutations. *Cardiovascular Research*, *99*(3), 382–394. https://doi.org/10.1093/cvr/cvt106

Bakkers, J. (2011). Zebrafish as a model to study cardiac development and human cardiac disease. *Cardiovascular Research*, *91*(2), 279–288.

Barbazuk, W. B., Korf, I., Kadavi, C., Heyen, J., Tate, S., Wun, E., Bedell, J. A., McPherson, J. D., & Johnson, S. L. (2000). The syntenic relationship of the zebrafish and human genomes. *Genome Research*, *10*(9), 1351–1358. https://doi.org/10.1101/gr.144700

Bartel, D. P. (2009). MicroRNAs: Target recognition and regulatory functions. *Cell*, *136*(2), 215–233. https://doi.org/10.1016/j.cell.2009.01.002

Bassett, D. I., Bryson-Richardson, R. J., Daggett, D. F., Gautier, P., Keenan, D. G., & Currie, P. D. (2003). Dystrophin is required for the formation of stable muscle attachments in the zebrafish embryo. *Development (Cambridge, England)*, *130*(23), 5851–5860. https://doi.org/10.1242/dev.00799

Bassett, D. I., & Currie, P. D. (2003). The zebrafish as a model for muscular dystrophy and congenital myopathy. *Human Molecular Genetics*, *12 Spec No 2*, R265-270. https://doi.org/10.1093/hmg/ddg279

Berger, J., Berger, S., Hall, T. E., Lieschke, G. J., & Currie, P. D. (2010). Dystrophin-deficient zebrafish feature aspects of the Duchenne muscular dystrophy pathology. *Neuromuscular Disorders: NMD*, *20*(12), 826–832. https://doi.org/10.1016/j.nmd.2010.08.004

Bertrand, A. T., Renou, L., Papadopoulos, A., Beuvin, M., Lacène, E., Massart, C., Ottolenghi, C., Decostre, V., Maron, S., Schlossarek, S., Cattin, M.-E., Carrier, L., Malissen, M., Arimura, T., & Bonne, G. (2012). DelK32-lamin A/C has abnormal location and induces

incomplete tissue maturation and severe metabolic defects leading to premature death. *Human Molecular Genetics*, *21*(5), 1037–1048. https://doi.org/10.1093/hmg/ddr534

Bertrand, A. T., Ziaei, S., Ehret, C., Duchemin, H., Mamchaoui, K., Bigot, A., Mayer, M., Quijano-Roy, S., Desguerre, I., Lainé, J., Ben Yaou, R., Bonne, G., & Coirault, C. (2014). Cellular microenvironments reveal defective mechanosensing responses and elevated YAP signaling in LMNA-mutated muscle precursors. *Journal of Cell Science*, *127*(Pt 13), 2873–2884. https://doi.org/10.1242/jcs.144907

Bilinska, Z. T., Sylvius, N., Grzybowski, J., Fidzianska, A., Michalak, E., Walczak, E., Walski, M., Bieganowska, K., Szymaniak, E., Kusmierczyk-Droszcz, B., Lubiszewska, B., Wagner, T., Tesson, F., & Ruzyllo, W. (2006). Dilated cardiomyopathy caused by LMNA mutations. Clinical and morphological studies. *Kardiologia Polska*, *64*(8), 812–819; discussion 820-1.

Bonne, G., Barletta, M. R. D., Varnous, S., Becane, H. M., Hammouda, E. H., Merlini, L., Muntoni, F., Greenberg, C. R., Gary, F., Urtizberea, J. A., Duboc, D., Fardeau, M., Toniolo, D., & Schwartz, K. (1999). Mutations in the gene encoding lamin A/C cause autosomal dominant Emery-Dreifuss muscular dystrophy. *Nature Genetics*, *21*(3), 285–288.

Bonne, G., Mercuri, E., Muchir, A., Urtizberea, A., Becane, H. M., Recan, D., Merlini, L., Wehnert, M., Boor, R., Reuner, U., Vorgerd, M., Wicklein, E. M., Eymard, B., Duboc, D., Penisson-Besnier, I., Cuisset, J. M., Ferrer, X., Desguerre, I., Lacombe, D., … Muntoni, F. (2000). Clinical and molecular genetic spectrum of autosomal dominant Emery-Dreifuss muscular dystrophy due to mutations of the lamin A/C gene. *Annals of Neurology*, *48*(2), 170–180.

Bonne, Gisèle, & Quijano-Roy, S. (2013). Emery-Dreifuss muscular dystrophy, laminopathies, and other nuclear envelopathies. *Handbook of Clinical Neurology*, *113*, 1367–1376. https://doi.org/10.1016/B978-0-444-59565-2.00007-1

Bornancin, F., & Parker, P. J. (1997). Phosphorylation of protein kinase C-alpha on serine 657 controls the accumulation of active enzyme and contributes to its phosphatase-resistant state. *The Journal of Biological Chemistry*, *272*(6), 3544–3549. https://doi.org/10.1074/jbc.272.6.3544

Boudreau, E., Labib, S., Bertrand, A. T., Decostre, V., Bolongo, P. M., Sylvius, N., Bonne, G., & Tesson, F. (2012). Lamin A/C mutants disturb sumo1 localization and sumoylation in vitro and in vivo. *PloS One*, *7*(9), e45918.

Bowling, N., Walsh, R. A., Song, G., Estridge, T., Sandusky, G. E., Fouts, R. L., Mintze, K., Pickard, T., Roden, R., Bristow, M. R., Sabbah, H. N., Mizrahi, J. L., Gromo, G., King, G. L., & Vlahos, C. J. (1999). Increased protein kinase C activity and expression of Ca2+-sensitive isoforms in the failing human heart. *Circulation*, *99*(3), 384–391.

Braz, J. C., Gregory, K., Pathak, A., Zhao, W., Sahin, B., Klevitsky, R., Kimball, T. F., Lorenz, J. N., Nairn, A. C., Liggett, S. B., Bodi, I., Wang, S., Schwartz, A., Lakatta, E. G., DePaoli-Roach, A. A., Robbins, J., Hewett, T. E., Bibb, J. A., Westfall, M. V., … Molkentin, J. D. (2004). PKC-alpha regulates cardiac contractility and propensity toward heart failure. *Nature Medicine*, *10*(3), 248–254.

Braz, Julian C., Bueno, O. F., De Windt, L. J., & Molkentin, J. D. (2002). PKC alpha regulates the hypertrophic growth of cardiomyocytes through extracellular signal-regulated kinase1/2 (ERK1/2). *The Journal of Cell Biology*, *156*(5), 905–919. https://doi.org/10.1083/jcb.200108062

Broers, J. L., Ramaekers, F. C., Bonne, G., Yaou, R. B., & Hutchison, C. J. (2006). Nuclear lamins: Laminopathies and their role in premature ageing. *Physiological Reviews*, *86*(3), 967–1008.

Brown, D. R., Samsa, L. A., Qian, L., & Liu, J. (2016). Advances in the Study of Heart Development and Disease Using Zebrafish. *Journal of Cardiovascular Development and Disease*, *3*(2). https://doi.org/10.3390/jcdd3020013

Calum MacRae. (2016, August 27). *Phase 2 Study of A797, an Oral, Selective p38 Mitogen-Activated Protein Kinase Inhibitor, in Patients With Lamin A/C-Related Dilated Cardiomyopathy*. European Society of Cardiology Congress, Rome, Italy.

Cargnello, M., & Roux, P. P. (2011). Activation and function of the MAPKs and their substrates, the MAPK-activated protein kinases. *Microbiology and Molecular Biology Reviews: MMBR*, *75*(1), 50–83. https://doi.org/10.1128/MMBR.00031-10

Cattin, M.-E., Bertrand, A. T., Schlossarek, S., Le Bihan, M.-C., Skov Jensen, S., Neuber, C., Crocini, C., Maron, S., Lainé, J., Mougenot, N., Varnous, S., Fromes, Y., Hansen, A., Eschenhagen, T., Decostre, V., Carrier, L., & Bonne, G. (2013). Heterozygous LmnadelK32 mice develop dilated cardiomyopathy through a combined pathomechanism of haploinsufficiency and peptide toxicity. *Human Molecular Genetics*, *22*(15), 3152–3164. https://doi.org/10.1093/hmg/ddt172

Cazaubon, S., Bornancin, F., & Parker, P. J. (1994). Threonine-497 is a critical site for permissive activation of protein kinase C alpha. *The Biochemical Journal*, *301 (Pt 2)*, 443–448. https://doi.org/10.1042/bj3010443

Charron, P., Arbustini, E., & Bonne, G. (2012). What Should the Cardiologist know about Lamin Disease? *Arrhythmia & Electrophysiology Review*, *1*(1), 22–28. https://doi.org/10.15420/aer.2012.1.1.22

Chen, Z., Huang, W., Dahme, T., Rottbauer, W., Ackerman, M. J., & Xu, X. (2008). Depletion of zebrafish essential and regulatory myosin light chains reduces cardiac function through distinct mechanisms. *Cardiovascular Research*, *79*(1), 97–108. https://doi.org/10.1093/cvr/cvn073

Collins, M. M., Ahlberg, G., Hansen, C. V., Guenther, S., Marín-Juez, R., Sokol, A. M., El-Sammak, H., Piesker, J., Hellsten, Y., Olesen, M. S., Stainier, D. Y. R., & Lundegaard, P. R. (2019). Early sarcomere and metabolic defects in a zebrafish pitx2c cardiac arrhythmia model. *Proceedings of the National Academy of Sciences of the United States of America*, *116*(48), 24115–24121. https://doi.org/10.1073/pnas.1913905116

Collins, M. M., Maischein, H.-M., Dufourcq, P., Charpentier, M., Blader, P., & Stainier, D. Y. (2018). Pitx2c orchestrates embryonic axis extension via mesendodermal cell migration. *ELife*, *7*. https://doi.org/10.7554/eLife.34880

Colombo, M. G., Botto, N., Vittorini, S., Paradossi, U., & Andreassi, M. G. (2008). Clinical utility of genetic tests for inherited hypertrophic and dilated cardiomyopathies. *Cardiovascular Ultrasound*, *6*, 62. https://doi.org/10.1186/1476-7120-6-62

D'Amico, A., Haliloglu, G., Richard, P., Talim, B., Maugenre, S., Ferreiro, A., Guicheney, P., Menditto, I., Benedetti, S., Bertini, E., Bonne, G., & Topaloglu, H. (2005). Two patients with "Dropped head syndrome" due to mutations in LMNA or SEPN1 genes. *Neuromuscular Disorders: NMD*, *15*(8), 521–524. https://doi.org/10.1016/j.nmd.2005.03.006

Davies, B. S. J., Barnes, R. H., Tu, Y., Ren, S., Andres, D. A., Spielmann, H. P., Lammerding, J., Wang, Y., Young, S. G., & Fong, L. G. (2010). An accumulation of non-farnesylated prelamin A causes cardiomyopathy but not progeria. *Human Molecular Genetics*, *19*(13), 2682–2694. https://doi.org/10.1093/hmg/ddq158

Delbarre, E., Tramier, M., Coppey-Moisan, M., Gaillard, C., Courvalin, J.-C., & Buendia, B. (2006). The truncated prelamin A in Hutchinson-Gilford progeria syndrome alters segregation of A-type and B-type lamin homopolymers. *Human Molecular Genetics*, *15*(7), 1113–1122. https://doi.org/10.1093/hmg/ddl026

Dhe-Paganon, S., Werner, E. D., Chi, Y.-I., & Shoelson, S. E. (2002). Structure of the globular tail of nuclear lamin. *The Journal of Biological Chemistry*, *277*(20), 17381–17384. https://doi.org/10.1074/jbc.C200038200

Dietzel, S., Zolghadr, K., Hepperger, C., & Belmont, A. S. (2004). Differential large-scale chromatin compaction and intranuclear positioning of transcribed versus non-transcribed transgene arrays containing beta-globin regulatory sequences. *Journal of Cell Science*, *117*(Pt 19), 4603–4614. https://doi.org/10.1242/jcs.01330

Disatnik, M. H., Buraggi, G., & Mochly-Rosen, D. (1994). Localization of protein kinase C isozymes in cardiac myocytes. *Experimental Cell Research*, *210*(2), 287–297. https://doi.org/10.1006/excr.1994.1041

Dittmer, T. A., & Misteli, T. (2011). The lamin protein family. *Genome Biology*, *12*(5), 222. https://doi.org/10.1186/gb-2011-12-5-222

Eckersley-Maslin, M. A., Bergmann, J. H., Lazar, Z., & Spector, D. L. (2013). Lamin A/C is expressed in pluripotent mouse embryonic stem cells. *Nucleus (Austin, Tex.)*, *4*(1), 53–60. https://doi.org/10.4161/nucl.23384

Eriksson, M., Brown, W. T., Gordon, L. B., Glynn, M. W., Singer, J., Scott, L., Erdos, M. R., Robbins, C. M., Moses, T. Y., Berglund, P., Dutra, A., Pak, E., Durkin, S., Csoka, A. B., Boehnke, M., Glover, T. W., & Collins, F. S. (2003). Recurrent de novo point mutations in lamin A cause Hutchinson-Gilford progeria syndrome. *Nature*, *423*(6937), 293–298. https://doi.org/10.1038/nature01629

Fabian, M. R., Sonenberg, N., & Filipowicz, W. (2010). Regulation of mRNA translation and stability by microRNAs. *Annual Review of Biochemistry*, *79*, 351–379. https://doi.org/10.1146/annurev-biochem-060308-103103

Fidzianska, A., Bilinska, Z. T., Tesson, F., Wagner, T., Walski, M., Grzybowski, J., Ruzyllo, W., & Hausmanowa-Petrusewicz, I. (2008). Obliteration of cardiomyocyte nuclear architecture in a patient with LMNA gene mutation. *Journal of the Neurological Sciences*, *271*(1–2), 91–96.

Finlan, L. E., Sproul, D., Thomson, I., Boyle, S., Kerr, E., Perry, P., Ylstra, B., Chubb, J. R., & Bickmore, W. A. (2008). Recruitment to the nuclear periphery can alter expression of genes in human cells. *PLoS Genetics*, *4*(3), e1000039. https://doi.org/10.1371/journal.pgen.1000039

Furukawa, K., Inagaki, H., & Hotta, Y. (1994). Identification and cloning of an mRNA coding for a germ cell-specific A-type lamin in mice. *Experimental Cell Research*, *212*(2), 426–430. https://doi.org/10.1006/excr.1994.1164

Genge, C. E., Lin, E., Lee, L., Sheng, X., Rayani, K., Gunawan, M., Stevens, C. M., Li, A. Y., Talab, S. S., Claydon, T. W., Hove-Madsen, L., & Tibbits, G. F. (2016). The Zebrafish Heart as a Model of Mammalian Cardiac Function. *Reviews of Physiology, Biochemistry and Pharmacology*, *171*, 99–136. https://doi.org/10.1007/112_2016_5

Gerace, L., Blum, A., & Blobel, G. (1978). Immunocytochemical localization of the major polypeptides of the nuclear pore complex-lamina fraction. Interphase and mitotic distribution. *The Journal of Cell Biology*, *79*(2 Pt 1), 546–566. https://doi.org/10.1083/jcb.79.2.546

Gerull, B., Gramlich, M., Atherton, J., McNabb, M., Trombitás, K., Sasse-Klaassen, S., Seidman, J. G., Seidman, C., Granzier, H., Labeit, S., Frenneaux, M., & Thierfelder, L. (2002). Mutations of TTN, encoding the giant muscle filament titin, cause familial dilated cardiomyopathy. *Nature Genetics*, *30*(2), 201–204. https://doi.org/10.1038/ng815

Glickman, N. S., & Yelon, D. (2002). Cardiac development in zebrafish: Coordination of form and function. *Seminars in Cell & Developmental Biology*, *13*(6), 507–513. https://doi.org/10.1016/s1084952102001040

Goldberg, M. W., Huttenlauch, I., Hutchison, C. J., & Stick, R. (2008). Filaments made from A- and B-type lamins differ in structure and organization. *Journal of Cell Science*, *121*(Pt 2), 215–225. https://doi.org/10.1242/jcs.022020

Goldman, R. D., Gruenbaum, Y., Moir, R. D., Shumaker, D. K., & Spann, T. P. (2002). Nuclear lamins: Building blocks of nuclear architecture. *Genes & Development*, *16*(5), 533–547. https://doi.org/10.1101/gad.960502

Goldman, R. D., Shumaker, D. K., Erdos, M. R., Eriksson, M., Goldman, A. E., Gordon, L. B., Gruenbaum, Y., Khuon, S., Mendez, M., Varga, R., & Collins, F. S. (2004a). Accumulation of mutant lamin A causes progressive changes in nuclear architecture in Hutchinson-Gilford progeria syndrome. *Proceedings of the National Academy of Sciences of the United States of America*, *101*(24), 8963–8968. https://doi.org/10.1073/pnas.0402943101

Goldman, R. D., Shumaker, D. K., Erdos, M. R., Eriksson, M., Goldman, A. E., Gordon, L. B., Gruenbaum, Y., Khuon, S., Mendez, M., Varga, R., & Collins, F. S. (2004b). Accumulation of mutant lamin A causes progressive changes in nuclear architecture in Hutchinson-Gilford progeria syndrome. *Proceedings of the National Academy of Sciences of the United States of America*, *101*(24), 8963–8968. https://doi.org/10.1073/pnas.0402943101

Gonzalez, F. A., Raden, D. L., Rigby, M. R., & Davis, R. J. (1992). Heterogeneous expression of four MAP kinase isoforms in human tissues. *FEBS Letters*, *304*(2–3), 170–178. https://doi.org/10.1016/0014-5793(92)80612-k

González, J. M., Navarro-Puche, A., Casar, B., Crespo, P., & Andrés, V. (2008). Fast regulation of AP-1 activity through interaction of lamin A/C, ERK1/2, and c-Fos at the nuclear envelope. *The Journal of Cell Biology*, *183*(4), 653–666. https://doi.org/10.1083/jcb.200805049

González-Cruz, R. D., Dahl, K. N., & Darling, E. M. (2018). The Emerging Role of Lamin C as an Important LMNA Isoform in Mechanophenotype. *Frontiers in Cell and Developmental Biology*, *6*, 151. https://doi.org/10.3389/fcell.2018.00151

Goodnight, J. A., Mischak, H., Kolch, W., & Mushinski, J. F. (1995). Immunocytochemical localization of eight protein kinase C isozymes overexpressed in NIH 3T3 fibroblasts. Isoform-specific association with microfilaments, Golgi, endoplasmic reticulum, and nuclear and cell membranes. *The Journal of Biological Chemistry*, *270*(17), 9991–10001. https://doi.org/10.1074/jbc.270.17.9991

Gupta, P., Bilinska, Z. T., Sylvius, N., Boudreau, E., Veinot, J. P., Labib, S., Bolongo, P. M., Hamza, A., Jackson, T., Ploski, R., Walski, M., Grzybowski, J., Walczak, E., Religa, G.,

Fidzianska, A., & Tesson, F. (2010). Genetic and ultrastructural studies in dilated cardiomyopathy patients: A large deletion in the lamin A/C gene is associated with cardiomyocyte nuclear envelope disruption. *Basic Research in Cardiology*, *105*(3), 365–377.

Guyon, J. R., Steffen, L. S., Howell, M. H., Pusack, T. J., Lawrence, C., & Kunkel, L. M. (2007). Modeling human muscle disease in zebrafish. *Biochimica et Biophysica Acta*, *1772*(2), 205–215. https://doi.org/10.1016/j.bbadis.2006.07.003

Haas, M., & Jost, E. (1993). Functional analysis of phosphorylation sites in human lamin A controlling lamin disassembly, nuclear transport and assembly. *European Journal of Cell Biology*, *62*(2), 237–247.

Hall, T. E., Bryson-Richardson, R. J., Berger, S., Jacoby, A. S., Cole, N. J., Hollway, G. E., Berger, J., & Currie, P. D. (2007). The zebrafish candyfloss mutant implicates extracellular matrix adhesion failure in laminin alpha2-deficient congenital muscular dystrophy. *Proceedings of the National Academy of Sciences of the United States of America*, *104*(17), 7092–7097. https://doi.org/10.1073/pnas.0700942104

Hambleton, M., Hahn, H., Pleger, S. T., Kuhn, M. C., Klevitsky, R., Carr, A. N., Kimball, T. F., Hewett, T. E., 2nd, G. W. D., Koch, W. J., & Molkentin, J. D. (2006). Pharmacological- and gene therapy-based inhibition of protein kinase Calpha/beta enhances cardiac contractility and attenuates heart failure. *Circulation*, *114*(6), 574–582.

Haque, F., Lloyd, D. J., Smallwood, D. T., Dent, C. L., Shanahan, C. M., Fry, A. M., Trembath, R. C., & Shackleton, S. (2006). SUN1 interacts with nuclear lamin A and cytoplasmic nesprins to provide a physical connection between the nuclear lamina and the

cytoskeleton. *Molecular and Cellular Biology*, *26*(10), 3738–3751. https://doi.org/10.1128/MCB.26.10.3738-3751.2006

Hasselberg, N. E., Haland, T. F., Saberniak, J., Brekke, P. H., Berge, K. E., Leren, T. P., Edvardsen, T., & Haugaa, K. H. (2018). Lamin A/C cardiomyopathy: Young onset, high penetrance, and frequent need for heart transplantation. *European Heart Journal*, *39*(10), 853–860. https://doi.org/10.1093/eurheartj/ehx596

Heald, R., & McKeon, F. (1990). Mutations of phosphorylation sites in lamin A that prevent nuclear lamina disassembly in mitosis. *Cell*, *61*(4), 579–589. https://doi.org/10.1016/0092-8674(90)90470-y

Helbling-Leclerc, A., Zhang, X., Topaloglu, H., Cruaud, C., Tesson, F., Weissenbach, J., Tomé, F. M., Schwartz, K., Fardeau, M., & Tryggvason, K. (1995). Mutations in the laminin alpha 2-chain gene (LAMA2) cause merosin-deficient congenital muscular dystrophy. *Nature Genetics*, *11*(2), 216–218. https://doi.org/10.1038/ng1095-216

Heller, F., Dabaj, I., Mah, J. K., Bergounioux, J., Essid, A., Bönnemann, C. G., Rutkowski, A., Bonne, G., Quijano-Roy, S., & Wahbi, K. (2017). Cardiac manifestations of congenital LMNA-related muscular dystrophy in children: Three case reports and recommendations for care. *Cardiology in the Young*, *27*(6), 1076–1082. https://doi.org/10.1017/S1047951116002079

Hernandez, O. M., Jones, M., Guzman, G., & Szczesna-Cordary, D. (2007). Myosin essential light chain in health and disease. *American Journal of Physiology. Heart and Circulatory Physiology*, *292*(4), H1643-1654. https://doi.org/10.1152/ajpheart.00931.2006

Hershberger, R. E., & Morales, A. (1993). LMNA-Related Dilated Cardiomyopathy. In M. P. Adam, H. H. Ardinger, R. A. Pagon, S. E. Wallace, L. J. Bean, K. Stephens, & A.

Amemiya (Eds.), *GeneReviews®*. University of Washington, Seattle. http://www.ncbi.nlm.nih.gov/books/NBK1674/

Ho, Y.-L., Shau, Y.-W., Tsai, H.-J., Lin, L.-C., Huang, P.-J., & Hsieh, F.-J. (2002). Assessment of zebrafish cardiac performance using Doppler echocardiography and power angiography. *Ultrasound in Medicine & Biology*, *28*(9), 1137–1143. https://doi.org/10.1016/s0301-5629(02)00564-1

Holt, I., Ostlund, C., Stewart, C. L., Man, N. thi, Worman, H. J., & Morris, G. E. (2003). Effect of pathogenic mis-sense mutations in lamin A on its interaction with emerin in vivo. *Journal of Cell Science*, *116*(Pt 14), 3027–3035. https://doi.org/10.1242/jcs.00599

Hu, N., Yost, H. J., & Clark, E. B. (2001). Cardiac morphology and blood pressure in the adult zebrafish. *The Anatomical Record*, *264*(1), 1–12. https://doi.org/10.1002/ar.1111

Hu, R., Morley, M. P., Brandimarto, J., Tucker, N. R., Parsons, V. A., Zhao, S. D., Meder, B., Katus, H. A., Rühle, F., Stoll, M., Villard, E., Cambien, F., Lin, H., Smith, N. L., Felix, J. F., Vasan, R. S., van der Harst, P., Newton-Cheh, C., Li, J., … Cappola, T. P. (2018). Genetic Reduction in Left Ventricular Protein Kinase C-α and Adverse Ventricular Remodeling in Human Subjects. *Circulation. Genomic and Precision Medicine*, *11*(3), e001901. https://doi.org/10.1161/CIRCGEN.117.001901

Igumenova, T. I. (2015). Dynamics and Membrane Interactions of Protein Kinase C. *Biochemistry*, *54*(32), 4953–4968. https://doi.org/10.1021/acs.biochem.5b00565

Inamdar, A. A., & Inamdar, A. C. (2016). Heart Failure: Diagnosis, Management and Utilization. *Journal of Clinical Medicine*, *5*(7). https://doi.org/10.3390/jcm5070062

Ivorra, C., Kubicek, M., González, J. M., Sanz-González, S. M., Alvarez-Barrientos, A., O'Connor, J.-E., Burke, B., & Andrés, V. (2006). A mechanism of AP-1 suppression

through interaction of c-Fos with lamin A/C. *Genes & Development*, *20*(3), 307–320. https://doi.org/10.1101/gad.349506

Jackson, H. E., & Ingham, P. W. (2013). Control of muscle fibre-type diversity during embryonic development: The zebrafish paradigm. *Mechanisms of Development*, *130*(9–10), 447–457. https://doi.org/10.1016/j.mod.2013.06.001

Jahn, D., Schramm, S., Schnolzer, M., Heilmann, C. J., de Koster, C. G., Schutz, W., Benavente, R., & Alsheimer, M. (2012). A truncated lamin A in the Lmna -/- mouse line: Implications for the understanding of laminopathies. *Nucleus (Austin, Tex.)*, *3*(5), 463–474. https://doi.org/10.4161/nucl.21676

Jalili, T., Takeishi, Y., Song, G., Ball, N. A., Howles, G., & Walsh, R. A. (1999). PKC translocation without changes in Galphaq and PLC-beta protein abundance in cardiac hypertrophy and failure. *The American Journal of Physiology*, *277*(6), H2298-2304. https://doi.org/10.1152/ajpheart.1999.277.6.H2298

Jensen, T. E., Maarbjerg, S. J., Rose, A. J., Leitges, M., & Richter, E. A. (2009). Knockout of the predominant conventional PKC isoform, PKCalpha, in mouse skeletal muscle does not affect contraction-stimulated glucose uptake. *American Journal of Physiology.Endocrinology and Metabolism*, *297*(2), E340-8.

Jeremy M. Berg, John L. Tymoczko, & Lubert Stryer. (2002). *Biochemistry. 5th edition* (5th ed.). W.H. Freeman.

Jr, R. R. (2012). ERK1/2 MAP kinases: Structure, function, and regulation. *Pharmacological Research : The Official Journal of the Italian Pharmacological Society*, *66*(2), 105–143.

Jung, H.-J., Coffinier, C., Choe, Y., Beigneux, A. P., Davies, B. S. J., Yang, S. H., Barnes, R. H., Hong, J., Sun, T., Pleasure, S. J., Young, S. G., & Fong, L. G. (2012). Regulation of

prelamin A but not lamin C by miR-9, a brain-specific microRNA. *Proceedings of the National Academy of Sciences of the United States of America*, *109*(7), E423-431. https://doi.org/10.1073/pnas.1111780109

Kim, S., Lee, J., Lee, S. K., Bae, S. Y., Kim, J., Kim, M., Kil, W. H., Kim, S. W., Lee, J. E., & Nam, S. J. (2014). Protein kinase C-α downregulates estrogen receptor-α by suppressing c-Jun phosphorylation in estrogen receptor-positive breast cancer cells. *Oncology Reports*, *31*(3), 1423–1428. https://doi.org/10.3892/or.2013.2936

Kimmel, C. B., Ballard, W. W., Kimmel, S. R., Ullmann, B., & Schilling, T. F. (1995). Stages of embryonic development of the zebrafish. *Developmental Dynamics: An Official Publication of the American Association of Anatomists*, *203*(3), 253–310. https://doi.org/10.1002/aja.1002030302

Kochin, V., Shimi, T., Torvaldson, E., Adam, S. A., Goldman, A., Pack, C.-G., Melo-Cardenas, J., Imanishi, S. Y., Goldman, R. D., & Eriksson, J. E. (2014). Interphase phosphorylation of lamin A. *Journal of Cell Science*, *127*(Pt 12), 2683–2696. https://doi.org/10.1242/jcs.141820

Koshimizu, E., Imamura, S., Qi, J., Toure, J., Jr, D. M. V., Carr, C. E., Hanai, J., & Kishi, S. (2011). Embryonic senescence and laminopathies in a progeroid zebrafish model. *PloS One*, *6*(3), e17688.

Krimm, I., Ostlund, C., Gilquin, B., Couprie, J., Hossenlopp, P., Mornon, J.-P., Bonne, G., Courvalin, J.-C., Worman, H. J., & Zinn-Justin, S. (2002). The Ig-like structure of the C-terminal domain of lamin A/C, mutated in muscular dystrophies, cardiomyopathy, and partial lipodystrophy. *Structure (London, England: 1993)*, *10*(6), 811–823.

Lammerding, J., Fong, L. G., Ji, J. Y., Reue, K., Stewart, C. L., Young, S. G., & Lee, R. T. (2006). Lamins A and C but not lamin B1 regulate nuclear mechanics. *The Journal of Biological Chemistry*, *281*(35), 25768–25780. https://doi.org/10.1074/jbc.M513511200

Lammerding, J., Schulze, P. C., Takahashi, T., Kozlov, S., Sullivan, T., Kamm, R. D., Stewart, C. L., & Lee, R. T. (2004). Lamin A/C deficiency causes defective nuclear mechanics and mechanotransduction. *The Journal of Clinical Investigation*, *113*(3), 370–378. https://doi.org/10.1172/JCI19670

Lanzicher, T., Martinelli, V., Long, C. S., Del Favero, G., Puzzi, L., Borelli, M., Mestroni, L., Taylor, M. R. G., & Sbaizero, O. (2015). AFM single-cell force spectroscopy links altered nuclear and cytoskeletal mechanics to defective cell adhesion in cardiac myocytes with a nuclear lamin mutation. *Nucleus (Austin, Tex.)*, *6*(5), 394–407. https://doi.org/10.1080/19491034.2015.1084453

Laurini, E., Martinelli, V., Lanzicher, T., Puzzi, L., Borin, D., Chen, S. N., Long, C. S., Lee, P., Mestroni, L., Taylor, M. R. G., Sbaizero, O., & Pricl, S. (2018). Biomechanical defects and rescue of cardiomyocytes expressing pathologic nuclear lamins. *Cardiovascular Research*, *114*(6), 846–857. https://doi.org/10.1093/cvr/cvy040

Leitges, M., Plomann, M., Standaert, M. L., Bandyopadhyay, G., Sajan, M. P., Kanoh, Y., Farese, R. V., & Letiges, M. (2002). Knockout of PKC alpha enhances insulin signaling through PI3K. *Molecular Endocrinology (Baltimore, Md.)*, *16*(4), 847–858. https://doi.org/10.1210/mend.16.4.0809

Leukel, M., & Jost, E. (1995). Two conserved serines in the nuclear localization signal flanking region are involved in the nuclear targeting of human lamin A. *European Journal of Cell Biology*, *68*(2), 133–142.

Li, M., Hromowyk, K. J., Amacher, S. L., & Currie, P. D. (2017). Muscular dystrophy modeling in zebrafish. *Methods in Cell Biology*, *138*, 347–380. https://doi.org/10.1016/bs.mcb.2016.11.004

Li, Mei, Andersson-Lendahl, M., Sejersen, T., & Arner, A. (2014). Muscle dysfunction and structural defects of dystrophin-null sapje mutant zebrafish larvae are rescued by ataluren treatment. *FASEB Journal: Official Publication of the Federation of American Societies for Experimental Biology*, *28*(4), 1593–1599. https://doi.org/10.1096/fj.13-240044

Li, W., Zhang, J., Flechner, L., Hyun, T., Yam, A., Franke, T. F., & Pierce, J. H. (1999). Protein kinase C-alpha overexpression stimulates Akt activity and suppresses apoptosis induced by interleukin 3 withdrawal. *Oncogene*, *18*(47), 6564–6572. https://doi.org/10.1038/sj.onc.1203065

Lin, F., & Worman, H. J. (1993). Structural organization of the human gene encoding nuclear lamin A and nuclear lamin C. *The Journal of Biological Chemistry*, *268*(22), 16321–16326.

Link, J., Jahn, D., Schmitt, J., Göb, E., Baar, J., Ortega, S., Benavente, R., & Alsheimer, M. (2013). The meiotic nuclear lamina regulates chromosome dynamics and promotes efficient homologous recombination in the mouse. *PLoS Genetics*, *9*(1), e1003261. https://doi.org/10.1371/journal.pgen.1003261

Liu, B., Wang, J., Chan, K. M., Tjia, W. M., Deng, W., Guan, X., Huang, J., Li, K. M., Chau, P. Y., Chen, D. J., Pei, D., Pendas, A. M., Cadiñanos, J., López-Otín, C., Tse, H. F., Hutchison, C., Chen, J., Cao, Y., Cheah, K. S. E., … Zhou, Z. (2005). Genomic instability in laminopathy-based premature aging. *Nature Medicine*, *11*(7), 780–785. https://doi.org/10.1038/nm1266

Lloyd, D. J., Trembath, R. C., & Shackleton, S. (2002). A novel interaction between lamin A and SREBP1: Implications for partial lipodystrophy and other laminopathies. *Human Molecular Genetics*, *11*(7), 769–777.

Machiels, B. M., Zorenc, A. H., Endert, J. M., Kuijpers, H. J., van Eys, G. J., Ramaekers, F. C., & Broers, J. L. (1996). An alternative splicing product of the lamin A/C gene lacks exon 10. *The Journal of Biological Chemistry*, *271*(16), 9249–9253.

Machowska, M., Piekarowicz, K., & Rzepecki, R. (2015). Regulation of lamin properties and functions: Does phosphorylation do it all? *Open Biology*, *5*(11). https://doi.org/10.1098/rsob.150094

Magracheva, E., Kozlov, S., Stewart, C. L., Wlodawer, A., & Zdanov, A. (2009). Structure of the lamin A/C R482W mutant responsible for dominant familial partial lipodystrophy (FPLD). *Acta Crystallographica. Section F, Structural Biology and Crystallization Communications*, *65*(Pt 7), 665–670. https://doi.org/10.1107/S1744309109020302

Martelli, A. M., Bortul, R., Tabellini, G., Faenza, I., Cappellini, A., Bareggi, R., Manzoli, L., & Cocco, L. (2002). Molecular characterization of protein kinase C-alpha binding to lamin A. *Journal of Cellular Biochemistry*, *86*(2), 320–330.

Mattar, P., Stevanovic, M., Nad, I., & Cayouette, M. (2018). Casz1 controls higher-order nuclear organization in rod photoreceptors. *Proceedings of the National Academy of Sciences of the United States of America*, *115*(34), E7987–E7996. https://doi.org/10.1073/pnas.1803069115

Mattioli, E., Andrenacci, D., Garofalo, C., Prencipe, S., Scotlandi, K., Remondini, D., Gentilini, D., Di Blasio, A. M., Valente, S., Scarano, E., Cicchilitti, L., Piaggio, G., Mai, A., & Lattanzi, G. (2018). Altered modulation of lamin A/C-HDAC2 interaction and p21

expression during oxidative stress response in HGPS. *Aging Cell*, *17*(5), e12824. https://doi.org/10.1111/acel.12824

Mattout, A., Goldberg, M., Tzur, Y., Margalit, A., & Gruenbaum, Y. (2007). Specific and conserved sequences in D. melanogaster and C. elegans lamins and histone H2A mediate the attachment of lamins to chromosomes. *Journal of Cell Science*, *120*(Pt 1), 77–85. https://doi.org/10.1242/jcs.03325

Mattout, A., Pike, B. L., Towbin, B. D., Bank, E. M., Gonzalez-Sandoval, A., Stadler, M. B., Meister, P., Gruenbaum, Y., & Gasser, S. M. (2011). An EDMD mutation in C. elegans lamin blocks muscle-specific gene relocation and compromises muscle integrity. *Current Biology: CB*, *21*(19), 1603–1614. https://doi.org/10.1016/j.cub.2011.08.030

Mauro, A., Ciccarelli, C., Cesaris, P. D., Scoglio, A., Bouche, M., Molinaro, M., Aquino, A., & Zani, B. M. (2002). PKCalpha-mediated ERK, JNK and p38 activation regulates the myogenic program in human rhabdomyosarcoma cells. *Journal of Cell Science*, *115*(Pt 18), 3587–3599.

McCord, R. P., Nazario-Toole, A., Zhang, H., Chines, P. S., Zhan, Y., Erdos, M. R., Collins, F. S., Dekker, J., & Cao, K. (2013). Correlated alterations in genome organization, histone methylation, and DNA-lamin A/C interactions in Hutchinson-Gilford progeria syndrome. *Genome Research*, *23*(2), 260–269. https://doi.org/10.1101/gr.138032.112

McKeon, F. D., Kirschner, M. W., & Caput, D. (1986). Homologies in both primary and secondary structure between nuclear envelope and intermediate filament proteins. *Nature*, *319*(6053), 463–468. https://doi.org/10.1038/319463a0

Meder, B., Laufer, C., Hassel, D., Just, S., Marquart, S., Vogel, B., Hess, A., Fishman, M. C., Katus, H. A., & Rottbauer, W. (2009). A single serine in the carboxyl terminus of cardiac

essential myosin light chain-1 controls cardiomyocyte contractility in vivo. *Circulation Research*, *104*(5), 650–659. https://doi.org/10.1161/CIRCRESAHA.108.186676

Meister, P., Towbin, B. D., Pike, B. L., Ponti, A., & Gasser, S. M. (2010). The spatial dynamics of tissue-specific promoters during C. elegans development. *Genes & Development*, *24*(8), 766–782. https://doi.org/10.1101/gad.559610

Milan, D. J., Jones, I. L., Ellinor, P. T., & MacRae, C. A. (2006). In vivo recording of adult zebrafish electrocardiogram and assessment of drug-induced QT prolongation. *American Journal of Physiology. Heart and Circulatory Physiology*, *291*(1), H269-273. https://doi.org/10.1152/ajpheart.00960.2005

Mione, M. C., & Trede, N. S. (2010). The zebrafish as a model for cancer. *Disease Models & Mechanisms*, *3*(9–10), 517–523. https://doi.org/10.1242/dmm.004747

Misteli, T., & Scaffidi, P. (2005). Genome instability in progeria: When repair gets old. *Nature Medicine*, *11*(7), 718–719. https://doi.org/10.1038/nm0705-718

Mitsuhashi, H., Hayashi, Y. K., Matsuda, C., Noguchi, S., Wakatsuki, S., Araki, T., & Nishino, I. (2010). Specific phosphorylation of Ser458 of A-type lamins in LMNA-associated myopathy patients. *Journal of Cell Science*, *123*(Pt 22), 3893–3900. https://doi.org/10.1242/jcs.072157

Moir, R. D., Yoon, M., Khuon, S., & Goldman, R. D. (2000). Nuclear lamins A and B1: Different pathways of assembly during nuclear envelope formation in living cells. *The Journal of Cell Biology*, *151*(6), 1155–1168. https://doi.org/10.1083/jcb.151.6.1155

Monje, P., Marinissen, M. J., & Gutkind, J. S. (2003). Phosphorylation of the carboxyl-terminal transactivation domain of c-Fos by extracellular signal-regulated kinase mediates the transcriptional activation of AP-1 and cellular transformation induced by platelet-derived

growth factor. *Molecular and Cellular Biology*, *23*(19), 7030–7043. https://doi.org/10.1128/mcb.23.19.7030-7043.2003

Muchir, A., Kim, Y. J., Reilly, S. A., Wu, W., Choi, J. C., & Worman, H. J. (2013). Inhibition of extracellular signal-regulated kinase 1/2 signaling has beneficial effects on skeletal muscle in a mouse model of Emery-Dreifuss muscular dystrophy caused by lamin A/C gene mutation. *Skeletal Muscle*, *3*(1), 17-5040-3–17.

Muchir, A., Pavlidis, P., Decostre, V., Herron, A. J., Arimura, T., Bonne, G., & Worman, H. J. (2007). Activation of MAPK pathways links LMNA mutations to cardiomyopathy in Emery-Dreifuss muscular dystrophy. *The Journal of Clinical Investigation*, *117*(5), 1282–1293.

Muchir, A., Reilly, S. A., Wu, W., Iwata, S., Homma, S., Bonne, G., & Worman, H. J. (2012). Treatment with selumetinib preserves cardiac function and improves survival in cardiomyopathy caused by mutation in the lamin A/C gene. *Cardiovascular Research*, *93*(2), 311–319.

Muchir, A., Shan, J., Bonne, G., Lehnart, S. E., & Worman, H. J. (2009). Inhibition of extracellular signal-regulated kinase signaling to prevent cardiomyopathy caused by mutation in the gene encoding A-type lamins. *Human Molecular Genetics*, *18*(2), 241–247.

Muchir, A., Wu, W., Choi, J. C., Iwata, S., Morrow, J., Homma, S., & Worman, H. J. (2012). Abnormal p38alpha mitogen-activated protein kinase signaling in dilated cardiomyopathy caused by lamin A/C gene mutation. *Human Molecular Genetics*, *21*(19), 4325–4333.

Muchir, A., Wu, W., & Worman, H. J. (2009). Reduced expression of A-type lamins and emerin activates extracellular signal-regulated kinase in cultured cells. *Biochimica et Biophysica Acta*, *1792*(1), 75–81.

Muchir, Antoine, van Engelen, B. G., Lammens, M., Mislow, J. M., McNally, E., Schwartz, K., & Bonne, G. (2003). Nuclear envelope alterations in fibroblasts from LGMD1B patients carrying nonsense Y259X heterozygous or homozygous mutation in lamin A/C gene. *Experimental Cell Research*, *291*(2), 352–362.

Müller, U. K., LEEUWEN, J. L. van, DUIN, S. van, & LIU, H. (2009). An Un-Momentous Start to Life: Can Hydrodynamics Explain Why Fish Larvae Change Swimming Style? *Journal of Biomechanical Science and Engineering*, *4*(1), 37–53. https://doi.org/10.1299/jbse.4.37

Müller, U. K., van den Boogaart, J. G. M., & van Leeuwen, J. L. (2008). Flow patterns of larval fish: Undulatory swimming in the intermediate flow regime. *The Journal of Experimental Biology*, *211*(Pt 2), 196–205. https://doi.org/10.1242/jeb.005629

Müller, U. K., & van Leeuwen, J. L. (2004). Swimming of larval zebrafish: Ontogeny of body waves and implications for locomotory development. *The Journal of Experimental Biology*, *207*(Pt 5), 853–868. https://doi.org/10.1242/jeb.00821

Muramatsu, M., Kaibuchi, K., & Arai, K. (1989). A protein kinase C cDNA without the regulatory domain is active after transfection in vivo in the absence of phorbol ester. *Molecular and Cellular Biology*, *9*(2), 831–836. https://doi.org/10.1128/mcb.9.2.831

Myant, K., Qiao, X., Halonen, T., Come, C., Laine, A., Janghorban, M., Partanen, J. I., Cassidy, J., Ogg, E.-L., Cammareri, P., Laiterä, T., Okkeri, J., Klefström, J., Sears, R. C., Sansom, O. J., & Westermarck, J. (2015). Serine 62-Phosphorylated MYC Associates with

Nuclear Lamins and Its Regulation by CIP2A Is Essential for Regenerative Proliferation. *Cell Reports*, *12*(6), 1019–1031. https://doi.org/10.1016/j.celrep.2015.07.003

Nakashima, S. (2002). Protein kinase C alpha (PKC alpha): Regulation and biological function. *Journal of Biochemistry*, *132*(5), 669–675.

Naskar, S., Datta, K., Mitra, A., Pathak, K., Datta, R., Bansal, T., & Sarkar, S. (2014). Differential and conditional activation of PKC-isoforms dictates cardiac adaptation during physiological to pathological hypertrophy. *PloS One*, *9*(8), e104711.

Nemtsas, P., Wettwer, E., Christ, T., Weidinger, G., & Ravens, U. (2010). Adult zebrafish heart as a model for human heart? An electrophysiological study. *Journal of Molecular and Cellular Cardiology*, *48*(1), 161–171. https://doi.org/10.1016/j.yjmcc.2009.08.034

Neri, L. M., Borgatti, P., Capitani, S., & Martelli, A. M. (1998). Nuclear diacylglycerol produced by phosphoinositide-specific phospholipase C is responsible for nuclear translocation of protein kinase C-alpha. *The Journal of Biological Chemistry*, *273*(45), 29738–29744. https://doi.org/10.1074/jbc.273.45.29738

Nicolas, H. A., Akimenko, M.-A., & Tesson, F. (2019). Cellular and Animal Models of Striated Muscle Laminopathies. *Cells*, *8*(4). https://doi.org/10.3390/cells8040291

Nishizuka, Y. (1988). The molecular heterogeneity of protein kinase C and its implications for cellular regulation. *Nature*, *334*(6184), 661–665. https://doi.org/10.1038/334661a0

Nmezi, B., Xu, J., Fu, R., Armiger, T. J., Rodriguez-Bey, G., Powell, J. S., Ma, H., Sullivan, M., Tu, Y., Chen, N. Y., Young, S. G., Stolz, D. B., Dahl, K. N., Liu, Y., & Padiath, Q. S. (2019). Concentric organization of A- and B-type lamins predicts their distinct roles in the spatial organization and stability of the nuclear lamina. *Proceedings of the National*

Academy of Sciences of the United States of America. https://doi.org/10.1073/pnas.1810070116

O'Brien, K. F., & Kunkel, L. M. (2001). Dystrophin and muscular dystrophy: Past, present, and future. *Molecular Genetics and Metabolism*, *74*(1–2), 75–88. https://doi.org/10.1006/mgme.2001.3220

Ollila, L., Nikus, K., Holmström, M., Jalanko, M., Jurkko, R., Kaartinen, M., Koskenvuo, J., Kuusisto, J., Kärkkäinen, S., Palojoki, E., Reissell, E., Piirilä, P., & Heliö, T. (2017). Clinical disease presentation and ECG characteristics of LMNA mutation carriers. *Open Heart*, *4*(1), e000474. https://doi.org/10.1136/openhrt-2016-000474

Parekh, D. B., Ziegler, W., & Parker, P. J. (2000). Multiple pathways control protein kinase C phosphorylation. *The EMBO Journal*, *19*(4), 496–503. https://doi.org/10.1093/emboj/19.4.496

Pasotti, M., Klersy, C., Pilotto, A., Marziliano, N., Rapezzi, C., Serio, A., Mannarino, S., Gambarin, F., Favalli, V., Grasso, M., Agozzino, M., Campana, C., Gavazzi, A., Febo, O., Marini, M., Landolina, M., Mortara, A., Piccolo, G., Viganò, M., … Arbustini, E. (2008). Long-term outcome and risk stratification in dilated cardiolaminopathies. *Journal of the American College of Cardiology*, *52*(15), 1250–1260. https://doi.org/10.1016/j.jacc.2008.06.044

Pass, J. M., Gao, J., Jones, W. K., Wead, W. B., Wu, X., Zhang, J., Baines, C. P., Bolli, R., Zheng, Y. T., Joshua, I. G., & Ping, P. (2001). Enhanced PKC beta II translocation and PKC beta II-RACK1 interactions in PKC epsilon-induced heart failure: A role for RACK1. *American Journal of Physiology. Heart and Circulatory Physiology*, *281*(6), H2500-2510. https://doi.org/10.1152/ajpheart.2001.281.6.H2500

Pelster, B., & Burggren, W. W. (1996). Disruption of hemoglobin oxygen transport does not impact oxygen-dependent physiological processes in developing embryos of zebra fish (Danio rerio). *Circulation Research*, *79*(2), 358–362. https://doi.org/10.1161/01.res.79.2.358

Ping, P., Zhang, J., Qiu, Y., Tang, X. L., Manchikalapudi, S., Cao, X., & Bolli, R. (1997). Ischemic preconditioning induces selective translocation of protein kinase C isoforms epsilon and eta in the heart of conscious rabbits without subcellular redistribution of total protein kinase C activity. *Circulation Research*, *81*(3), 404–414. https://doi.org/10.1161/01.res.81.3.404

Pinto, Y. M., Elliott, P. M., Arbustini, E., Adler, Y., Anastasakis, A., Böhm, M., Duboc, D., Gimeno, J., de Groote, P., Imazio, M., Heymans, S., Klingel, K., Komajda, M., Limongelli, G., Linhart, A., Mogensen, J., Moon, J., Pieper, P. G., Seferovic, P. M., … Charron, P. (2016). Proposal for a revised definition of dilated cardiomyopathy, hypokinetic non-dilated cardiomyopathy, and its implications for clinical practice: A position statement of the ESC working group on myocardial and pericardial diseases. *European Heart Journal*, *37*(23), 1850–1858. https://doi.org/10.1093/eurheartj/ehv727

Poon, K. L., & Brand, T. (2013). The zebrafish model system in cardiovascular research: A tiny fish with mighty prospects. *Global Cardiology Science & Practice*, *2013*(1), 9–28. https://doi.org/10.5339/gcsp.2013.4

Quijano-Roy, S., Mbieleu, B., Bönnemann, C. G., Jeannet, P.-Y., Colomer, J., Clarke, N. F., Cuisset, J.-M., Roper, H., De Meirleir, L., D'Amico, A., Ben Yaou, R., Nascimento, A., Barois, A., Demay, L., Bertini, E., Ferreiro, A., Sewry, C. A., Romero, N. B., Ryan, M., … Estournet, B. (2008). De novo LMNA mutations cause a new form of congenital

muscular dystrophy. *Annals of Neurology*, *64*(2), 177–186. https://doi.org/10.1002/ana.21417

Raffaele Di Barletta, M., Ricci, E., Galluzzi, G., Tonali, P., Mora, M., Morandi, L., Romorini, A., Voit, T., Orstavik, K. H., Merlini, L., Trevisan, C., Biancalana, V., Housmanowa-Petrusewicz, I., Bione, S., Ricotti, R., Schwartz, K., Bonne, G., & Toniolo, D. (2000). Different mutations in the LMNA gene cause autosomal dominant and autosomal recessive Emery-Dreifuss muscular dystrophy. *American Journal of Human Genetics*, *66*(4), 1407–1412. https://doi.org/10.1086/302869

Raharjo, W. H., Enarson, P., Sullivan, T., Stewart, C. L., & Burke, B. (2001). Nuclear envelope defects associated with LMNA mutations cause dilated cardiomyopathy and Emery-Dreifuss muscular dystrophy. *Journal of Cell Science*, *114*(Pt 24), 4447–4457.

Röber, R. A., Weber, K., & Osborn, M. (1989). Differential timing of nuclear lamin A/C expression in the various organs of the mouse embryo and the young animal: A developmental study. *Development (Cambridge, England)*, *105*(2), 365–378.

Rodríguez, J., Calvo, F., González, J. M., Casar, B., Andrés, V., & Crespo, P. (2010). ERK1/2 MAP kinases promote cell cycle entry by rapid, kinase-independent disruption of retinoblastoma-lamin A complexes. *The Journal of Cell Biology*, *191*(5), 967–979. https://doi.org/10.1083/jcb.201004067

Rouet-Benzineb, P., Mohammadi, K., Pérennec, J., Poyard, M., Bouanani Nel-H, null, & Crozatier, B. (1996). Protein kinase C isoform expression in normal and failing rabbit hearts. *Circulation Research*, *79*(2), 153–161. https://doi.org/10.1161/01.res.79.2.153

Roy, A., Yang, J., & Zhang, Y. (2012). COFACTOR: an accurate comparative algorithm for structure-based protein function annotation. *Nucleic Acids Research*, *40*(Web Server issue), W471-477. https://doi.org/10.1093/nar/gks372

Ruvolo, P. P., Deng, X., Carr, B. K., & May, W. S. (1998). A functional role for mitochondrial protein kinase Calpha in Bcl2 phosphorylation and suppression of apoptosis. *The Journal of Biological Chemistry*, *273*(39), 25436–25442. https://doi.org/10.1074/jbc.273.39.25436

Samson, C., Petitalot, A., Celli, F., Herrada, I., Ropars, V., Le Du, M.-H., Nhiri, N., Jacquet, E., Arteni, A.-A., Buendia, B., & Zinn-Justin, S. (2018). Structural analysis of the ternary complex between lamin A/C, BAF and emerin identifies an interface disrupted in autosomal recessive progeroid diseases. *Nucleic Acids Research*, *46*(19), 10460–10473. https://doi.org/10.1093/nar/gky736

Sarmah, S., & Marrs, J. A. (2016). Zebrafish as a Vertebrate Model System to Evaluate Effects of Environmental Toxicants on Cardiac Development and Function. *International Journal of Molecular Sciences*, *17*(12). https://doi.org/10.3390/ijms17122123

Scaffidi, P., & Misteli, T. (2005). Reversal of the cellular phenotype in the premature aging disease Hutchinson-Gilford progeria syndrome. *Nature Medicine*, *11*(4), 440–445. https://doi.org/10.1038/nm1204

Schmalz, D., Kalkbrenner, F., Hucho, F., & Buchner, K. (1996). Transport of protein kinase C alpha into the nucleus requires intact cytoskeleton while the transport of a protein containing a canonical nuclear localization signal does not. *Journal of Cell Science*, *109 (Pt 9)*(Pt 9), 2401–2406.

Schönwasser, D. C., Marais, R. M., Marshall, C. J., & Parker, P. J. (1998). Activation of the mitogen-activated protein kinase/extracellular signal-regulated kinase pathway by conventional, novel, and atypical protein kinase C isotypes. *Molecular and Cellular Biology*, *18*(2), 790–798. https://doi.org/10.1128/mcb.18.2.790

Sedmera, D., Reckova, M., deAlmeida, A., Sedmerova, M., Biermann, M., Volejnik, J., Sarre, A., Raddatz, E., McCarthy, R. A., Gourdie, R. G., & Thompson, R. P. (2003). Functional and morphological evidence for a ventricular conduction system in zebrafish and Xenopus hearts. *American Journal of Physiology. Heart and Circulatory Physiology*, *284*(4), H1152-1160. https://doi.org/10.1152/ajpheart.00870.2002

Seeley, M., Huang, W., Chen, Z., Wolff, W. O., Lin, X., & Xu, X. (2007). Depletion of zebrafish titin reduces cardiac contractility by disrupting the assembly of Z-discs and A-bands. *Circulation Research*, *100*(2), 238–245. https://doi.org/10.1161/01.RES.0000255758.69821.b5

Shi, X., Chen, R., Zhang, Y., Yun, J., Brand-Arzamendi, K., Liu, X., & Wen, X.-Y. (2018). Zebrafish heart failure models: Opportunities and challenges. *Amino Acids*, *50*(7), 787–798. https://doi.org/10.1007/s00726-018-2578-7

Shih, Y.-H., Zhang, Y., Ding, Y., Ross, C. A., Li, H., Olson, T. M., & Xu, X. (2015). Cardiac transcriptome and dilated cardiomyopathy genes in zebrafish. *Circulation. Cardiovascular Genetics*, *8*(2), 261–269. https://doi.org/10.1161/CIRCGENETICS.114.000702

Shimi, T., Kittisopikul, M., Tran, J., Goldman, A. E., Adam, S. A., Zheng, Y., Jaqaman, K., & Goldman, R. D. (2015). Structural organization of nuclear lamins A, C, B1, and B2

revealed by superresolution microscopy. *Molecular Biology of the Cell*, *26*(22), 4075–4086. https://doi.org/10.1091/mbc.E15-07-0461

Shimi, T., Pfleghaar, K., Kojima, S., Pack, C.-G., Solovei, I., Goldman, A. E., Adam, S. A., Shumaker, D. K., Kinjo, M., Cremer, T., & Goldman, R. D. (2008). The A- and B-type nuclear lamin networks: Microdomains involved in chromatin organization and transcription. *Genes & Development*, *22*(24), 3409–3421. https://doi.org/10.1101/gad.1735208

Singh, R. K., Kumar, S., Gautam, P. K., Tomar, M. S., Verma, P. K., Singh, S. P., Kumar, S., & Acharya, A. (2017). Protein kinase C-α and the regulation of diverse cell responses. *Biomolecular Concepts*, *8*(3–4), 143–153. https://doi.org/10.1515/bmc-2017-0005

Singh, R. M., Cummings, E., Pantos, C., & Singh, J. (2017). Protein kinase C and cardiac dysfunction: A review. *Heart Failure Reviews*, *22*(6), 843–859. https://doi.org/10.1007/s10741-017-9634-3

Smyth, M. S., & Martin, J. H. (2000). X ray crystallography. *Molecular Pathology: MP*, *53*(1), 8–14. https://doi.org/10.1136/mp.53.1.8

Soh, J. W., Lee, E. H., Prywes, R., & Weinstein, I. B. (1999). Novel roles of specific isoforms of protein kinase C in activation of the c-fos serum response element. *Molecular and Cellular Biology*, *19*(2), 1313–1324.

Soh, J.-W., & Weinstein, I. B. (2003). Roles of specific isoforms of protein kinase C in the transcriptional control of cyclin D1 and related genes. *The Journal of Biological Chemistry*, *278*(36), 34709–34716. https://doi.org/10.1074/jbc.M302016200

Solovei, I., Wang, A. S., Thanisch, K., Schmidt, C. S., Krebs, S., Zwerger, M., Cohen, T. V., Devys, D., Foisner, R., Peichl, L., Herrmann, H., Blum, H., Engelkamp, D., Stewart, C.

L., Leonhardt, H., & Joffe, B. (2013). LBR and lamin A/C sequentially tether peripheral heterochromatin and inversely regulate differentiation. *Cell*, *152*(3), 584–598. https://doi.org/10.1016/j.cell.2013.01.009

Spann, T. P., Moir, R. D., Goldman, A. E., Stick, R., & Goldman, R. D. (1997). Disruption of nuclear lamin organization alters the distribution of replication factors and inhibits DNA synthesis. *The Journal of Cell Biology*, *136*(6), 1201–1212. https://doi.org/10.1083/jcb.136.6.1201

Staudt, D., & Stainier, D. (2012). Uncovering the molecular and cellular mechanisms of heart development using the zebrafish. *Annual Review of Genetics*, *46*, 397–418. https://doi.org/10.1146/annurev-genet-110711-155646

Steffen, L. S., Guyon, J. R., Vogel, E. D., Beltre, R., Pusack, T. J., Zhou, Y., Zon, L. I., & Kunkel, L. M. (2007). Zebrafish orthologs of human muscular dystrophy genes. *BMC Genomics*, *8*, 79.

Stewart, C., & Burke, B. (1987). Teratocarcinoma stem cells and early mouse embryos contain only a single major lamin polypeptide closely resembling lamin B. *Cell*, *51*(3), 383–392.

Strelkov, S. V., Schumacher, J., Burkhard, P., Aebi, U., & Herrmann, H. (2004). Crystal structure of the human lamin A coil 2B dimer: Implications for the head-to-tail association of nuclear lamins. *Journal of Molecular Biology*, *343*(4), 1067–1080. https://doi.org/10.1016/j.jmb.2004.08.093

Stuurman, N., Heins, S., & Aebi, U. (1998). Nuclear lamins: Their structure, assembly, and interactions. *Journal of Structural Biology*, *122*(1–2), 42–66.

Sullivan, T., Escalante-Alcalde, D., Bhatt, H., Anver, M., Bhat, N., Nagashima, K., Stewart, C. L., & Burke, B. (1999). Loss of A-type lamin expression compromises nuclear envelope integrity leading to muscular dystrophy. *The Journal of Cell Biology*, *147*(5), 913–920.

Swift, J., Ivanovska, I. L., Buxboim, A., Harada, T., Dingal, P. C. D. P., Pinter, J., Pajerowski, J. D., Spinler, K. R., Shin, J.-W., Tewari, M., Rehfeldt, F., Speicher, D. W., & Discher, D. E. (2013). Nuclear lamin-A scales with tissue stiffness and enhances matrix-directed differentiation. *Science (New York, N.Y.)*, *341*(6149), 1240104. https://doi.org/10.1126/science.1240104

Sylvius, N., Bilinska, Z. T., Veinot, J. P., Fidzianska, A., Bolongo, P. M., Poon, S., McKeown, P., Davies, R. A., Chan, K. L., Tang, A. S., Dyack, S., Grzybowski, J., Ruzyllo, W., McBride, H., & Tesson, F. (2005). In vivo and in vitro examination of the functional significances of novel lamin gene mutations in heart failure patients. *Journal of Medical Genetics*, *42*(8), 639–647.

Sylvius, N., Hathaway, A., Boudreau, E., Gupta, P., Labib, S., Bolongo, P. M., Rippstein, P., McBride, H., Bilinska, Z. T., & Tesson, F. (2008). Specific contribution of lamin A and lamin C in the development of laminopathies. *Experimental Cell Research*, *314*(13), 2362–2375.

Taniura, H., Glass, C., & Gerace, L. (1995). A chromatin binding site in the tail domain of nuclear lamins that interacts with core histones. *The Journal of Cell Biology*, *131*(1), 33–44. https://doi.org/10.1083/jcb.131.1.33

Taylor, M. R., Fain, P. R., Sinagra, G., Robinson, M. L., Robertson, A. D., Carniel, E., Lenarda, A. D., Bohlmeyer, T. J., Ferguson, D. A., Brodsky, G. L., Boucek, M. M., Lascor, J., Moss, A. C., Li, W. L., Stetler, G. L., Muntoni, F., Bristow, M. R., Mestroni, L., &

Group, F. D. C. R. R. (2003). Natural history of dilated cardiomyopathy due to lamin A/C gene mutations. *Journal of the American College of Cardiology*, *41*(5), 771–780.

Tesson, F., Saj, M., Uvaize, M. M., Nicolas, H., Płoski, R., & Bilińska, Z. (2014). Lamin A/C mutations in dilated cardiomyopathy. *Cardiology Journal*, *21*(4), 331–342. https://doi.org/10.5603/CJ.a2014.0037

The PyMOL Molecular Graphics System, Version 2.3.4 Schrödinger, LLC (2.3.4). (n.d.). [Computer software].

Turgay, Y., Eibauer, M., Goldman, A. E., Shimi, T., Khayat, M., Ben-Harush, K., Dubrovsky-Gaupp, A., Sapra, K. T., Goldman, R. D., & Medalia, O. (2017). The molecular architecture of lamins in somatic cells. *Nature*, *543*(7644), 261–264. https://doi.org/10.1038/nature21382

Uhlén, M., Fagerberg, L., Hallström, B. M., Lindskog, C., Oksvold, P., Mardinoglu, A., Sivertsson, Å., Kampf, C., Sjöstedt, E., Asplund, A., Olsson, I., Edlund, K., Lundberg, E., Navani, S., Szigyarto, C. A.-K., Odeberg, J., Djureinovic, D., Takanen, J. O., Hober, S., … Pontén, F. (2015). Proteomics. Tissue-based map of the human proteome. *Science (New York, N.Y.)*, *347*(6220), 1260419. https://doi.org/10.1126/science.1260419

van Berlo, J. H., de Voogt, W. G., van der Kooi, A. J., van Tintelen, J. P., Bonne, G., Yaou, R. B., Duboc, D., Rossenbacker, T., Heidbüchel, H., de Visser, M., Crijns, H. J. G. M., & Pinto, Y. M. (2005). Meta-analysis of clinical characteristics of 299 carriers of LMNA gene mutations: Do lamin A/C mutations portend a high risk of sudden death? *Journal of Molecular Medicine (Berlin, Germany)*, *83*(1), 79–83. https://doi.org/10.1007/s00109-004-0589-1

van Rijsingen, I. A. W., Nannenberg, E. A., Arbustini, E., Elliott, P. M., Mogensen, J., Hermans-van Ast, J. F., van der Kooi, A. J., van Tintelen, J. P., van den Berg, M. P., Grasso, M., Serio, A., Jenkins, S., Rowland, C., Richard, P., Wilde, A. A. M., Perrot, A., Pankuweit, S., Zwinderman, A. H., Charron, P., … Pinto, Y. M. (2013). Gender-specific differences in major cardiac events and mortality in lamin A/C mutation carriers. *European Journal of Heart Failure*, *15*(4), 376–384. https://doi.org/10.1093/eurjhf/hfs191

Vaughan, A., Alvarez-Reyes, M., Bridger, J. M., Broers, J. L., Ramaekers, F. C., Wehnert, M., Morris, G. E., Whitfield WGF, null, & Hutchison, C. J. (2001). Both emerin and lamin C depend on lamin A for localization at the nuclear envelope. *Journal of Cell Science*, *114*(Pt 14), 2577–2590.

Vergnes, L., Péterfy, M., Bergo, M. O., Young, S. G., & Reue, K. (2004). Lamin B1 is required for mouse development and nuclear integrity. *Proceedings of the National Academy of Sciences of the United States of America*, *101*(28), 10428–10433. https://doi.org/10.1073/pnas.0401424101

Verkerk, A. O., & Remme, C. A. (2012). Zebrafish: A novel research tool for cardiac (patho)electrophysiology and ion channel disorders. *Frontiers in Physiology*, *3*, 255. https://doi.org/10.3389/fphys.2012.00255

Verma, A. D., & Parnaik, V. K. (2017). Heart-specific expression of laminopathic mutations in transgenic zebrafish. *Cell Biology International*, *41*(7), 809–819. https://doi.org/10.1002/cbin.10784

Vogel, B., Meder, B., Just, S., Laufer, C., Berger, I., Weber, S., Katus, H. A., & Rottbauer, W. (2009). In-vivo characterization of human dilated cardiomyopathy genes in zebrafish. *Biochemical and Biophysical Research Communications*, *390*(3), 516–522.

Vytopil, M., Ricci, E., Dello Russo, A., Hanisch, F., Neudecker, S., Zierz, S., Ricotti, R., Demay, L., Richard, P., Wehnert, M., Bonne, G., Merlini, L., & Toniolo, D. (2002). Frequent low penetrance mutations in the Lamin A/C gene, causing Emery Dreifuss muscular dystrophy. *Neuromuscular Disorders: NMD*, *12*(10), 958–963.

Wang, J., Liu, X., Arneja, A. S., & Dhalla, N. S. (1999). Alterations in protein kinase A and protein kinase C levels in heart failure due to genetic cardiomyopathy. *The Canadian Journal of Cardiology*, *15*(6), 683–690.

Wang, Jingwei, Liu, X., Sentex, E., Takeda, N., & Dhalla, N. S. (2003). Increased expression of protein kinase C isoforms in heart failure due to myocardial infarction. *American Journal of Physiology. Heart and Circulatory Physiology*, *284*(6), H2277-2287. https://doi.org/10.1152/ajpheart.00142.2002

Wetsel, W. C., Khan, W. A., Merchenthaler, I., Rivera, H., Halpern, A. E., Phung, H. M., Negro-Vilar, A., & Hannun, Y. A. (1992). Tissue and cellular distribution of the extended family of protein kinase C isoenzymes. *The Journal of Cell Biology*, *117*(1), 121–133. https://doi.org/10.1083/jcb.117.1.121

Wolf, C. M., Wang, L., Alcalai, R., Pizard, A., Burgon, P. G., Ahmad, F., Sherwood, M., Branco, D. M., Wakimoto, H., Fishman, G. I., See, V., Stewart, C. L., Conner, D. A., Berul, C. I., Seidman, C. E., & Seidman, J. G. (2008). Lamin A/C haploinsufficiency causes dilated cardiomyopathy and apoptosis-triggered cardiac conduction system disease. *Journal of Molecular and Cellular Cardiology*, *44*(2), 293–303. https://doi.org/10.1016/j.yjmcc.2007.11.008

Woods, I. G., Kelly, P. D., Chu, F., Ngo-Hazelett, P., Yan, Y. L., Huang, H., Postlethwait, J. H., & Talbot, W. S. (2000). A comparative map of the zebrafish genome. *Genome Research*, *10*(12), 1903–1914. https://doi.org/10.1101/gr.10.12.1903

Wortzel, I., & Seger, R. (2011). The ERK Cascade: Distinct Functions within Various Subcellular Organelles. *Genes & Cancer*, *2*(3), 195–209. https://doi.org/10.1177/1947601911407328

Wu, W., Shan, J., Bonne, G., Worman, H. J., & Muchir, A. (2010). Pharmacological inhibition of c-Jun N-terminal kinase signaling prevents cardiomyopathy caused by mutation in LMNA gene. *Biochimica et Biophysica Acta*, *1802*(7–8), 632–638.

Wydner, K. L., McNeil, J. A., Lin, F., Worman, H. J., & Lawrence, J. B. (1996). Chromosomal assignment of human nuclear envelope protein genes LMNA, LMNB1, and LBR by fluorescence in situ hybridization. *Genomics*, *32*(3), 474–478. https://doi.org/10.1006/geno.1996.0146

Xu, X., Meiler, S. E., Zhong, T. P., Mohideen, M., Crossley, D. A., Burggren, W. W., & Fishman, M. C. (2002). Cardiomyopathy in zebrafish due to mutation in an alternatively spliced exon of titin. *Nature Genetics*, *30*(2), 205–209. https://doi.org/10.1038/ng816

Yang, J., & Zhang, Y. (2015). I-TASSER server: New development for protein structure and function predictions. *Nucleic Acids Research*, *43*(W1), W174-181. https://doi.org/10.1093/nar/gkv342

Yang, S. H., Andres, D. A., Spielmann, H. P., Young, S. G., & Fong, L. G. (2008). Progerin elicits disease phenotypes of progeria in mice whether or not it is farnesylated. *The Journal of Clinical Investigation*, *118*(10), 3291–3300. https://doi.org/10.1172/JCI35876

Yang, S. H., Bergo, M. O., Toth, J. I., Qiao, X., Hu, Y., Sandoval, S., Meta, M., Bendale, P., Gelb, M. H., Young, S. G., & Fong, L. G. (2005). Blocking protein farnesyltransferase improves nuclear blebbing in mouse fibroblasts with a targeted Hutchinson-Gilford progeria syndrome mutation. *Proceedings of the National Academy of Sciences of the United States of America*, *102*(29), 10291–10296. https://doi.org/10.1073/pnas.0504641102

Yang, S. H., Meta, M., Qiao, X., Frost, D., Bauch, J., Coffinier, C., Majumdar, S., Bergo, M. O., Young, S. G., & Fong, L. G. (2006). A farnesyltransferase inhibitor improves disease phenotypes in mice with a Hutchinson-Gilford progeria syndrome mutation. *The Journal of Clinical Investigation*, *116*(8), 2115–2121. https://doi.org/10.1172/JCI28968

Yang, Y., He, Y., Wang, X., Liang, Z., He, G., Zhang, P., Zhu, H., Xu, N., & Liang, S. (2017). Protein SUMOylation modification and its associations with disease. *Open Biology*, *7*(10). https://doi.org/10.1098/rsob.170167

Zhang, Y. (2009). I-TASSER: fully automated protein structure prediction in CASP8. *Proteins*, *77 Suppl 9*, 100–113. https://doi.org/10.1002/prot.22588

Zhang, Y.-Q., & Sarge, K. D. (2008). Sumoylation regulates lamin A function and is lost in lamin A mutants associated with familial cardiomyopathies. *The Journal of Cell Biology*, *182*(1), 35–39. https://doi.org/10.1083/jcb.200712124

Appendix
Reviews 1 and 2

1. Review 1: Lamin A/C mutations in Dilated Cardiomyopathy

A. Citation:

Tesson, F., Saj, M., Uvaize, M. M., Nicolas, H., Płoski, R., & Bilińska, Z. (2014). Lamin A/C mutations in dilated cardiomyopathy. *Cardiology Journal*, *21*(4), 331–342. https://doi.org/10.5603/CJ.a2014.0037

B. Author Contributions:

F Tesson – contributed to the content of the manuscript

M Saj – contributed to the content of the manuscript

M Mohamed Uvaize – contributed to the content of the manuscript

H Nicolas – contributed to the content of the manuscript

R Płoski – edited the manuscript

Z Bilińska – contributed to the content of the manuscript

C. Abstract

Dilated cardiomyopathy (DCM) is one of the leading causes of heart failure and heart transplant. Mutations in 60 genes have been associated with DCM. Approximately 6% of all DCM cases are caused by mutations in the lamin A/C gene (LMNA). LMNA codes for type-V intermediate filaments that support the structure of the nuclear membrane and are involved in chromatin structure and gene expression. Most LMNA mutations result in striated muscle diseases while the rest affects the adipose tissue, peripheral nervous system, multiple tissues or lead to progeroid syndromes/overlapping syndromes. Patients with LMNA mutations exhibit a variety of cellular and physiological phenotypes. This paper explores the current phenotypes observed in LMNA-caused DCM, the results and implications of the cellular and animal models of DCM and the prevailing theories on the pathogenesis of laminopathies.

1. Introduction

Dilated cardiomyopathy (DCM) is a disease of the heart muscle characterized by the dilatation of the left or both ventricles and reduced systolic function in the absence of abnormal loading conditions (hypertension, valve disease) or coronary artery disease sufficient to cause global systolic impairment [1]. DCM is a significant health concern. It is the third most frequent cause of heart failure in the United States after coronary artery disease and hypertension [2]. Furthermore, DCM is also a primary indication for heart transplantation [2] and is marked by considerable morbidity as well as mortality. It is believed that 20% to 50% of IDC cases have familial causation [3-4]. So far, more than 60 genes including the lamin A/C gene (*LMNA*) have been associated with DCM. The pattern of the disease inheritance is mostly autosomal dominant [4]. Despite recent technological progress that makes gene screening both less time-consuming and cost-efficient, genetic screening currently reveals that only 30 to 35% of familial DCM follow the Mendelian model of disease inheritance [5] while the remaining have a more complex multi-variant origin, which also encompasses the non-rare variants. In majority of the cases, incomplete age-related penetrance is observed [6-8] It was reported that seven percent of LMNA mutation carriers exhibit cardiac-related phenotypes if under 20 years of age, 66% when carriers are between 20 and 39, 86% when carriers are between 40 and 59 years, and 100% when carriers are over 60 years of age [6]. Another complicating factor that clouds the genetic diagnosis is the variability of expression within one phenotype. While some mutation carriers may develop all the symptoms of the disease, other family members carrying the mutation exhibit only some aspects of it and may remain with a subclinical form of the disease. The onset of DCM can vary greatly as can the severity and the rate of progression of the disease. The variability may also pertain to the range of phenotypes such as in the case of 960delT *LMNA* mutation, which presented with three differing

phenotypes within one family: pure DCM, DCM with EDMD-like symptoms and DCM with LGMD-like symptoms [9].

Mutations in *LMNA* were first identified in a family with EDMD in 1999 [10]. In the same year, the association between *LMNA* mutations and DCM was reported [11]. Since then, an ever-growing number of mutations in *LMNA* have been identified defining a group of diseases called laminopathies. Laminopathies can be divided according to the observed phenotype. Most *LMNA* mutations have been associated with striated muscle diseases (79.1%), followed by adipose tissue (8.6%) and peripheral nervous tissue disorders (0.3%). 9.3% of *LMNA* mutations lead to progeroid syndromes while 10.9% cause overlapping syndromes with multiple tissue involvement [12].

Table 1 encompasses the most current list of *LMNA* mutations that lead to DCM, either isolated, with sole cardiac features or as a part of diagnosis of other, more complex conditions commonly affecting skeletal muscle such as EDMD or LGMD, but also encompassing other tissues which for instance leads to Charcot-Marie-Tooth disease, familial partial lipodystrophy, general lipodystrophy, hypogonadism, Hutchinson-Gilford progeria syndrome or diabetes mellitus. Table 1 also summarizes the span of phenotypic traits reported to be associated with a given mutation. It was created by combining information from four main *LMNA* mutation databases: the Human Intermediate Filament Database [13], the Leiden Muscular Dystrophy website (www.dmd.nl), the HGMD® Professional 2012.4, the Universal Mutation Database (www.umd.be/LMNA/) and from the literature. We were able to find 165 *LMNA* mutations leading to DCM (Figure 1).

Nucleotide change	Protein change	DCM phenotype range	Domain	Reference *
674bp deletion incl. start codon	deletion of 5' part	1º AVB, LBBB, AF, PVB, VT, HF, SCD	Head	[1]
c.16C>T	p.Gln6X	1º-2º AVB, AF, AFLu, PAB, PVB, VT, HF, SCD	Head	[2]
c.28_29insA	p.Thr10AsnfsX31	1º-2º AVB, AF, PVB, MD	Head	[3]
c.31delC	p.Arg11AlafsX85	(2º) AVB	Head	[4,5]
c.46_49dup	p.Ser18GlnfsX24	AVB	Head	[6]
c.48_51dupCAGC	p.Ser18GlnfsX23	n/a	Head	[6]
c.65C>T	p.Ser22Leu	PVB, HF	Head	[7]
c.73C>T	p.Arg25Cys	CA, AF, PVB, MD, HF	Head	[8]
c.73C>G	p.Arg25Gly	1º/3º AVB, TC, AF, PVB, PAB, LGMD, HF	Head	[9]
c.78C>T	p.Ile26Ile	HF, LBBB, AF	Head	[10]
c.82C>T	p.Arg28Trp	AVB, AF, PM, FPLD, HF	Head	[4,11]
c.94_96delAAG	p.Lys32del	LAFB, CA, AF, EDMD	Head	[12,13]
c.99G>T	p.Glu33Asp	1º AVB, Br, AF, CA, CMT2, MD, leuconychia	Head	[14]
c.106C>T	p.Gln36X	1º-2º AVB, VT	Coil 1A	[15]
c.134A>G	p.Tyr45Cys	AF, AFL, MD	Coil 1A	[16]
c.154C>G	p.Leu52Val	n/a	Coil 1A	[17]
c.155T>C	p.Leu52Pro	AVB, LBBB, RBBB, AF, PVB, HF	Coil 1A	[18]
c.158A>T	p.Glu53Val	AVB, AF, HF	Coil 1A	[19]

c.165delC	p.Asn56ThrfsX40	2º AVB, HF	Coil 1A	[5]
c.169G>C	p.Ala57Pro	atypical WS, hypogonadism, sloping shoulders	Coil 1A	[20]
c.176T>G	p.Leu59Arg	CCD, hypogonadism, ovarian failure, MAD	Coil 1A	[21,22]
c.178C>G	p.Arg60Gly	1º/3º AVB, LBBB, Br, AF, VA, DM, FPLD, PN, HF, SCD	Coil 1A	[23-26]
c.184C>G	p.Arg62Gly	CCD, 1º AVB, AF, PM, FPLD, HF	Coil 1A	[11,26]
c.203_208delAGGTGG	p.Glu68_Val69del	3º AVB, EDMD2	Coil 1A	[4,27]
c.215G>T	p.Arg72Leu	n/a	Linker 1	[17]
c.232A>G	p.Lys78Glu	1º AVB, VT, ICD	Linker 1	[96]
c.244G>A	p.Glu82Lys	1º-3º AVB, LBBB, AF, VF, SVT, HF	Coil 1B	[28,29]
c.254T>G	p.Leu85Arg	CCD, PM, AF, HF, SCD	Coil 1B	[23]
c.266G>T	p.Arg89Leu	1º-3º AVB, AF, VT, MA, HF / AVB, AF, VT, EDMD, HF	Coil 1B	[4,5,30-32]
c.274C>T	p.Leu92Phe	LBBB, AF, PVB, HF	Coil 1B	[33,34]
c.289A>G	p.Lys97Glu	1º/3º AVB, LBBB, PVB, HF	Coil 1B	[4,5,35]
c.302G>C	p.Arg101Pro	AF, HF / AVB, AF, PVB, VT, LGMD	Coil 1B	[31]/ [94]
c.331G>T	p.Glu111X	3º AVB, PVB, HF	Coil 1B	[4,5,35]
c.348_349insG	p.Lys117GlufsX10	AVB, AF, SCD	Coil 1B	[36]
c.356+1G>T	n/a	n/a	Coil 1B	[37]
c.357-1G>T	n/a	LBBB, AF, PVB, VT, VF, HF	Coil 1B	[4,31,34]
c.357C>T	p.Arg119Arg	CCD, PM, LGMD, HF	Coil 1B	[16]
c.367_369del	p.Lys123del	1º-3º AVB, LBBB, PVB, VT, VF, MP, SCD	Coil 1B	[38]
c.380_381ins24bp	p.Ile128_Ala129insArg ValThrLeuIleSerSerArg	CCD	Coil 1B	[34]

c.384ins24	p.Ile128delinsIleSer	n/a	Coil 1B	[33]
c.394G>C	p.Ala132Pro	1º AVB, Br, AF, HF	Coil 1B	[39]
c.398G>T	p.Arg133Leu	CCD, LD	Head	[40]
c.405_425dup	p.Asn142delinsLysLys	1º AVB, AF, VT, PVB	Coil 1B	[41]
c.425_426insGGCACTGGAGGCTCTGCTGAA	p.Leu141_Asn142insLysAspLeuAspAlaLeuLeu	1º AVB, AF, PVB, VT, HF	Coil 1B	[41]
c.427T>C	p.Ser143Pro	1º-3º AVB, LBBB, LAFB, SSS, Br, AF, PVB, VF, VT, HF	Coil 1B	[39,42]
c.481G>A	p.Glu161Lys	AVB, LBBB, Br, AF, PVB, LAFB, VT, HF	Coil 1B	[4,3,19,34,43]
c.497G>C	p.Arg166Pro	AVB, LBBB, AF, VT, HF	Coil 1B	[31,44]
c.514-1G>A	n/a	VT, VF	Coil 1B	[4]
c.548T>C	p.Leu183Pro	AVB	Coil 1B	[4]
c.556G>A	p.Glu186Lys	CCD, HF	Coil 1B	[19]
c.565C>T	p.Arg189Trp	PVB	Coil 1B	[45]
c.568C>T	p.Arg190Trp	1º AVB, RBBB, Br, LAFB, AF, AFL, PVB, HF	Coil 1B	[4,5,7,19,35,39,46,47]
c.569G>A	p.Arg190Gln	1º-3º AVB, Br, AF, AFL, VT, HF	Coil 1B	[31,43]
c.575A>G	p.Asp192Gly	1º AVB, LAFB, HF	Coil 1B	[46,48,49]
c.575A>T	p.Asp192Val	LBBB, FLPD, HF	Coil 1B	[26]
c.585C>G	p.Asn195Lys	1º-3º AVB, Br, AF, HF, SCD	Coil 1B	[8,23]
c.585C>A	p.Asn195Lys	1º, 3º AVB, AF, HF, SCD	Coil 1B	[8]
c.607G>A	p.Glu203Lys	1º AVB, LBBB, RBBB, HF	Coil 1B	[50]
c.608A>G	p.Glu203Gly	1º-2º AVB, AF, HF, SCD	Coil 1B	[23]

c.608A>T	p.Glu203Val	2º AVB, Br, SWMA, HF	Coil 1B	[23,43]
c.622_624delAAG	p.Lys208del	1º AVB, PVB, VT, LGMD	Coil 1B	[8]
c.629T>G	p.Ile210Ser	AF, HF	Coil 1B	[31,51]
c.640-10A>G	n/a	1º-3º AVB, LBBB, RBBB, AF, VT, HF	Coil 1B	[52]
c.644T>C	p.Leu215Pro	1º-2º AVB, SSS, Br, LBBB, AF, AFL, SVT, VT, PVB, SCD, HF	Coil 1B	[53]
c.656A>C	p.Lys219Thr	(3º) AVB	Linker 2	[4,43]
c.657G>C	p.Lys219Asn	1º AVB, VT, PM	Linker 2	[54]
c.673C>T	p.Arg225X	(1º) AVB, Br, AF, LVE, PVB, SCD	Linker 2	[8,44,50]
c.676C>G	p.Leu226Val	n/a	Linker 2	[37]
c.694G>C	p.Gly232Arg	AVB, RBBB, PVB, EDMD	Linker 2	[18]
c.700C>T	p.Gln234X	2º AVB, Br, HF	Linker 2	[31]
c.736C>T	p.Gln246X	AVB	Coil 2	[4]
c.746G>A	p.Arg249Gln	AVB, PVB, EDMD or LGMD1B	Coil 2	[18]
c.767T>G	p.Val256lGy	AVB	Coil 2	[55]
c.775T>C	p.Tyr259His	AVB, AF, VT	Coil 2	[44]
c.780G>C	p.Lys260Asn	AVB, SSS, ASS, HF	Coil 2	[4,56]
c.781_783del3ins18	p.Lys261delins6	AVB, LBBB, AF, PVC, EDMD2	Coil 2	[18]
c.799T>C	p.Tyr267His	CCD, SCD	Coil 2	[57]
c.800A>G	p.Tyr267Cys	AVB, TC, EDMD2	Coil 2	[4,58]
c.810G>A	p.Lys270Lys	CCD, AF, PM, EDMD, LGMD	Coil 2	[16]
c.811-3C>T	n/a	n/a	Coil 2	[37]

c.812T>C	p.Leu271Pro	AF, Br, SVT, VT, EDMD, HF	Coil 2	[16,59]
c.815_818delACAAinsCCAGAC	p.Asp272AlafsX208	AVB, AF, VT	Coil 2	[44]
c.832G>A	p. Ala278hTr	AVB, AF, VF, SVT, PM, PVB	Coil 2	[60]
c.855delG	p.Ala287LeufsX191	AF, ASS, LGMD	Coil 2	[58]
c.859insC	p.Ala287fs	AF	Coil 2	[34]
c.883T>C	p.Ser295Pro	CCD, MD	Coil 2	[16]
c.906_907delCT	p.Ser303CysfsX27	AVB, PM, HF, Br, PAB, PVB, CCD, SVA, AF, SCD	Coil 2	[95]
c.908_909delCT	p.Ser303CysfsX26	1º AVB, Br, SSS, AF / 1º-3º AVB, AF, PVB, VT, LGMD, HF	Coil 2	[61,62]
c.936G>C	p.Gln312His	AVB, AF, CCD, HF	Coil 2	[63]
c.976T>A	p.Ser326Thr	VT, AVB, CCD, XL-EDMD, MP, PM	Coil 2	[97]
c.IVS5+1G>T (c.936+1G>T)	n/a	1º-2º AVB, VT, PM	Coil 2	[4, 56, 64]
c.937-11C>G	p.Leu313GlyfsX31	1º-3º AVB, LGMD1B, VT, AF	Coil 2	[65]
c.949G>A	p.Glu317Lys	1º/3º AVB, AFL, LBBB, HF	Coil 2	[4,5,35,34]
c.952G>A	p.Ala318Thr	TC, PVB, HF	Coil 2	[31]
c.958delC	p.Leu320fs	n/a	Coil 2	[17]
c.959delT	p.Leu320fsX160	2º-3º AVB, LBBB, AF, VT, SVT, PVB, LGMD, EDMD, HF, SCD	Coil 2	[66,67]
c.961C>T	p.Arg321X	1º AVB, RBBB, AF, VT, HF	Coil 2	[68,69]
c.[992G>A; =]+[=; 1039G>A]	p.[Arg331Glu; =]+[=; Glu347Lys]	AF, PM	Coil 2	[58]
c.992G>C	p.Arg331Pro	AVB, PM, LGMD	Coil 2	[58]
c.992G>A	p.Arg331Gln	1º AVB, AFL, VT, HF	Coil 2	[69]
c.1003C>T	p.Arg335Trp	3º AVB, RBBB, SSS, AF, VT	Coil 2	[17,70]

c.1004G>A	p.Arg335Gln	n/a	Coil 2	[37]
c.1039G>A	p.Glu347Lys	AF, PM, SCD	Coil 2	[13,71]
c.1044G>T	p.Met348Ile	EDMD, PM, CCD	Coil 2	[72]
c.1045C>T	p.Arg349Trp	CCD, SVA, MD, HF, SCD	Coil 2	[8]
c.1046G>T	p.Arg349Leu	AF, HF	Coil 2	[73]
c.1048G>C	p.Ala350Pro	AVB, LBBB, AF, PVB	Coil 2	[18]
c.1057C>A	p.Gln353Lys	CA, MP, HF	Coil 2	[48]
c.1063C>T	p.Gln355X	2º AVB, AF, VT, HF	Coil 2	[7,69]
c.1069G>C	p.Asp357His	AVB, VT	Coil 2	[74]
c.1070A>C	p.Asp357Ala	2º AVB, Br, AF, VES, VT, VF, HF, SCD	Coil 2	[70]
c.1072G>T	p.Glu358X	1º-2º AVB, VT	Coil 2	[75]
c.1085_1085delT	p.Leu363TrpfsX117	1º-2º AVB, AF, VT, HF	Coil 2	[39]
c.1102_1130dupGCCCTGGACATGGAGATCCACGCCTACCG	p.Lys378ProfsX112	LBBB, VT, LGMD, HF	Coil 2	[76]
c.1111_1125del15	p.Met371_Ala375del	n/a	Coil 2	[17]
c.1114delG	p.Glu372ArgfsX107	1º AVB, Br, AF, HF	Coil 2	[31]
c.1129C>T	p.Arg377Cys	LGMD, HF	Coil 2	[77]
c.1130G>A	p.Arg377His	1º-3º AVB, LBBB, RBBB, AF, PVB, VT, VF, LGMD, EDMD, HF, SCD	Coil 2	[3,8,18,30, 41,78]
c.1130G>T	p.Arg377Leu	(2º) AVB, Br, SSS, AF, AFL, ASS, ATC, VT, LGMD1B, EDMD, HF, SCD	Coil 2	[4,8,79,80]
c.1157G>C	p.Arg386Thr	FPLD, CCD	Tail	[81]

c.1157+1G>A	n/a	VT, VF	Tail	[4]
c.1157+1G>T	p.Arg386SerfsX21	VES, VF, HF	Tail	[70]
c.1163G>A	p.Arg388His	Br, PVB, HF, SCD	Tail	[31]
c.1189C>T	p.Arg397Cys	n/a	Tail	[37]
c.1195C>T	p.Arg399Cys	HF	Tail	[31]
c.1197_1240del44	p.Gly400Argfs*11	AVB, SSS	Tail	[55]
c.1292C>G	p.Ser431*_	AVB	Tail	[55]
c.1294C>T	p.Gln432X	3º AVB, LBBB, RBBB, AF, VT, HF	Tail	[69]
c.1303C>T	p.Arg435Cys	HF	Tail	[13]
c.1307_1308insGCAC	p.Ser437HisfsX1	2º AVB, Br, TC, AF, PVB, HF, SCD	Tail	[31]
c.1318G>A	p.Val440Met	LAFB, VES	Tail	[69]
c.1370delA	p.Lys457SerfsX21	AF, LGMD	Tail	[58]
c.1380+1G>A	n/a	(1º) AVB, AF, VF, HF	Tail	[8,34]
c.1397_1397delA	p.Asn466IlefsX14	1º AVB, LBBB, Br, AF, VF, VT, HF, SCD	Tail	[41,82]
c.1412G>A	p.Arg471His	AF, VT, HF	Tail	[31]
c.1424_1425insAGA	p.Gly474_Asp475insGlu	HF, ICD	Tail	[31]
c.1443C>G	p.Tyr481X	2º AVB, RBBB, SVT, VT, HF	Tail	[46,48,49]
c.1489-1G>T	p. Ile497-Glu536del	2º AVB, Br, AF, AFL, VT, EDMD	Tail	[70]
c.1492T>A	p.Trp498Arg	AVB, EDMD2	Tail	[4]
c.1493_1493delG	p.Ala499LeufsX47	AF, VT, HF	Tail	[39]
c.1496delC	p.Ala499Val	1º-2º AVB, RBBB, Br, ATC, ASS, AN	Tail	[83]

c.1512_1513insAG	p.Thr505ArgfsX44	1º AVB, AF, PVB, HF, SCD	Tail	[8]
c.1526_1527insC	p.Thr510TyrfsX42	1º AVB / AVB, EDMD2	Tail	[4] /[84]
c.1549C>T	p.Gln517X	3º AVB , AF, EDMD, VF, SCD	Tail	[70]
c.1560G>A	p.Trp520X	2º AVB, LBBB, Br	Tail	[70]
c.1567G>A	p.Gly523Arg	LBBB	Tail	[33,34]
c.1579_1580insCTGC	p.Arg527ProfsX26	1º-2º AVB, LBBB, LAFB, HF	Tail	[4,5,35]
c.1583C>T	p.Thr528Met	1º-3º AVB, Br, AF, SVA	Tail	[10]
c.1608+1G>T	n/a	n/a	Tail	[37]
c.IVS9-3C>G (c.1609-3C>G)	loss of exon 10	3º AVB, Br, PM, LGMD1B	Tail	[85]
c.1621C>T	p.Arg541Cys	LBBB, VT, VF, PVB, fibrosis, SWMA, SCD	Tail	[86-88]
c.1621C>A	p.Arg541Ser	VT, HF / LGMD1B, HF	Tail	[16]/ [46,39,48]
c.1621C>G	p.Arg541Gly	IVB, LBBB, Br, SVA, PVB, VA, TC	Tail	[89]
c.1622G>A	p.Arg541His	AVB, AF, PVB	Tail	[18]
c.1622G>C	p.Arg541Pro	PVB, VT, HF	Tail	[8]
c.1711C>A	p.Arg571Ser	1º-3º AVB, Br, AF	Tail	[23]
c.1713C>A	p.Ser571Arg	2º, 3º AVB, PM, HF, AF	Tail	[23]
c.1714insCTGC	p.Ser572LeufsX8	1º, 2º AVB, PM, LBBB	Tail	[35]
c.1718C>T	p.Ser573Leu	AVB, VT	Tail	[4,30]
c.1904G>A	p.Gly645Asp	HF	Tail	[90]
c.1930C>T	p.Arg644Cys	AVB, AF, VT, HF / LGMD1B, HF, SCD	Tail	[4,43,69]/ [91]
c.1960C>T	p.Arg654X	AVB, LBBB, SSS, AF, VT, HF, SCD	Tail	[31]

c.1964_1965insG	p.Thr655fsX49	PM, VT, MH, POS, HF, SCD	Tail	[92]
c.[1699 to 183_1699–160inv24; 568_1699–184del; 1699 to 159_1995+6997del]	double deletion with break points in exon 3, intron 10, downstream of gene	1º-3º AVB, AF, AFL, Br, VA, SCD	Coil/Tail	[93]
deletion exons 3-12	deletion > 4,704 bp	VT, HF	Coil/Tail	[48]

Table 1. *LMNA* mutations associated with dilated cardiomyopathy from four databases - Human Intermediate Filament Database [13] (database updated 2014-01-15), Leiden Muscular Dystrophy website (www.dmd.nl; database updated 2014-01-05), HGMD® Professional 2014.4 (database updated 2014-02-02) and the Universal Mutation Database (www.umd.be/LMNA/). 1º, 2º, 3º - atrio-ventricular block degree, in parenthesis when degree specified only in some studies, AF - atrial fibrillation, AFL - atrial flutter, AN - axonal neuropathy, ASS - atrial standstill, ATC - atrial tachycardia, AVB - atrio-ventricular block, Br - bradycardia, CA - cardiac abnormalities, CCD - cardiac conduction disease, CMT2 - Charcot-Marie-Tooth disease, DM - diabetes mellitus, EDMD(2) - Emery-Dreifuss muscular dystrophy (type 2), FPLD - familial partial lipodystrophy, HF - heart failure, IVB - intra-ventricular block, ICD – implantable cardiac defibrillator, LAFB - left anterior fascicular block, LBBB - left bundle branch block, LGMD(1B) - limb girdle muscular dystrophy (type 1B), LVE - left ventricular exosystoly, MA - muscular atrophy, MAD - mandibuloacral dysplasia, MD - muscular dystrophy, MH - muscular hypertrophy, MP - myopathy, PAB - premature atrial beats, PM - pacemaker implantation, PN - peripheral neuropathy, POS - polycystic ovary syndrome, PVB - premature ventricular beats, RBBB - right bundle branch block, SCD - sudden cardiac death, SSS - sick sinus syndrome, SVA - supraventricular arrhythmia, SVT - supraventricular tachycardia, SWMA - segmental wall motion abnormalities, TC - tachycardia, VA- ventricular arrhythmia, VES - ventricular extra systoles, VF - ventricular fibrillation, VT - ventricular tachycardia, LD - lipodystrophy, WS - Werner syndrome, "/" used to separate differing phenotypes. *: References are listed in "Supplementary file."

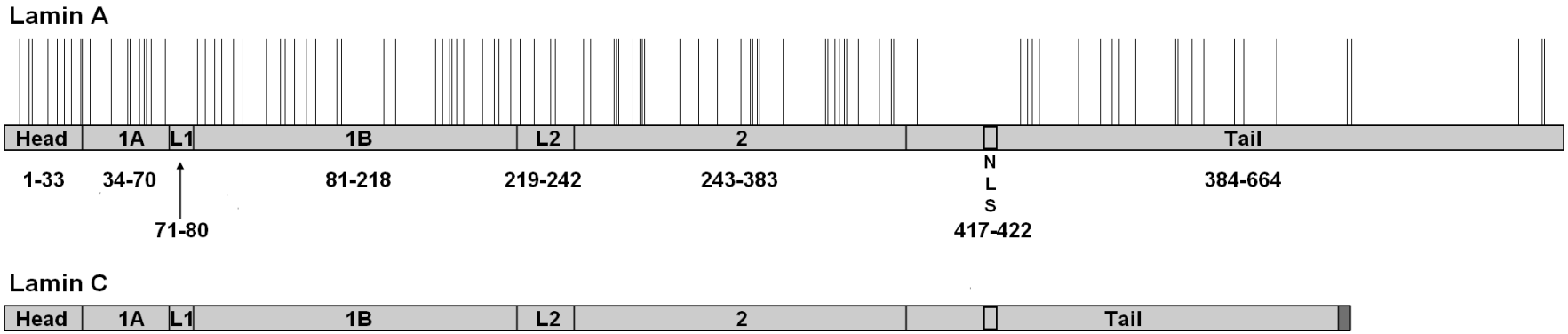

Figure1. Protein map of lamin A and lamin C with currently known mutations of both transcripts plotted onto lamin A protein. NLS - nuclear localization signal. Dark shaded area at the C-terminal of lamin C represents lamin C-unique sequence.

LMNA gene encodes the A-type lamins which are involved in maintaining the structural integrity of the nucleus, chromatin organization and gene expression [14]. *LMNA* is composed of 12 exons and encodes lamin A and lamin C by alternative splicing in exon 10 [15]. Both lamin isoforms are identical for the first 566 amino acids after which lamin C contains a unique sequence of five basic amino acids while amino acids from 567 to 664 are unique to lamin A [15]. In addition, prelamin A contains a CaaX motif at the COOH-terminal, which undergoes posttranslational modifications [15]. Lamins are divided into three domains: a short globular head, an α-helical rod and a globular tail. The rod domain comprises several coiled-coil domains separated by linker regions which are evolutionarily highly conserved (Figure 1) [16].

Most lamin mutations leading to DCM are found in the head and rod domains covering more than half of lamin A and two-thirds of lamin C. DCM mutations are rarely found in the tail domain which contains many phosphorylation sites as opposed to mutations linked to EDMD, familial partial lipodystrophy and Hutchinson-Gilford progeria syndrome ([13]; Human Genome Mutation Database). However, hot spot(s) for DCM or other diseases affecting the striated muscle cannot be identified. Conversely, in adipose tissue defects, approximately 80% of cases carry a substitution of the p.Arg482 residue while 85% of mandibuloacral dysplasia cases are caused by a homozygous mutation at the p.527 residue and 77% of HGPS patients carry the c.1827C>T substitution within exon 11[16].

2. Studies of Cellular Phenotypes Associated with LMNA mutations

DCM patients with *LMNA* mutations display highly variable cardiomyocyte phenotype. A DCM patient encompassing exons 3-12 deletion showed diminished lamin A and C staining in the endomyocardial biopsy with discontinuous nuclear envelopes and invasion of mitochondria into the nuclear space [17]. Another DCM patient carrying a *LMNA* mutation displayed dramatic

morphological alterations in approximately 30% of the cardiomyocyte's nuclei including a complete loss of the nuclear envelope [18]. However, other mutation carriers did not present with such dramatic abnormalities [17,18]. Nevertheless, cardiomyocytes from DCM patients with *LMNA* mutations usually display reduced lamin A and C in the nuclei with nuclear membrane damage such as focal disruptions, blebs and nuclear pore clustering [19,20].

Skin fibroblasts isolated from patients with cardiac-or-skeletal-specific laminopathies most often had abnormal nuclear shape including blebs and herniation [21]. Lamin A and C distribution were affected in these cells and were either present in a honeycomb pattern [21] or distributed unevenly along the inner nuclear lamina [22]. Some fibroblasts had lamin A and C aggregates close to the lamina which did not interact with emerin, DNA or RNA [23]. Patient tissue heart samples and skin fibroblasts provide a method to visualize the pathophysiology of disease-associated mutations; however, they are not easy to acquire. Currently, no specific therapy exists for patients with *LMNA*-related DCM. This has encouraged researchers to establish both mice and cellular models in an effort to elucidate the mechanisms leading to the disease phenotypes. Unraveling the molecular mechanisms might provide insights into the pathophysiology of this disease which could be translated into novel therapy in the future.

A *Lmna* null mouse based on genetrap technology has been developed ([24]. The mouse is characterized by postnatal maturation defects of cardiac, muscle, and adipose tissues. Premature death occurred by 2-3 weeks of age. However, in this study, age matched heterozygous mice were indistinguishable from wild-type mice [24]. Only one study reported $Lmna^{+/-}$ mice with 50% of normal cardiac lamin A/C levels and displaying cardiac abnormalities [25]. The $Lmna^{H222P/H222P}$ mice harbouring the EDMD mutation developed muscular dystrophy and DCM with atrio-ventricular conduction defect at adulthood and died by 13 months of age [26]. Male

Lmna$^{H222P/H222P}$ mice developed significant left ventricular dilatation and by 16 weeks of age had decreased ejection fraction [26]. In another study, *Lmna*$^{N195K/N195K}$ mice harboring a DCM with conduction system disease mutation, died at an early age due to arrhythmia. Surprisingly, both *Lmna*$^{H222P/+}$ and *Lmna*$^{N195K/+}$ mice were found to have a phenotype and life expectancy similar to the wild-type [26,27]. Cells derived from both *Lmna*$^{-/-}$ and *Lmna*$^{N195K/N195K}$ mice were observed to have damaged and misshapen nuclei, showed increased fragility under mechanical strain and impaired gene transcription [27-30].

Lamin A/C is found in almost all cells except in certain differentiated cells of hematopoietic origins [31]. Cellular models have shown that lamin A and C proteins are found distributed together in a homogeneous meshwork. However, wild type lamin A transfected alone has consistently shown to localize to the inner nuclear lamina with some nucleoplasmic localization. Conversely, lamin C has been shown to localize as intranuclear aggregate [18,32-36]. Intranuclear lamin C has shown to be more mobile than intranuclear lamin A [36,37]. Likewise, the lamin C only mouse model expressed lamin C at the inner nuclear lamina as established in wild type cells [35]; thus indicating the existence of compensatory mechanisms. Pugh et al. [32] studied the incorporation of the lamin A and C in Swiss 3T3 cells and found that the incorporation of lamin C into the lamina was made possible by lamin A.

In an attempt to identify deregulation in striated muscle specific laminopathies including DCM and EDMD, researches have been focused on skeletal muscle differentiations. Lamin A and C play a pivotal role in myoblast differentiation. *In vitro,* cells expressing disease-associated *LMNA* mutations displayed an inhibition of myoblast differentiation [38] (F. Tesson personal communication) and myoblasts lacking lamin A and C expression showed decreased differentiation potential with downregulation of MyoD and pRb and upregulation of Myf5 [39].

These studies suggest that disruption of lamin A and C may weaken contractile tissues such as skeletal and cardiac muscle.

Lamin A and C also play a role in the regulation of signaling cascades such as the Sumo pathway. Sumo pathway regulates a wide range of cellular processes through the attachment of small ubiquitin-related modifier (sumo) to various substrates. Sumo1 was found to be mislocalized in the presence of lamin A and C mutants both *in vitro* (C2C12 and Cos7 cells) and *in vivo* (primary myoblasts and myopathic muscle tissue from the $Lmna^{H222P/H222P}$ mice) [18,40]. In cell models, trapping of sumo1 correlated with an increased steady-state level of sumoylation. Ubc9, the E2 conjugating enzyme of the Sumo pathway was also mislocalized to the mutant aggregates [40]. Lamin A has been shown to be covalently modified by Sumo 2 and 3 [41]. The disruption of a critical post-translational modifying process has the potential to affect the post-translational regulation of tissue-specific sumoylated proteins which may lead to the tissue-specific symptoms observed in patients with various laminopathies [40].

Recent studies using induced pluripotent stem cells derived cardiomyocytes (iPSCS-CMs) from DCM patients with *LMNA* mutations showed accelerated nuclear senescence and apoptosis under electrical stimulation. This study also showed that activation of stress response MEK1/ERK1/2 pathway contributes to increased apoptosis in $LMNA^{R225X/WT}$dermal fibroblasts after electrical stimulation [42]. Moreover, this apoptotic effect could be attenuated by pharmacological blockade of the MEK1/ERK1/2 pathway. Study of gene expression profile showed that mouse models of laminopathies also displayed ERK pathway activation in heart muscle [43,44]. Importantly, the pharmacological blockade of the ERK1/2 pathway prevented the development of DCM in this model [45]. These studies have shed new light on MEK1 pathway as a potential therapeutic target in *LMNA*-associated DCM.

3. Conclusion: The mechanistic hypotheses

Until now, three main hypotheses have been proposed to explain the mechanism of pathogenesis of laminopathies: the structural, the gene expression and the toxicity hypotheses. The structural hypothesis states that mutations within lamin A/C lead to disorganization of the proteinaceous meshwork, instability of the nuclear envelope and disorganization of chromatin, which in turn leads to the overall inability of the cell to properly function in contracting tissue environment such as striated muscles [46,47]. Building on this hypothesis, recent studies identified repetitive disruptions of the nuclear envelope in the presence of lamin A/C mutations [17,48]. These disruptions impaired protein distribution into cell compartments. Translocations of large amounts of protein into the cytoplasm could trigger aggresome formation or even induce cell apoptosis [48]. On the other hand, translocation of transcription factors into the cytoplasm might impair gene expression. The gene expression hypothesis is based on the regulatory role of lamin A/C in chromatin organization and DNA transcription. Mutated lamins might disrupt the protein meshwork through their interaction with other proteins of the nuclear envelope which may lead to epigenetic changes in the chromatin, which may then in turn disrupt various complex signaling pathways [49]. Lastly, the cell toxicity hypothesis proposes that mutated prelamin A may accumulate within patients' nuclei to the point that they might become toxic to the cell and lead to development of the disease [50]. These hypotheses are likely to be not mutually exclusive and combining them might allow describing the mechanisms underlying the initiation and/or the development of laminopathies. Ultimately, a better understanding of the pathogenesis of the disease may suggest novel strategies targeting the underlying molecular defects.

4. Acknowledgements: None

5. Statement of competing interests: None declared

6. References

1. Elliott P, Andersson B, Arbustini E, Bilinska Z, Cecchi F, Charron P, Dubourg O, Kuhl U, Maisch B, McKenna WJ, Monserrat L, Pankuwelt S, Rapezzi C, Seferovic P, Tavazzi L, Keren A: **[Classification of the cardiomyopathies].** *Kardiol Pol* 2008, **66:**533-40, discussion.

2. Maron BJ, Towbin JA, Thiene G, Antzelevitch C, Corrado D, Arnett D, Moss AJ, Seidman CE, Young JB: **Contemporary definitions and classification of the cardiomyopathies: an American Heart Association Scientific Statement from the Council on Clinical Cardiology, Heart Failure and Transplantation Committee; Quality of Care and Outcomes Research and Functional Genomics and Translational Biology Interdisciplinary Working Groups; and Council on Epidemiology and Prevention.** *Circulation* 2006, **113:**1807-1816.

3. Ghosh N, Haddad H: **Recent progress in the genetics of cardiomyopathy and its role in the clinical evaluation of patients with cardiomyopathy.** *Curr Opin Cardiol* 2011, **26:**155-164.

4. Taylor MR, Carniel E, Mestroni L: **Cardiomyopathy, familial dilated.** *Orphanet J Rare Dis* 2006, **1:**27.

5. Hershberger RE, Siegfried JD: **Update 2011: clinical and genetic issues in familial dilated cardiomyopathy.** *J Am Coll Cardiol* 2011, **57:**1641-1649.

6. Pasotti M, Klersy C, Pilotto A, Marziliano N, Rapezzi C, Serio A, Mannarino S, Gambarin F, Favalli V, Grasso M, Agozzino M, Campana C, Gavazzi A, Febo O, Marini M, Landolina M, Mortara A, Piccolo G, Vigano M, Tavazzi L, Arbustini E: **Long-term outcome and risk stratification in dilated cardiolaminopathies.** *J Am Coll Cardiol* 2008, **52:**1250-1260.

7. Mangin L, Charron Ph, Tesson F, Mallet A, Dubourg O, Desnos M, Benaiche A, Gayet C, Gibelin P, Logeais Y, Davy J-M, Sidi D, Schwartz K, Komajda M. **Familial dilated cardiomyopathy: clinical features in French families**. *J Heart Failure* 1999, **1**:353-361.

8. Mestroni L, Rocco C, Gregori D, Sinagra G, Di Lenarda A, Miocic S, Vatta M, Pinamonti B, Muntoni F, Caforio AL, McKenna WJ, Falaschi A, Giacca M, Camerini, Heart Muscle Disease Study Group. **Familial dilated cardiomyopathy: evidence for genetic and phenotypic heterogeneity**. *J Am Coll Cardiol* 1999, **34**: 181-190.

9. Brodsky GL, Muntoni F, Miocic S, Sinagra G, Sewry C, Mestroni L: **Lamin A/C gene mutation associated with dilated cardiomyopathy with variable skeletal muscle involvement.** *Circulation* 2000, **101:**473-476.

10. Bonne G, Di Barletta MR, Varnous S, Becane HM, Hammouda EH, Merlini L, Muntoni F, Greenberg CR, Gary F, Urtizberea JA, Duboc D, Fardeau M, Toniolo D, Schwartz K:

Mutations in the gene encoding lamin A/C cause autosomal dominant Emery-Dreifuss muscular dystrophy. *Nat Genet* 1999, **21:**285-288.

11. Fatkin D, MacRae C, Sasaki T, Wolff MR, Porcu M, Frenneaux M, Atherton J, Vidaillet HJ, Jr., Spudich S, De Girolami U, Seidman JG, Seidman C, Muntoni F, Muehle G, Johnson W, McDonough B: **Missense mutations in the rod domain of the lamin A/C gene as causes of dilated cardiomyopathy and conduction-system disease.** *N Engl J Med* 1999, **341:**1715-1724.

12. Bertrand AT, Chikhaoui K, Yaou RB, Bonne G: **Clinical and genetic heterogeneity in laminopathies.** *Biochem Soc Trans* 2011, **39:**1687-1692.

13. Szeverenyi I, Cassidy AJ, Chung CW, Lee BT, Common JE, Ogg SC, Chen H, Sim SY, Goh WL, Ng KW, Simpson JA, Chee LL, Eng GH, Li B, Lunny DP, Chuon D, Venkatesh A, Khoo KH, McLean WH, Lim YP, Lane EB: **The Human Intermediate Filament Database: comprehensive information on a gene family involved in many human diseases.** *Hum Mutat* 2008, **29:**351-360.

14. Broers JL, Ramaekers FC, Bonne G, Yaou RB, Hutchison CJ: **Nuclear lamins: laminopathies and their role in premature ageing.** *Physiol Rev* 2006, **86**:967–1008.

15. Lin F, Worman HJ. **Structural Organization of the Human Gene Encoding Nuclear Lamin A and Nuclear Lamin C.** *J Biol Chem* 1993, **268:**16321-16326.

16. Bertrand AT, Chikhaoui K, Yaou RB, Bonne G: **Clinical and genetic heterogeneity in laminopathies.** *Biochem Soc Trans* 2011, **39:**1687-1692.

17. Gupta P, Bilinska ZT, Sylvius N, Boudreau E, Veinot JP, Labib S, Bolongo PM, Hamza A, Jackson T, Ploski R, Walski M, Grzybowski J, Walczak E, Religa G, Fidzianska A, Tesson F: **Genetic and ultrastructural studies in dilated cardiomyopathy patients: a large deletion in the lamin A/C gene is associated with cardiomyocyte nuclear envelope disruption.** *Basic Res Cardiol* 2010, **105:**365-377.

18. Sylvius N, Bilinska ZT, Veinot JP, Fidzianska A, Bolongo PM, Poon S, McKeown P, Davies RA, Chan KL, Tang AS, Dyack S, Grzybowski J, Ruzyllo W, McBride H, Tesson F: **In vivo and in vitro examination of the functional significances of novel lamin gene mutations in heart failure patients.** *J Med Genet* 2005, **42:**639-647.

19. Arbustini E, Pilotto A, Repetto A, Grasso M, Negri A, Diegoli M, Campana C, Scelsi L, Baldini E, Gavazzi A, Tavazzi L: **Autosomal dominant dilated cardiomyopathy with atrioventricular block: a lamin A/C defect-related disease.** *J Am Coll Cardiol* 2002, **39:**981-990.

20. Fidzianska A, Bilinska ZT, Tesson F, Wagner T, Walski M, Grzybowski J, Ruzyllo W, Hausmanowa-Petrusewicz I: **Obliteration of cardiomyocyte nuclear architecture in a patient with LMNA gene mutation.** *J Neurol Sci* 2008, **271:**91-96.

21. Muchir A, Worman HJ: **The nuclear envelope and human disease.** *Physiology (Bethesda)* 2004, **19:**309-314.

22. Favreau C, Dubosclard E, Ostlund C, Vigouroux C, Capeau J, Wehnert M, Higuet D, Worman HJ, Courvalin JC, Buendia B: **Expression of lamin A mutated in the carboxyl-terminal tail generates an aberrant nuclear phenotype similar to that observed in cells from patients with Dunnigan-type partial lipodystrophy and Emery-Dreifuss muscular dystrophy.** *Exp Cell Res* 2003, **282:**14-23.

23. Muchir A, Medioni J, Laluc M, Massart C, Arimura T, van der Kooi AJ, Desguerre I, Mayer M, Ferrer X, Briault S, Hirano M, Worman HJ, Mallet A, Wehnert M, Schwartz K, Bonne G: **Nuclear envelope alterations in fibroblasts from patients with muscular dystrophy, cardiomyopathy, and partial lipodystrophy carrying lamin A/C gene mutations.** *Muscle Nerve* 2004, **30:**444-450.

24. Kubben N, Voncken JW, Konings G, van Weeghel M, van den Hoogenhof MM, Gijbels M, van Erk A, Schoonderwoerd K, van den Bosch B, Dahlmans V, Calis C, Houten SM, Misteli T, Pinto YM. **Post-natal myogenic and adipogenic developmental: defects and metabolic impairment upon loss of A-type lamins.** *Nucleus* 2011, **2**:195-207.

25. Wolf CM, Wang L, Alcalai R, Pizard A, Burgon PG, Ahmad F, Sherwood M, Branco DM, Wakimoto H, Fishman GI, See V, Stewart CL, Conner DA, Berul CI, Seidman CE, Seidman JG: **Lamin A/C haploinsufficiency causes dilated cardiomyopathy and apoptosis-triggered cardiac conduction system disease.** *J Mol Cell Cardiol* 2008, **44:**293-303.

26. Arimura T, Helbling-Leclerc A, Massart C, Varnous S, Niel F, Lacene E, Fromes Y, Toussaint M, Mura AM, Keller DI, Amthor H, Isnard R, Malissen M, Schwartz K, Bonne G: **Mouse model carrying H222P-Lmna mutation develops muscular dystrophy and dilated cardiomyopathy similar to human striated muscle laminopathies.** *Hum Mol Genet* 2005, **14:**155-169.

27. Mounkes LC, Kozlov SV, Rottman JN, Stewart CL: **Expression of an LMNA-N195K variant of A-type lamins results in cardiac conduction defects and death in mice.** *Hum Mol Genet* 2005, **14:**2167-2180.

28. Sullivan T, Escalante-Alcalde D, Bhatt H, Anver M, Bhat N, Nagashima K, Stewart CL, Burke B: **Loss of A-type lamin expression compromises nuclear envelope integrity leading to muscular dystrophy.** *J Cell Biol* 1999, **147:**913-920.

29. Lammerding J, Schulze PC, Takahashi T, Kozlov S, Sullivan T, Kamm RD, Stewart CL, Lee RT: **Lamin A/C deficiency causes defective nuclear mechanics and mechanotransduction.** *J Clin Invest* 2004, **113:**370-378.

30. Nikolova V, Leimena C, McMahon AC, Tan JC, Chandar S, Jogia D, Kesteven SH, Michalicek J, Otway R, Verheyen F, Rainer S, Stewart CL, Martin D, Feneley MP, Fatkin D: **Defects in nuclear structure and function promote dilated cardiomyopathy in lamin A/C-deficient mice.** *J Clin Invest* 2004, **113:**357-369.

31. Broers JL, Machiels BM, Kujipers HJ, Smedts F, van den Kieboom, Raymond Y, Ramaekers FC. **A-and B-type lamins are differentially expressed in normal human tissues.** *Histochem Cell Biol* 1997, **107**:505-517.

32. Pugh GE, Coates PJ, Lane EB, Raymond Y, Quinlan RA: **Distinct nuclear assembly pathways for lamins A and C lead to their increase during quiescence in Swiss 3T3 cells.** *J Cell Sci* 1997, **110 (Pt 19):**2483-2493.

33. Raharjo WH, Enarson P, Sullivan T, Stewart CL, Burke B: **Nuclear envelope defects associated with LMNA mutations cause dilated cardiomyopathy and Emery-Dreifuss muscular dystrophy.** *J Cell Sci* 2001, **114:**4447-4457.

34. Vaughan A, Alvarez-Reyes M, Bridger JM, Broers JL, Ramaekers FC, Wehnert M, Morris GE, Whitfield WGF, Hutchison CJ: **Both emerin and lamin C depend on lamin A for localization at the nuclear envelope.** *J Cell Sci* 2001, **114:**2577-2590.

35. Fong LG, Ng JK, Lammerding J, Vickers TA, Meta M, Cote N, Gavino B, Qiao X, Chang SY, Young SR, Yang SH, Stewart CL, Lee RT, Bennett CF, Bergo MO, Young SG: **Prelamin A and lamin A appear to be dispensable in the nuclear lamina.** *J Clin Invest* 2006, **116:**743-752.

36. Sylvius N, Hathaway A, Boudreau E, Gupta P, Labib S, Bolongo PM, Rippstein P, McBride H, Bilinska ZT, Tesson F: **Specific contribution of lamin A and lamin C in the development of laminopathies.** *Exp Cell Res* 2008, **314:**2362-2375.

37. Broers JL, Kuijpers HJ, Ostlund C, Worman HJ, Endert J, Ramaekers FC: **Both lamin A and lamin C mutations cause lamina instability as well as loss of internal nuclear lamin organization.** *Exp Cell Res* 2005, **304:**582-592.

38. Favreau C, Higuet D, Courvalin JC, Buendia B: **Expression of a mutant lamin A that causes Emery-Dreifuss muscular dystrophy inhibits in vitro differentiation of C2C12 myoblasts.** *Mol Cell Biol* 2004, **24:**1481-1492.

39. Frock RL, Kudlow BA, Evans AM, Jameson SA, Hauschka SD, Kennedy BK: **Lamin A/C and emerin are critical for skeletal muscle satellite cell differentiation.** *Genes Dev* 2006, **20:**486-500.

40. Boudreau E, Labib S, Bertrand AT, Decostre V, Bolongo PM, Sylvius N, Bonne G, Tesson F: **Lamin A/C mutants disturb sumo1 localization and sumoylation in vitro and in vivo.** *PLoS One* 2012, **7:**e45918.

41. Zhang YQ, Sarge KD: **Sumoylation regulates lamin A function and is lost in lamin A mutants associated with familial cardiomyopathies.** *J Cell Biol* 2008, **182:**35-39.

42. Siu CW, Lee YK, Ho JC, Lai WH, Chan YC, Ng KM, Wong LY, Au KW, Lau YM, Zhang J, Lay KW, Colman A, Tse HF: **Modeling of lamin A/C mutation premature cardiac aging using patient-specific induced pluripotent stem cells.** *Aging (Albany NY)* 2012, **4:**803-822.

43. Muchir A, Pavlidis P, Decostre V, Herron AJ, Arimura T, Bonne G, Worman HJ: **Activation of MAPK pathways links LMNA mutations to cardiomyopathy in Emery-Dreifuss muscular dystrophy.** *J Clin Invest* 2007, **117:**1282-1293.

44. Muchir A, Pavlidis P, Bonne G, Hayashi YK, Worman HJ: **Activation of MAPK in hearts of EMD null mice: similarities between mouse models of X-linked and autosomal dominant Emery Dreifuss muscular dystrophy.** *Hum Mol Genet* 2007, **16:**1884-1895.

45. Muchir A, Shan J, Bonne G, Lehnart SE, Worman HJ: **Inhibition of extracellular signal-regulated kinase signaling to prevent cardiomyopathy caused by mutation in the gene encoding A-type lamins.** *Hum Mol Genet* 2009, **18:**241-247.

46. Broers JL, Peeters EA, Kuijpers HJ, Endert J, Bouten CV, Oomens CW, Baaijens FP, Ramaekers FC: **Decreased mechanical stiffness in LMNA-/- cells is caused by defective nucleo-cytoskeletal integrity: implications for the development of laminopathies.** *Hum Mol Genet* 2004, **13:**2567-2580.

47. Fidzianska A, Hausmanowa-Petrusewicz I: **Architectural abnormalities in muscle nuclei. Ultrastructural differences between X-linked and autosomal dominant forms of EDMD.** *J Neurol Sci* 2003, **210:**47-51.

48. De Vos WH, Houben F, Kamps M, Malhas A, Verheyen F, Cox J, Manders EM, Verstraeten VL, van Steensel MA, Marcelis CL, van den WA, Vaux DJ, Ramaekers FC, Broers JL: **Repetitive disruptions of the nuclear envelope invoke temporary loss of cellular compartmentalization in laminopathies.** *Hum Mol Genet* 2011, **20:**4175-4186.

49. Maraldi NM, Capanni C, Cenni V, Fini M, Lattanzi G: **Laminopathies and lamin-associated signaling pathways.** *J Cell Biochem* 2011, **112:**979-992.

50. Navarro CL, Cau P, Levy N: **Molecular bases of progeroid syndromes.** *Hum Mol Genet* 2006, **15 Spec No 2:**R151-R161.

7. Supplementary File

1. van Tintelen JP, Tio RA, Kerstjens-Frederikse WS, van Berlo JH, Boven LG, Suurmeijer AJ, White SJ, den Dunnen JT, te Meerman GJ, Vos YJ, van der Hout AH, Osinga J, van den Berg MP, van Veldhuisen DJ, Buys CH, Hofstra RM, Pinto YM: Severe myocardial fibrosis caused by a deletion of the 5' end of the lamin A/C gene. J Am Coll Cardiol 2007, 49:2430-2439.

2. Becane HM, Bonne G, Varnous S, Muchir A, Ortega V, Hammouda EH, Urtizberea JA, Lavergne T, Fardeau M, Eymard B, Weber S, Schwartz K, Duboc D: High incidence of sudden death with conduction system and myocardial disease due to lamins A and C gene mutation. Pacing Clin Electrophysiol 2000, 23:1661-1666.

3. Sebillon P, Bouchier C, Bidot LD, Bonne G, Ahamed K, Charron P, Drouin-Garraud V, Millaire A, Desrumeaux G, Benaiche A, Charniot JC, Schwartz K, Villard E, Komajda M: Expanding the phenotype of LMNA mutations in dilated cardiomyopathy and functional consequences of these mutations. *J Med Genet* 2003, 40:560-567.

4. Pasotti M, Klersy C, Pilotto A, Marziliano N, Rapezzi C, Serio A, Mannarino S, Gambarin F, Favalli V, Grasso M, Agozzino M, Campana C, Gavazzi A, Febo O, Marini M, Landolina M, Mortara A, Piccolo G, Vigano M, Tavazzi L, Arbustini E: Long-term outcome and risk stratification in dilated cardiolaminopathies. J Am Coll Cardiol 2008, 52:1250-1260.

5. Verga L, Concardi M, Pilotto A, Bellini O, Pasotti M, Repetto A, Tavazzi L, Arbustini E: Loss of lamin A/C expression revealed by immuno-electron microscopy in dilated cardiomyopathy with atrioventricular block caused by LMNA gene defects. Virchows Arch 2003, 443:664-671.

6. Ho JC, Zhou T, Lai WH, Huang Y, Chan YC, Li X, Wong NL, Li Y, Au KW, Guo D, Xu J, Siu CW, Pei D, Tse HF, Esteban MA: Generation of induced pluripotent stem cell lines from 3 distinct laminopathies bearing heterogeneous mutations in lamin A/C. Aging (Albany NY) 2011, 3:380-390.

7. Pethig K, Genschel J, Peters T, Wilhelmi M, Flemming P, Lochs H, Haverich A, Schmidt HH: LMNA mutations in cardiac transplant recipients. Cardiology 2005, 103:57-62.

8. van Tintelen JP, Hofstra RM, Katerberg H, Rossenbacker T, Wiesfeld AC, du Marchie Sarvaas GJ, Wilde AA, van Langen IM, Nannenberg EA, van der Kooi AJ, Kraak M, van Gelder IC, van Veldhuisen DJ, Vos Y, van den Berg MP: High yield of LMNA mutations in patients with dilated cardiomyopathy and/or conduction disease referred to cardiogenetics outpatient clinics. Am Heart J 2007, 154:1130-1139.

9. Yuan WL, Huang CY, Wang JF, Xie SL, Nie RQ, Liu YM, Liu PM, Zhou SX, Chen SQ, Huang WJ: R25G mutation in exon 1 of LMNA gene is associated with dilated cardiomyopathy and limb-girdle muscular dystrophy 1B. Chin Med J (Engl) 2009, 122:2840-2845.

10. Saj M, Dabrowski R, Labib S, Jankowska A, Szperl M, Broda G, Szwed H, Tesson F, Bilinska ZT, Ploski R: Variants of the lamin A/C (LMNA) gene in non-valvular atrial fibrillation patients: a possible pathogenic role of the Thr528Met mutation. Mol Diagn Ther 2012, 16:99-107.

11. Garg A, Speckman RA, Bowcock AM: Multisystem dystrophy syndrome due to novel missense mutations in the amino-terminal head and alpha-helical rod domains of the lamin A/C gene. Am J Med 2002, 112:549-555.

12. Vytopil M, Ricci E, Dello RA, Hanisch F, Neudecker S, Zierz S, Ricotti R, Demay L, Richard P, Wehnert M, Bonne G, Merlini L, Toniolo D: Frequent low penetrance mutations in the Lamin A/C gene, causing Emery Dreifuss muscular dystrophy. Neuromuscul Disord 2002, 12:958-963.

13. Vytopil M, Benedetti S, Ricci E, Galluzzi G, Dello RA, Merlini L, Boriani G, Gallina M, Morandi L, Politano L, Moggio M, Chiveri L, Hausmanova-Petrusewicz I, Ricotti R, Vohanka S, Toman J, Toniolo D: Mutation analysis of the lamin A/C gene (LMNA) among patients with different cardiomuscular phenotypes. J Med Genet 2003, 40:e132.

14. Goizet C, Yaou RB, Demay L, Richard P, Bouillot S, Rouanet M, Hermosilla E, Le Masson G, Lagueny A, Bonne G, Ferrer X: A new mutation of the lamin A/C gene leading to autosomal dominant axonal neuropathy, muscular dystrophy, cardiac disease, and leuconychia. J Med Genet 2004, 41:e29.

15. Arbustini E, Pilotto A, Grasso M, Marziliano N, Serio A, Gambarin F, Pasotti M, Serafini E, Cassini P, Digiorgio B: Novel human pathological mutations. Gene symbol: LMNA. Disease: cardiomyopathy, dilated with conduction defects. Hum Genet 2009, 125:350.

16. Scharner J, Brown CA, Bower M, Iannaccone ST, Khatri IA, Escolar D, Gordon E, Felice K, Crowe CA, Grosmann C, Meriggioli MN, Asamoah A, Gordon O, Gnocchi VF, Ellis JA, Mendell JR, Zammit PS: Novel LMNA mutations in patients with Emery-Dreifuss muscular dystrophy and functional characterization of four LMNA mutations. Hum Mutat 2011, 32:152-167.

17. Lakdawala NK, Funke BH, Baxter S, Cirino AL, Roberts AE, Judge DP, Johnson N, Mendelsohn NJ, Morel C, Care M, Chung WK, Jones C, Psychogios A, Duffy E, Rehm HL, White E, Seidman JG, Seidman CE, Ho CY: Genetic testing for dilated cardiomyopathy in clinical practice. J Card Fail 2012, 18:296-303.

18. Rudenskaya GE, Polyakov AV, Tverskaya SM, Zaklyazminskaya EV, Chukhrova AL, Groznova OE, Ginter EK: Laminopathies in Russian families. Clin Genet 2008, 74:127-133.

19. Song K, Dube MP, Lim J, Hwang I, Lee I, Kim JJ: Lamin A/C mutations associated with familial and sporadic cases of dilated cardiomyopathy in Koreans. Exp Mol Med 2007, 39:114-120.

20. Chen L, Lee L, Kudlow BA, Dos Santos HG, Sletvold O, Shafeghati Y, Botha EG, Garg A, Hanson NB, Martin GM, Mian IS, Kennedy BK, Oshima J: LMNA mutations in atypical Werner's syndrome. Lancet 2003, 362:440-445.

21. Nguyen D, Leistritz DF, Turner L, MacGregor D, Ohson K, Dancey P, Martin GM, Oshima J: Collagen expression in fibroblasts with a novel LMNA mutation. Biochem Biophys Res Commun 2007, 352:603-608.

22. McPherson E, Turner L, Zador I, Reynolds K, MacGregor D, Giampietro PF: Ovarian failure and dilated cardiomyopathy due to a novel lamin mutation. Am J Med Genet A 2009, 149A:567-572.

23. Fatkin D, MacRae C, Sasaki T, Wolff MR, Porcu M, Frenneaux M, Atherton J, Vidaillet HJ, Jr., Spudich S, De Girolami U, Seidman JG, Seidman C, Muntoni F, Muehle G, Johnson W, McDonough B: Missense mutations in the rod domain of the lamin A/C gene as causes of dilated cardiomyopathy and conduction-system disease. N Engl J Med 1999, 341:1715-1724.

24. van der Kooi AJ, Bonne G, Eymard B, Duboc D, Talim B, Van d, V, Reiss P, Richard P, Demay L, Merlini L, Schwartz K, Busch HF, de Visser M: Lamin A/C mutations with lipodystrophy, cardiac abnormalities, and muscular dystrophy. Neurology 2002, 59:620-623.

25. Carboni N, Porcu M, Mura M, Cocco E, Marrosu G, Maioli MA, Solla E, Tranquilli S, Orru P, Marrosu MG: Evolution of the phenotype in a family with an LMNA gene mutation presenting with isolated cardiac involvement. Muscle Nerve 2010, 41:85-91.

26. Subramanyam L, Simha V, Garg A: Overlapping syndrome with familial partial lipodystrophy, Dunnigan variety and cardiomyopathy due to amino-terminal heterozygous missense lamin A/C mutations. Clin Genet 2010, 78:66-73.

27. Arbustini Eloisa AE, Pilotto A, Pasotti M, Grasso M, Diegoli M, Ghio S, Tagliani M, Tavazzi L: Gene symbol: LMNA. Disease: EDMD2. Hum Genet 2005, 117:294.

28. Wang H, Wang J, Zheng W, Wang X, Wang S, Song L, Zou Y, Yao Y, Hui R: Mutation Glu82Lys in lamin A/C gene is associated with cardiomyopathy and conduction defect. Biochem Biophys Res Commun 2006, 344:17-24.

29. Wu X, Wang QK, Gui L, Liu M, Zhang X, Jin R, Li W, Yan L, Du R, Wang Q, Zhu J, Yang J: Identification of a new lamin A/C mutation in a chinese family affected with atrioventricular block as the prominent phenotype. J Huazhong Univ Sci Technolog Med Sci 2010, 30:103-107.

30. Taylor MR, Fain PR, Sinagra G, Robinson ML, Robertson AD, Carniel E, Di Lenarda A, Bohlmeyer TJ, Ferguson DA, Brodsky GL, Boucek MM, Lascor J, Moss AC, Li WL, Stetler GL, Muntoni F, Bristow MR, Mestroni L: Natural history of dilated cardiomyopathy due to lamin A/C gene mutations. J Am Coll Cardiol 2003, 41:771-780.

31. Parks SB, Kushner JD, Nauman D, Burgess D, Ludwigsen S, Peterson A, Li D, Jakobs P, Litt M, Porter CB, Rahko PS, Hershberger RE: Lamin A/C mutation analysis in a cohort of 324 unrelated patients with idiopathic or familial dilated cardiomyopathy. Am Heart J 2008, 156:161-169.

32. Redondo-Verge L, Yaou RB, Fernandez-Recio M, Dinca L, Richard P, Bonne G: Cardioembolic stroke prompting diagnosis of LMNA-associated Emery-Dreifuss muscular dystrophy. Muscle Nerve 2011, 44:587-589.

33. Millat G, Chanavat V, Julia S, Crehalet H, Bouvagnet P, Rousson R: Validation of high-resolution DNA melting analysis for mutation scanning of the LMNA gene. Clin Biochem 2009, 42:892-898.

34. Millat G, Bouvagnet P, Chevalier P, Sebbag L, Dulac A, Dauphin C, Jouk PS, Delrue MA, Thambo JB, Le Metayer P, Seronde MF, Faivre L, Eicher JC, Rousson R: Clinical and mutational spectrum in a cohort of 105 unrelated patients with dilated cardiomyopathy. Eur J Med Genet 2011, 54:e570-e575.

35. Arbustini E, Pilotto A, Repetto A, Grasso M, Negri A, Diegoli M, Campana C, Scelsi L, Baldini E, Gavazzi A, Tavazzi L: Autosomal dominant dilated cardiomyopathy with atrioventricular block: a lamin A/C defect-related disease. J Am Coll Cardiol 2002, 39:981-990.

36. Pan H, Richards AA, Zhu X, Joglar JA, Yin HL, Garg V: A novel mutation in LAMIN A/C is associated with isolated early-onset atrial fibrillation and progressive atrioventricular block followed by cardiomyopathy and sudden cardiac death. Heart Rhythm 2009, 6:707-710.

37. Narula N, Favalli V, Tarantino P, Grasso M, Pilotto A, Bellazzi R, Serio A, Gambarin FI, Charron P, Meder B, Pinto Y, Elliott PM, Mogensen J, Bolognesi M, Bollati M, Arbustini E: Quantitative expression of the mutated lamin A/C gene in patients with cardiolaminopathy. J Am Coll Cardiol 2012, 60:1916-1920.

38. Keller H, Finsterer J, Steger C, Wexberg P, Gatterer E, Khazen C, Stix G, Gerull B, Hoftberger R, Weidinger F: Novel c.367_369del LMNA mutation manifesting as severe arrhythmias, dilated cardiomyopathy, and myopathy. Heart Lung 2012, 41:382-386.

39. Karkkainen S, Reissell E, Helio T, Kaartinen M, Tuomainen P, Toivonen L, Kuusisto J, Kupari M, Nieminen MS, Laakso M, Peuhkurinen K: Novel mutations in the lamin A/C gene in heart transplant recipients with end stage dilated cardiomyopathy. Heart 2006, 92:524-526.

40. Lupsa BC, Sachdev V, Lungu AO, Rosing DR, Gorden P. Cardiomyopathy in congenital and acquired generalized lipodystrophy: a clinical assessment. Medicine (Baltimore) 2010, 89:245-50.

41. Perrot A, Sigusch HH, Nagele H, Genschel J, Lehmkuhl H, Hetzer R, Geier C, Leon P, V, Reinhard D, Dietz R, Josef OK, Schmidt HH: Genetic and phenotypic analysis of dilated cardiomyopathy with conduction system disease: demand for strategies in the management of presymptomatic lamin A/C mutant carriers. Eur J Heart Fail 2006, 8:484-493.

42. Karkkainen S, Helio T, Miettinen R, Tuomainen P, Peltola P, Rummukainen J, Ylitalo K, Kaartinen M, Kuusisto J, Toivonen L, Nieminen MS, Laakso M, Peuhkurinen K: A novel mutation, Ser143Pro, in the lamin A/C gene is common in finnish patients with familial dilated cardiomyopathy. Eur Heart J 2004, 25:885-893.

43. Perrot A, Hussein S, Ruppert V, Schmidt HH, Wehnert MS, Duong NT, Posch MG, Panek A, Dietz R, Kindermann I, Bohm M, Michalewska-Wludarczyk A, Richter A, Maisch B, Pankuweit S, Ozcelik C: Identification of mutational hot spots in LMNA encoding lamin A/C in patients with familial dilated cardiomyopathy. Basic Res Cardiol 2009, 104:90-99.

44. Saga A, Karibe A, Otomo J, Iwabuchi K, Takahashi T, Kanno H, Kikuchi J, Keitoku M, Shinozaki T, Shimokawa H: Lamin A/C gene mutations in familial cardiomyopathy with advanced atrioventricular block and arrhythmia. Tohoku J Exp Med 2009, 218:309-316.

45. Botto N, Vittorini S, Colombo MG, Biagini A, Paradossi U, Aquaro G, Andreassi MG: A novel LMNA mutation (R189W) in familial dilated cardiomyopathy: evidence for a 'hot spot' region at exon 3: a case report. Cardiovasc Ultrasound 2010, 8:9.

46. Sylvius N, Bilinska ZT, Veinot JP, Fidzianska A, Bolongo PM, Poon S, McKeown P, Davies RA, Chan KL, Tang AS, Dyack S, Grzybowski J, Ruzyllo W, McBride H, Tesson F: In vivo and in vitro examination of the functional significances of novel lamin gene mutations in heart failure patients. J Med Genet 2005, 42:639-647.

47. Fernandez X, Dumont CA, Monserrat L, Hermida-Prieto M, Castro-Beiras A: Sudden death in a patient with lamin A/C gene mutation and near normal left ventricular systolic function. Int J Cardiol 2008, 126:136-137.

48. Gupta P, Bilinska ZT, Sylvius N, Boudreau E, Veinot JP, Labib S, Bolongo PM, Hamza A, Jackson T, Ploski R, Walski M, Grzybowski J, Walczak E, Religa G, Fidzianska A, Tesson F: Genetic and ultrastructural studies in dilated cardiomyopathy patients: a large deletion in the lamin A/C gene is associated with cardiomyocyte nuclear envelope disruption. Basic Res Cardiol 2010, 105:365-377.

49. Bilinska ZT, Sylvius N, Grzybowski J, Fidzianska A, Michalak E, Walczak E, Walski M, Bieganowska K, Szymaniak E, Kusmierczyk-Droszcz B, Lubiszewska B, Wagner T, Tesson F, Ruzyllo W: Dilated cardiomyopathy caused by LMNA mutations. Clinical and morphological studies. Kardiol Pol 2006, 64:812-819.

50. Jakobs PM, Hanson EL, Crispell KA, Toy W, Keegan H, Schilling K, Icenogle TB, Litt M, Hershberger RE: Novel lamin A/C mutations in two families with dilated cardiomyopathy and conduction system disease. J Card Fail 2001, 7:249-256.

51. Cowan J, Li D, Gonzalez-Quintana J, Morales A, Hershberger RE: Morphological analysis of 13 LMNA variants identified in a cohort of 324 unrelated patients with idiopathic or familial dilated cardiomyopathy. Circ Cardiovasc Genet 2010, 3:6-14.

52. Otomo J, Kure S, Shiba T, Karibe A, Shinozaki T, Yagi T, Naganuma H, Tezuka F, Miura M, Ito M, Watanabe J, Matsubara Y, Shirato K: Electrophysiological and histopathological characteristics of progressive atrioventricular block accompanied by familial dilated cardiomyopathy caused by a novel mutation of lamin A/C gene. J Cardiovasc Electrophysiol 2005, 16:137-145.

53. Hershberger RE, Hanson EL, Jakobs PM, Keegan H, Coates K, Bousman S, Litt M: A novel lamin A/C mutation in a family with dilated cardiomyopathy, prominent conduction system disease, and need for permanent pacemaker implantation. Am Heart J 2002, 144:1081-1086.

54. Arbustini E, Pasotti M, Pilotto A, Diegoli M, Brega A, Disabella E, Grasso M, Marziliano N: Gene symbol: LMNA. Disease: Dilated cardiomyopathy with conduction defect CMD1A. Hum Genet 2007 120:910.

55. Saj M, Bilinska ZT, Tarnowska A, Sioma A, Bolongo P, Sobieszczanska-Malek M, Michalak E, Golen D, Mazurkiewicz L, Malek L, Walczak E, Fidzianska A, Grzybowski J, Przybylski A, Zielinski T, Korewicki J, Tesson F, Ploski R: LMNA mutations in Polish patients with dilated cardiomyopathy: prevalence, clinical characteristics, and in vitro studies. BMC Med Genet 2013 23:14:55.

56. Arbustini Eloisa AE, Pilotto A, Pasotti M, Grasso M, Diegoli M, Campana C, Gavazzi A, Alessandra R, Tavazzi L: Gene symbol: LMNA. Disease: Cardiomyopathy, dilated, with conduction defect 1. Hum Genet 2005, 117:298.

57. Carboni N, Mura M, Marrosu G, Cocco E, Ahmad M, Solla E, Mateddu A, Maioli MA, Marini S, Nissardi V, Frau J, Mallarini G, Mercuro G, Marrosu MG: Muscle MRI findings in patients with an apparently exclusive cardiac phenotype due to a novel LMNA gene mutation. Neuromuscul Discord 2008 18:291-298.

58. Benedetti S, Menditto I, Degano M, Rodolico C, Merlini L, D'Amico A, Palmucci L, Berardinelli A, Pegoraro E, Trevisan CP, Morandi L, Moroni I, Galluzzi G, Bertini E, Toscano A, Olive M, Bonne G, Mari F, Caldara R, Fazio R, Mammi I, Carrera P, Toniolo D, Comi G, Quattrini A, Ferrari M, Previtali SC: Phenotypic clustering of lamin A/C mutations in neuromuscular patients. Neurology 2007, 69:1285-1292.

59. Kichuk Chrisant MR, Drummond-Webb J, Hallowell S, Friedman NR: Cardiac transplantation in twins with autosomal dominant Emery-Dreifuss muscular dystrophy. J Heart Lung Transplant 2004, 23:496-498.

60. Beckmann BM, Holinski-Feder E, Walter MC, Haserück N, Reithmann C, Hinterseer M, Wilde AA, Kääb S: Laminopathy presenting as familial atrial fibrillation. Int J Cardiol 2010 145:394-396.

61. MacLeod HM, Culley MR, Huber JM, McNally EM: Lamin A/C truncation in dilated cardiomyopathy with conduction disease. BMC Med Genet 2003, 4:4.

62. Antoniades L, Eftychiou C, Kyriakides T, Christodoulou K, Katritsis DG: Malignant mutation in the lamin A/C gene causing progressive conduction system disease and early sudden death in a family with mild form of limb-girdle muscular dystrophy. J Interv Card Electrophysiol 2007, 19:1-7.

63. Ben Yaou R, Bécane HM, Demay L, Laforet P, Mannequin D, Bohu PA, Drouin-Garraud V, Ferrer X, Mussini JM, Oolongs E, Petiot P, Penisson-Besnier I, Streichenberger N, Toutain A, Richard P, Eymard B, Bonne G: La dystrophie musculaire des ceintures autosomique dominante associée à des troubles de la conduction cardiaque (LGMD1B). Description de 8 nouvelles familles avec mutations du gène LMNA. Rev Neurol (Paris) 2005 161:42-54.

64. Arbustini E, Pilotto A, Porcu E, Landolina M, Pasotti M, Lucchelli C, Disabella E, Tavazzi L: Gene symbol: LMNA. Disease: Cardiomyopathy, dilated, with conduction tissue defect 1. Hum Genet 2005 117:300.

65. Carboni N, Floris M, Mateddu A, Porcu M, Marrosu G, Solla E, Cocco E, Mura M, Marini S, Maioli MA, Piras R, Aste R, Marrosu MG: Aberrant splicing in the LMNA gene caused by a novel mutation on the polypyrimidine tract of intron 5. Muscle Nerve 2011, 43:688-693.

66. Brodsky GL, Muntoni F, Miocic S, Sinagra G, Sewry C, Mestroni L: Lamin A/C gene mutation associated with dilated cardiomyopathy with variable skeletal muscle involvement. Circulation 2000, 101:473-476.

67. Raffaele DB, Ricci E, Galluzzi G, Tonali P, Mora M, Morandi L, Romorini A, Voit T, Orstavik KH, Merlini L, Trevisan C, Biancalana V, Housmanowa-Petrusewicz I, Bione S, Ricotti R, Schwartz K, Bonne G, Toniolo D: Different mutations in the LMNA gene cause autosomal dominant and autosomal recessive Emery-Dreifuss muscular dystrophy. Am J Hum Genet 2000, 66:1407-1412.

68. Zeller R, Ivandic BT, Ehlermann P, Mucke O, Zugck C, Remppis A, Giannitsis E, Katus HA, Weichenhan D: Large-scale mutation screening in patients with dilated or hypertrophic cardiomyopathy: a pilot study using DGGE. J Mol Med (Berl) 2006, 84:682-691.

69. Moller DV, Pham TT, Gustafsson F, Hedley P, Ersboll MK, Bundgaard H, Andersen CB, Torp-Pedersen C, Kober L, Christiansen M: The role of Lamin A/C mutations in Danish patients with idiopathic dilated cardiomyopathy. Eur J Heart Fail 2009, 11:1031-1035.

70. Stallmeyer B, Koopmann M, Schulze-Bahr E: Identification of novel mutations in LMNA associated with familial forms of dilated cardiomyopathy. Genet Test Mol Biomarkers 2012, 16:543-549.

71. Benedetti S, Menditto I, Degano M, Rodolico C, Merlini L, D'Amico A, Palmucci L, Berardinelli A, Pegoraro E, Trevisan CP, Morandi L, Moroni I, Galluzzi G, Bertini E, Toscano A, Olivè M, Bonne G, Mari F, Caldara R, Fazio R, Mammì I, Carrera P, Toniolo D, Comi G, Quattrini A, Ferrari M, Previtali SC: Phenotypic clustering of lamin A/C mutations in neuromuscular patients. Neurology 2007 69:1285-1292.

72. Meinke P, Nguyen TD, Wehnert MS: The LINC complex and human disease. Biochem Soc Trans 2011 39:1693-1697.

73. Hermida-Prieto M, Monserrat L, Castro-Beiras A, Laredo R, Soler R, Peteiro J, Rodriguez E, Bouzas B, Alvarez N, Muniz J, Crespo-Leiro M: Familial dilated cardiomyopathy and isolated left ventricular noncompaction associated with lamin A/C gene mutations. Am J Cardiol 2004, 94:50-54.

74. Fujimori Y, Okimatsu H, Kashiwagi T, Sanda N, Okumura K, Takagi A, Nagata K, Murate T, Uchida A, Node K, Saito H, Kojima T: Molecular defects associated with antithrombin deficiency and dilated cardiomyopathy in a Japanese patient. Intern Med 2008, 47:925-931.

75. De Backer J, Van Beeumen K, Loeys B, Duytschaever M: Expanding the phenotype of sudden cardiac death-An unusual presentation of a family with a Lamin A/C mutation. Int J Cardiol 2010, 138:97-99.

76. Volpi L, Ricci G, Passino C, Di Pierri E, Ali G, Maccherini M, Benedetti S, Lattanzi G, Columbaro M, Ferrari M, Caramella D, Tanganelli P, Emdin M, Siciliano G: Prevalent cardiac phenotype resulting in heart transplantation in a novel LMNA gene duplication. Neuromuscul Disord 2010, 20:512-516.

77. Komaki H, Hayashi YK, Tsuburaya R, Sugie K, Kato M, Nagai T, Imataka G, Suzuki S, Saitoh S, Asahina N, Honke K, Higuchi Y, Sakuma H, Saito Y, Nakagawa E, Sugai K, Sasaki M, Nonaka I, Nishino I: Inflammatory changes in infantile-onset LMNA-associated myopathy. Neuromuscul Disord 2011, 21:563-568.

78. Charniot JC, Pascal C, Bouchier C, Sebillon P, Salama J, Duboscq-Bidot L, Peuchmaurd M, Desnos M, Artigou JY, Komajda M: Functional consequences of an LMNA mutation associated with a new cardiac and non-cardiac phenotype. Hum Mutat 2003, 21:473-481.

79. Boriani G, Gallina M, Merlini L, Bonne G, Toniolo D, Amati S, Biffi M, Martignani C, Frabetti L, Bonvicini M, Rapezzi C, Branzi A: Clinical relevance of atrial fibrillation/flutter, stroke, pacemaker implant, and heart failure in Emery-Dreifuss muscular dystrophy: a long-term longitudinal study. Stroke 2003, 34:901-908.

80. Hong JS, Ki CS, Kim JW, Suh YL, Kim JS, Baek KK, Kim BJ, Ahn KJ, Kim DK: Cardiac dysrhythmias,cardiomyopathy and muscular dystrophy in patients with Emery-Dreifuss muscular dystrophy and limb-girdle muscular dystrophy type 1B. J Korean Med Sci 2005, 20:283-290.

81. Balavoine AS, Laurent JM, Brigadeau F, Lascols O, Vantyghem MC: Atteinte cardiaque et diabète lié à une mutation de la lamine A/C habituellement rencontrée dans les dystrophies musculaires d'Emery Dreifuss. Congress Abstract P206. 36ième congrès annuel de la société francophone du diabète. Diabetes & Metabolism 2010 36:A87.

82. Genschel J, Baier P, Kuepferling S, Proepsting MJ, Buettner C, Ewert R, Hetzer R, Lochs H, Schmidt HH: A new frameshift mutation at codon 466 (1397delA) within the LMNA gene. Hum Mutat 2000, 16:278.

83. Duparc A, Cintas P, Somody E, Bieth E, Richard P, Maury P, Delay M: A cardio-neurological form of laminopathy: dilated cardiomyopathy with permanent partial atrial standstill and axonal neuropathy. Pacing Clin Electrophysiol 2009, 32:410-415.

84. Arbustini EA, Pasotti M, Pilotto A, Repetto A, Grasso M, Diegoli M: Gene symbol: CMD1A. Disease: Dilated cardiomyopathy associated with conduction system disease. Hum Genet 2005, 117:295.

85. Chrestian N, Valdmanis PN, Echahidi N, Brunet D, Bouchard JP, Gould P, Rouleau GA, Champagne J, Dupré N: A novel mutation in a large French-Canadian family with LGMD1B. Can J Neurol Sci 2008 35:331-334.

86. Forissier JF, Bonne G, Bouchier C, Duboscq-Bidot L, Richard P, Wisnewski C, Briault S, Moraine C, Dubourg O, Schwartz K, Komajda M: Apical left ventricular aneurysm without atrio-ventricular block due to a lamin A/C gene mutation. Eur J Heart Fail 2003, 5:821-825.

87. Hookana E, Junttila MJ, Sarkioja T, Sormunen R, Niemela M, Raatikainen MJ, Uusimaa P, Lizotte E, Peuhkurinen K, Brugada R, Huikuri HV: Cardiac arrest and left ventricular fibrosis in a Finnish family with the lamin A/C mutation. J Cardiovasc Electrophysiol 2008, 19:743-747.

88. Saj M, Jankowska A, Lewandowski M, Szwed H, Szperl M, Ploski R, Bilinska ZT: Dilated cardiomyopathy with profound segmental wall motion abnormalities and ventricular arrhythmia caused by the R541C mutation in the LMNA gene. Int J Cardiol 2010, 144:e51-e53.

89. Malek LA, Labib S, Mazurkiewicz L, Saj M, Ploski R, Tesson F, Bilinska ZT: A new c.1621 C > G, p.R541G lamin A/C mutation in a family with DCM and regional wall motion abnormalities (akinesis/dyskinesis): genotype-phenotype correlation. J Hum Genet 2011, 56:83-86.

90. Duboscq-Bidot L, Charron P, Ruppert V, Fauchier L, Richter A, Tavazzi L, Arbustini E, Wichter T, Maisch B, Komajda M, Isnard R, Villard E: Mutations in the ANKRD1 gene encoding CARP are responsible for human dilated cardiomyopathy. Eur Heart J 2009, 30:2128-2136.

91. Mercuri E, Brown SC, Nihoyannopoulos P, Poulton J, Kinali M, Richard P, Piercy RJ, Messina S, Sewry C, Burke MM, McKenna W, Bonne G, Muntoni F: Extreme variability

of skeletal and cardiac muscle involvement in patients with mutations in exon 11 of the lamin A/C gene. Muscle Nerve 2005, 31:602-609.

92. Decaudain A, Vantyghem MC, Guerci B, Hecart AC, Auclair M, Reznik Y, Narbonne H, Ducluzeau PH, Donadille B, Lebbe C, Bereziat V, Capeau J, Lascols O, Vigouroux C: New metabolic phenotypes in laminopathies: LMNA mutations in patients with severe metabolic syndrome. J Clin Endocrinol Metab 2007, 92:4835-4844.

93. Marsman RF, Bardai A, Postma AV, Res JC, Koopmann TT, Beekman L, van der Wal AC, Pinto YM, Lekanne Deprez RH, Wilde AA, Jordaens LJ, Bezzina CR: A complex double deletion in LMNA underlies progressive cardiac conduction disease, atrial arrhythmias, and sudden death. Circ Cardiovasc Genet 2011, 4:280-287.

94. Chang SH, Tsai CT, Lai LP, Lei MH: Identification of a lamin A/C gene mutation in a Taiwanese family with limb girdle muscular dystrophy and cardiomyopathy. Int J Cardiol 2010, 145:598-599.

95. Sparks EA, Boudoulas KD, Raman SV, Sasaki T, Graber HL, Nelson SD, Seidman CE, Boudoulas H. **Heritable cardiac conduction and myocardial disease: from the clinic to the basic science laboratory and back to the clinic.** *Cardiology* 2011, **118:**179-186.

96. Kourgiannidis G, Anastasakis A, Lampropoulos K, Iliopoulos T. **A patient with ventricular tachycardia due to a novel mutation of the lamin A/C gene: case presentation and mini review.** *Hellenic J Cardiol* 2013, **54:**326-330.

97. Muntoni F, Bonne G, Goldfarb LG, Mercuri E, Piercy RJ, Burke M, Yaou RB, Richard P, Récan D, Shatunoy A, Sewry CA, Brown SC. **Disease severity in dominant Emery Dreifuss is increased by mutations in both emerin and desmin proteins.** *Brain* 2006 **129:**1260-1268.

2. Review 2: Cellular and Animal Models of Striated Muscle Laminopathies

A. Citation:

Nicolas, H. A., Akimenko, M.-A., & Tesson, F. (2019). Cellular and Animal Models of Striated Muscle Laminopathies. *Cells*, *8*(4). https://doi.org/10.3390/cells8040291

B. Author Contributions:

HA Nicolas – drafted the manuscript

MA Akimenko – critiqued and edited the manuscript

F Tesson – contributed to the content of the manuscript, critiqued and edited the manuscript

C. Abstract

The lamin A/C (*LMNA*) gene codes for nuclear intermediate filaments constitutive of the nuclear lamina. *LMNA* has 12 exons and alternative splicing of exon 10 results in two major isoforms—lamins A and C. Mutations found throughout the *LMNA* gene cause a group of diseases collectively known as laminopathies, of which the type, diversity, penetrance and severity of phenotypes can vary from one individual to the other, even between individuals carrying the same mutation. The majority of the laminopathies affect cardiac and/or skeletal muscles. The underlying molecular mechanisms contributing to such tissue-specific phenotypes caused by mutations in a ubiquitously expressed gene are not yet well elucidated. This review will explore the different phenotypes observed in established models of striated muscle laminopathies and their respective contributions to advancing our understanding of cardiac and skeletal muscle-related laminopathies. Potential future directions for developing effective treatments for patients with lamin A/C mutation-associated cardiac and/or skeletal muscle conditions will be discussed.

1. Introduction

Laminopathies consist of a variety of diseases that affect different tissue types ranging from cardiac muscle (e.g., dilated cardiomyopathy (DCM)), skeletal muscles (e.g., Emery–Dreifuss Muscular Dystrophy (EDMD)), adipose tissues (e.g. familial partial lipodystrophy Dunnigan-type 2(FPLD2)) to nervous system (e.g., Charcot–Marie–Tooth disease type 2B1 (CMT2B1)) or affect several systems (e.g., Hutchison Gilford Progeria Syndrome (HGPS)). Mutations in the nuclear A-type lamins coding gene *LMNA* cause primary (classical) laminopathies, while secondary laminopathies are caused by mutations in B-type lamins, proteins involved in prelamin A maturation, or lamin binding partners. In addition, Lamin A/C mutations are also associated with arrhythmogenic right ventricular cardiomyopathy and hypertrophic cardiomyopathy [1–5]. The

LMNA gene (approximately 24 kb) is located on chromosome 1q22 and has 12 exons. It is expressed in most differentiated cells, with the expression in mice starting during early embryogenesis (8th day post-implantation) [6,7]. Alternative splicing of exon 10 results in the generation of the two major lamin splice variants, A and C [6]. Lamins A and C are identical up until amino acid (a.a) 566, after which six lamin C specific a.a are added [8]. Prelamin A is further processed to produce mature lamin A, firstly by the farnesylation of the cysteine residue in the C-terminal C*AAX* motif [9]. This is followed by the removal of the *AAX* a.a in the motif, then the methylation of the farnesylated cysteine, and lastly by the cleavage of the last 15 a.a (including the cysteine that was both methylated and farnesylated), resulting in a 646 a.a-long mature lamin A [9]. The other isoforms of lamin A/C are lamin C2 (utilizing an alternative exon 1; found in mammalian sperm cells) and lamin AΔ10 (which lacks exon 10; a less abundant form) [10–12]. The A-type lamins possess three main parts: the carboxy (C) head and amino (N) tail involved in the assembly of lamin A/C homodimers into anti-parallel protofilaments, and the central rod domain involved in the formation of the lamin A/C homodimers [13]. The A-type lamins, which are nuclear intermediate filaments, have a range of functions including nuclear structural support, anchoring of nuclear pores, chromatin and protein binding [14]. Examples of A-type lamins' binding partners are the sterol regulatory element binding transcription factor 1 (SREBF-1), the LEM-domain integral membrane protein emerin, and the spectrin repeat-containing nuclear envelope protein 1 (syne1), in which both emerin and syne1 are involved in mediating anchorage to the cytoskeleton [15–18].

The mechanism(s) by which the same *LMNA* mutation can sometimes lead to different phenotypes and mutations found throughout the ubiquitously expressed gene can lead to tissue specific phenotypes is not yet well elucidated. However, based on the current data, three

hypotheses seek to explain this diversity in phenotypes. The first suggests that the accumulation of misprocessed/unprocessed lamin A is toxic to cells, as in HGPS [19,20]. The second relates to the role of lamin A/C in interacting with chromatin and proteins. This is evidenced, for instance, by the increased expression and activation of MAPK pathway members in EDMD and DCM [21]. Similarly, the most frequent mutation causing FPLD2 affects a lamin A/C domain critical for binding of SREBF-1, a transcription factor (TF) involved in modulating transcription of sterol-regulated genes and adipocyte differentiation [15,22–28]. Lastly, it was postulated that the disruption of the protein network that connects the nucleus to the rest of the cell results in exacerbated effects of external stimuli such as mechanical forces on myocytes, leading to aberrant cellular structure and response (e.g. disruption of the cytoskeleton and cellular mechanical and adhesion properties in cells expressing the DCM lamin A/C p.D192G variant) [29–36].

The majority of reported cases of laminopathies (79%) affect the cardiac and/or skeletal muscles and are predominantly autosomal dominant [37]. DCM associated with *LMNA* mutations accounts for up to at least one-third of reported genotyped families with DCM, and presents with dilation of the left ventricle, thinning of the ventricular wall and conduction defects [38]. Patients with *LMNA*-related DCM also tend to have more severe phenotype and poorer prognosis with a recent study reporting 19% required heart transplants [39,40]. *LMNA*-related congenital muscular dystrophy (L-CMD) and EDMD are skeletal muscle conditions caused by *LMNA* mutations with overlapping clinical phenotypes, which include wasting of the upper arm and lower front leg muscles [41]. However, L-CMD is more severe and has earlier onset but less definitive cardiac presentation compared to EDMD [42]. 1B Limb-girdle muscular dystrophy (LGMD1B), associated with *LMNA* mutations, also affects the skeletal and cardiac muscles [43]. It is characterized by progressive muscle weakness, age-related cardiac conduction defects and no or

minimal late-onset joint contractures [43]. With the first paper identifying *LMNA* as a causal gene in EDMD in 1999, massive efforts involving both cellular and animal models have since been undertaken to understand the underlying mechanisms in cardiac and skeletal muscle conditions caused by mutations in *LMNA* [6,44]. Thus, this review will examine the different phenotypes observed in these established models and their respective contributions to unravelling the mechanisms underlying the development of striated muscle laminopathies. Potential future directions for developing more effective treatments for patients with *LMNA* mutation-associated conditions will also be discussed.

2. Cellular Models

Cellular models facilitate the characterization of the striated muscle laminopathy phenotype at both the cellular and nuclear level, and the identification of potential molecular markers for the conditions. This section gives an overview of the results obtained using patients' and mice models' cells and various cell lines.

2.1. Evidence of Abnormal Nuclear Morphology Coupled with Aberrant Lamin A/C Phenotype and Mislocalization of Several Lamin A/C Binding Proteins in LMNA-Related Cardiac and Skeletal Muscle Disease

A rare lamin A/C null case in humans was discovered from a deceased newborn who was homozygous for the nonsense p.Y259X mutation [45]. This variant causes complete absence of the A-type lamins in the homozygous state and half the amount of wild-type (WT) lamin A/C in the heterozygous state, resulting in LGMD1B [45,46]. The homozygous child presented with severe under development and abnormalities including dystrophic muscles [45]. Skin fibroblasts from the heterozygous grandmother were comparable to WT controls, while the *LMNA* null cells

presented with misshapen nuclei and abnormal localization of nuclear proteins such as lamin B1, B2, emerin, and syne1 [46]. B-type lamins are intimately connected to A-type lamins, and appear to be involved in several cellular functions ranging from regulation of gene expression and mitotic spindle assembly to cellular senescence [47]. Moreover, the skin fibroblasts from the child had impaired cell division capacity [46]. RNAi knockdown of *LMNA* in HeLa cells, however, did not affect cell growth but indeed resulted in emerin mislocalization in the endoplasmic reticulum, similar to what was seen in the *LMNA* null fibroblasts [46,48]. To determine whether emerin was also mislocalized in the presence of other *LMNA* mutations, mutant lamins A and C were transfected in various cell lines including the P19 embryonic carcinoma stem cells, which do not have endogenous lamin A/C [30,49]. The results were contradictory and, regardless of the position of the mutation along *LMNA*, emerin was either clearly mislocalized in some studied DCM or EDMD mutant lamin A/C or normally expressed and distributed [30,49,50]. Nonetheless, many *LMNA* mutations affecting the rod domain of the protein and causing muscular laminopathies also presented with aggregates of lamin A/C proteins, particularly lamin C, in the nucleoplasm of transfected cells [49,50]. Emerin was found in these nuclear foci [50]. On the other hand, a.a substitutions affecting the globular end of the lamin A/C protein did not result in punctate lamin A structures and emerin remained mislocalized [50]. Analyses of fibroblasts from muscular laminopathy patients with mutations affecting the head or tail domains of the protein had overt nuclear structure aberrations [51]. Specifically, immunostaining for lamin A/C revealed defects including honeycomb staining, punctate structures or blebbing [51]. Moreover, emerin and lamin B were also noted to be mislocalized [51]. All of these results therefore demonstrate that lamin A/C mutations cause profound nuclear abnormalities and the mislocalization of a variety of proteins.

Transient transfection in HeLa cells of the p.E203G lamin A variant, which is associated with DCM with conduction defects (DCM-CD), resulted in lamin aggregates and the absence of the lamin A variant in the nuclear periphery [15]. However, Ostlund and colleagues did not show this effect when they transiently transfected C2C12 cells with the p.E203G prelamin A variant [52,53]. The difference between the observed lamin phenotypes might be attributed to the cell line used. Nevertheless, the transient expression (lamin A only, lamin C only or both lamins A and C (to maintain the 1:1 stoichiometry of lamin A/C)) of other variants for DCM (p.D192G, p.N195K) or EDMD (p.R386K) in Cos7 and H9C2 (rat cardiomyoblast cell line) cells resulted in large and multiple lamin aggregates, which also fail to connect to the nuclear envelope unlike cells expressing WT or an FPLD (p. R482W) mutant lamin A/C [54]. An interesting exceptionwas the DCM-causing lamin A/C variant p.L85R, which produced a WT lamin phenotype if mutant lamin A only was expressed but an aberrant phenotype (multiple speckles) when mutant lamin C only was expressed; nevertheless, the abnormal mutant lamin C phenotype was rescued if co-expressed with the mutant lamin A [54]. This therefore suggests that mutations can differently affect the properties of lamins A and C. Indeed, interactions between emerin and lamin A, and emerin and lamin C, are differently affected by *LMNA* mutations [55]. Furthermore, fibroblasts from mice expressing only lamin C ($Lmna^{LCO}$) (discussed in the later part of the review) displayed normal emerin localization [56]. These results illustrate that the structural abnormalities due to *LMNA* mutations can result in the inability of the A-type lamins to properly connect to the nuclear envelope and can negatively impact their interaction with their binding partners. To further explore the effects of *LMNA* mutations on the interaction between A-type lamins and their binding partners, studies involving mutations found in regions known to interact with lamin A/C partners were performed.

2.2. Evidence of Disrupted Lamin A/C Interaction with Binding Partners, which Can Result in Multiple Tissue Phenotypes

Mutations found throughout the *LMNA* gene affect sites that are known to interact with various proteins. An example of one of these mutations—the substitution of C with T at nucleotide position 1444, producing the p.R482W lamin A/C variant and causing both FPLD and LGMD in some patients—is located in a region known to bind actin and/or influence SREBF1 interaction [15,57–60]. Similar to p.L530P, an EDMD variant, the p.R482W FPLD variant showed a notable decrease in binding capacity to SREBF1, thus suggesting that in some mutations that cause striated muscle laminopathies, binding capacity to TF involved in adipocyte metabolism can be affected, which can then lead to lipodystrophic features in some patients with primary presentation of muscular laminopathy [15]. This could also explain why the *Lmna*$^{\Delta 8\text{-}11}$ mice, which primarily exhibited striated muscle laminopathy, also notably lacked subcutaneous fat and presented with some metabolic parameter abnormalities [61,62]. To further investigate the consequences of changes in lamin A/C structure and the resulting abnormal lamin A/C phenotypes conferred by the mutations, mobility experiments were performed.

2.3. Evidence of Impaired Lamin A/C Structural Stability and Dynamics in Striated Muscle Laminopathies

As a consequence of the change in lamin A/C structure caused by *LMNA* mutations, the structural stability and dynamics of various lamin A/C variants were studied. Gilchrist et al. transfected epitope-tagged WT lamin A or lamin A variants in HT1080 cells, a human fibrosarcoma cell line [63]. The lamin A variants studied were p.L85R, p.N195K (both associated with DCM-CD), p.L530P (associated with EDMD) and p.R482W (associated with FPLD in some individuals co-presenting LGMD) [63]. The transfected cells showed no significant or overt

nuclear shape/size abnormalities [63]. Fluorescence recovery after photobleaching (FRAP) analysis was performed on these transiently transfected cells to determine the dynamics of WT lamin A and variant lamin A. The DCM-CD and EDMD variants were more mobile and showed faster dynamics (especially the p.N195K variant) compared to WT [63]. However, the predominant lipodystrophy causing variant p.R482W had comparable mobility to WT lamin A [63]. FRAP experiments on Cos7 cells also demonstrated increased mobility for the p.D192G (DCM-CD) and p.R386K (EDMD) lamin C only expressing variants compared to either WT lamin C or the p.L85R (DCM-CD) lamin C variant [54]. Fluorescence loss in photobleaching (FLIP) experiments further showed faster diffusion of lamin A p.N195K compared to WT [63]. Such increased mobility suggests less stability in the lamin A/C structures of the said variants [54,63]. To determine if these unstable A-type lamins affect the mechanical properties of the nucleoskeleton and/or the cytoskeleton, studies were performed on WT and mutant *LMNA*-expressing cells.

2.4. Evidence of Compromised Nuclear and Cytoskeletal Mechanics in the Presence of LMNA Mutations Causing Muscular Laminopathies

Putative alterations of the nucleoskeleton and/or the cytoskeleton were examined by assessing their mechanical properties in the presence of *LMNA* mutations. A cardiac sample from the p.D192G DCM patient presented with immense nuclear aberrations including rupture of nuclear envelope, chromatin disorganization and mislocalization of the mitochondria in the nucleoplasm in about 30% of the cardiomyocytes [38,64]. Similarly, nuclear envelope breaks were observed in the $Lmna^{\Delta K32/+}$ DCM mice model (discussed later part in the review) [65]. Furthermore, skin fibroblasts from DCM, EDMD and LGMD patients carrying *LMNA* mutations displayed a loss of nuclear stiffness [30]. Mouse embryo fibroblasts (MEFs) and skeletal myotubes from the $Lmna^{\Delta 8-}$

^{11} mice (discussed later in the review) also presented with reduced nuclear stiffness and a notable increase in nuclear deformity when strain was applied to the cells compared to WT [31]–[33]. Both low- and medium-pressure micro-injection of dextran into the nucleus resulted in dextran leaking into the cytoplasm, suggesting compromised nuclear integrity in fibroblasts of *Lmna*$^{\Delta 8\text{-}11}$ mice [31]. Viral transfection of different mutant *LMNA* cDNA (p.E161K, p.D192G, p.N195K variants) causing DCM with or without conduction defects in neonatal rat ventricular myocytes, resulted in nuclear morphology defects including blebbing [34]. Analyses of nuclear stiffness showed that the mutant *LMNA*-expressing cells are stiffer, particularly the p.D192G variant, compared to the controls [34]. On the other hand, *LMNA* mutations that were not associated with striated muscle laminopathies did not result in nuclear deformability [30]. Nucleoplasmic localization and large aggregates of lamin A/C were described in transfected cells, suggesting impaired assembly of lamin A/C mutants [30,34,38,54]. These mutations are found in the rod domain of the A-type lamins, which is involved in dimerization and the formation of a higher-order lamin structure (Figure 1).

Moreover, although no overt differences were detected between the cytoskeletal architecture of WT and *Lmna*$^{\Delta 8\text{-}11}$ MEFs, a significant decrease in cytoskeletal stiffness, cytoplasmic elasticity and viscosity was observed in the *Lmna*$^{\Delta 8\text{-}11}$ fibroblasts compared to WT cells, indicating that lamin A/C regulates the cytoskeleton plasticity [31,32]. Even skin fibroblasts with EDMD mutations that did not result in nuclear deformability displayed defects in force transmission between the nucleus and the cytoskeleton [30]. Neonatal rat ventricular myocytes expressing mutant *LMNA* showed disorganized actin and lower levels of actin staining compared to WT and uninfected controls [34]. They also have impaired adhesion and increased plasticity, suggesting a poorer capacity to handle and transmit mechanical stress due to actin defects [34]. Accordingly,

left ventricular *Lmna*$^{\Delta 8\text{-}11}$ myocytes displayed contractile dysfunction [66]. Actin and the p38 MAPK, which was shown to be associated with *LMNA*-related DCM, are thought to interact, and the inhibition of p38 restored the mutant actin and mechanical phenotypes back to WT [34,67,68]. Defects in mechano-transduction in *LMNA* mutant cells have been further explored using L-CMD patients' myoblasts cultured on matrix stiffness close to that of muscle (12kPa) [35,36]. Mutant cells displayed accumulation and disorganization of contractile actin stress fibres and increased traction forces, supporting the hypothesis that mutant cells are unable to sustain high external mechanical stretching because of impaired functional integrity of nuclear–cytoskeletal linkages [35,36]. Furthermore, *LMNA*-mutated myoblasts showed aberrant activation of regulators of the mechano-response (including yes-associated protein involved in cell adaptation to its microenvironment and formins known to affect actin polymerisation and depolymerisation in a force-sensitive manner) [35,36]. Interestingly, nuclear shape and chromatin organization can be improved in lamin A/C-depleted U2OS cells (derived from human osteosarcoma) in HGPS-derived patients cells, or in aged vascular smooth muscle cell by treatment with remodelin [69,70]. Remodelin is a small molecule that inhibits N-Acetyltransferase 10 (NAT10) activity to induce a microtubule reorganization [70]. These results emphasize the significance of nuclear structural deformity in laminopathies, demonstrating that mutations in *LMNA* impair the mechanical capacity and integrity of both the nucleus and the whole cell by the disruption of the cytoskeleton, thus resulting in defects in mechano-transduction signalling. To determine if these structural changes also affect the post-translational modification status of lamin A/C, experiments looking at such were undertaken.

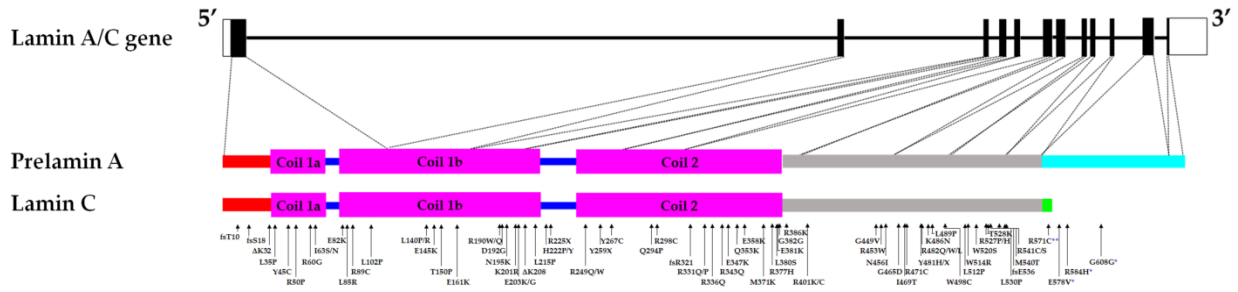

Figure 1. Schematic of prelamin A and lamin C proteins with the corresponding coding exons of the *LMNA* gene and the positions of the affected amino acids cited in this review. In red is the N terminus head, in bright pink are coils 1a, b and 2, in blue are linkers 1 and 2, in grey is the part of the C terminal tail common to both lamins A and C, in cyan is the part of the C terminal tail specific to lamin A and in bright green is the part of the C terminal tail specific to lamin C. fs means frameshift starting at the indicated amino acid. * and ** denote lamin-A- or lamin-C-specific amino acid substitution respectively.

2.5. Evidence of Altered Lamin A/C Post-Translational Modification Status in Striated Muscle Laminopathy

As discussed in the previous paragraphs, many of the disease-causing mutations result in alteration of the lamin A/C protein structure as well as the nuclear envelope properties. Therefore, would such changes in conformation also result in aberrant post-translational protein modifications? A-type lamins are known to be phosphorylated and the phosphorylation status may influence nuclear deformability [71]. Lamin A/C phosphorylation determines the nuclear localization, assembly, and plays a role in mobility and cytoplasmic transport of nuclear lamins during interphase [72]. There are three main regions of lamin A that are phosphorylated during interphase: the N-terminal head, the proximal C-terminal region and the far C-terminal region found in lamin A only [72]. Mitsuhashi et al. demonstrated abnormal Akt phosphorylation of the serine residue at position 458 (located in the proximal C-terminal region) in muscle tissues and fibroblasts of patients with myopathies caused by *LMNA* mutations located in the Ig fold in the protein C-terminus [73]. Resolved structure of the lamin A/C C-terminus showed that in WT, S458

was partially buried; therefore, it was plausible that certain mutations in the Ig fold altered the protein structure and caused the exposure of S458, rendering it accessible for abnormal phosphorylation by Akt [73,74]. Moreover, the EDMD variant p.R453W not only increased S458 phosphorylation, but also decreased S390 phosphorylation as compared to WT lamin A [75]. In addition, N-terminus lamin A phosphorylation was found to be lower in myoblasts from EDMD and LGMD patients compared to the control [76]. Furthermore, immunostaining for phosphorylated lamin A/C (phos-lamin A/C) in muscle fibres from these patients was markedly reduced [76]. Lower phos-lamin A/C was also observed in the regenerating muscle of a patient with EDMD compared to a sample from a patient with another type of muscular dystrophy, Duchenne Muscular Dystrophy (DMD) [76]. Such reduction in phos-lamin A/C was only observed in myocytes but not in fibroblasts and inflammatory cells, suggesting a tissue-specific process involving kinases and lamin A/C in muscles [76]. Overall, the data showed how a mutation that affects a particular region of the protein may confer structural and chemical changes that result in a molecular hallmark common to the different types of *LMNA*-related myopathies.

Lamin A has also been shown to be sumoylated by SUMO2 [77]. Fibroblasts from a p.E203K DCM patient or HeLa-transfected cells showed decreased lamin A sumoylation and increased cell death [77]. Moreover, transient transfection of p.D192G lamin C only or both p.D192G lamins A and C in fibroblast-like Cos7 cells derived from monkey kidney tissue or in C2C12 cells, a mouse skeletal myoblast cell line, resulted in large lamin foci, which co-localized with SUMO1, a protein involved in post-translational modification [38,78]. Mislocalization of SUMO1 was also observed in *Lmna*$^{H222P/H222P}$ mice's (discussed later in the review) primary myoblasts and in *Lmna*$^{H222P/H222P}$ mice's skeletal muscle tissue [78]. These results therefore suggest that lamin A sumoylation impairment is involved in the disease mechanism underlying striated muscle laminopathies.

Overall, the data from patient cells and immortalized cell lines demonstrate the wide breadth of the effects caused by mutations in the lamin A/C gene. Nonetheless, such cellular phenotypic analyses can be further characterized using derived cells from the patients' induced pluripotent stem cells (iPSCs). These iPSCs can be of immense benefit, particularly in cases when multiple tissue phenotypes are co-present, as there will be no need to collect multiple cell types from the patients. Some studies using laminopathy patient iPSCs are discussed in the next section.

2.6. Derived Myogenic or Cardiac Cells from Patients' Induced iPSCs Replicated Previously Demonstrated Muscular Laminopathy Cellular Phenotypes with 3D Culturing: A Promising Method of Identifying and Examining More Subtle Morphological Defects in Mutant Cells

In primary culture, dermal fibroblasts from the p.R225X lamin A/C DCM-CD patient presented with decreased lamin A/C and profound nuclear defects including condensed heterochromatin clumps, nuclear blebs, nuclear pore complexes (NPCs) clustering, and mitochondria around the nuclear envelope [79]. Electrical induction of these fibroblasts resulted in a significant increase in the senescence and apoptosis in the mutant cells; inhibition of the ERK 1/2 branch of the MAPK pathway ameliorated this phenotype [79]. Cardiomyocytes were then derived from the iPSCs obtained from the fibroblasts of the p.R225X patient and another DCM-CD patient with a different lamin A/C truncation [79,80]. Surprisingly, both the mutant cardiomyocytes were morphologically comparable to WT [79]. However, upon electrical stimulation, these mutant cardiomyocytes presented with nuclear senescence and a marked increase in apoptosis [79]. The electrical susceptibility of these cardiomyocytes seems to be caused by lamin A/C haploinsufficiency as electrical stimulation of *LMNA* knocked-down control cells resulted in the same phenotype as the mutant cells [79]. Another study using derived myogenic cells from the iPSCs of patients with various striated muscle laminopathies (p.K32del, p.L35P and

p.R249W) presented with deformed nuclei and aberrant localization of emerin (localized in one pole of the cells) and lamin B1 [81]. Lamins A and C also formed aggregates or displayed a honeycomb pattern [81]. Although an abnormal nuclear shape (observed in p.L35P and p.R249W cells) and mislocalized lamin A/C (observed in p.R249W cells) were noted in the myotubes (differentiated myoblasts), the phenotype tended to be less pronounced in the myotubes than in the myoblasts [81]. Interestingly, 3D culturing of these mutant myotubes, which better simulate the cellular environment in patients, enhanced the phenotypes observed compared to what was seen in the monolayer-cultured myotubes [81]. These data therefore highlight the immense potential of iPSCs to model striated laminopathies and the promising use of 3D culturing as a means to detect, identify and more accurately characterize cellular changes that might not be readily observable in 2D culturing.

3. Animal Models

In order to further confirm the pathogenicity of certain *LMNA* mutations and to study the phenotypes and tease out disease-associated pathways while minimizing confounding variables such as comorbidity, defined and controlled strains of different animal models have been used to study striated laminopathies.

3.1. Caenorhabditis elegans (Worm) Models

Worm Models Mimicked Patient Cellular Phenotypes, Highlighted the Role of Lamin A/C in Germ Cells and Reproduction, and Further Confirmed Results from Cell Lines and Mice Models

The worm species *Caenorhabditis elegans* (*C. elegans*) possesses one lamin gene (*lmn-1*) that codes for lamin-1, the equivalent of the B-type lamins but functionally similar to both A and B

type lamins [82]. Gonadal knockdown of *lmn-1* via RNAi resulted in abnormal embryos that are developmentally arrested and have abnormal nuclear morphology and disrupted chromatin [83]. Animals that survived lmn-1 knockdown and grew to adulthood were either sterile or semi-sterile [83]. The sterile animals presented with a significant reduction of germ cells, some of which showed abnormalities [83]. Similarly, meiotic arrest and apoptosis were observed in *Lmna*$^{\Delta 8\text{-}11}$ male mice germ cells (however, oogenesis in mice was unaffected) [84]. Moreover, siRNA knockdown of *Lmna* in the seminiferous tubules of mice resulted in sperm with abnormal heads [85]. Nevertheless, the progenies of the semi-sterile adult *C. elegans* were fertile and had an increased male proportion compared to WT [83]. NPCs were also misarranged in the nuclei of embryonic cells with decreased lamin-1, and such defects have been observed in cell lines, other animal models and patients [45, 61, 83,86]. Expression of GFP-tagged p.K46del lamin-1 variant, an equivalent of the p.K32del EDMD/L-CMD human lamin A/C variant, also resulted in lamin misassembly, nuclear aggregates, emerin mislocalization (due to decreased binding to lamin) and muscle/movement abnormalities [87–89]. Further evaluation of 14 laminopathic variants (including EDMD and DCM variants) located throughout the protein showed abnormal homodimer assembly, as well as mislocalization and abnormal dynamics of lamin-1 and/or aberrant mislocalization/dynamics and even lethality in vivo [90]. Moreover, as in cells transfected with certain lamin A/C variants, emerin was found in some of the lamin-1 variant aggregates [50,90]. The expression of the p.Y59C EDMD lamin-1 variant led to tissue-specific muscle promoter inactivation, coupled with aberrant muscle gene expression changes, resulting in muscle disruption and decreased muscle function [91].

3.2. Drosophila melanogaster (Fruit Fly) Models

Fruit Fly Models Phenocopied Early Lethality in *LMNA* Null Patients, Demonstrated Cytosketal Disturbance, Presented with Muscle and Mobility Defects, and Associated the Oxidative/Reductive Stress Signalling Pathway (via Nrf2) to Striated Muscle Laminopathies

Similar to the *lmn-1* gene of *C. elegans*, the *Drosophila melanogaster LamC* gene encoding lamin-C is also a paralogue of the lamin A/C gene in vertebrates [92]. *LamC* null fruit fly and truncated Lamin-C variants fruit flies (deletion of the first 42 or 48 N-terminal residues) were generated and resulted in developmental delay and prepupal death [93,94]. Larval muscle-specific expression of the 42 a.a. N-terminal truncated lamin C variant, however resulted in some viability but the survivors presented with deformed legs in adulthood, caused by the absence of muscular function and the disturbance of ecdysone (moulting) hormone signalling [94]. Immunostaining for the fruit fly B-type lamin (lamin Dm0) in both the null and the N-terminal deleted mutants showed lamin B nuclear aggregation [93]. On the other hand, ectopic overexpression of a 9 a.a truncated lamin C variant resulted in formation of melanotic tumours, lag in growth, inhibition of pupation and morbidity at the larval stage [95]. In the *LamC* null fruit fly, localization of B-type lamins and heterochromatin was normal, but NPC clustering was observed [96]. Furthermore, nuclear aberrations including chromatin leakage were detected in the cells of imaginal discs of *LamC* null larvae compared to WT [96]. Abnormal nuclear shape and actin localization in the nucleus were also seen in muscle samples from *LamC* null flies [96].

Expression of a variety of EDMD and DCM *LMNA* variants in fruit fly resulted in a host of nuclear aberrations such as lamin-C aggregates and/or increased nuclear blebbing, which are similar to what were previously observed in transfected cells expressing striated muscle laminopathy mutations [53,93,96]. C-terminal and N-terminal truncated lamin-C expression also

both resulted in nuclear abnormalities [96]. In addition, when the N-terminal truncated lamin-C or the p.W557S (human equivalent: p.W520S) variant was expressed either ubiquitously or in a muscle-specific manner, lethality was observed [96]. Evaluation of nuclear stiffness in WT and mutant lamin-C demonstrated increased nuclear fragility in the 48 a.a. N-terminal truncated lamin C variant, further illustrating the importance of the lamin N-terminus in muscles [97]. Muscle-specific expression of another set of muscular laminopathy mutations resulted in larval muscular and mobility defects, actin disruption, nuclear protein mislocalization in the cytoplasm and varying degrees of mortality in mutant pupae [97,98]. Transcriptome analyses from mutant and WT body muscle wall samples showed elevated expression levels of detoxification genes in mutant samples compared to WT [97]. An increase in the TF Nrf2 involved in activating detoxification genes was observed, along with an increase in p62/SQSTM1, an autophagosome cargo protein involved in capturing Keap1, a protein that sequesters Nrf2 [97]. The release of Nrf2 from Keap1 allows Nrf2 to translocate to the nucleus, where it upregulates genes coding for antioxidant proteins [97]. Muscle biopsies from striated muscle laminopathy patients presented with increased staining for p62/SQSTM1 [97]. This illustrated the activation of the oxidative/reductive stress signalling pathway (via Nrf2) in muscles [97].

3.3. Danio rerio (Zebrafish) Models

Zebrafish models mirrored patient and mice model cardiac and skeletal muscle phenotypes, and presented a feasible avenue to facilitate high throughput drug and therapeutic target screening

Danio rerio (*D. rerio*), popularly known as the zebrafish, belongs to the osteichthyan branch, which also includes mice and humans. The zebrafish *lmna* is an orthologue of human *LMNA*. The

zebrafish is an established model of cardiac diseases owing to its cardiac system's relative comparability to its mammalian counterpart, its transparency during early development, which allows for organ observation, its high fecundity and its ability to tolerate severe cardiac dysfunction that would be lethal at the foetal level in mammals [99,100]. A study by Koshimizu et al. showed that morpholino (MO) knockdown of zebrafish *lmna* resulted in slow skeletal muscle fibres damage at 24 h post-fertilization (hpf) [101]. Moreover, about half of the morphants also presented with craniofacial deformity and an increase in apoptosis in the brain and trunk [101]. Such an increase in apoptosis is further verified by impaired cell cycle progression [101]. Decreased lipid levels associated with decreased levels of zebrafish PPAR-gamma, suggestive of defects in adipocyte differentiation, were also observed [101]. Another study with MO-mediated *lmna* knockdown showed that the zebrafish lamin A/C morphants presented with blood congestion at 24 hpf, cardiac oedema, decreased heart rate, and decreased cardiac function during the period of observation (48–96 hpf) [100]. Such phenotypes are indicative of progression towards heart failure. Furthermore, some of the *lmna* morphants presented with some form of cardiac arrhythmia including atrial fibrillation, thus closely phenocopying *LMNA* mutation-caused DCM disease presentation in humans [100]. A disrupted nuclear membrane was also observed [100].

Aside from morphants, zebrafish mutant lamin A/C transgenic lines have also been generated to study striated muscle laminopathies. Two transgenic lines with cardiac-specific expression of GFP-tagged zebrafish *lmna* EDMD variants were created by Verma and Parnaik [102]. Homozygous mutant lamin A/C transgenic zebrafish have comparable fertility and longevity as WT lamin A/C transgenics up to one year old [102]. However, mutant zebrafish cardiomyocytes presented with abnormal nuclear shape, lamin aggregates (particularly the p.Q291P mutants) and an increase in heart rate at 3.5 and 5.5 d post-fertilization compared to WT [102]. Moreover, an

upregulation of the expression of genes involved in cardiac regeneration was observed in whole embryo extracts from homozygous mutant lamin A/C transgenic embryos compared to WT lamin A/C transgenics [102]. In addition, PCNA, a marker for proliferation, was increased in the adult hearts of mutant transgenic lines compared to WT transgenic [102].

3.4. Mus musculus (Mice) Models

Out of the animal models discussed in this review, *Mus musculus* (*M. musculus*) is the species most closely related to us. The mice prelamin A shares 96.4% amino acid sequence identity with human prelamin A (Table S1). Such conservation between humans and mice lamin A/C also extends to numerous aspects of anatomy and physiology, including both species having a four-chambered heart that functions comparably. Thus, mice models provide a means to reproduce the human disease phenotype in a more closely phylogenetically related species. Various genetic modifications—knock-out, transgenesis and knock-in—have been used and yielded high fidelity in vivo striated muscle laminopathy models.

3.4.1. *Lmna* Null Mice Models Proved the Causal Link between Lamin and Human Laminopathy Phenotypes, Resulting in Lethality in the Young—but Heterozygous Mice Failed to Show the Laminopathy Phenotype.

To further elucidate the importance and function of A-type lamins, *Lmna* knock-out mice were created. The lamin A/C null mice were generated using the gene trap technology [103]. No lamin A/C transcript or protein was detectable in the $Lmna^{GT-/-}$ mice and both emerin and NPCs were mislocalized [103]. The $Lmna^{GT-/-}$ mice presented with severe growth delay starting at seven days after birth and died at 2–3 weeks after birth [103]. No notable phenotype was observed in the heterozygous mice [103]. Transcriptome analyses prior to onset and after the onset of phenotype

in the lamin A/C null mice showed deregulation of genes involved in metabolism, adipogenesis, muscle contraction and cardiac differentiation compared to WT. Unlike in some patient samples and other striated laminopathy mouse models, there were no observed disorganized or dystrophic muscles and no fibrosis in cardiac tissues of the *Lmna*$^{GT-/-}$ mice [38,103]. Although cell proliferation levels were comparable to WT, notable cardiac hypotrophy, which worsened with age, was observed in homozygous mice [103]. However, no functional or anatomical abnormalities (i.e., enlarged cardiac chambers/thinning of cardiac walls) were observed in homozygous hearts, except for a moderate decrease in heart rate when compared to WT [103]. Skeletal muscle was also evaluated in the homozygous mice as these animals exhibited a hunched posture and abnormal gait by 13 days of age [103]. Similar to cardiomyocytes, skeletal myocytes were hypotrophic but were neither disorganized nor dystrophic [103]. Although gonadal fat stores and brown fat were present and normal in the *Lmna*$^{GT-/-}$ mice, subcutaneous fat was lacking [103]. Thus, adipogenic differentiation was induced in MEFs of the lamin A/C null mice and it was discovered that there was an impairment in the ability of the cells to differentiate into adipocytes when compared to induced cells from WT [103]. Metabolic parameters were also assessed and mice without lamin A/*C* become hypoglycemic and increasingly catabolic compared to WT [103]. All of these thereby illustrated the significance of lamin A/C in the context of striated muscle and fat cell differentiation, development and growth during the early stages after birth.

Another *Lmna* null (*Lmna*$^{\Delta/\Delta}$) mice was created using a different technique, Cre-mediated recombination [104]. The *Lmna*$^{\Delta/\Delta}$ mice were indistinguishable from their littermates at birth [104]. However, after two weeks, *Lmna*$^{\Delta/\Delta}$ mice weighed about half as much as their siblings and died by 16–18 days of age [104]. Haematoxylin and eosin staining of skeletal muscle of 15-day-old *Lmna*$^{\Delta/\Delta}$ mice showed significantly smaller muscle fibres compared to WT mice [104]. These

characteristics were comparable to those observed in the *Lmna*$^{GT-/-}$ mice [103,104]. In order to characterize and highlight the importance of each A-type lamin and its proper processing, another group of mice models was examined.

3.4.2. Homozygous C-Terminal Truncated Lamin A Mice Model Recapitulated the *Lmna* Null Mice Phenotype and the Heterozygous Mice Displayed a Late-Onset Cardiac Phenotype

A very well characterized model is the *Lmna*$^{\Delta 8\text{-}11}$ mice expressing a truncated lamin A that lacks its C-terminus [61,105]. It was the first (unsuccessful) attempt to create a Lamin A/C null mouse and was made by deleting exon 8 to mid-exon 11 of the *Lmna* gene [61]. The *Lmna*$^{\Delta 8\text{-}11}$ mice were comparable at birth to their heterozygous and WT siblings [61]. However, significant growth retardation was noted starting at 2–3 weeks after birth and by week 3–4, major gait defects were observed and all homozygous mice were dead by eight weeks [61]. In addition, the homozygous mice weighed considerably less than their siblings (about half their weight) [61,62]. Moreover, there was a significant increase in the organ to body weight ratio in most tissues of the *Lmna*$^{\Delta 8\text{-}11}$ mice compared to WT [62]. This could be a result of increased organ function (e.g., kidneys) or a maladaptive organ enlargement (e.g., heart) [62]. Histological analyses of the cardiac and skeletal muscle tissues of *Lmna*$^{\Delta 8\text{-}11}$ mice showed dystrophy, although no significant increase in creatine kinase was observed [61]. Lamin A/C transcript levels between affected (e.g., skeletal muscles) and unaffected (e.g., adipose tissues) tissues also did not seem to differ [106]. This suggested that lamin A/C levels do not contribute to the tissue-specific expression of disease phenotype in this model [106]. Furthermore, although the homozygous mice exhibited a deficit in fat tissue, analyses of metabolic parameters of these mice did not show strong lipodystrophic traits reminiscent of FPLD [61,106]. However, results from a more recent biochemical serum test hinted at potential liver dysfunction due to a significant increase in alanine aminotransferase and aspartate

transaminase, which are markers for liver disease, when compared to levels found in their heterozygous and WT siblings [62]. Immunostaining of MEFs from *Lmna*$^{\Delta 8\text{-}11}$ mice for lamina-associated polypeptide 2 (LAP2), Nup153 (component of NPCs) and lamin B showed misshapen nuclei and mislocalization of proteins such as lamin B and emerin, mimicking what was observed in the lamin A/C null cells of the child homozygous for the p.Y259X lamin A/C variant [46,61].

On the other hand, heterozygous mice (*Lmna*$^{\Delta 8\text{-}11/+}$) displayed late-onset cardiomyopathy (with or without CD) with no skeletal muscle defect [107]. At 10 weeks, 62% (n = 18) of *Lmna*$^{\Delta 8\text{-}11/+}$ mice exhibited rhythm or conduction abnormalities compared to none in WT mice (n = 17) [107]. Histochemical analyses of cardiac tissue also showed increased atrioventricular node fibrosis and apoptosis, and elongated nuclei in conductive cells compared to WT [107]. Moreover, aged (>50 weeks) heterozygous mice presented with significantly enlarged cardiac chambers and decreased fractional shortening indicative of both morphological and functional abnormalities [107]. However, levels of MAPK members were normal, unlike in the p.H222P EDMD mice model (to be discussed later in the review) [21,107].

3.4.3. Mice Expressing Non-Farnesylated Prelamin A Only, Mature Lamin A Only or Lamin C Only Showed the Importance of Lamin A Processing and the Respective Roles of Lamins A and C in the Pathogenesis of Laminopathies

As opposed to the *Lmna*$^{\Delta 8\text{-}11}$ and *Lmna*$^{\Delta 8\text{-}11/+}$ mice models that express a truncated lamin A, this next mice model expresses non-farnesylated prelamin A only (*Lmna*$^{\text{nPLAO/nPLAO}}$) [61,107,108]. These *Lmna*$^{\text{nPLAO/nPLAO}}$ mice presented with and died because of dilated cardiomyopathy [108]. Fibroblasts from *Lmna*$^{\text{nPLAO/nPLAO}}$ mice had increased nucleoplasmic prelamin A localization and nuclear blebs, but there was no significant change in the nuclear stiffness [108]. However, Coffinier et al. demonstrated a notable decrease in nuclear stiffness in the *Lmna*$^{\text{nPLAO/nPLAO}}$ MEFs

compared to WT [109]. Overall, *Lmna*$^{nPLAO/nPLAO}$ mice died prematurely (all males died by 44 weeks and females by 80 weeks) [108]. Cardiac assessment and histology showed a dilated left ventricle, decreased left ventricular ejection fraction, and mild to moderate fibrosis [108]. Moreover, as in cardiomyopathy, qRT-PCR revealed decreased myosin heavy-chain alpha (*Myh6*) expression and increased myosin heavy-chain beta (*Myh7*) expression [108]. It was suggested that non-farnesylated prelamin A acted as a poison or that non-farnesylated prelamin A is less effective than mature lamin A, leading to haploinsufficiency [108]. Both hypotheses have been suggested for the development of dilated cardiomyopathy in humans [64,110,111]. Although inhibition of farnesyltransferase has been shown to improve the progeroid phenotypes, the accumulation of non-farnesylated prelamin A may result in the development of cardiomyopathy [108,112].

In contrast to the *Lmna*$^{nPLAO/nPLAO}$ mice, mature lamin-A-only-expressing mice (*Lmna*^{LAO}) were normal, healthy, did not present any discernible pathological phenotype and had comparable survival (>24 months) to WT mice [109]. Lamin A was predominantly located in the nuclear rim, similar to WT [109]. However, a significant increase in the frequency of misshapen nuclei and nuclear blebs was observed in fibroblasts from the *Lmna*^{LAO} mice compared to WT [109]. Closer inspection of the blebs showed a honeycomb staining pattern for both lamin A and LAP2β, but no difference was observed between the nuclear stiffness of WT and *Lmna*^{LAO} mice [109]. This suggested that more localized lamina structural defects such as blebbing do not necessarily result in significant global nuclear mechanical defects and subsequent clinical onset of laminopathy [109].

A mouse model that lacks lamin A but expresses lamin C only (*Lmna*^{LCO}) was comparable to WT with no overt physiological and cellular defects (in either cardiac or skeletal muscles) over two years of observation [56]. Analyses of primary fibroblasts from *Lmna*^{LCO} embryos also

showed that lamin C, emerin and LAP2 localization was normal and that there was no significant alteration in nuclear lamina structure [56]. However, a notable increase in nuclear strain in response to mechanical stress was observed in *Lmna*^{LCO} cells when compared to WT cells [56]. This showed that lamin A is essential to the nuclear lamina's ability to respond to mechanical stress.

Although the mice models discussed so far provide valuable information to determine and understand the respective roles of lamins A and C and their importance as a whole, such models do not recapitulate the genetic context in most laminopathy patients. The knock-in and transgenic mice allow for better mimicking of the diseased state found in patients.

3.4.4. *Lmna* Knock-In and Transgenic Mice Further Established the Genotype and Phenotype Correlation and Revealed Several Signalling Pathways Involved in the Development of Myopathies Caused by *LMNA* Mutations

The p.N195K lamin A/C variant is associated with DCM-CD in humans [52]. The homozygous p.N195K lamin A/C mice (*Lmna*$^{N195K/N195K}$) had a mild delay in weight gain beginning at four weeks but appeared to be otherwise healthy until an acute period of deterioration followed by death at 12–14 weeks after birth [86]. The homozygous males died before the homozygous females [86]. The heterozygous p.N195K mice had a comparable life span to the WT [86]. No hallmark signs of muscular dystrophy were observed in *Lmna*$^{N195K/N195K}$ mice but mild muscular degeneration and cardiac chamber dilatation coupled with thinning of the chamber walls were noted in cardiac tissues [86]. In line with the restructuring occurring in cardiac tissues in DCM, there was an increase in interstitial fibrosis and upregulation of foetal genes such as the atrial natriuretic peptide (ANP) and brain natriuretic peptide (BNP) [86]. Furthermore, *Lmna*$^{N195K/N195K}$ mice presented with a significant decrease in fractional shortening compared to

their siblings at eight weeks, and the condition worsened with age [86]. Close monitoring and examination of the heart further revealed that the homozygous p.N195K mice presented with episodes of severe bradycardia and conduction defects, which caused death in these animals [86]. Characterization of the ventricular myocyte action potential showed longer duration associated with an increase in late sodium (Na^+) current in the homozygous mice compared to WT [113]. Primary mouse embryonic fibroblasts from homozygous mice also showed abnormal nuclear shape, mislocalization of emerin and Nup154 (a component of NPCs), disruption of the cytoskeleton and seemingly enlarged endoplasmic reticulum and mitochondria [86]. The muscle-specific intermediate filament desmin, which connects the contractile apparatus to the sarcolemmal cytoskeleton, the organelles and the nucleus, was disorganized and less expressed in cardiac tissues from the *Lmna*$^{N195K/N195K}$ mice [86]. In addition, connexin (CX) 40 and 43, proteins involved in gap junctions responsible for pulse relay, were mislocalized, with slightly lower amounts of CX40 in mutant atria compared to WT [86]. These therefore show that *LMNA* mutations impact the physiology of the entire cell, including the plasma membrane organization, through their effect on an intermediate filament protein like desmin. Mis-expression of the transcription factor Hf1b/Sp4, which is important in cardiac cell differentiation, particularly for the development of the cardiac conduction system, was also noted [86,114]. This model therefore mimicked the presentation of the disease in humans and demonstrated the involvement of gap junction proteins and Hf1b/Sp4 in the aberrant cardiac electrical relay that is seen in *LMNA*-related DCM-CD.

Another model for DCM-CD is transgenic mice with cardiac-specific expression of the p.E82K lamin A/C variant (*Lmna*^{E82K}) [115]. This variant results from an exon 1 *LMNA* mutation identified in a Chinese family with DCM-CD (atrioventricular block) [116,117]. Transgenics were comparable to their non-transgenic siblings at birth and at a young age [115]. A portion (11–16%)

of transgenic mice died starting at three months old [115]. Gross morphological changes include increased heart to body weight ratio and dilation of both cardiac chambers [115]. Cardiac functional assessment also showed a decrease in heart rate and cardiac function [115]. Moreover, like in the p.H222P mice model, interstitial fibrosis and disorganized cardiac muscle cells were also observed [115,118]. The nuclear membrane was compromised, and enlarged mitochondria and sarcoplasmic reticulum were noted [115]. In addition, elevated levels of markers for hypertrophy such as BNP, actin alpha 1 and collagen III alpha 1 were observed [115]. Thus, the mutation affecting a region in the lamin A/C protein involved in forming homodimers negatively affected actin alpha 1 and collagen III alpha 1 structural proteins that are both involved in contractility, thereby potentially causing cardiac dysfunction in the p.E82K transgenic mice. Furthermore, the transgenic mice heart displayed an increase in apoptosis, which may be linked to the decrease in left ventricular function and eventual heart failure [115].

To model another type of striated muscle laminopathy, EDMD, which also oftentimes co-present with a cardiac phenotype, a transgenic mouse with cardiac-specific expression of the p.M371K lamin A variant causing EDMD in humans was created [41,119]. This variant resulted in high prenatal deaths in the transgenics [119]. Furthermore, transgenic mice live for 2–7 weeks only [119]. Histology of cardiac tissues from transgenic mice showed cardiac lesions, pulmonary and cardiac oedema; however, unlike other models, they did not present fibrosis [119]. Immunostaining of cardiac sections showed deformed nuclei and lamin A aggregates that were colocalized with lamin B1 [119]. Similar to some patient tissues and other mouse models, electron microscopy of p.M371K mice cardiac samples also showed chromatin clumps and lipid pseudo-inclusions in the deformed nuclei [119]. However, the fibres containing these nuclei were generally

neither apoptotic nor necrotic [119]. These results illustrated that, when overexpressed in the heart, an EDMD mutant acted in a dominant negative manner, mimicking human DCM presentation.

To model another EDMD laminopathy associated with arrhythmia, the *LMNA* mutation substituting A to C at nucleotide position 665, resulting in the lamin A/C protein p.H222P variant, was expressed in mice [41]. The homozygous p.H222P knock-in mice model (*Lmna*$^{H222P/H222P}$) presented with skeletal and cardiac phenotypes mimicking the human disease presentation. All homozygous mice died at 13 months [118]. Analyses of tissue samples showed dilatation of the ventricles, accompanied by thinning of the ventricular wall, cardiomyocyte degeneration and fibrosis [118]. Locomotor behaviour was also impaired and further examination of muscle tissues showed a wide range of abnormalities [118]. A significant increase in nuclear localization of phosphorylated-Smad2/3 was observed in *Lmna*$^{H222P/H222P}$ mice compared to their heterozygous and WT siblings [118]. These proteins are part of the TGF-β signalling pathway, which is involved in the fibrotic process [118]. Moreover, as in the human disease presentation, there was a difference between the severity and temporal onset of the phenotype between genders in the H222P mice [118, 120,121]. Investigating this difference, Arimura et al. showed an increase in the nuclear accumulation of androgen receptors and their co-factors (serum response factor [SRF] and four-and-a half LIM protein-2 (FHL2)) in male cardiac tissues from patients with DCM associated with *LMNA* mutations [121]. Furthermore, castration or flutamide (an antagonist of androgen receptors) treatment improved the symptoms of the diseased p.H222P male mice, while testosterone administration to female p.H222P mice exacerbated their phenotype [121]. Therefore, phenotype severity of *LMNA*-related DCM may depend on sex hormone levels and inhibition of the androgen receptor–SRF–FHL2 complex may provide a potential therapeutic benefit [121]. The MAPK kinase pathway (ERK 1/2, p38α, JNK branches) and its downstream targets were also involved in

striated muscle laminopathies in both patients and *Lmna*$^{H222P/H222P}$ mice cardiac and/or skeletal muscle samples [21,67,122]. Inhibition of the ERK 1/2, JNK, or p38α signalling pathways rescued the cardiac and/or skeletal muscle phenotypes of the *Lmna*$^{H222P/H222P}$ mice [67,122–126]. Similarly, a combination of angiotensin II converting enzyme (ACE) and MEK 1/2 inhibitors improved the cardiac phenotype in the p.H222P mice [127]. Further analyses of the *Lmna*$^{H222P/H222P}$ mice implicated the AKT/mTor and WNT/β-catenin pathways [67,128,129]. Indeed, inhibition of mTor and activation of WNT/β-catenin signalling improved the cardiac function in the homozygous p.H222P mice [67,128,129]. Impaired autophagy has also been observed in the cardiac tissues of both the human patients and the *Lmna*$^{H222P/H222P}$ mice and the inhibition of mTor improved autophagy in the p.H222P mice hearts [128]. Gap junction architecture was disturbed in the *Lmna*$^{H222P/H222P}$ mice as seen in the *Lmna*$^{N195K/N195K}$ mice [86,129]. However, the localization of emerin was normal in striated muscles [118]. Therefore, this EDMD mouse model revealed new pathways that underlie striated muscle laminopathies, and that can potentially be targeted for therapeutic intervention.

A third EDMD mice model expressing another variant, the truncated p.K32del lamin A/C variant (*Lmna*$^{\Delta K32/\Delta K32}$), which results in severe EDMD or L-CMD in patients, was generated [88,89]. The *Lmna*$^{\Delta K32/\Delta K32}$ mice presented with major growth retardation and died three weeks after birth due to severe metabolic deficiencies associated with the repression of SREBF-1 [130]. Moreover, similar to what was observed in *C. elegans*, this lamin A/C protein variant is present in low amounts, suggesting its instability compared to the WT lamins [87,130]. The p.K32del variant also remained nucleoplasmic compared to the WT lamin A/C, which was found in both the nucleoplasm and nuclear rim [130]. On the other hand, the heterozygous p.K32del lamin A/C mice (*Lmna*$^{\Delta K32/+}$) progressively developed DCM and died at between 35 and 70 weeks of age [65]. No

phenotype difference was observed between males and females [65]. Upregulation of mRNA levels for cardiac remodelling markers (*Nppb*, *Myh7*) was noted at 10 weeks (a time point that precedes notable phenotype) [65]. Immunostaining and electron microscopy revealed overt nuclear aberrations in the cardiomyocytes of heterozygous mice, particularly towards the end stage of the disease [65]. In the heterozygous mice heart tissue, total lamin A/C protein (WT and variant) levels were deemed to be 50% lower than the amounts in age-matched (10 weeks, 30 weeks) WT mice, but this discrepancy was abrogated at 57 weeks when an increase in total lamin A/C was observed [65]. The restoration of total cardiac lamin A/C in older $Lmna^{\Delta K32/+}$ mice was caused by the impairment of the ubiquitin–proteasome system [65]. This system was determined to be involved in the degradation of lamin A/C variant proteins in the hearts of younger $Lmna^{\Delta K32/+}$ mice [65]. Thus, the results suggested that the p.K32del lamin A/C variant acted as a toxic molecule and its increasing amount with age was detrimental to the $Lmna^{\Delta K32/+}$ mice, which eventually developed cardiomyopathy.

However, not all mice models faithfully mimic the human phenotype. The p.L530P lamin A/C variant was discovered in a patient with autosomal dominant EDMD [44]. Heterozygous p.L530P knock-in mice were comparable to their WT siblings up to six months old [131]. However, the homozygous p.L530P mice ($Lmna^{L530P/L530P}$) started presenting phenotype reminiscent of HGPS at 4–6 days old and died within 4–5 weeks [131]. Mild to intermediate degeneration, hypoplasia and atrophy of the cardiac and skeletal muscles were observed in $Lmna^{L530P/L530P}$mice [131]. Furthermore, there were fewer myocytes but an increase in fibrocytes in mutant tissues was observed [12]. At the cellular level, nuclear disruption was also observed in $Lmna^{L530P/L530P}$ MEFs as well as a decrease in nuclear lamin A, and a mislocalization of lamin C to the cytoplasm instead of in the nucleus [131]. Nevertheless, no hallmarks of muscular dystrophy (e.g., centrally located

nuclei and muscle fibres of various diameters) were noted and the mouse phenotype was consistent with progeria even though this mutation at the heterozygous state was associated with skeletal muscle laminopathy in humans [44], [131].

4. Discussion and Conclusions

The evidence thus far demonstrates the wide array and importance of the presence and function of A-type lamins in maintaining cellular processes, as indicated by the diversity of diseases caused by *LMNA* mutations. Although *LMNA* mutations are known to cause distinct laminopathy disorders in humans, there is a large spectrum of sometimes contradictory findings obtained in cellular and animal models. One should not underestimate the fact that most mechanistic outcomes stem from models with inherent pitfalls. Differences in results between cell lines can be attributed to various reasons including the type of cell line used, the plasmid used for transfection (e.g., a difference in expression levels of transgene based on the promoter used), the presence or absence of a C or N termini reporter tag of various sizes, the duration of transient transfection, and which lamin (A or C) is being transfected [49,50,53]. Selecting a cell line based on the tissue-specific presentation of the disease (e.g., skeletal muscle cell lines for EDMD) is more appropriate because the cellular context in which the mutant transgene will be expressed corresponds to the cell type affected in the patients. The importance of the cell line selection can be seen in the transfection of the DCM mutant lamin A producing the p.E203G variant. In p.E203G lamin A-expressing HeLa cells, lamin aggregates were found but no such aggregates were observed upon expression in C2C12 cells [15,53]. Transfection of both lamins A and C maintains the endogenous stoichiometry between the two isoforms, therefore mimicking the naturally occurring state in cells. It also better recapitulates the autosomal dominant form of laminopathies in humans because double-transfected cells express both the WT lamin A/C (endogenous) and the

mutated lamin A/C (transfected; exogenous). However, only lamin A has been expressed in most cellular models. Derived cells from iPSCs of patients, especially when cultured in 3D, present a promising means to model laminopathies as these cells demonstrate high fidelity in mimicking the patient cellular phenotypes [81]. Moreover, iPSCs not only allow for the derivation of various cell types, which is very useful in laminopathies affecting multiple tissue types, but can also circumvent the limitations associated with senescence in primary cells after prolonged culturing [51]. In addition, since these cells are from the patients themselves, they may help reconcile the diversity in phenotypes observed in cellular and animal models. The cells can also be used for personalized therapeutic tests. However, as we progress in the use of iPSCs to model diseases and conduct clinical tests, we must consider the efficiency (currently typically low (<1%)) and methods used (via viruses or synthesized RNAs or proteins or small molecules) to generate iPSCs [132]. Moreover, iPSCs have been shown to differ from the original cells in terms of somatic mutations, copy number variations and DNA methylation [132,133]. Further investigation and understanding of such genomic changes in iPSCs will ensure not only the fidelity of the derived cells in reproducing the disease but, more importantly, their safety when administered to humans as treatment. Nevertheless, iPSCs and 3D culturing possess immense potential to model laminopathies and advance the field.

Although cell line models are more manageable to handle and cheaper than in vivo models, both cellular and animal models are complementary when modelling a complex human disorder. The animal models enable not only the identification of the molecular mechanisms affected by the variant protein, but also frame the results in the context of a living organism as a whole with the opportunity to further probe the phenotype and molecular implications in specific and relevant organs/tissues in real time and/or post-mortem, as well as to eventually test for treatments.

Differences or inconsistencies between the phenotypes of animal models of the same species can be a consequence of the respective techniques used. Such is the case in *Lmna*$^{\Delta 8\text{-}11}$ mice, which were initially deemed to be null but later proven to express a C-terminal truncated lamin A, and the real *Lmna* null—the *Lmna* KO mice (*Lmna*$^{GT\text{-}/\text{-}}$) created using gene trap technology, in which no lamin A/C transcript or protein was detectable [61,103,105]. The genetic background of the strain used can also have an effect on the phenotype [103]. Furthermore, the expression pattern of the transgene can cause a varying phenotype. Such a situation was observed in fruit flies, where a difference in viability was noted depending on whether the transgene was expressed ubiquitously, in a tissue-specific manner, or temporally induced (e.g., under heat-shock-driven expression) [96].

On the other hand, despite the immense progress afforded by both cellular and animal models, there are still differences in phenotypes between the actual human disease presentation and the models. For instance, both knock-out/knock-in mice models and transgenic zebrafish primarily presented a phenotype at the homozygous state, while in humans the conditions are predominantly autosomal dominant [61,86,102,103,108,115]. The heterozygous animals had milder or no symptoms, a different phenotype, or the disease onset was considerably delayed compared to their homozygous siblings (e.g., *Lmna*$^{GT\text{-}/\text{-}}$ mice; *Lmna*$^{\Delta 8\text{-}11}$ and *Lmna*$^{\Delta 8\text{-}11/+}$ mice; *Lmna*$^{\Delta K32/\Delta K32}$ and *Lmna*$^{\Delta K32/+}$ mice) [61,65,103,107,130]. In addition, some mutations result in a different laminopathy when expressed in the model organism (e.g., the *Lmna*$^{L530P/L530P}$ mice, see above). Furthermore, in humans, not all *LMNA* mutation carriers actually present a phenotype. Some individuals bearing the same mutation as their affected family members remain asymptomatic. This is not usually the case in the published animal models (i.e., all homozygous mice presented a phenotype). Nevertheless, the fact that animal models do not perfectly recapitulate human phenotype can be partly attributed to the genetic modification used (knockdown versus knock-out

or transgenesis or knock-in), species differences and external variables. Neither a knock-down (transient) nor a knock-out (permanent) animal model that seeks to significantly lower or completely abolish gene function is a blanket representative of the human disease context because most patients possess pathogenic mutations that do not abrogate *LMNA* gene function but instead result in the production of variant lamin A/C proteins. Moreover, although transgenesis enables tissue-specific expression of mutant transgenes, the results are influenced by the fact that endogenous WT lamin A/C is still being expressed in the animals. The insertion sites, number of insertions and expression levels of transgene are less defined and are usually not consistent between lines. In addition, in some studies, the phenotype in the transgenics becomes less overt or disappears after a few generations [134]. Knock-in models, on the other hand, would be the most faithful at recapitulating the genetic context of the mutation, but differences between species might influence and/or cause discrepancies between the human phenotype and animal models. Alignment (Figure S1) and percentage sequence identity (Table S1) between human prelamin A and its orthologues/paralogs in the different animal models cited show a range of sequence identity from 30% in *C. elegans* lamin-1 to 96.4% in *M. musculus*. Another example of species difference is with zebrafish, which underwent genome duplication, resulting in functional duplicates of orthologues for some human genes. Though the *LMNA* gene has one identified orthologue in zebrafish, *SYNE1*, which codes for the lamin A/C interacting partner Syne1, has two orthologues in zebrafish, *syne1a* and *syne1b*. In terms of anatomy, fruit flies, for instance, have a tubal heart and zebrafish only have two cardiac chambers. Thus, these species differences could contribute to the differences in phenotype between animal models and the actual human disease presentation. Other variables that can influence the phenotype also include the gene pool, environmental conditions, co-morbidities and technology. Humans have vast genetic diversity compared to that

of laboratory animals. Co-morbidities include hypertension, myocarditis, autosomal disorders, diabetes, obesity, high cholesterol, inactivity, as well as aging and treatments such as chemotherapy. The effects of the environment/lifestyle on the organism are also important, particularly since for each human being the experience is unique, while lab animals live in unnatural and controlled standard lab settings. Lastly, the lag in our capacity to identify and/or characterize phenotypes in human and animal models limits our understanding of the scale and intricacies of the disease.

Altogether, the insights learned from both cellular and animal models so far suggest that there is no one hypothesis that can completely explain the mechanisms underlying striated muscle laminopathies. However, the gene and/or mechanical hypotheses seem to provide an explanation for the cardiac and/or skeletal muscles phenotypes in most cases. The overlap in phenotypes between humans and models, particularly the phenotypic features common to more than one model, highlights the important and conserved pathways involved in the pathogenesis of striated muscle laminopathies. Tables 1 and 2 highlight these affected proteins and signalling pathways. An example of such commonality due to the presence of pathogenic muscular *LMNA* mutations is the nuclear membrane disturbance(s) that compromises the structure, integrity, shape and/or size of the nucleus [15,38,46,50,51,54,73,87,90,91,96]. These changes can impair the ability of A-type lamins to interact with each other or with other proteins and/or chromatin. In turn, such disturbances affect the function and regulation of lamin A/C binding partners as well as the accessibility of certain chromatin regions, thereby affecting gene expression and overall cell function, including mechano-transduction signalling. Tissue-specific effects that present as the primary overt phenotype of an affected individual might be partly attributed to the resulting physical and chemical properties changes in the lamin A/C protein variants that negatively impact

tissue-specific interactions and functions. Such vulnerabilities can result in mishandled cellular stimuli that feed back into the already compromised network, further magnifying the malignant cell response, with the most affected system(s) presenting as the dominant clinical symptom. In cases where the same mutation presents a different phenotype (e.g., symptomatic versus asymptomatic; difference in affected tissue) between individuals, such a contrast in disease presentation might be attributed to several factors including the state of zygosity, genetic background, epigenetic background and lifestyle. Some *LMNA* mutations exert their effects on a recessive mode. An example is the *LMNA* mutation resulting in the p.H222Y variant that caused severe EDMD for the homozygous patient, while both his heterozygous parents were asymptomatic [135]. Another lamin A/C variant, p.R298C, was identified in multiple families from Algeria and Morocco, where individuals carrying the mutation at the heterozygous state were unaffected or presented with EDMD or isolated cardiac disease and, at the homozygous state, predominantly presented with the neuropathic disease CMT2B1 [136–140]. The prevalence and presence (or absence) of a particular tissue-specific primary phenotype plus the varying onset and severity of clinical presentation in the families are probably influenced by differences in the genetic, epigenetic and lifestyle contexts.

Table 1. Summary of prominent and overlapping protein mislocalization in cellular and animal laminopathy models.

Mislocalized Proteins	Role	Mislocalization	Model(s)/Patient sample(s)
1. Lap2 (α, β)	regulation of nuclear architecture	absence in nuclear poles and/or lobules, honeycomb pattern in nuclear blebs	fibroblasts from homozygous p.Y259X patient [46], *Lmna* ^{LAO} mice [109], *Lmna*$^{\Delta 8\text{-}11}$ mice MEFs [61]
2. Emerin	anchorage to the cytoskeleton	cytoplasmic, concentration in one pole, sequestration within nuclear lamin foci, honeycomb pattern	fibroblasts from homozygous p.Y259X patient [46], RNAi *LMNA* knockdown in HeLa cells [48], various lamin A/C variants expressed in different cell lines[49,50], *C. elegans* [90], fibroblasts from patients with various lamin A/C

			mutations[51], myogenic cells derived from myopathies patients' iPSCs [81], *Lmna*$^{\Delta 8\text{-}11}$ mice [50,61], *Lmna*$^{N195K/N195K}$ mice [86], p.K46del lamin-1 variant *C. elegans* [87]
3. Syne1	anchorage to the cytoskeleton	cytoplasmic	fibroblasts from homozygous p.Y259X patient [46]
4. B-type lamins	involved in a variety of functions including regulation of expression, mitosis, cellular senescence	absence in one pole (i.e., concentration in one pole only) and/or absence in nuclear lobules, honeycomb pattern	fibroblasts from homozygous p.Y259X patient [46], fibroblasts from patients with various lamin A/C mutations [51], myogenic cells derived from myopathies patients' iPSCs [81], *LamC* null and Lamin-C N-terminal deleted *D. melanogaster* mutants [93], *Lmna*$^{\Delta 8\text{-}11}$ mice MEFs [61], cardiac expressing p.M371K lamin A/C mice [119]
5. Nup153, Nup154	component of the nuclear pore complex	absence in nuclear poles and/or lobules, clustering	fibroblasts from homozygous p.Y259X patient [46], fibroblasts from p. R225X patient [79], RNAi *lmn-1* knockdown in *C. elegans* [83], *Lmna*$^{\Delta 8\text{-}11}$ mice [61], *Lmna*$^{N195K/N195K}$ mice [86], *LamC* null and various lamin A/C mutations expressed in *D. melanogaster* [96], *Lmna*$^{GT\text{-}/\text{-}}$ mice [103], *Lmna*$^{\Delta 8\text{-}11}$ mice MEFs [61]
6. SUMO1	post-translational modifications	sequestration within nuclear lamin foci	various lamin A/C variants expressed in Cos7 cells [38], C2C12 cells [78], *Lmna*$^{H222P/H222P}$ mice primary myoblasts [78], *Lmna*$^{H222P/H222P}$ mice skeletal muscle tissue [78]
7. Actin	cytoskeletal component	filament disorganization, increased nuclear localization, and decreased expression	neonatal rat ventricular myocytes expressing various mutant lamin A/C [34], *LamC* null *D. melanogaster* [96], Lamin-C N-terminal deleted and various lamin A/C mutations expressed in *D. melanogaster* [97], patient myoblasts expressing various L-CMD variants [35, 36]
8. ERK ½ (phosphorylated)	involved in a variety of cellular responses	increased nuclear localization	*Lmna*$^{H222P/H222P}$ mice, p.H222P lamin A expressing Cos7 and C2C12 cells [21]
9. Smad2/3 (phosphorylated)	TGF-β signalling pathway	increased nuclear localization	*Lmna*$^{H222P/H222P}$ mice [118]
10. Androgen receptors, SRF - FHL2	mediating actions of androgens	nuclear accumulation	neonatal rat cardiomyocytes expressing p.H222P variant or p.R225X variant [121], *Lmna*$^{H222P/H222P}$ mice and cardiac tissue from DCM patients [121]

11. Cx40, Cx43	gap junction proteins	Diffused pattern and decreased expression in atria	*Lmna* $^{N195K/N195K}$ mice [86]

Table 2. Summary of prominent and overlapping affected proteins and signalling pathways in cellular and animal laminopathy models.

Models		Affected Proteins and Signalling Pathways	Reference(s)
Cellular Models	1. Fibroblasts from p.E203K DCM patient or HeLa transfected cells	↓ sumoylation	[77]
	2. Various lamin A/C variants expressed in neonatal rat ventricular myocytes	inhibition of p38 = rescue of actin and mechanical phenotype	[34]
	3. p. L530P (EDMD)	↓ binding to SREBF1	[15]
	4. Fibroblasts from p. R225X patient	inhibition of MEK/ERK 1/2 = rescue (decreased apoptosis and senescence)	[79]
	5. Myoblasts from patients expressing various L-CMD variants	deregulation of yes-associated protein and formins	[35, 36]
Animal Models	6. Various lamin A/C variants expressed in *D. melanogaster*	↑ Nrf2, p62/SQSTM1	[97]
	7. *D. rerio lmna* morphants	↓ pparγ, ↓ PCNA	[101]
	8. *D. rerio lmna* transgenics	↑ PCNA	[102]
	9. *Lmna*$^{nPLAO/nPLAO}$ mice	↓ Myh6, ↑ Myh7	[108]
	10. *Lmna*$^{N195K/N195K}$ mice	reactivation of foetal genes (↑ANP, ↑ BNP), inhibition of Na^+ channel = improve symptom, ↓ connexin 40, mis-expression of Hf1b/Sp4	[86]
	11. Mice cardiac tissue only expression of p.E82K lamin A/C variant	hypertrophy markers (↑ in BNP, actin alpha 1, collagen type III alpha 1), ↑ FAS, ↑ cytochrome C	[115]
	12. *Lmna*$^{H222P/H222P}$ mice	TGFβ (↑ nuclear phos-Smad 2/3), ↑ MAPK members (ERK 1/2, p38, JNK),	[21, 67,121–129]

	↑ AKT/mTor, ↓ WNT/β-catenin	
13. *Lmna*$^{\Delta K32/\Delta K32}$ mice	repression of SREBF1	[130]
14. Muscle tissues from patients with various myopathies	phos-lamin A/C (Ser458) by Akt	[73]
15. *Lmna*$^{\Delta K32/+}$ mice	↑ Nppb, ↑ Myh7	[65]

With the advent of the CRISPR/Cas9 technology, genetic manipulation has become more accessible and more precise; thus, the modelling of human diseases can be even further improved. Creating knock-in *LMNA* mutations in more relevant cellular models would usher an improved model that can better mimic what is found in patient cells. The use of iPSCs from patients also allows for a superior simulation of the cell type and tissue-specific conditions. Moreover, since iPSCs are patient-specific, derived cells can be used to conduct personalized drug screens, therefore facilitating a personalized medicine approach to treating the disease. In terms of vertebrate in vivo models, the zebrafish, with its quick, transparent development and high fecundity, allows for mass drug screening. In addition, the determination of specific molecular signatures prior to disease onset is now more feasible, thus eventually enabling clinicians to improve predictive diagnostic capabilities that may allow for prophylactic treatments to either prevent or delay disease onset and attenuate the severity of the disease. Lastly, as evidenced by the progress in the field arising from results obtained from animal models (specifically the H222P EDMD mice), a clinical trial involving a p38 inhibitor (ARRY-371797) to treat patients with DCM caused by *LMNA* mutations is in progress. Phase 2 results showed improved functional capacity (assessed by a 6-min walking test) and cardiac function with mild to moderate adverse effects (Clinical Trials ID: NCT03439514), thus raising our hopes that it can be used to treat laminopathies in the future [141].

5. Funding: This review received no external funding.

6. Conflicts of Interest: The authors declare no conflict of interest.

7. References

1. Mercuri, E.; Brown, S.C.; Nihoyannopoulos, P.; Poulton, J.; Kinali, M.; Richard, P.; Piercy, R.J.; Messina, S.; Sewry, C.; Burke, M.M.; et al. Extreme variability of skeletal and cardiac muscle involvement in patients with mutations in exon 11 of the lamin A/C gene. *Muscle Nerve*. **2005**, *31*, 602–609, doi:10.1002/mus.20293.
2. Francisco, A.R.G.; Santos Gonçalves, I.; Veiga, F.; Mendes Pedro, M.; Pinto, F.J.; Brito, D. Complex phenotype linked to a mutation in exon 11 of the lamin A/C gene: Hypertrophic cardiomyopathy, atrioventricular block, severe dyslipidemia and diabetes. *Revista Portuguesa Cardiol.* **2017**, *36*, 699.e1–699.e4, doi:10.1016/j.repc.2016.07.018.
3. Forleo, C.; Carmosino, M.; Resta, N.; Rampazzo, A.; Valecce, R.; Sorrentino, S.; Iacoviello, M.; Pisani, F.; Procino, G.; Gerbino, A.; et al. Clinical and functional characterization of a novel mutation in lamin a/c gene in a multigenerational family with arrhythmogenic cardiac laminopathy. *PLoS ONE* **2015**, *10*, e0121723, doi:10.1371/journal.pone.0121723.
4. Kato, K.; Takahashi, N.; Fujii, Y.; Umehara, A.; Nishiuchi, S.; Makiyama, T.; Ohno, S.; Horie, M. LMNA cardiomyopathy detected in Japanese arrhythmogenic right ventricular cardiomyopathy cohort. *J. Cardiol*. **2016**, *68*, 346–351, doi:10.1016/j.jjcc.2015.10.013.
5. Quarta, G.; Syrris, P.; Ashworth, M.; Jenkins, S.; Zuborne Alapi, K.; Morgan, J.; Muir, A.; Pantazis, A.; McKenna, W.J.; Elliott, P.M. Mutations in the Lamin A/C gene mimic arrhythmogenic right ventricular cardiomyopathy. *Eur. Heart J*. **2012**, *33*, 1128–1136, doi:10.1093/eurheartj/ehr451.
6. Lin, F.; Worman, H.J. Structural organization of the human gene encoding nuclear lamin A and nuclear lamin C. *J. Biol. Chem*. **1993**, *268*, 16321–16326.
7. Stewart, C.; Burke, B. Teratocarcinoma stem cells and early mouse embryos contain only a single major lamin polypeptide closely resembling lamin B. *Cell* **1987**, *51*, 383–392.
8. McKeon, F.D.; Kirschner, M.W.; Caput, D. Homologies in both primary and secondary structure between nuclear envelope and intermediate filament proteins. *Nature* **1986**, *319*, 463–468, doi:10.1038/319463a0.
9. Agarwal, A.K.; Fryns, J.-P.; Auchus, R.J.; Garg, A. Zinc metalloproteinase, ZMPSTE24, is mutated in mandibuloacral dysplasia. *Hum. Mol. Genet*. **2003**, *12*, 1995–2001.
10. Machiels, B.M.; Zorenc, A.H.; Endert, J.M.; Kuijpers, H.J.; van Eys, G.J.; Ramaekers, F.C.; Broers, J.L. An alternative splicing product of the lamin A/C gene lacks exon 10. *J. Biol. Chem*. **1996**, *271*, 9249–9253.
11. Furukawa, K.; Inagaki, H.; Hotta, Y. Identification and cloning of an mRNA coding for a germ cell-specific A-type lamin in mice. *Exp. Cell Res*. **1994**, *212*, 426–430, doi:10.1006/excr.1994.1164.
12. Alsheimer, M.; Benavente, R. Change of karyoskeleton during mammalian spermatogenesis: Expression pattern of nuclear lamin C2 and its regulation. *Exp. Cell Res*. **1996**, *228*, 181–188, doi:10.1006/excr.1996.0315.

13. Stuurman, N.; Heins, S.; Aebi, U. Nuclear lamins: Their structure, assembly, and interactions. *J. Struct. Biol*. **1998**, *122*, 42–66.
14. Broers, J.L.; Ramaekers, F.C.; Bonne, G.; Yaou, R.B.; Hutchison, C.J. Nuclear lamins: Laminopathies and their role in premature ageing. *Physiol. Rev*. **2006**, *86*, 967–1008.
15. Lloyd, D.J.; Trembath, R.C.; Shackleton, S. A novel interaction between lamin A and SREBP1: Implications for partial lipodystrophy and other laminopathies. *Hum. Mol. Genet*. **2002**, *11*, 769–777.
16. Clements, L.; Manilal, S.; Love, D.R.; Morris, G.E. Direct interaction between emerin and lamin A. *Biochem. Biophys. Res. Commun*. **2000**, *267*, 709–714, doi:10.1006/bbrc.1999.2023.
17. Sakaki, M.; Koike, H.; Takahashi, N.; Sasagawa, N.; Tomioka, S.; Arahata, K.; Ishiura, S. Interaction between emerin and nuclear lamins. *J. Biochem. (Tokyo)* **2001**, *129*, 321–327.
18. Cartegni, L.; di Barletta, M.R.; Barresi, R.; Squarzoni, S.; Sabatelli, P.; Maraldi, N.; Mora, M.; Di Blasi, C.; Cornelio, F.; Merlini, L. Heart-specific localization of emerin: New insights into Emery-Dreifuss muscular dystrophy. *Hum. Mol. Genet.* **1997**, *6*, 2257–2264.
19. Eriksson, M.; Brown, W.T.; Gordon, L.B.; Glynn, M.W.; Singer, J.; Scott, L.; Erdos, M.R.; Robbins, C.M.; Moses, T.Y.; Berglund, P.; et al. Recurrent de novo point mutations in lamin A cause Hutchinson-Gilford progeria syndrome. *Nature* **2003**, *423*, 293–298, doi:10.1038/nature01629.
20. Yang, S.H.; Meta, M.; Qiao, X.; Frost, D.; Bauch, J.; Coffinier, C.; Majumdar, S.; Bergo, M.O.; Young, S.G.; Fong, L.G. A farnesyltransferase inhibitor improves disease phenotypes in mice with a Hutchinson-Gilford progeria syndrome mutation. *J. Clin. Invest*. **2006**, *116*, 2115–2121, doi:10.1172/JCI28968.
21. Muchir, A.; Pavlidis, P.; Decostre, V.; Herron, A.J.; Arimura, T.; Bonne, G.; Worman, H.J. Activation of MAPK pathways links LMNA mutations to cardiomyopathy in Emery-Dreifuss muscular dystrophy. *J. Clin. Invest.* **2007**, *117*, 1282–1293.
22. Yokoyama, C.; Wang, X.; Briggs, M.R.; Admon, A.; Wu, J.; Hua, X.; Goldstein, J.L.; Brown, M.S. SREBP-1, a basic-helix-loop-helix-leucine zipper protein that controls transcription of the low density lipoprotein receptor gene. *Cell* **1993**, *75*, 187–197.
23. Tontonoz, P.; Kim, J.B.; Graves, R.A.; Spiegelman, B.M. ADD1: A novel helix-loop-helix transcription factor associated with adipocyte determination and differentiation. *Mol. Cell Biol*. **1993**, *13*, 4753–4759.
24. Kim, J.B.; Spiegelman, B.M. ADD1/SREBP1 promotes adipocyte differentiation and gene expression linked to fatty acid metabolism. *Genes Dev*. **1996**, *10*, 1096–1107.
25. Diraison, F.; Ravier, M.A.; Richards, S.K.; Smith, R.M.; Shimano, H.; Rutter, G.A. SREBP1 is required for the induction by glucose of pancreatic beta-cell genes involved in glucose sensing. *J. Lipid Res*. **2008**, *49*, 814–822, doi:10.1194/jlr.M700533-JLR200.
26. Hasty, A.H.; Shimano, H.; Yahagi, N.; Amemiya-Kudo, M.; Perrey, S.; Yoshikawa, T.; Osuga, J.; Okazaki, H.; Tamura, Y.; Iizuka, Y.; et al. Sterol regulatory element-binding protein-1 is regulated by glucose at the transcriptional level. *J. Biol. Chem*. **2000**, *275*, 31069–31077, doi:10.1074/jbc.M003335200.
27. Boguslavsky, R.L.; Stewart, C.L.; Worman, H.J. Nuclear lamin A inhibits adipocyte differentiation: Implications for Dunnigan-type familial partial lipodystrophy. *Hum. Mol. Genet.* **2006**, *15*, 653–663, doi:10.1093/hmg/ddi480.
28. Wojtanik, K.M.; Edgemon, K.; Viswanadha, S.; Lindsey, B.; Haluzik, M.; Chen, W.; Poy, G.; Reitman, M.; Londos, C. The role of LMNA in adipose: A novel mouse model of

lipodystrophy based on the Dunnigan-type familial partial lipodystrophy mutation. *J. Lipid Res*. **2009**, *50*, 1068–1079, doi:10.1194/jlr.M800491-JLR200.
29. Lanzicher, T.; Martinelli, V.; Puzzi, L.; Del Favero, G.; Codan, B.; Long, C.S.; Mestroni, L.; Taylor, M.R.; Sbaizero, O. The Cardiomyopathy Lamin A/C D192G Mutation Disrupts Whole-Cell Biomechanics in Cardiomyocytes as Measured by Atomic Force Microscopy Loading-Unloading Curve Analysis. *Sci. Rep*. **2015**, *5*, 13388, doi:10.1038/srep13388.
30. Zwerger, M.; Jaalouk, D.E.; Lombardi, M.L.; Isermann, P.; Mauermann, M.; Dialynas, G.; Herrmann, H.; Wallrath, L.L.; Lammerding, J. Myopathic lamin mutations impair nuclear stability in cells and tissue and disrupt nucleo-cytoskeletal coupling. *Hum. Mol. Genet.* **2013**, *22*, 2335–2349, doi:10.1093/hmg/ddt079.
31. Lammerding, J.; Schulze, P.C.; Takahashi, T.; Kozlov, S.; Sullivan, T.; Kamm, R.D.; Stewart, C.L.; Lee, R.T. Lamin A/C deficiency causes defective nuclear mechanics and mechanotransduction. *J. Clin. Invest.* **2004**, *113*, 370–378, doi:10.1172/JCI19670.
32. Lee, J.S.H.; Hale, C.M.; Panorchan, P.; Khatau, S.B.; George, J.P.; Tseng, Y.; Stewart, C.L.; Hodzic, D.; Wirtz, D. Nuclear lamin A/C deficiency induces defects in cell mechanics, polarization, and migration. *Biophys. J.* **2007**, *93*, 2542–2552, doi:10.1529/biophysj.106.102426.
33. Lammerding, J.; Fong, L.G.; Ji, J.Y.; Reue, K.; Stewart, C.L.; Young, S.G.; Lee, R.T. Lamins A and C but not lamin B1 regulate nuclear mechanics. *J. Biol. Chem*. **2006**, *281*, 25768–25780, doi:10.1074/jbc.M513511200.
34. Laurini, E.; Martinelli, V.; Lanzicher, T.; Puzzi, L.; Borin, D.; Chen, S.N.; Long, C.S.; Lee, P.; Mestroni, L.; Taylor, M.R.G.; et al. Biomechanical defects and rescue of cardiomyocytes expressing pathologic nuclear lamins. *Cardiovasc. Res*. **2018**, *114*, 846–857, doi:10.1093/cvr/cvy040.
35. Schwartz, C.; Fischer, M.; Mamchaoui, K.; Bigot, A.; Lok, T.; Verdier, C.; Duperray, A.; Michel, R.; Holt, I.; Voit, T.; et al. Lamins and nesprin-1 mediate inside-out mechanical coupling in muscle cell precursors through FHOD1. *Sci. Rep*. **2017**, *7*, 1253, doi:10.1038/s41598-017-01324-z.
36. Bertrand, A.T.; Ziaei, S.; Ehret, C.; Duchemin, H.; Mamchaoui, K.; Bigot, A.; Mayer, M.; Quijano-Roy, S.; Desguerre, I.; Lainé, J.; et al. Cellular microenvironments reveal defective mechanosensing responses and elevated YAP signaling in LMNA-mutated muscle precursors. *J. Cell Sci*. **2014**, *127 Pt 13*, 2873–2884, doi:10.1242/jcs.144907.
37. Tesson, F.; Saj, M.; Uvaize, M.M.; Nicolas, H.; Płoski, R.; Bilińska, Z. Lamin A/C mutations in dilated cardiomyopathy. *Cardiol. J*. **2014**, *21*, 331–342, doi:10.5603/CJ.a2014.0037.
38. Sylvius, N.; Bilinska, Z.T.; Veinot, J.P.; Fidzianska, A.; Bolongo, P.M.; Poon, S.; McKeown, P.; Davies, R.A.; Chan, K.L.; Tang, A.S.; et al. In vivo and in vitro examination of the functional significances of novel lamin gene mutations in heart failure patients. *J. Med. Genet*. **2005**, *42*, 639–647.
39. Taylor, M.R.; Fain, P.R.; Sinagra, G.; Robinson, ML.; Robertson, A.D.; Carniel, E.; Di Lenarda, A.; Bohlmeyer, T.J.; Ferguson, D.A.; Brodsky, G.L.; et al. Natural history of dilated cardiomyopathy due to lamin A/C gene mutations. *J. Am. Coll. Cardiol*. **2003**, *41*, 771–780.
40. Hasselberg, N.E.; Haland, T.F.; Saberniak, J.; Brekke, P.H.; Berge, K.E.; Leren, T.P.; Edvardsen, T.; Haugaa, K.H. Lamin A/C cardiomyopathy: Young onset, high penetrance, and frequent need for heart transplantation. *Eur. Heart J*. **2018**, *39*, 853–860, doi:10.1093/eurheartj/ehx596.

41. Bonne, G.; Mercuri, E.; Muchir, A.; Urtizberea, A.; Bécane, H.M.; Recan, D.; Merlini, L.; Wehnert, M.; Boor, R.; Reuner, U.; et al. Clinical and molecular genetic spectrum of autosomal dominant Emery-Dreifuss muscular dystrophy due to mutations of the lamin A/C gene. *Ann. Neurol*. **2000**, *48*, 170–180.
42. Quijano-Roy, S.; Mbieleu, B.; Bönnemann, C.G.; Jeannet, P.Y.; Colomer, J.; Clarke, N.F.; Cuisset, J.M.; Roper, H.; De Meirleir, L.; D'Amico, A.; et al. De novo LMNA mutations cause a new form of congenital muscular dystrophy. *Ann. Neurol*. **2008**, *64*, 177–186, doi:10.1002/ana.21417.
43. Muchir, A.; Bonne, G.; van der Kooi, A.J.; van Meegen, M.; Baas, F.; Bolhuis, P.A.; de Visser, M.; Schwartz, K.. Identification of mutations in the gene encoding lamins A/C in autosomal dominant limb girdle muscular dystrophy with atrioventricular conduction disturbances (LGMD1B). *Hum. Mol. Genet.* **2000**, *9*, 1453–1459.
44. Bonne, G.; Barletta, M.R.D.; Varnous, S.; Bécane, H.M.; Hammouda, E.H.; Merlini, L.; Muntoni, F.; Greenberg, C.R.; Gary, F.; Urtizberea, J.A.; et al. Mutations in the gene encoding lamin A/C cause autosomal dominant Emery-Dreifuss muscular dystrophy. *Nat. Genet*. **1999**, *21*, 285–288.
45. van Engelen, B.G.M.; Muchir, A.; Hutchison, C.J.; van der Kooi, A.J.; Bonne, G.; Lammens, M. The lethal phenotype of a homozygous nonsense mutation in the lamin A/C gene. *Neurology* **2005**, *64*, 374–376, doi:10.1212/01.WNL.0000149763.15180.00.
46. Muchir, A.; van Engelen, B.G.; Lammens, M.; Mislow, J.M.; McNally, E.; Schwartz, K.; Bonne, G. Nuclear envelope alterations in fibroblasts from LGMD1B patients carrying nonsense Y259X heterozygous or homozygous mutation in lamin A/C gene. *Exp. Cell Res*. **2003**, *291*, 352–362.
47. Hutchison, C.J. B-type lamins in health and disease. *Semin. Cell Dev. Biol*. **2014**, *29*, 158–163, doi:10.1016/j.semcdb.2013.12.012.
48. Harborth, J.; Elbashir, S.M.; Bechert, K.; Tuschl, T.; Weber, K. Identification of essential genes in cultured mammalian cells using small interfering RNAs. *J. Cell Sci.* **2001**, *114 Pt 24*, 4557–4565.
49. Raharjo, W.H.; Enarson, P.; Sullivan, T.; Stewart, C.L.; Burke, B. Nuclear envelope defects associated with LMNA mutations cause dilated cardiomyopathy and Emery-Dreifuss muscular dystrophy. *J. Cell Sci.* **2001**, *114 Pt 24*, 4447–4457.
50. Holt, I.; Ostlund, C.; Stewart, C.L.; thi Man, N.; Worman, H.J.; Morris, G.E. Effect of pathogenic mis-sense mutations in lamin A on its interaction with emerin in vivo. *J. Cell Sci.* **2003**, *116 Pt 14*, 3027–3035, doi:10.1242/jcs.00599.
51. Muchir, A.; Medioni, J.; Laluc, M.; Massart, C.; Arimura, T.; van der Kooi, A.J.; Desguerre, I.; Mayer, M.; Ferrer, X.; Briault, S.; et al. Nuclear envelope alterations in fibroblasts from patients with muscular dystrophy, cardiomyopathy, and partial lipodystrophy carrying lamin A/C gene mutations. *Muscle Nerve*. **2004**, *30*, 444–450.
52. Fatkin, D.; MacRae, C.; Sasaki, T.; Wolff, M.R.; Porcu, M.; Frenneaux, M.; Atherton, J.; Vidaillet, H.J. Jr.; Spudich, S.; De Girolami, U.; et al. Missense mutations in the rod domain of the lamin A/C gene as causes of dilated cardiomyopathy and conduction-system disease. *N. Engl. J. Med*. **1999**, *341*, 1715–1724.
53. Ostlund, C.; Bonne, G.; Schwartz, K.; Worman, H.J. Properties of lamin A mutants found in Emery-Dreifuss muscular dystrophy, cardiomyopathy and Dunnigan-type partial lipodystrophy. *J. Cell Sci.* **2001**, *114 Pt 24*, 4435–4445.

54. Sylvius, N.; Hathaway, A.; Boudreau, E.; Gupta, P.; Labib, S.; Bolongo, P.M.; Rippstein, P.; McBride, H.; Bilinska, Z.T.; Tesson, F. Specific contribution of lamin A and lamin C in the development of laminopathies. *Exp. Cell Res.* **2008**, *314*, 2362–2375.
55. Motsch, I.; Kaluarachchi, M.; Emerson, L.J.; Brown, C.A.; Brown, S.C.; Dabauvalle, M.C.; Ellis, J.A. Lamins A and C are differentially dysfunctional in autosomal dominant Emery-Dreifuss muscular dystrophy. *Eur. J. Cell Biol*. **2005**, *84*, 765–781, doi:10.1016/j.ejcb.2005.04.004.
56. Fong, L.G.; Ng, J.K.; Lammerding, J.; Vickers, T.A.; Meta, M.; Coté, N.; Gavino, B.; Qiao, X.; Chang, S.Y.; Young, S.R.; et al. Prelamin A and lamin A appear to be dispensable in the nuclear lamina. *J. Clin. Invest.* **2006**, *116*, 743–752, doi:10.1172/JCI27125.
57. Vigouroux, C.; Magré, J.; Vantyghem, M.C.; Bourut, C.; Lascols, O.; Shackleton, S.; Lloyd, D.J.; Guerci, B.; Padova, G.; Valensi, P.; et al. Lamin A/C gene: Sex-determined expression of mutations in Dunnigan-type familial partial lipodystrophy and absence of coding mutations in congenital and acquired generalized lipoatrophy. *Diabetes* **2000**, *49*, 1958–1962.
58. Simon, D.N.; Zastrow, M.S.; Wilson, K.L. Direct actin binding to A- and B-type lamin tails and actin filament bundling by the lamin A tail. *Nucl. Austin Tex*. **2010**, *1*, 264–272, doi:10.4161/nucl.1.3.11799.
59. Buendia, B. LMNA p.R482W mutation related to FPLD2 alters SREBP1-A type lamin interactions in human fibroblasts and adipose stem cells. *Orphanet J. Rare Dis*. **2015**, *10*, O13, doi:10.1186/1750-1172-10-S2-O13.
60. Vadrot, N.; Duband-Goulet, I.; Cabet, E.; Attanda, W.; Barateau, A.; Vicart, P.; Gerbal, F.; Briand, N.; Vigouroux, C.; Oldenburg, A.R.; et al. The p.R482W substitution in A-type lamins deregulates SREBP1 activity in Dunnigan-type familial partial lipodystrophy. *Hum. Mol. Genet.* **2015**, *24*, 2096–2109, doi:10.1093/hmg/ddu728.
61. Sullivan, T.; Escalante-Alcalde, D.; Bhatt, H.; Anver, M.; Bhat, N.; Nagashima, K.; Stewart, C.L.; Burke, B. Loss of A-type lamin expression compromises nuclear envelope integrity leading to muscular dystrophy. *J. Cell Biol*. **1999**, *147*, 913–920.
62. Ruan, J.; Liu, X.G.; Zheng, H.L.; Li, J.B.; Xiong, X.D.; Zhang, C.L.; Luo, C.Y.; Zhou, Z.J.; Shi, Q.; Weng, Y.G. Deletion of the lmna gene induces growth delay and serum biochemical changes in C57BL/6 mice. *Asian-Australas J. Anim. Sci*. **2014**, *27*, 123–130, doi:10.5713/ajas.2013.13246.
63. Gilchrist, S.; Gilbert, N.; Perry, P.; Ostlund, C.; Worman, H.J.; Bickmore, W.A. Altered protein dynamics of disease-associated lamin A mutants. *BMC Cell Biol*. **2004**, *5*, 46, doi:10.1186/1471-2121-5-46.
64. Gupta, P.; Bilinska, Z.T.; Sylvius, N.; Boudreau, E.; Veinot, J.P.; Labib, S.; Bolongo, P.M.; Hamza, A.; Jackson, T.; Ploski, R.; et al. Genetic and ultrastructural studies in dilated cardiomyopathy patients: A large deletion in the lamin A/C gene is associated with cardiomyocyte nuclear envelope disruption. *Basic Res. Cardiol*. **2010**, *105*, 365–377.
65. Cattin, M.-E.; Bertrand, A.T.; Schlossarek, S.; Le Bihan, M.C.; Skov Jensen, S.; Neuber, C.; Crocini, C.; Maron, S.; Lainé, J.; Mougenot, N.; et al. Heterozygous LmnadelK32 mice develop dilated cardiomyopathy through a combined pathomechanism of haploinsufficiency and peptide toxicity. *Hum. Mol. Genet.* **2013**, *22*, 3152–3164, doi:10.1093/hmg/ddt172.
66. Nikolova, V.; Leimena, C.; McMahon, A.C.; Tan, J.C.; Chandar, S.; Jogia, D.; Kesteven, S.H.; Michalicek, J.; Otway, R.; Verheyen, F.; et al. Defects in nuclear structure and function promote dilated cardiomyopathy in lamin A/C-deficient mice. *J. Clin. Invest.* **2004**, *113*, 357–369.

67. Muchir, A.; Wu, W.; Choi, J.C.; Iwata, S.; Morrow, J.; Homma, S.; Worman, H.J. Abnormal p38alpha mitogen-activated protein kinase signaling in dilated cardiomyopathy caused by lamin A/C gene mutation. *Hum. Mol. Genet.* **2012**, *21*, 4325–4333.
68. Cargnello, M.; Roux, P.P. Activation and function of the MAPKs and their substrates, the MAPK-activated protein kinases. *Microbiol. Mol. Biol. Rev*. **2011**, *75*, 50–83, doi:10.1128/MMBR.00031-10.
69. Cobb, A.M.; Larrieu, D.; Warren, D.T.; Liu, Y.; Srivastava, S.; Smith, A.J.O.; Bowater, R.P.; Jackson, S.P.; Shanahan, C.M. Prelamin A impairs 53BP1 nuclear entry by mislocalizing NUP153 and disrupting the Ran gradient. *Aging Cell*. **2016**, *15*, 1039–1050, doi:10.1111/acel.12506.
70. Larrieu, D.; Britton, S.; Demir, M.; Rodriguez, R.; Jackson, S.P. Chemical inhibition of NAT10 corrects defects of laminopathic cells. *Science* **2014**, *344*, 527–532, doi:10.1126/science.1252651.
71. Davidson, P.M.; Lammerding, J. Broken nuclei--lamins, nuclear mechanics, and disease. *Trends Cell Biol*. **2014**, *24*, 247–256, doi:10.1016/j.tcb.2013.11.004.
72. Kochin, V.; Shimi, T.; Torvaldson, E.; Adam, S.A.; Goldman, A.; Pack, C.G.; Melo-Cardenas, J.; Imanishi, S.Y.; Goldman, R.D.; Eriksson, J.E. Interphase phosphorylation of lamin A. *J. Cell Sci.* **2014**, *127 Pt 12*, 2683–2696, doi:10.1242/jcs.141820.
73. Mitsuhashi, H.; Hayashi, Y.K.; Matsuda, C.; Noguchi, S.; Wakatsuki, S.; Araki, T.; Nishino, I. Specific phosphorylation of Ser458 of A-type lamins in LMNA-associated myopathy patients. *J. Cell Sci.* **2010**, *123 Pt 22*, 3893–3900, doi:10.1242/jcs.072157.
74. Krimm, I.; Ostlund, C.; Gilquin, B.; Couprie, J.; Hossenlopp, P.; Mornon, J.P.; Bonne, G.; Courvalin, J.C.; Worman, H.J.; Zinn-Justin, S. The Ig-like structure of the C-terminal domain of lamin A/C, mutated in muscular dystrophies, cardiomyopathy, and partial lipodystrophy. *Struct. Lond. Engl. 1993*. **2002**, *10*, 811–823.
75. Swift, J.; Ivanovska, I.L.; Buxboim, A.; Harada, T.; Dingal, P.C.; Pinter, J.; Pajerowski, J.D.; Spinler, K.R.; Shin, J.W.; Tewari, M.; et al. Nuclear lamin-A scales with tissue stiffness and enhances matrix-directed differentiation. *Science* **2013**, *341*, 1240104, doi:10.1126/science.1240104.
76. Cenni, V.; Sabatelli, P.; Mattioli, E.; Marmiroli, S.; Capanni, C.; Ognibene, A.; Squarzoni, S.; Maraldi, N.M.; Bonne, G.; Columbaro, M.; et al. Lamin A N-terminal phosphorylation is associated with myoblast activation: Impairment in Emery-Dreifuss muscular dystrophy. *J. Med. Genet*. **2005**, *42*, 214–220, doi:10.1136/jmg.2004.026112.
77. Zhang, Y.-Q.; Sarge, K.D. Sumoylation regulates lamin A function and is lost in lamin A mutants associated with familial cardiomyopathies. *J. Cell Biol*. **2008**, *182*, 35–39, doi:10.1083/jcb.200712124.
78. Boudreau, E.; Labib, S.; Bertrand, A.T.; Decostre, V.; Bolongo, P.M.; Sylvius, N.; Bonne, G.; Tesson, F. Lamin A/C mutants disturb sumo1 localization and sumoylation in vitro and in vivo. *PLoS ONE* **2012**, *7*, e45918.
79. Siu, C.-W.; Lee, Y.-K.; Ho, J.C.-Y.; Lai, W.H.; Chan, Y.C.; Ng, K.M.; Wong, L.Y.; Au, K.W.; Lau, Y.M.; Zhang, J.; et al. Modeling of lamin A/C mutation premature cardiac aging using patient-specific induced pluripotent stem cells. *Aging* **2012**, *4*, 803–822, doi:10.18632/aging.100503.
80. Ho, J.C.Y.; Zhou, T.; Lai, W.-H.; Huang, Y.; Chan, Y.C.; Li, X.; Wong, N.L.; Li, Y.; Au, K.W.; Guo, D.; et al. Generation of induced pluripotent stem cell lines from 3 distinct

laminopathies bearing heterogeneous mutations in lamin A/C. *Aging* **2011**, *3*, 380–390, doi:10.18632/aging.100277.
81. Steele-Stallard, H.B.; Pinton, L.; Sarcar, S.; Ozdemir, T.; Maffioletti, S.M.; Zammit, P.S.; Tedesco, F.S. Modeling Skeletal Muscle Laminopathies Using Human Induced Pluripotent Stem Cells Carrying Pathogenic LMNA Mutations. *Front. Physiol*. **2018**, *9*, 1332, doi:10.3389/fphys.2018.01332.
82. Riemer, D.; Dodemont, H.; Weber, K. A nuclear lamin of the nematode Caenorhabditis elegans with unusual structural features; cDNA cloning and gene organization. *Eur. J. Cell Biol*. **1993**, *62*, 214–223.
83. Liu, J.; Rolef Ben-Shahar, T.; Riemer, D.; Treinin, M.; Spann, P.; Weber, K.; Fire, A.; Gruenbaum, Y. Essential roles for Caenorhabditis elegans lamin gene in nuclear organization, cell cycle progression, and spatial organization of nuclear pore complexes. *Mol. Biol. Cell* **2000**, *11*, 3937–3947, doi:10.1091/mbc.11.11.3937.
84. Alsheimer, M.; Liebe, B.; Sewell, L.; Stewart, C.L.; Scherthan, H.; Benavente, R. Disruption of spermatogenesis in mice lacking A-type lamins. *J. Cell Sci.* **2004**, *117 Pt 7*, 1173–1178, doi:10.1242/jcs.00975.
85. Shen, J.; Chen, W.; Shao, B.; Qi, Y.; Xia, Z.; Wang, F.; Wang, L.; Guo, X.; Huang, X.; Sha, J. Lamin A/C proteins in the spermatid acroplaxome are essential in mouse spermiogenesis. *Reprod. Camb. Engl*. **2014**, *148*, 479–487.
86. Mounkes, L.C.; Kozlov, S.V.; Rottman, J.N.; Stewart, C.L. Expression of an LMNA-N195K variant of A-type lamins results in cardiac conduction defects and death in mice. *Hum. Mol. Genet.* **2005**, *14*, 2167–2180, doi:10.1093/hmg/ddi221.
87. Bank, E.M.; Ben-Harush, K.; Wiesel-Motiuk, N.; Barkan, R.; Feinstein, N.; Lotan, O.; Medalia, O.; Gruenbaum, Y. A laminopathic mutation disrupting lamin filament assembly causes disease-like phenotypes in Caenorhabditis elegans. *Mol. Biol. Cell* **2011**, *22*, 2716–2728, doi:10.1091/mbc.E11-01-0064.
88. D'Amico, A.; Haliloglu, G.; Richard, P.; Talim, B.; Maugenre, S.; Ferreiro, A.; Guicheney, P.; Menditto, I.; Benedetti, S.; Bertini, E.; et al. Two patients with "Dropped head syndrome" due to mutations in LMNA or SEPN1 genes. *Neuromuscul. Disord. NMD* **2005**, *15*, 521–524, doi:10.1016/j.nmd.2005.03.006.
89. Vytopil, M.; Ricci, E.; Dello Russo, A.; Hanisch, F.; Neudecker, S.; Zierz, S.; Ricotti, R.; Demay, L.; Richard, P.; Wehnert, M.; et al. Frequent low penetrance mutations in the Lamin A/C gene, causing Emery Dreifuss muscular dystrophy. *Neuromuscul. Disord. NMD* **2002**, *12*, 958–963.
90. Wiesel, N.; Mattout, A.; Melcer, S.; Melamed-Book, N.; Herrmann, H.; Medalia, O.; Aebi, U.; Gruenbaum, Y. Laminopathic mutations interfere with the assembly, localization, and dynamics of nuclear lamins. *Proc. Natl. Acad. Sci. USA* **2008**, *105*, 180–185, doi:10.1073/pnas.0708974105.
91. Mattout, A.; Pike, B.L.; Towbin, B.D.; Bank, E.M.; Gonzalez-Sandoval, A.; Stadler, M.B.; Meister, P.; Gruenbaum, Y.; Gasser, S.M. An EDMD mutation in C. elegans lamin blocks muscle-specific gene relocation and compromises muscle integrity. *Curr. Biol.* **2011**, *21*, 1603–1614, doi:10.1016/j.cub.2011.08.030.
92. Riemer, D.; Stuurman, N.; Berrios, M.; Hunter, C.; Fisher, P.A.; Weber, K. Expression of Drosophila lamin C is developmentally regulated: Analogies with vertebrate A-type lamins. *J. Cell Sci.* **1995**, *108 Pt 10*, 3189–3198.

93. Schulze, S.R.; Curio-Penny, B.; Li, Y.; Imani, R.A.; Rydberg, L.; Geyer, P.K.; Wallrath, L.L. Molecular genetic analysis of the nested Drosophila melanogaster lamin C gene. *Genetics* **2005**, *171*, 185–196, doi:10.1534/genetics.105.043208.
94. Dialynas, G.; Speese, S.; Budnik, V.; Geyer, P.K.; Wallrath, L.L. The role of Drosophila Lamin C in muscle function and gene expression. *Dev. Camb. Engl*. **2010**, *137*, 3067–3077, doi:10.1242/dev.048231.
95. Stuurman, N.; Delbecque, J.P.; Callaerts, P.; Aebi, U. Ectopic overexpression of Drosophila lamin C is stage-specific lethal. *Exp. Cell Res.* **1999**, *248*, 350–357, doi:10.1006/excr.1999.4396.
96. Schulze, S.R.; Curio-Penny, B.; Speese, S.; Dialynas, G.; Cryderman, D.E.; McDonough, C.W.; Nalbant, D.; Petersen, M.; Budnik, V.; Geyer, P.K.; et al. A comparative study of Drosophila and human A-type lamins. *PLoS ONE* **2009**, *4*, e7564, doi:10.1371/journal.pone.0007564.
97. Dialynas, G.; Shrestha, O.K.; Ponce, J.M.; Zwerger, M.; Thiemann, D.A.; Young, G.H.; Moore, S.A.; Yu, L.; Lammerding, J.; Wallrath, L.L. Myopathic lamin mutations cause reductive stress and activate the nrf2/keap-1 pathway. *PLoS Genet*. **2015**, *11*, e1005231, doi:10.1371/journal.pgen.1005231.
98. Dialynas, G.; Flannery, K.M.; Zirbel, L.N.; Nagy, P.L.; Mathews, K.D.; Moore, S.A.; Wallrath, L.L. LMNA variants cause cytoplasmic distribution of nuclear pore proteins in Drosophila and human muscle. *Hum. Mol. Genet.* **2012**, *21*, 1544–1556, doi:10.1093/hmg/ddr592.
99. Shi, X.; Chen, R.; Zhang, Y.; Yun, J.; Brand-Arzamendi, K.; Liu, X.; Wen, X.Y. Zebrafish heart failure models: Opportunities and challenges. *Amino Acids*. **2018**, *50*, 787–798, doi:10.1007/s00726-018-2578-7.
100. Vogel, B.; Meder, B.; Just, S.; Laufer, C.; Berger, I.; Weber, S.; Katus, H.A.; Rottbauer, W. In-vivo characterization of human dilated cardiomyopathy genes in zebrafish. *Biochem. Biophys. Res. Commun*. **2009**, *390*, 516–522.
101. Koshimizu, E.; Imamura, S.; Qi, J.; Toure, J.; Valdez, D.M. Jr.; Carr, C.E.; Hanai, J.; Kishi, S. Embryonic senescence and laminopathies in a progeroid zebrafish model. *PLoS ONE* **2011**, *6*, e17688.
102. Verma, A.D.; Parnaik, V.K. Heart-specific expression of laminopathic mutations in transgenic zebrafish. *Cell Biol. Int*. **2017**, *41*, 809–819, doi:10.1002/cbin.10784.
103. Kubben, N.; Voncken, J.W.; Konings, G.; van Weeghel, M.; van den Hoogenhof, M.M.; Gijbels, M.; van Erk, A.; Schoonderwoerd, K.; van den Bosch, B.; Dahlmans, V.; et al. Post-natal myogenic and adipogenic developmental: Defects and metabolic impairment upon loss of A-type lamins. *Nucl. Austin Tex*. **2011**, *2*, 195–207, doi:10.4161/nucl.2.3.15731.
104. Kim, Y.; Zheng, Y. Generation and characterization of a conditional deletion allele for Lmna in mice. *Biochem Biophys. Res. Commun*. **2013**, *440*, 8–13, doi:10.1016/j.bbrc.2013.08.082.
105. Jahn, D.; Schramm, S.; Schnolzer, M.; Heilmann, C.J.; de Koster, C.G.; Schütz, W.; Benavente, R.; Alsheimer, M. A truncated lamin A in the Lmna -/- mouse line: Implications for the understanding of laminopathies. *Nucl. Austin Tex*. **2012**, *3*, 463–474, doi:10.4161/nucl.21676.
106. Cutler, D.A.; Sullivan, T.; Marcus-Samuels, B.; Stewart, C.L.; Reitman, M.L. Characterization of adiposity and metabolism in Lmna-deficient mice. *Biochem. Biophys. Res. Commun*. **2002**, *291*, 522–527, doi:10.1006/bbrc.2002.6466.

107. Wolf, C.M.; Wang, L.; Alcalai, R.; Pizard, A.; Burgon, P.G.; Ahmad, F.; Sherwood, M.; Branco, D.M.; Wakimoto, H.; Fishman, G.I.; et al. Lamin A/C haploinsufficiency causes dilated cardiomyopathy and apoptosis-triggered cardiac conduction system disease. *J. Mol. Cell. Cardiol*. **2008**, *44*, 293–303, doi:10.1016/j.yjmcc.2007.11.008.
108. Davies, B.S.J.; Barnes, R.H.; Tu, Y.; Ren, S.; Andres, D.A.; Spielmann, H.P.; Lammerding, J.; Wang, Y.; Young, S.G.; Fong, L.G. An accumulation of non-farnesylated prelamin A causes cardiomyopathy but not progeria. *Hum. Mol. Genet.* **2010**, *19*, 2682–2694, doi:10.1093/hmg/ddq158.
109. Coffinier, C.; Jung, H.-J.; Li, Z.; Nobumori, C.; Yun, U.J.; Farber, E.A.; Davies, B.S.; Weinstein, M.M.; Yang, S.H.; Lammerding, J.; et al. Direct synthesis of lamin A, bypassing prelamin a processing, causes misshapen nuclei in fibroblasts but no detectable pathology in mice. *J. Biol. Chem*. **2010**, *285*, 20818–20826, doi:10.1074/jbc.M110.128835.
110. Benedetti, S.; Menditto, I.; Degano, M.; Rodolico, C.; Merlini, L.; D'Amico, A.; Palmucci, L.; Berardinelli, A.; Pegoraro, E.; Trevisan, C.P.; et al. Phenotypic clustering of lamin A/C mutations in neuromuscular patients. *Neurology* **2007**, *69*, 1285–1292, doi:10.1212/01.wnl.0000261254.87181.80.
111. Sébillon, P.; Bouchier, C.; Bidot, L.D.; Bonne, G.; Ahamed, K.; Charron, P.; Drouin-Garraud, V.; Millaire, A.; Desrumeaux, G.; Benaïche, A.; et al. Expanding the phenotype of LMNA mutations in dilated cardiomyopathy and functional consequences of these mutations. *J. Med. Genet*. **2003**, *40*, 560–567.
112. Gordon, L.B.; Kleinman, M.E.; Miller, D.T.; Neuberg, D.S.; Giobbie-Hurder, A.; Gerhard-Herman, M.; Smoot, L.B.; Gordon, C.M.; Cleveland, R.; Snyder, B.D.; et al. Clinical trial of a farnesyltransferase inhibitor in children with Hutchinson-Gilford progeria syndrome. *Proc. Natl. Acad. Sci. USA* **2012**, *109*, 16666–16671, doi:10.1073/pnas.1202529109.
113. Markandeya, Y.S.; Tsubouchi, T.; Hacker, T.A.; Wolff, M.R.; Belardinelli, L.; Balijepalli, R.C. Inhibition of late sodium current attenuates ionic arrhythmia mechanism in ventricular myocytes expressing LaminA-N195K mutation. *Heart Rhythm*. **2016**, *13*, 2228–2236, doi:10.1016/j.hrthm.2016.08.007.
114. Nguyên-Trân, V.T.; Kubalak, S.W.; Minamisawa, S.; Fiset, C.; Wollert, K.C.; Brown, A.B.; Ruiz-Lozano, P.; Barrere-Lemaire, S.; Kondo, R.; Norman, L.W.; et al. A novel genetic pathway for sudden cardiac death via defects in the transition between ventricular and conduction system cell lineages. *Cell* **2000**, *102*, 671–682.
115. Lu, D.; Lian, H.; Zhang, X.; Shao, H.; Huang, L.; Qin, C.; Zhang, L. LMNA E82K mutation activates FAS and mitochondrial pathways of apoptosis in heart tissue specific transgenic mice. *PLoS ONE* **2010**, *5*, e15167, doi:10.1371/journal.pone.0015167.
116. Wu, X.; Wang, Q.K.; Gui, L.; Liu, M.; Zhang, X.; Jin, R.; Li, W.; Yan, L.; Du, R.; Wang, Q. Identification of a new lamin A/C mutation in a Chinese family affected with atrioventricular block as the prominent phenotype. *J. Huazhong Univ. Sci. Technol. Med. Sci. Hua Zhong Ke Ji Xue Xue Bao Yi Xue Ying Wen Ban Huazhong Keji Daxue Xuebao Yixue Yingdewen Ban* **2010**, *30*, 103–107, doi:10.1007/s11596-010-0119-z.
117. Wang, H.; Zheng, W.; Wang, J.; Wang, X.J.; Zhen, Y.S.; Song, L.; Zou, Y.B.; Hui, R.T. A novel LMNA gene mutation E82K associated with familial dilated cardiomyopathy. *Zhonghua Xin Xue Guan Bing Za Zhi* **2005**, *33*, 875–879.
118. Arimura, T.; Helbling-Leclerc, A.; Massart, C.; Varnous, S.; Niel, F.; Lacène, E.; Fromes, Y.; Toussaint, M.; Mura, A.M.; Keller, D.I.; et al. Mouse model carrying H222P-Lmna mutation

develops muscular dystrophy and dilated cardiomyopathy similar to human striated muscle laminopathies. *Hum. Mol. Genet.* **2005**, *14*, 155–169.
119. Wang, Y.; Herron, A.J.; Worman, H.J. Pathology and nuclear abnormalities in hearts of transgenic mice expressing M371K lamin A encoded by an LMNA mutation causing Emery-Dreifuss muscular dystrophy. *Hum. Mol. Genet.* **2006**, *15*, 2479–2489, doi:10.1093/hmg/ddl170.
120. van Rijsingen, I.A.W.; Nannenberg, E.A.; Arbustini, E.; Elliott, P.M.; Mogensen, J.; Hermans-van Ast, J.F.; van der Kooi, A.J.; van Tintelen, J.P.; van den Berg, M.P.; Grasso, M.; et al. Gender-specific differences in major cardiac events and mortality in lamin A/C mutation carriers. *Eur. J. Heart Fail*. **2013**, *15*, 376–384, doi:10.1093/eurjhf/hfs191.
121. Arimura, T.; Onoue, K.; Takahashi-Tanaka, Y.; Ishikawa, T.; Kuwahara, M.; Setou, M.; Shigenobu, S.; Yamaguchi, K.; Bertrand, A.T.; Machida, N.; et al. Nuclear accumulation of androgen receptor in gender difference of dilated cardiomyopathy due to lamin A/C mutations. *Cardiovasc. Res*. **2013**, *99*, 382–394, doi:10.1093/cvr/cvt106.
122. Muchir, A.; Reilly, S.A.; Wu, W.; Iwata, S.; Homma, S.; Bonne, G.; Worman, H.J. Treatment with selumetinib preserves cardiac function and improves survival in cardiomyopathy caused by mutation in the lamin A/C gene. *Cardiovasc. Res*. **2012**, *93*, 311–319.
123. Muchir, A.; Kim, Y.J.; Reilly, S.A.; Wu, W.; Choi, J.C.; Worman, H.J. Inhibition of extracellular signal-regulated kinase 1/2 signaling has beneficial effects on skeletal muscle in a mouse model of Emery-Dreifuss muscular dystrophy caused by lamin A/C gene mutation. *Skelet. Muscle* **2013**, *3*, 17–5040-3-17.
124. Muchir, A.; Shan, J.; Bonne, G.; Lehnart, S.E.; Worman, H.J. Inhibition of extracellular signal-regulated kinase signaling to prevent cardiomyopathy caused by mutation in the gene encoding A-type lamins. *Hum. Mol. Genet.* **2009**, *18*, 241–247.
125. Wu, W.; Shan, J.; Bonne, G.; Worman, H.J.; Muchir, A. Pharmacological inhibition of c-Jun N-terminal kinase signaling prevents cardiomyopathy caused by mutation in LMNA gene. *Biochim. Biophys. Acta* **2010**, *1802*, 632–638.
126. Wu, W.; Muchir, A.; Shan, J.; Bonne, G.; Worman, H.J. Mitogen-activated protein kinase inhibitors improve heart function and prevent fibrosis in cardiomyopathy caused by mutation in lamin A/C gene. *Circulation* **2011**, *123*, 53–61.
127. Muchir, A.; Wu, W.; Sera, F.; Homma, S.; Worman, H.J. Mitogen-activated protein kinase kinase 1/2 inhibition and angiotensin II converting inhibition in mice with cardiomyopathy caused by lamin A/C gene mutation. *Biochem. Biophys. Res. Commun*. **2014**, *452*, 958–961.
128. Choi, J.C.; Muchir, A.; Wu, W.; Iwata, S.; Homma, S.; Morrow, J.P.; Worman, H.J. Temsirolimus activates autophagy and ameliorates cardiomyopathy caused by lamin A/C gene mutation. *Sci. Transl. Med*. **2012**, *4*, 144ra102, doi:10.1126/scitranslmed.3003875.
129. Le Dour, C.; Macquart, C.; Sera, F.; Homma, S.; Bonne, G.; Morrow, J.P.; Worman, H.J.; Muchir, A. Decreased WNT/β-catenin signalling contributes to the pathogenesis of dilated cardiomyopathy caused by mutations in the lamin a/C gene. *Hum. Mol. Genet.* **2017**, *26*, 333–343, doi:10.1093/hmg/ddw389.
130. Bertrand, A.T.; Renou, L.; Papadopoulos, A.; Beuvin, M.; Lacène, E.; Massart, C.; Ottolenghi, C.; Decostre, V.; Maron, S.; Schlossarek, S.; et al. DelK32-lamin A/C has abnormal location and induces incomplete tissue maturation and severe metabolic defects leading to premature death. *Hum. Mol. Genet.* **2012**, *21*, 1037–1048, doi:10.1093/hmg/ddr534.

131. Mounkes, L.C.; Kozlov, S.; Hernandez, L.; Sullivan, T.; Stewart, C.L. A progeroid syndrome in mice is caused by defects in A-type lamins. *Nature* **2003**, *423*, 298–301, doi:10.1038/nature01631.
132. Yamanaka, S. Induced pluripotent stem cells: Past, present, and future. *Cell Stem Cell* **2012**, *10*, 678–684, doi:10.1016/j.stem.2012.05.005.
133. Yoshihara, M.; Hayashizaki, Y.; Murakawa, Y. Genomic Instability of iPSCs: Challenges Towards Their Clinical Applications. *Stem Cell Rev*. **2017**, *13*, 7–16, doi:10.1007/s12015-016-9680-6.
134. Davis, J.; Maillet, M.; Miano, J.M.; Molkentin, J.D. Lost in transgenesis: A user's guide for genetically manipulating the mouse in cardiac research. *Circ. Res*. **2012**, *111*, 761–777, doi:10.1161/CIRCRESAHA.111.262717.
135. Di Barletta, R.M.; Ricci, E.; Galluzzi, G.; Tonali, P.; Mora, M.; Morandi, L.; Romorini, A.; Voit, T.; Orstavik, K.H.; Merlini, L.; et al. Different mutations in the LMNA gene cause autosomal dominant and autosomal recessive Emery-Dreifuss muscular dystrophy. *Am. J. Hum. Genet*. **2000**, *66*, 1407–1412, doi:10.1086/302869.
136. Ben Yaou, R.; Toutain, A.; Arimura, T.; Demay, L.; Massart, C.; Peccate, C.; Muchir, A.; Llense, S.; Deburgrave, N.; Leturcq, F.; et al. Multitissular involvement in a family with LMNA and EMD mutations: Role of digenic mechanism? *Neurology* **2007**, *68*, 1883–1894, doi:10.1212/01.wnl.0000263138.57257.6a.
137. De Sandre-Giovannoli, A.; Chaouch, M.; Kozlov, S.; Vallat, J.M.; Tazir, M.; Kassouri, N.; Szepetowski, P.; Hammadouche, T.; Vandenberghe, A.; Stewart, C.L.; et al. Homozygous defects in LMNA, encoding lamin A/C nuclear-envelope proteins, cause autosomal recessive axonal neuropathy in human (Charcot-Marie-Tooth disorder type 2) and mouse. *Am. J. Hum. Genet*. **2002**, *70*, 726–736, doi:10.1086/339274.
138. Chaouch, M.; Allal, Y.; De Sandre-Giovannoli, A.; Vallat, J.M.; Amer-el-Khedoud, A.; Kassouri, N.; Chaouch, A.; Sindou, P.; Hammadouche, T.; Tazir, M.; et al. The phenotypic manifestations of autosomal recessive axonal Charcot-Marie-Tooth due to a mutation in Lamin A/C gene. *Neuromuscul. Disord. NMD* **2003**, *13*, 60–67.
139. Tazir, M.; Azzedine, H.; Assami, S.; Sindou, P.; Nouioua, S.; Zemmouri, R.; Hamadouche, T.; Chaouch, M.; Feingold, J.; Vallat, J.M.; et al. Phenotypic variability in autosomal recessive axonal Charcot-Marie-Tooth disease due to the R298C mutation in lamin A/C. *Brain J. Neurol*. **2004**, *127 Pt 1*, 154–163, doi:10.1093/brain/awh021.
140. Bouhouche, A.; Birouk, N.; Azzedine, H.; Benomar, A.; Durosier, G.; Ente, D.; Muriel, M.P.; Ruberg, M.; Slassi, I.; Yahyaoui, M.; et al. Autosomal recessive axonal Charcot-Marie-Tooth disease (ARCMT2): Phenotype-genotype correlations in 13 Moroccan families. *Brain J. Neurol*. **2007**, *130 Pt 4*, 1062–1075, doi:10.1093/brain/awm014.
141. MacRae, C. Phase 2 Study of A797, an Oral, Selective p38 Mitogen-Activated Protein Kinase Inhibitor, in Patients With Lamin A/C-Related Dilated Cardiomyopathy. In Proceedings of the European Society of Cardiology Congress, Rome, Italy, 27 August 2016.